



**HAL**  
open science

# Enzymatically initiated synthesis of biomimetic receptors based on molecularly imprinted polymers by free radical polymerization

Mira Daoud Attieh

► **To cite this version:**

Mira Daoud Attieh. Enzymatically initiated synthesis of biomimetic receptors based on molecularly imprinted polymers by free radical polymerization. *Biotechnology*. Université de Technologie de Compiègne; Université Libanaise, 2016. English. NNT : 2016COMP2266 . tel-01384244

**HAL Id: tel-01384244**

**<https://theses.hal.science/tel-01384244>**

Submitted on 19 Oct 2016

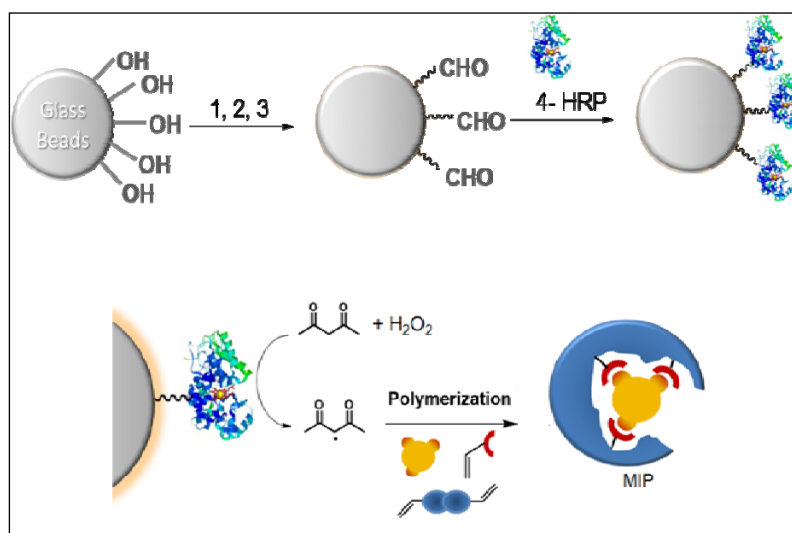
**HAL** is a multi-disciplinary open access archive for the deposit and dissemination of scientific research documents, whether they are published or not. The documents may come from teaching and research institutions in France or abroad, or from public or private research centers.

L'archive ouverte pluridisciplinaire **HAL**, est destinée au dépôt et à la diffusion de documents scientifiques de niveau recherche, publiés ou non, émanant des établissements d'enseignement et de recherche français ou étrangers, des laboratoires publics ou privés.

Par Mira DAOUD ATTIEH

*Enzymatically initiated synthesis of biomimetic receptors based on molecularly imprinted polymers by free radical polymerization*

Thèse présentée pour l'obtention  
du grade de Docteur de l'UTC en  
cotutelle



Soutenu le 1<sup>er</sup> avril 2016  
**Spécialité** : Biotechnologie

D2266



## **THESE EN COTUTELLE**

Pour obtenir le grade de Docteur délivré par

**L'UNIVERSITE de TECHNOLOGIE de COMPIEGNE**

et

**L'Ecole Doctorale des Sciences et Technologie  
(Université Libanaise)**

**Spécialité Biotechnologie**

Présentée et soutenue publiquement par

**Mira DAOUD ATTIEH**

**Enzymatically initiated synthesis of biomimetic receptors based on  
molecularly imprinted polymers by free radical polymerization**

Thèse dirigée par le Professeur Karsten Haupt, la Dr. Aude Falcimaigne-Cordin  
et le Professeur Assem Elkak

Soutenance prévue le 1 Avril 2016, devant le jury composé de :

M <sup>me</sup> Clovia Holdsworth, Pr.	University of Newcastle, Australie	Rapporteur
M <sup>me</sup> Alessandra Maria Bossi, Pr.	University of Verona, Verona, Italie	Rapporteur
M <sup>me</sup> Hélène Greige-Gerges, Pr.	Université Libanaise	Rapporteur
M <sup>me</sup> Catherine Sarazin, Pr.	Université de Picardie Jules Vernes, Amiens	Examineur
M. Bernard Cathala, Dr.	Institut National de la Recherche Agronomique, Nantes	Examineur
M. Karsten Haupt, Pr.	Université de Technologie de Compiègne	Directeur
M <sup>me</sup> Aude Cordin, Dr.	Université de Technologie de Compiègne	Co-directeur
M. Assem Elkak, Pr.	Université Libanaise	Directeur





*To all who believe that courage is  
sometimes the quiet inner voice  
saying at the end of the day: " I  
will try again tomorrow"*



---

*Table of contents*

<b><i>Acknowledgments</i></b>	<b>I</b>
<b><i>List of Figures</i></b>	<b>III</b>
<b><i>List of Tables</i></b>	<b>IX</b>
<b><i>Abbreviations</i></b>	<b>XI</b>
<b><i>Abstract in English</i></b>	<b>XIII</b>
<b><i>Résumé en Français</i></b>	<b>XIV</b>
<b>Introduction</b>	<b>1</b>
<b>Chapter I:</b>	
<b>Literature Review</b>	<b>5</b>
<b><i>I.1. Enzymatic polymer synthesis</i></b> .....	<b>6</b>
<b>I.1.1. Polymer synthesis by enzyme-mediated polymerization</b> .....	<b>8</b>
I.1.1.1. Synthesis of Polysaccharides.....	9
I.1.1.2. Synthesis of polyesters.....	16
I.1.1.3. Oxidative polymerization of polyaromatics and vinyl monomers.....	19
<b>I.1.2. Polymer synthesis via Enzymatic Polymer Modification</b> .....	<b>27</b>
<b>I.1.3. Enzyme-initiated radical polymerization</b> .....	<b>29</b>
I.1.3.1. Enzymes.....	29
I.1.3.2. Catalytic mechanism.....	35
I.1.3.3. Influence of different parameters on the polymerization.....	39
<b>I.1.4. Potential applications of enzymatic polymerization</b> .....	<b>46</b>
I.1.4.1. Biocatalysts in fine and bulk chemical industries.....	47
I.1.4.2. Biocatalysts in food industry.....	47

1.1.4.3.	Application of biocatalysts in biomedical and pharmaceutical fields.....	47
<b>1.2.</b>	<b>Molecularly imprinted polymers.....</b>	<b>49</b>
<b>1.2.1.</b>	<b>Principle of molecular imprinting.....</b>	<b>50</b>
1.2.1.1.	Background of the molecular imprinting technique.....	51
1.2.1.2.	Imprinting matrix.....	52
<b>1.2.2.</b>	<b>Development of water-compatible molecularly imprinted polymers.....</b>	<b>62</b>
1.2.2.1.	Synthesis of water-compatible MIPs in organic solvents.....	62
1.2.2.2.	Synthesis of water-compatible MIPs in aqueous media.....	68
<b>1.2.3.</b>	<b>Molecular imprinting of macromolecules.....</b>	<b>70</b>
1.2.3.1.	Limitations of the protein imprinting.....	70
1.2.3.2.	Imprinting in hydrogels and sol-gels.....	71
1.2.3.3.	Surface imprinting.....	76
1.2.3.4.	Imprinting by epitope approach.....	79
1.2.3.5.	Microorganisms and cells imprinting.....	80
<b>References.....</b>	<b>.....</b>	<b>82</b>

## Chapter II:

### Preparation and characterization of hydrogels synthesized by biochemically initiated free radical polymerization

#### – Results and discussion

97

<b>II.1.</b>	<b>Introduction.....</b>	<b>98</b>
<b>II.2.</b>	<b>Materials and Methods.....</b>	<b>101</b>
II.2.1.	Materials.....	101
II.2.2.	Synthesis of linear polymers.....	103
II.2.3.	Synthesis of Hydrogels.....	104
II.2.4.	Polymer characterization.....	105
II.2.5.	Study of the polymerization kinetics.....	106
II.2.6.	Evaluation of HRP entrapment within hydrogel matrix.....	106
II.2.7.	Cytotoxicity test of nanoparticles.....	109
<b>II.3.</b>	<b>Results and discussion.....</b>	<b>110</b>
<b>II.3.1.</b>	<b>Linear polymers synthesis by biochemical initiation.....</b>	<b>110</b>
II.3.1.1.	Synthesis of linear polyacrylamides.....	110
II.3.1.2.	Polymerization of other acrylic and vinyl monomers.....	114
<b>II.3.2.</b>	<b>Hydrogel synthesis by biocatalyst-mediated initiation.....</b>	<b>114</b>
II.3.2.1.	Characterization of hydrogels synthesis by HRP-mediated free radical polymerization.....	115
II.3.2.2.	Efficiency of different heme-containing proteins for FRP.....	118

II.3.1.	Linear polymers synthesis by biochemical initiation.....	110
II.3.1.1.	Synthesis of linear polyacrylamides .....	110
II.3.1.2.	Polymerization of other acrylic and vinyl monomers .....	114
II.3.2.	<b>Hydrogel synthesis by biocatalyst-mediated initiation .....</b>	<b>Table of contents</b>
II.3.2.1.	Characterization of hydrogels synthesis by HRP-mediated free radical polymerization .....	115
II.3.2.2.	Efficiency of different heme-containing proteins for FRP .....	118
II.3.2.3.	Versatility of enzyme-mediated polymerization for hydrogel synthesis .....	124
II.3.2.4.	Optimization of the enzymatic initiation system .....	127
II.3.2.5.	Comparison between HRP-mediated and chemical initiations of free radical polymerization .....	136
II.3.2.6.	Cytotoxicity of the enzymatically synthesized nanoparticles .....	138
II.4.	<b>Conclusion .....</b>	<b>140</b>
References.....		141

## Chapter III:

### Immobilization of horseradish peroxidase for the initiation of the free radical polymerization

– Results and discussion .....		145
III.1.	<b>Introduction .....</b>	<b>146</b>
III.1.	<b>Introduction .....</b>	<b>146</b>
III.2.	<b>Materials and Methods .....</b>	<b>149</b>
III.2.	<b>Materials and Methods .....</b>	<b>149</b>
III.2.1.	Materials .....	149
III.2.1.	Materials .....	149
III.2.2.	HRP immobilization .....	150
III.2.2.	HRP immobilization .....	150
III.2.3.	Characterization of the immobilized enzyme .....	151
III.2.3.	Characterization of the immobilized enzyme .....	151
III.2.4.	Characterization of the immobilized enzyme .....	151
III.2.4.	Synthesis of hydrogels using immobilized HRP and their characterization.....	154
III.2.4.1.	Synthesis of hydrogels using immobilized HRP and their characterization.....	154
III.2.4.2.	Experimental design in the hydrogel matrix .....	157
III.2.4.2.	Entrapment of HRP in the hydrogel matrix for hydrogels synthesis.....	157
III.2.4.3.	Comparison of free and immobilized enzyme for hydrogels synthesis .....	158
III.3.	<b>Results and discussion .....</b>	<b>159</b>
III.3.	<b>Results and discussion .....</b>	<b>159</b>
III.3.1.	HRP immobilization .....	159
III.3.1.	HRP immobilization .....	159
III.3.1.1.	HRP immobilization .....	159
III.3.1.2.	Optimization of HRP immobilization .....	169
III.3.1.2.	Enzyme activities in HRP immobilization mixtures .....	171
III.3.1.3.	Enzyme stability in hydro-organic mixtures .....	174
III.3.1.4.	Storage stability .....	175
III.3.2.	<b>HRP-mediated synthesis of hydrogels .....</b>	<b>176</b>
III.3.2.1.	Influence of the experimental conditions on the hydrogels synthesis .....	177
III.3.2.2.	Models validation .....	184
III.3.2.3.	Emphasis of the enzyme absence within the hydrogel matrix .....	186
III.3.2.4.	Comparison between the free and immobilized HRP-mediated syntheses of hydrogels .....	188
III.4.	<b>Conclusion .....</b>	<b>189</b>
References .....		191

---

<b>Chapter IV:</b>	
<b>Enzyme-mediated synthesis of molecularly imprinted hydrogels</b>	
<b>– Results and discussion</b>	<b>193</b>
<i>IV.1. Introduction</i>	<i>194</i>
<i>IV.2. Materials and Methods</i>	<i>197</i>
IV.2.1. Materials	197
IV.2.2. Synthesis of MIP Hydrogels	198
IV.2.2.1. Molecular imprinting of 2,4-dichlorophenoxyacetic acid	198
IV.2.2.2. Molecular imprinting of salicylic acid	200
IV.2.2.3. Trypsin imprinting	201
IV.2.3. Polymers characterization	202
IV.2.3.1. Particle size measurements	202
IV.2.3.2. Polymer morphology	202
IV.2.3.3. Binding properties of MIPs	202
<i>IV.3. Results and discussion</i>	<i>206</i>
IV.3.1. Free HRP-mediated synthesis of MIPs	206
IV.3.1.1. Synthesis of MIP for 2,4-dichlorophenoxyacetic acid	206
IV.3.1.2. Synthesis of a MIP for salicylic acid	219
IV.3.1.3. Molecular imprinting of a protein: trypsin	221
IV.3.2. Synthesis of MIP nanoparticles by immobilized HRP	223
IV.3.2.1. Optimization of MIP synthesis	223
IV.3.2.2. Molecular recognition properties	226
IV.3.2.3. Reusability of the immobilized HRP	227
<i>IV.4. Conclusion</i>	<i>231</i>
<i>References</i>	<i>232</i>
<b>Conclusions and perspectives</b>	<b>235</b>
<b>Annexes</b>	<b>239</b>
<i>Annexes 1-List of Achievements</i>	<i>239</i>
<i>Annexes 2-Posters</i>	<i>240</i>

## Remerciements

A l'issue de la rédaction de cette recherche, je suis convaincue que la thèse est loin d'être un travail solitaire. En effet, il faut remercier tous ceux qui, sans leur contribution, je n'aurais pas pu réaliser mon travail de thèse. Je leur dois leur bonne humeur, et surtout leur intérêt manifesté à l'égard de mon projet de recherche.

En premier lieu, je tiens à remercier mes directeurs de thèse. J'aimerai, tout d'abord, remercier mon directeur libanais, Pr. Assem ELKAK, pour la confiance qu'il m'a accordée en acceptant de me recruter en tant que thésarde en co-tutelle. Mes remerciements vont également à mon directeur de thèse français, Pr. Karsten HAUPT, et j'aimerai lui dire à quel point j'ai apprécié sa grande disponibilité, malgré ses occupations et ses charges, et que j'ai été extrêmement sensible à ses qualités humaines de compréhension manifestées dans les différents axes financiers et scientifiques de ce travail doctoral. Et je n'oublie pas de le remercier pour m'avoir accueilli, en tant que directeur de laboratoire de génie enzymatique et cellulaire (GEC).

J'exprime aussi mes remerciements à Dr. Aude FALCIMAIGNE-CORDIN, mon multivitamines de tous les jours, d'avoir co-encadré ce travail de thèse. Elle était toujours disponible, à l'écoute de mes nombreuses questions ; et sa capacité d'enthousiasme et d'analyse, durant nos réunions, m'ont vraiment bien encouragé, surtout qu'elle m'a fait confiance malgré les connaissances, plutôt légères, que j'avais quand j'ai commencé la thèse. Enfin, je lui dis que ses nombreuses relectures et corrections de mes rapports, mes présentations, et de ma thèse, sont bien appréciées. Finalement, tous mes travaux de recherche et ma thèse vous doit beaucoup, mes directeurs de thèses, et pour tout cela, un grand merci !

Je n'oublie pas de remercier Prof Fawaz El-OMAR, Doyen de l'école doctorale de l'UL, et Prof Mohamad KHALIL, directeur de la plateforme de Biotechnologie (AZM) à l'école doctorale de l'UL pour toute leur compréhension et leur soutien qu'ils m'ont offerts lors de ce trajet doctoral.

Il me sera très difficile de remercier, un par un, tous les membres de l'Unité Génie Enzymatique et Cellulaire, et j'adresse mes remerciements chaleureux à tous le personnel en tant que techniciens et administratifs, les profs et les maitres de conférences dans les autres équipes, les doctorants que j'ai eu la chance de connaître, ainsi que les étudiants en master. Vraiment un grand merci surtout pour Dr Claire Rossi pour sa contribution dans l'élaboration du plan d'expérience et sa très bonne humeur. Je passe également mon merci à tous les stagiaires qui ont contribué à ce travail : Yiming SONG, Laure BONNEMAISON, Eugène CHRISTO-FOROUX, et Paulina Ximena MEDINA RANGEL.

Un remerciement un peu chaleureux à mes collègues les plus sincères Yi, Marcelina, et Laeticia, avec qui j'ai partagé le bureau pour des années, ainsi que pour tous les autres MIPièns que j'ai eu la chance de partager de très beaux moments avec. Finalement, j'adresse des remerciements distingués pour Hassan ISBER et Rita MAALOUF pour l'amitié à la libanaise qu'ils m'ont accordée avec tout genre de soutien qu'ils m'ont offert quand j'avais besoin d'une épaule sur laquelle verser mes larmes et mes problèmes.

J'exprime mes sentiments les plus sincères à Marie-Curie, dans le cadre du projet ITN CHEBANA, ainsi que les autres sources financières pour les co-financements alloués à ces travaux de thèse.



## List of figures

## Chapter I

<b>Figure I-1:</b> Enzyme applications in Materials Science.....	7
<b>Figure I-2:</b> Enzyme-substrate relationship for enzymatic reactions: (A) an in vivo reaction obeying the “key and lock” theory and (B) an in vitro reaction involving an enzyme-artificial substrate complex leading to a product with bond formation, where the artificial substrate desirably possesses a close structure of the natural substrate at the active site vicinity. The black part in the enzyme indicates the active site. Reprinted from [1, 24].....	10
<b>Figure I-3:</b> Typical enzymatic polymerization of cellobiosyl fluoride and N,N'-diacetylchitobiose oxazoline catalyzed by cellulose and chitinase, respectively. [15].....	11
<b>Figure I-4:</b> Examples of hyaluronidase multi-catalyses for enzymatic polymerizations of sugar oxazoline monomers. Adapted from [1,17].....	15
<b>Figure I-5:</b> Lipase-catalyzed synthesis of aliphatic polyesters via polycondensation. from [66].....	17
<b>Figure I-6:</b> Lipase-catalyzed synthesis of polyesters via ring-opening polymerization. from [75].....	18
<b>Figure I-7:</b> Lipase-catalyzed ring-opening polymerization of phosphates. Reprinted from [75].....	19
<b>Figure I-8:</b> Detailed reaction scheme applied for Free radical polymerization. I: Initiator; PR <sup>•</sup> : Primary radical; R <sup>•</sup> <sub>1</sub> ; M: monomer molecule. Reprinted from [77].....	20
<b>Figure I-9:</b> Schematic representation of laccase and peroxidase mediator systems-initiated polymerization reactions. Upper: the mediator is used as true catalyst transferring the radical to a monomer; Lower: the oxidized mediator radical itself initiates the polymerization process and hence is incorporated into the polymer. Reprinted from [79].....	21
<b>Figure I-10:</b> Chemical structures of the tested vinyl monomers in the enzyme-initiated polymerization.....	23
<b>Figure I-11:</b> Mechanism of HRP-catalyzed polymerization under ARGET ATRP conditions. (Asc=ascorbate, DHA=dehydroascorbic acid). Reprinted from [101].....	25
<b>Figure I-12:</b> Schematic representation of glucose oxidase (GOx)-HRP cascade catalyzed radical generation in air for the initiation of RAFT polymerization of dimethylacrylamide. Modified from [103].....	26
<b>Figure I-13:</b> Schematic representation of enzymes involved in the enzymatic modification. from [105].....	28
<b>Figure I-14:</b> Three-dimensional representation of Horseradish peroxidase (HRP); helices and loops are shown in blue and yellow. One short $\beta$ -sheet region is shown in pink. The two calcium ions are shown as green spheres. The heme group is shown in red and stand between the distal and the proximal domain; the proximal His170 residue (light blue) coordinates to the heme [109].....	31
<b>Figure I-15:</b> A: General 3D structure of laccase ( <i>Trametes Trogii</i> laccase). The three cupredoxin-like domain (D1, D2, and D3) are shown in green, cyan, and magenta, respectively. B: Schematic representation of the active site of laccase (from <i>T. versicolor</i> laccase). It represents the copper ions from T1 Cu to the T2/T3 trinuclear cluster. Residues involved in the coordination sphere of the catalytic coppers are also represented. Modified from [102,118].....	34
<b>Figure I-16:</b> Mechanism of the HRP catalytic cycle, showing compounds I and II as enzyme intermediates. Reprinted from [108].....	36

<b>Figure I-17:</b> The classical peroxidase cycle and the pathways for the production of the redox forms ferrous and compound III (HRP-III). Reactions 1-3: classical cycle; Reaction 4: reduction of the ferric enzyme to the ferrous form; Reactions 5, 6, and 7: possible pathways for the formation of compound III. from [114].....	37
<b>Figure I-18:</b> Schematic representation of a laccase catalytic cycle producing two molecules of water from the reduction of one molecule of molecular oxygen and the concomitant oxidation (at the T1 copper site) of four substrate molecules to the corresponding radicals. Sub: substrate molecule; Sub <sup>•</sup> : oxidized substrate radicals. Adapted from [125].....	38
<b>Figure I-19:</b> Chemical structures of the most common laccase mediators.....	39
<b>Figure I-20:</b> Chemical structures of the $\beta$ -diketones that have been mostly investigated for the enzyme-mediated initiation of the acrylamide and styrene polymerization. Modified form [93,100].....	42
<b>Figure I-21:</b> Commonly accepted reaction scheme of HRP catalytic cycle. Adapted from [92].....	43
<b>Figure I-22:</b> Variation of the polymer molecular weight depending on the initial concentration of horseradish peroxidase. [AAM] <sub>0</sub> = 0.64 mol/l; [Acac] <sub>0</sub> = 0.02 mol/l; [H <sub>2</sub> O <sub>2</sub> ] <sub>0</sub> = 7*10 <sup>-4</sup> mol/l. from [96]. ....	43
<b>Figure I-23:</b> Highly schematic representation of the molecular imprinting process. from [167].....	51
<b>Figure I-24:</b> Functional monomers commonly used in the non-covalent molecular imprinting.....	54
<b>Figure I-25:</b> Cross-linkers most commonly used in the non-covalent imprinting.....	55
<b>Figure I-26:</b> Characterization of different physical forms for molecularly imprinted polymers synthesized by different strategies: (A) SEM photos for MIP membrane prepared by immersion polymerization [197]; (B): SEM photos for magnetic MIP beads prepared by suspension polymerization [185]; (C): TEM photos for MIP silica beads [198]; (D): TEM photos for MIP nanoparticles (43 nm) prepared by precipitation polymerization [199]; (E): TEM photos for MIP nanocapsule prepared by emulsion polymerization [198]; (F): TEM photo for a side view of MIP nanofilm [162]; (G): SEM photos for MIP microspheres prepared by two-step seed swelling polymerization [200]; (H): SEM photo for monolithic MIP prepared by In situ polymerization [201]; (I): TEM photos for core-shell MIP prepared by emulsion polymerization [192]......	61
<b>Figure I-27:</b> Chemical structures of the specially designed functional monomers for the preparation of water-compatible MIPs. A: N-N'-diethyl(4-vinylphenyl)amidine; B: 9-(guanidinomethyl)-10-vinylanthracene; C: 1-(3,5-bis(trifluoromethyl)phenyl)-3-(4-vinylphenyl)urea); D: 2,6-bis(acrylamide)pyridine; E: 2,2'-((1-carboxy-5-methacrylamidopentyl)azanediyl)diacetic acid-Nickel(II); F: 2-(4-vinylphenoxy)-3,5,6-trichlorobenzoquinone; G: 5-(4''-vinyl)benzyloxy-1,3-bis[2'-(3''',3''',4'',4''-tetramethyl-2'',5''-dioxaborolanyl)phenylcarbomoyl]benzene. Reprinted from [209].....	64
<b>Figure I-28:</b> Strategy for preparation of protein-imprinted beads with double thermo-responsive gates by surface-initiated living radical polymerization. (a) Generation of mesoporous chloromethylated polystyrene beads (MCP beads) modified. (b) Use of the supports (modified MCP beads) for the grafting of lysozyme-imprinted polymers (MIP beads) and then coating with poly(N-isopropylacrylamide) (coated MIP beads) by two-step polymerization. (c) Schematic illustration of coated MIP beads with thermosensitive swelling/collapse phase transitions for selective adsorption of proteins. Reprinted from [235]......	74
<b>Figure I-29:</b> Schematic representation of the solid-phase synthesis of MIP-NPs. 1: Polymerization; 2: Release of thermoresponsive MIP-NPs (temperature change from 37 °C to room temperature, 25 °C) [236].....	75
<b>Figure I-30:</b> Outline of CRP micro-contact imprinting and re-binding: (a) protein is adsorbed onto the microscope cover glass together with the functional monomer; (b) the cover glass is brought into contact with the support carrying the cross-linker and initiator and then placed in UV reactor; (c) the cover glass is removed; (d) template protein is extracted by washing; (e) rebinding of template or competitor proteins [241].....	77
<b>Figure I-31:</b> Protein imprinting using a sacrificial wide-pore silica support modified with a submonolayer of adsorbed protein (IgG or HSA), filling of the pores of the protein-silica template with a monomer solution, polymerization, and subsequent removal of the protein and silica porogen by fluoride etching and washing. The	

last step leaves behind an inverse replica of the silica template that features highly accessible protein-complementary binding sites at the pore walls of the polymeric beads. Reprinted from [247].....	78
<b>Figure I-32:</b> Schematic representation of the epitope approach for MIP synthesis. Reprinted from [228].....	79

## Chapter II

<b>Figure II-1:</b> Representation of the accepted HRP catalytic cycle, showing compounds I and II as enzyme intermediates, and the formation of radical species.....	100
<b>Figure II-2:</b> Representation of the enzyme-mediated free-radical polymerization for hydrogel preparation.....	100
<b>Figure II-3:</b> Standard curve for protein quantification by Bradford.....	107
<b>Figure II-4:</b> Chemical structures of (A) Protoporphyrin IV and (B) Hemin.....	111
<b>Figure II-5:</b> SEM images for poly(4-VP/PDA) nanoparticles synthesized by free-radical polymerization initiated by: (A) HRP catalysis; (B) UV with Vazo <sup>®</sup> 56.....	115
<b>Figure II-6:</b> Activity of the possibly entrapped HRP within Hydrogels 1 and 2.....	116
<b>Figure II-7:</b> Sodium Dodecyl Sulfate Gel Electrophoresis (SDS-PAGE) under reducing conditions of nanoparticles. Lane 1: molecular weight markers (10000-250000 Da), Lane 2: commercial pure HRP solution, Lane 3: Hydrogel 1 prior to washing, Lane 4: Hydrogel 1 after washing, Lane 6: Hydrogel 2 prior to washing, Lane 7: Hydrogel 2 after washing.....	117
<b>Figure II-8:</b> Hydrodynamic diameters and PDI (as obtained by DLS) of the particles obtained by free radical polymerization of different functional monomers and PDA as cross-linker, initiated by different biocatalysts, using $[Monomers]_0 = 57.2 \text{ mmol/l}$ , $[Biocatalyst]_0 = 0.023 \text{ mM}$ , $[Acac]_0 = 2.8 \text{ mM}$ , and $[H_2O_2]_0 = 1.76 \text{ mM}$ , in 0.1 M phosphate buffer pH 7.0.....	119
<b>Figure II-9:</b> SEM images of poly(4-VP/PDA) particles synthesized by free radical polymerization initiated by (A) HRP, (B) cytochrome c, (C) myoglobin, using $[Monomers]_0 = 57.2 \text{ mmol/l}$ , $[Biocatalyst]_0 = 0.023 \text{ mM}$ , $[Acac]_0 = 2.8 \text{ mM}$ , and $[H_2O_2]_0 = 1.76 \text{ mM}$ , in 0.1 M phosphate buffer pH 7.0.....	121
<b>Figure II-10:</b> Kinetics for acrylamide-based hydrogels synthesis by free-radical polymerization via different biocatalysts, in term of: (A) Polymerization yield (%), (B) Particles size (nm) measured by DLS and (C) spectrophotometric monitoring.....	122
<b>Figure II-11:</b> Kinetics for HRP-initiated polymerization of different functional monomers in presence of PDA as cross-linker, in term of: (A) Polymerization yield (%) and (B) Particles size (nm), using $[Monomers]_0 = 57.2 \text{ mmol/l}$ , $[Biocatalyst]_0 = 0.023 \text{ mM}$ , $[Acac]_0 = 2.8 \text{ mM}$ , and $[H_2O_2]_0 = 1.76 \text{ mM}$ , in 0.1 M phosphate buffer pH 7.0.....	123
<b>Figure II-12:</b> Sizes of the particles obtained by HRP-initiated free radical polymerization of different functional and cross-linking monomers, using $[Monomers]_0 = 57.2 \text{ mmol/l}$ , $[HRP]_0 = 0.08 \text{ g/l}$ , $[Acac]_0 = 2.8 \text{ mM}$ , and $[H_2O_2]_0 = 1.76 \text{ mM}$ , in 0.1 M phosphate buffer pH 7.0.....	125
<b>Figure II-13:</b> Sizes of the particles obtained by HRP-initiated free radical polymerization of different functional and cross-linking monomers, using different monomer concentrations.....	126
<b>Figure II-14:</b> Sizes and yields of poly(4-VP/PDA) particles obtained by free radical polymerization initiated with different hydrogen peroxide concentrations, using $[monomers]_0 = 57.2 \text{ mM}$ , $[HRP]_0 = 0.08 \text{ g/L}$ , and $[Acac]_0 = 2.78 \text{ mM}$ .....	128
<b>Figure II-15:</b> 4-VP/PDA particles sizes and yields obtained by free radical polymerization initiated by HRP and different acetylacetone concentrations, using $[monomers]_0 = 57.2 \text{ mmol/L}$ , $[HRP]_0 = 0.08 \text{ g/l}$ , and $[H_2O_2]_0 = 1.76 \text{ mM}$ .....	130

<b>Figure II-16:</b> 4-VP/PDA particle sizes and yields obtained by free radical polymerization initiated by different HRP concentrations, using $[\text{monomers}]_0 = 57.2 \text{ mM}$ , $[\text{Acac}]_0 = 2.8 \text{ mM}$ , and $[\text{H}_2\text{O}_2]_0 = 1.76 \text{ mM}$ .....	132
<b>Figure II-17:</b> 4-VP/PDA particles sizes and yields obtained by free radical polymerization initiated in different buffers using $[\text{monomers}]_0 = 57.2 \text{ mM}$ , $[\text{HRP}]_0 = 0.08 \text{ g/L}$ , $[\text{Acac}]_0 = 2.8 \text{ mM}$ , and $[\text{H}_2\text{O}_2]_0 = 1.76 \text{ mM}$ .....	135
<b>Figure II-18:</b> Particles sizes with their corresponding PDI obtained by different initiations methods for the free radical polymerization of acidic, neutral, and basic monomers cross-linked by PDA.....	137
<b>Figure II-19:</b> HaCat Cells viability for different polymer concentrations of (4-VP/PDA) nanoparticles polymerized by HRP-mediated initiation (green bars), and photochemical initiation with Vazo <sup>®</sup> 56 (blue bars). The errors bars are means of 5 replicates.....	139

### Chapter III

<b>Figure III-1:</b> schematic representation of the detailed protocol for HRP immobilization.....	147
<b>Figure III-2:</b> Calibration curve for Orange Test.....	152
<b>Figure III-3:</b> Amounts of amino groups on the surface of activated glass beads according to different activation and silanization protocols .....	161
<b>Figure III-4:</b> Optimization of the activation step by boiling in 4 M NaOH. (A) Effect of the incubation time on the amino group density. (B) Effect of the increase in amino groups number on the amount of the immobilized HRP. The immobilization reactions were conducted using 2% APTES/toluene for silanization, 2.5 wt% glutaraldehyde for 1 hour, and 2 mg/ml HRP solution for overnight at 25°C.....	162
<b>Figure III-5:</b> Effect of the different silanization protocols on the amino group density on the surface of the glass beads. Activation was by boiling in 4 M NaOH for 2 hours.....	163
<b>Figure III-6:</b> Influence of the glutaraldehyde incubation time on HRP immobilization. The reactions were achieved by boiling the beads for 2 hours in 4 M NaOH and incubation in 2% APTES/toluene overnight. The HRP coupling Step is achieved at 25°C, with an enzyme concentration of 2 mg/ml.....	165
<b>Figure III-7:</b> Influence of the pretreatment with water prior to glutaraldehyde incubation on HRP immobilization. The reactions were achieved by boiling the beads for 2 hours in NaOH 4M, and incubation in 2% APTES/toluene overnight, and by activating in 2.5-wt% glutaraldehyde for 1 hour. The HRP coupling step is achieved at 25°C, with an enzyme concentration of 2 mg/ml.....	167
<b>Figure III-8:</b> Influence of the coupling agent on HRP immobilization. The reactions were carried out by boiling the beads for 2 hours in 4 M NaOH and incubating in 2% APTES/toluene overnight. The HRP coupling step is achieved at 25°C, with an enzyme concentration of 2mg/ml.....	168
<b>Figure III-9:</b> Influence of the incubation temperature on HRP immobilization. The reaction is carried out by boiling the beads for 2 hours in 4 M NaOH, then by incubating successively in 2% APTES/toluene overnight, 2.5-wt% glutaraldehyde for 1 hour, and 2 mg/ml HRP solution.....	170
<b>Figure III-10:</b> Influence of the enzyme concentration on HRP immobilization. The reaction is carried out by boiling the beads for 2 hours in 4 M NaOH, then by incubating successively in 2% APTES/toluene overnight, in 2.5 wt-% glutaraldehyde for 1 hour. The HRP coupling step is done at 25°C.....	171
<b>Figure III-11:</b> SEM images of glass beads (GB) at the different stages of the HRP immobilization protocol: (A): Native GB; (B): GB after activation by 4 M NaOH (C): GB after silanization in APTES/toluene; (D): GB after activation via glutaraldehyde; (D): GB after coupling of HRP.....	173
<b>Figure III-12:</b> Residual enzyme activity of free and immobilized HRP in hydro-organic solvents according to the percentage of organic solvents in 50 mM sodium phosphate buffer (pH 7.0). The remaining activities (%) refers to the percentages of the initial reaction rates obtained for the free and immobilized HRP measured	



<i>directly upon dissolving the free HRP in buffer, and directly upon immobilization and washing of the glass beads.....</i>	<i>175</i>
<b>Figure III-13:</b> Storage stabilities of free and immobilized HRP in 50 mM phosphate buffer pH 7.0. The remaining activity (%) refers to the percentages of the initial reaction rates obtained for the free and immobilized HRP measured directly after dissolving the free HRP in buffer, and directly after immobilization and washing of the glass beads.....	<i>176</i>
<b>Figure III-14:</b> 3D representation of response surfaces for the polymerization yield according to total monomers (%) concentrations and the Acac amount (mmol).....	<i>181</i>
<b>Figure III-15:</b> 3D representation of response surfaces for the particles size according to different parameters: (A) H <sub>2</sub> O <sub>2</sub> and Acac; (B) H <sub>2</sub> O <sub>2</sub> and [Monomers]; (C) [Monomers] and Acac .....	<i>183</i>
<b>Figure III-16:</b> Prediction profile of the optimum experimental conditions in order to obtain small-sized hydrogel with high polymerization yield.....	<i>184</i>
<b>Figure III-17:</b> Particles size of the poly(4-VP/PDA) hydrogel synthesized by the optimal synthesis protocol predicted by the desirability function .....	<i>186</i>
<b>Figure III-18:</b> Sodium dodecyl sulfate gel electrophoresis (SDS-PAGE) under reducing conditions of hydrogels. Lane 1: molecular weight markers (10000-250000 Da), Lane 2: commercial pure HRP (2 µg), Lane 3: commercial pure HRP (10 ng), Lane 5: Hydrogel solution (5 mg), Lane 7: Hydrogel solution (10 mg).....	<i>187</i>

## Chapter IV

<b>Figure IV-1:</b> Schematic representation of HRP immobilization and the synthesis of molecularly imprinted nanoparticles by immobilized HRP-initiated free-radical polymerization. (1): preparation of the solid carrier by activation in 4 M NaOH solution at 100°C for 2 hours, (2): silanization step with (3-Aminopropyl)triethoxysilane solution prepared in toluene at 2% (v/v), (3): glass beads activation via glutaraldehyde 2.5% (v/v, in 50 mM sodium phosphate buffer pH 7.0), (4): coupling of HRP on activated glass beads by 2 mg/ml HRP solution (prepared in the same buffer).....	<i>196</i>
<b>Figure IV-2:</b> Calibration curve of trypsin between 20 and 120 nM in 50 mM Tris-HCl pH 8.0.....	<i>205</i>
<b>Figure IV-3:</b> Effect of the acetylacetone (Acac) initial concentrations on the 2,4-D binding on MIPs and NIP synthesized via HRP-catalysis : (A) 0.9 mM; (B) 1.4 mM; (C) 2.1 mM; (D) 2.8 mM. The synthesis was achieved by using [HRP] <sub>0</sub> = 0.08 g/l, and [H <sub>2</sub> O <sub>2</sub> ] <sub>0</sub> = 0.88 mM. The binding tests are carried out by radioactive assays, in 20 mM pH 7.0 sodium phosphate buffer + 0.1% triton X-100 using [ <sup>14</sup> C]-2,4-D (0.04 nmol, 2 nCi).....	<i>208</i>
<b>Figure IV-4:</b> Effect of the HRP concentrations (from 0.04 g/l to 0.4 g/l) on the binding isotherms of MIPs and NIP synthesized via HRP-catalysis in 20 mM pH 7.0 sodium phosphate buffer + 0.1% triton X-100 using [ <sup>14</sup> C]-2,4-D (0.04 nmol, 2nCi), [Acac] <sub>0</sub> = 1.4 mM, and [H <sub>2</sub> O <sub>2</sub> ] <sub>0</sub> = 0.88 mM.....	<i>211</i>
<b>Figure IV-5:</b> Effect of polymerization media on the 2,4-D binding by MIPs and NIP synthesized via HRP-initiated free radical polymerization in water (left) or in 20 mM phosphate buffer pH 7.0 (right). The radioligand binding assays were performed in 20 mM sodium phosphate buffer pH 7.0 + 0.1% triton X-100 with [ <sup>14</sup> C]-2,4-D (0.04 nmol, 2nCi).....	<i>212</i>
<b>Figure IV-6:</b> SEM images of the MIPs (left) and NIPs (right) synthesized by HRP-mediated initiation of free radical polymerization .....	<i>214</i>
<b>Figure IV-7:</b> SEM images of the MIPs (left) and NIPs (right) synthesized by U.V-initiated free radical polymerization.....	<i>214</i>
<b>Figure IV-8:</b> Comparison of the binding isotherms of the MIPs and NIPs synthesized by free radical polymerization initiated by enzyme-catalysis (left) or UV (right), using 4-VP and PDA as functional and cross-	

linking monomers at 2%. The tests are performed by radioactivity binding assays in 20 mM sodium phosphate buffer pH 7.0 + 0.1% triton X-100 using [ <sup>14</sup> C]-2,4-D (0.04 nmol, 2nCi).....	215
<b>Figure IV-9:</b> Comparison of the binding for MIPs and NIPs synthesized by free radical polymerization initiated by enzyme-catalysis (left) or UV (right), using 4-VP and EbAAm as functional and cross-linking monomers at 1% total concentration. The binding tests were performed by radioligand binding assays in 20 mM sodium phosphate buffer pH 7.0 + 0.1% triton X-100 with [ <sup>14</sup> C]-2,4-D (0.04 nmol, 2nCi).....	216
<b>Figure IV-10:</b> Langmuir isotherms of the MIPs synthesized by free radical polymerization initiated by enzyme-catalysis (left) or U.V (right), using 4-VP and PDA as functional and cross-linking monomers at 2%. The binding tests are performed by radioactive binding assays in 20 mM pH 7.0 sodium phosphate buffer + 0.1% triton X-100 using [ <sup>14</sup> C]-2,4-D (0.04 nmol, 2nCi) and increasing concentrations of cold 2,4-D.....	217
<b>Figure IV-11:</b> Displacement of [ <sup>14</sup> C]-2,4-dichlorophenoxyacetic (0.04nmol, 2nCi) , binding to (A) enzyme-mediated synthesized MIPs and to (B) photochemically synthesized MIPs (right), by increasing concentrations of competing ligands, in 20mM sodium phosphate buffer pH 7.0 +0.1% triton X-100. Chemical structures of the corresponding competitors are drawn below.....	219
<b>Figure IV-12:</b> Equilibrium binding isotherms in 20 mM acetate phosphate buffer, pH 6.0 with 10 nmol SA, on MIP (full symbols) and NIP (open symbols) nanoparticles that have been prepared through: (A) HRP-catalysis, (B) UV-initiation.....	220
<b>Figure IV-13:</b> Chemical structure of the anchoring N-acryloyol-p-aminobenzamidine.HCl monomer (AB)...	221
<b>Figure IV-14:</b> Equilibrium binding isotherms of MIP and NIP nanoparticles for trypsin (0.6 nmol) in 5 mM Tris-HCl buffer pH 8.0 + 10 mM CaCl <sub>2</sub> , in: (A) the presence of the anchoring monomer AB, and (B) the absence of AB in the polymer formulation. Polymerization was initiated by HRP.....	222
<b>Figure IV-15:</b> 2,4-D radioactive binding assays in 20 mM pH 7.0 sodium phosphate buffer + 0.1% triton X-100 with [ <sup>14</sup> C]-2,4-D (0.04 nmol, 2nCi) for MIPs/NIPs prepared by immobilized HRP catalysis in: (A) different molar ratios of [Acac]/[Monomers], (B): different total monomers concentrations.....	225
<b>Figure IV-16:</b> Equilibrium binding isotherms using [ <sup>14</sup> C]-2,4-D (0.04 nmol, 2 nCi), in 20 mM sodium phosphate buffer pH 7.0 + 0.1% triton X-100 for MIP (filled symbols) and NIP (open symbols) nanoparticles prepared with immobilized HRP catalysis. Data points are means from three independent experiments with three different polymer batches issued from different HRP immobilizations.....	226
<b>Figure IV-17:</b> Displacement of [ <sup>14</sup> C]-2,4-D (0.04 nmol, 2nCi) binding to 1.5 mg of MIP, by increasing concentrations of competing ligands, in 20 mM pH 7.0 sodium phosphate buffer + 0.1% triton X-100. B/B0 is the ratio of the amounts of radioactive 2,4-D bound in the presence and absence of displacing ligand.....	227
<b>Figure IV-18:</b> (A): DLS measurement of particle sizes for MIP and NIP obtained in every cycle of free radical polymerization catalyzed by the same immobilized HRP. (B): Binding assays using [ <sup>14</sup> C]-2,4-D (0.04 nmol, 2 nCi) for MIP and NIP nanoparticles (1 mg/ml) synthesized in every cycle by immobilized HRP-mediated FRP in 20 mM pH 7.0 sodium phosphate buffer + 0.1% triton X-100.0 Data are mean values from three different batches of polymers synthesized within 3 separate HRP immobilizations.....	228
<b>Figure IV- 19:</b> Particles sizes, measured by STEM, upon washing and drying, of the MIP (left) and NIP (right) nanoparticles synthesized by free radical polymerization catalyzed by the reusable HRP immobilized on glass beads in every cycle.....	230

## List of tables

### Chapter I

<b>Table I-1:</b> Classification of the polymerization types, the enzymes that are incorporated in their catalysis, as well as the typical polymers synthesized. Modified from [1,9,14] .....	8
<b>Table I-2:</b> Polyphenols polymerized for improved antioxidant activity .....	22
<b>Table I-3:</b> Common substrates for horseradish peroxidase. [108] .....	32
<b>Table I-4:</b> Summary for water-compatible MIPs applied as analytical devices .....	67

### Chapter II

<b>Table II-1:</b> Chemical structure and molecular weight of functional monomers used in this study .....	102
<b>Table II-2:</b> Chemical structure and molecular weight of cross-linking monomers used in this study .....	103
<b>Table II-3:</b> Linear polymerization assays of acrylamide by free radical polymerization initiated by different catalysts .....	110
<b>Table II-4:</b> Yields and average molecular weights of linear polyacrylamides synthesized by enzyme-mediated initiation of free-radical polymerization, through different biocatalysts .....	113
<b>Table II-5:</b> Yields of linear polymers based on neutral and basic monomers by free-radical polymerization initiated by enzyme-mediation .....	114
<b>Table II-6:</b> Polymerization yields obtained with different functional monomers and PDA as cross-linker, initiated by different biocatalysts, using $[\text{Monomers}]_0 = 57.2 \text{ mmol/l}$ , $[\text{Biocatalyst}]_0 = 0.023 \text{ mM}$ , $[\text{Acac}]_0 = 2.8 \text{ mM}$ , and $[\text{H}_2\text{O}_2]_0 = 1.76 \text{ mM}$ , in $0.1 \text{ M}$ phosphate buffer pH 7.0. ....	119
<b>Table II-7:</b> Yield of the particles based on various functional and cross-linking monomers by HRP-mediated free-radical polymerization using $[\text{monomers}]_0 = 57.2 \text{ mmol/l}$ , $[\text{H}_2\text{O}_2]_0 = 1.76 \text{ mM}$ , $[\text{Acac}]_0 = 2.78 \text{ mM}$ , and $[\text{HRP}]_0 = 0.08 \text{ g/l}$ , in $0.1 \text{ M}$ phosphate buffer pH 7.0 .....	125
<b>Table II-8:</b> Hydrogels yields based on various functional monomers in different monomers concentrations by HRP-mediated free-radical polymerization. ....	126
<b>Table II-9:</b> yield of the 4-VP/PDA particles with different HRP and hydrogen peroxide initial concentrations ( $[\text{Monomers}]_0 = 57.2 \text{ mM}$ , and $[\text{Acac}]_0 = 2.78 \text{ mM}$ ) .....	133
<b>Table II-10:</b> Polymerization yields obtained by free radical polymerization, in water or in $0.1 \text{ M}$ PB pH 7.0, using $[\text{Monomers}]_0 = 57.2 \text{ mM}$ , $[\text{HRP}]_0 = 0.08 \text{ g/l}$ , $[\text{Acac}]_0 = 2.8 \text{ mM}$ , and $[\text{H}_2\text{O}_2]_0 = 1.76 \text{ mM}$ .....	134
<b>Table II-11:</b> Polymerization yields for polymer based on acidic, neutral, and basic functional monomers, synthesized by free-radical polymerization initiated by enzyme catalysis, redox chemical and photochemical initiation. ....	137

### Chapter III

<b>Table III-1:</b> The chemical structure of the chemicals used in this study for activation and coupling steps.....	149
<b>Table III-2:</b> Four-parameter Doelhart matrix showing the number of experiments and the factors.....	156
<b>Table III-3:</b> Four-parameter Doelhart matrix showing the number of experiments, the real values of the factors and the responses values obtained for 22 runs of hydrogels synthesis by immobilized HRP-mediated initiation of free-radical polymerization.....	179
<b>Table III-4:</b> Sorted parameter estimates of the polymerization yield (%), where X1= amount of glass beads, X2= [Monomers], X3= amount of acetylacetone, X4= amount of H <sub>2</sub> O <sub>2</sub> .....	180
<b>Table III-5:</b> Sorted parameter estimates of the particles size (nm), where X1= amount of glass beads, X2= [Monomers], X3=amount of acetylacetone, X4=amount of H <sub>2</sub> O <sub>2</sub> .....	182
<b>Table III-6:</b> coded and real values of the factors in the optimal protocol in the Doelhart experimental design.....	185
<b>Table III-7:</b> Comparison of the predicted values in the Doelhart's experimental design and the real experimental ones for the particles sizes (nm) and the polymerization yield (%) in HRP-mediated synthesis of hydrogels.....	185
<b>Table III-8:</b> Experimental conditions and polymer characteristics for the hydrogels synthesized by free and immobilized HRP-initiated polymerization via an enzymatic catalytic activity of 3*10 <sup>-6</sup> mol/min in the polymerization medium.....	188

### Chapter IV

<b>Table VI-1:</b> Particles sizes and polymerization yields of the MIP/NIP polymers according to different acetylacetone initial concentrations.....	207
<b>Table IV-2:</b> Q <sub>max</sub> and K <sub>50</sub> of MIPs synthesized via HRP-catalysis by different acetylacetone (Acac) initial concentrations.....	209
<b>Table IV-3:</b> Yields and imprinting factors for the MIPs and NIPs synthesized according to different molar ratios of [Acac]/[Monomer] and [Acac]/[H <sub>2</sub> O <sub>2</sub> ].....	209
<b>Table IV-4:</b> Particles sizes and polymerization yields of the MIP/NIP polymers according to different HRP initial concentrations.....	210
<b>Table IV-5:</b> Q <sub>max</sub> , K <sub>50</sub> and imprinting factors of the different MIPs synthesized via HRP-catalysis by different HRP initial concentrations.....	211
<b>Table IV-6:</b> Maximum capacities and dissociation constants of the MIPs synthesized via different initiation methods.....	217
<b>Table IV-7:</b> Parameters of cross-reactivity for MIP of enzymatic and photochemical initiations.....	218
<b>Table IV-8:</b> Particles sizes and polymerization yields of the MIP/NIP polymers according to the initiation way of free-radical polymerization.....	222
<b>Table IV-9:</b> Influence of total monomers concentrations and the acetylacetone concentration on the characteristics of MIP-NPs synthesized by immobilized-HRP catalyzed free radical polymerization.....	224
<b>Table IV-10:</b> Polymerization yields (mg) for the MIPs and NIPs in every cycle.....	228



## Abbreviations

<b>2,4-D</b> : 2,4-Dichlorophenoxyacetic acid	<b>FRP</b> : Free radical polymerization
<b>4-VP</b> : 4-Vinylpyridine	<b>FT-IR</b> : Fourier Transform Infrared spectroscopy
<b>AA</b> : Acrylic acid	<b>GACs</b> : Glycosamines
<b>Aam</b> : Acrylamide	<b>GB</b> : Glass beads
<b>AB</b> : <i>N</i> -acryloyl- <i>p</i> -aminobenzamidine.HCl	<b>GOx</b> : Glucose oxidase
<b>ABTS</b> : 2,2'-azino-bis(3-ethylbenzothiazoline-6-sulfinoc acid)	<b>GPC</b> : Gel Permeation Chromatography
<b>Acac</b> : Acetylacetone	<b>H<sub>2</sub>O</b> : water molecule
<b>ACN</b> : Acetonitrile	<b>H<sub>2</sub>O<sub>2</sub></b> : Hydrogen peroxide
<b>APTES</b> : (3-aminopropyl)triethoxusilane	<b>Hb</b> : Hemoglobin
<b>ATRP</b> : Atom transfer radical polymerization	<b>HCl</b> : Hydrogen chloride
<b>AuNPs</b> : gold nanoparticles	<b>HEC</b> : Hydroxyethyl cellulose
<b>BS<sub>3</sub></b> : Bis(sulfosuccimidyl) suberate	<b>HEMA</b> : 2-Hydroxyethyl methacrylate
<b>BSA</b> : Bovin serum albumin	<b>HMDI</b> : Hexamethyl diisocyanate
<b>CEA</b> : carboxyethyl acrylate	<b>HNO<sub>3</sub></b> : Nitric acid
<b>CPOAc</b> : chlorophenoxyacetic acid	<b>HRP</b> : Horseradish peroxidase
<b>Cyt <i>c</i></b> : Cytochrome <i>c</i>	<b>KPS</b> : Potassium persulfate
<b>DEAEM</b> : 2-(diethylamino)ethyl methacrylate	<b>MAA</b> : methacrylic acid
<b>DLS</b> : Dynamic light scattering	<b>MeAam</b> : Methacrylamide
<b>DMF</b> : Dimethylformamide	<b>MeBAam</b> : <i>N,N'</i> -methylenebis(acrylamide)
<b>DMSO</b> : Dimethyl sulfoxide	<b>MeOH</b> : Methanol
<b>EBAam</b> : <i>N,N'</i> -ethylenebis(acrylamide)	<b>MIP</b> : Molecularly imprinted polymers

---

<b>Myo:</b> Myoglobin	<b>PNIPAm:</b> poly( <i>N</i> -isopropyl acrylamide)
<b>NaOH:</b> Sodium hydroxide	<b>QCM:</b> Quartz cristal microbalance
<b>NIP:</b> Non-imprinted polymers	<b>RAFT:</b> Reversible addition-fragmentation
<b>NIPAm:</b> <i>N</i> -isopropyl acrylamide	<b>ROP:</b> Ring-opening polymerization
<b>PDA:</b> 1,4-Bis(acryloyl)piperazine	<b>SA:</b> Salicylic acid
<b>PDI:</b> Polydispersity Index	<b>SBP:</b> Soybean peroxidase
<b>PET:</b> Polyethylene terephthalate	<b>SEM:</b> Scanning electron microscopy
<b>pH:</b> power of hydrogen	<b>STEM:</b> Scanning transmission electron microscopy
<b>Ph-AcOH:</b> phenoxyacetic acid	
<b>Phenyl TMS:</b> 1-phenyl-2-trimethylsilylacetylene	
<b>TAME:</b> <i>N</i> $\alpha$ - <i>p</i> -tosyl-L-arginine-methyl ester hydrochloride	
<b>TEM:</b> Transition electron microscopy	
<b>TEMED:</b> Tetramethylethylenediamine	
<b>THF:</b> Tetrahydrofuran	
<b>TSAS:</b> transition-state analog substrate	
<b>Vazo<sup>®</sup> 56:</b> 2,2'-Azobis(2-amidinopropane) dichloride	
<b><math>\beta</math>-CF:</b> $\beta$ -Cellobiosyl fluoride	

## Abstract in English

### **Enzymatically initiated synthesis of biomimetic receptors based on molecularly imprinted polymers by free radical polymerization**

**Keywords:** *molecularly imprinted polymers, water-compatible nanoparticles, free radical polymerization, enzymatic catalysis, horseradish peroxidase*

Enzyme-catalyzed synthesis of natural and synthetic polymers has been developed since several decades, as an eco-friendly process. Compared to the conventional methods, enzymes offer high selectivity, ability to operate under mild conditions and to recycle the catalyst. On the other hand, molecularly imprinted polymers (MIPs) are synthetic materials with specific recognition properties for target molecules. They have recently attracted increasing attention in environmental and newly in biomedical applications for their specificity and selectivity. However, concerns about MIP toxicity for human and environment safety are of great importance. Herein, carrying forward the concept of green chemistry, an enzyme-mediated synthesis approach is described to prepare molecularly imprinted nanoparticles (MIP-NPs) in aqueous media. Horseradish peroxidase (HRP) is used to initiate the polymerization of methacrylate-based monomers and cross-linkers by catalyzing the generation of free radicals. Different hydrogels are synthesized and characterized. “Greener” hydrogels are obtained with lower cytotoxicity than that of polymers synthesized by traditional way. The hydrogels synthesis is optimized in order to control the particles sizes and polymerization yields. Moreover, water-compatible MIP nanoparticles for the recognition of different small molecules and proteins are prepared in aqueous media by HRP-initiated free radical polymerization and compared to MIPs prepared by the thermal or photopolymerization methods. HRP immobilization is also performed for hydrogels synthesis as well as MIP preparation. The reusability of immobilized enzyme is investigated for the preparation of several MIP batches with the same morphology, yield as well as good specificity and selectivity. We believe that this new synthesis method for MIPs will provide new opportunities to enlarge the use of molecular imprinting technology in biomedical and environmental applications.



## Résumé en Français

### **Synthèse de récepteurs biomimétiques basés sur les polymères à empreintes moléculaires par polymérisation radicalaire libre initiée par catalyse enzymatique**

*Mots-clés : polymères à empreintes moléculaires, hydrogel, polymérisation radicalaire libre, catalyse enzymatique, peroxydase de raifort*

Depuis de nombreuses années, l'utilisation d'enzyme pour la synthèse de polymères naturels ou synthétiques a largement été développée en tant que procédé alternatif plus vert et plus respectueux de l'environnement. En effet, comparée aux méthodes conventionnelles de synthèse, les enzymes offrent une sélectivité élevée, une capacité à réagir dans des conditions de réaction douces, ainsi que la possibilité de recyclage du biocatalyseur. D'autre part, les polymères à empreintes moléculaires (MIPs) sont des matériaux synthétiques avec des propriétés de reconnaissance moléculaire spécifique envers une molécule cible. Récemment, les MIPs ont été utilisés dans les applications environnementales et biomédicales de part leur propriétés de reconnaissance moléculaire, leur spécificité et sélectivité. Cependant, leur application reste limitée en raison de leur faible biocompatibilité et de la présence de résidu de polymérisation potentiellement nocif. Ce travail de thèse a pour objectif de proposer une méthode alternative pour la synthèse de MIPs basée sur le concept de chimie verte. La peroxydase de raifort (HRP) est utilisée pour initier la co-polymérisation en milieux aqueux de monomères fonctionnels méthacrylates et d'agents réticulants en catalysant la génération des radicaux libres. Différents hydrogels ont été synthétisés et caractérisés, en particulier une cytotoxicité plus faible a été obtenue comparée à celle des polymères synthétisés traditionnellement. La synthèse a été optimisée afin de pouvoir contrôler la taille des particules et le rendement de polymérisation. Des MIPs sous forme de nanoparticules ont été préparés en milieu aqueux pour plusieurs molécules de faible poids moléculaire ainsi que pour des protéines par polymérisation radicalaire libre initiée par HRP. L'effet de la méthode d'initiation a été évalué en comparant les propriétés de ces MIPs à ceux préparés par les méthodes traditionnellement. L'immobilisation de l'HRP a été aussi effectuée pour synthétiser des hydrogels et des MIPs. L'enzyme immobilisée a pu être réutilisée pour synthétiser des MIPs avec les mêmes performances en termes de morphologie, rendement, spécificité et sélectivité. Ces nouveaux matériaux offrent de nombreuses perspectives pour des applications environnementales et biomédicales.



## Introduction

Polymers, as natural and synthetic materials, are widely used in industry as well as in people's daily life, such as pharmacy, cosmetics, packaging, and many more applications. Functional polymers have received considerable attention in Polymer Science for their advanced chemical, physical and biological properties, which are highly required in specific and sophisticated areas such as nanotechnology and medicine. For polymer preparation, today's synthetic techniques allow a much better control of the polymers' structure, architecture, functionality, molar mass and dispersity, and hence allow the tailoring of chemically and mechanically stable polymers according to the needs of a specific application. However, such materials are not necessarily biodegradable or biocompatible, thus they present a certain toxicity from an ecological or environmental point of view. In this context, green or sustainable chemistry has emerged as an innovative set of principles to manufacture products by eliminating or reducing the use or generation of hazardous substances. Benign design criteria of green chemistry had provided a framework for scientists to use when preparing new materials, products and systems as solutions to a wide range of problems. Green chemistry is then making significant contributions in the drive toward sustainability for the simultaneous benefit of the environment, economy and society.

During 1980s and 1990s, many researches have been focusing on the development of greener functional polymers. In response to the increasing needs of such polymers regarding commercial and ecological requirements, new approaches have been developed by using renewable resources or even biocompatible and biodegradable components or catalysts. Enzymes have become increasingly attractive for the development of more efficient and cleaner chemical processes in polymers synthesis. Compared to traditional chemical synthesis, higher specificity and selectivity, as well as the use of mild reaction conditions such as temperature, pH and solvents

---

gives in general an excellent green profile to reactions catalyzed by enzymes. Biocatalysts have thus been used to prepare a wide range of natural and synthetic materials.

One example of functional polymers are molecularly imprinted polymers (MIPs). The concept of molecular imprinting was firstly established by Wulff and Mosbach. Robust molecular recognition elements were achieved by introducing specific recognition properties into polymers that are able to specifically interact with a given target molecule. MIPs are therefore referred to as plastic antibodies. The antibody-like ability to bind and discriminate between molecules or other structures is due to the binding sites within the polymeric cavities that are complementary to the template or to analogous structures in size, shape and position of the functional groups. Recently, much effort has been directed towards the preparation of uniformly sized MIPs at the nanometer scale, leading to new polymers with superior properties for example in biomedical applications. However, the use of MIPs in biocompatible applications such as environmental and drug delivery fields remains very challenging since biodegradable and non-toxic polymeric building blocks are highly required.

Recognizing the potential of molecularly imprinted nanoparticles in the environmental and biomedical fields, the multidisciplinary research project, BIOMIP, has been funded in 2013 by the Regional Council of Picardy in order to propose more eco-friendly and biocompatibility materials. This project aimed to develop advanced biosynthesized, biocompatible and biodegradable molecularly imprinted polymers. My Ph.D. thesis was carried out in the context of the “BIOMIP” project, in the Institute of Enzyme and Cell Engineering at Université de Technologie de Compiègne, in co-tutelle with the Lebanese University. It was co-funded by the FP7 CHEBANA-Marie Curie Network, and AZM and SAADE.

**The objective of this thesis** was the synthesis in aqueous solvents of water-compatible molecularly imprinted polymers based on a new method using an immobilized enzymatic initiator system, instead of the thermal or photochemical initiation methods traditionally used in free radical polymerization. This may help to promote the application of MIPs in environmental and biomedical fields, Horseradish peroxidase was the biocatalyst of choice in this study. The goals involved not only the study of imprinted hydrogels synthesis by using free enzyme as the biocatalyst, but also the immobilization of the enzyme on solid carrier and its application for the



---

catalyzed MIP synthesis. The MIPs recognition ability was optimized towards small molecules and proteins.

This Ph.D. manuscript is divided into four chapters:

**Chapter I** offers a literature overview on the enzymatic polymerization, with emphasis on the different kinds of polymers accessible, and the enzymes involved in the polymerization processes. The second part of this chapter is dedicated to MIPs and their applications, and to the remaining challenges in the molecular imprinting field. Special attention is been paid to molecular imprinting in aqueous media for small molecules as well as biomacromolecules.

**Chapter II** describes and discusses experimental work on the enzyme-mediated synthesis of hydrogels. Since hydrogels have become very popular and are widely used in biomedical application, it is interesting to develop a new green approach for their synthesis. The effect of each compound in the enzymatic initiation system, including the nature of biocatalyst, on the efficiency of the polymerization and the polymer characteristics was investigated. Optimal experimental conditions for nanoparticles synthesis were determined and applied for the polymerization of a wide range of functional and cross-linking monomers. Nanoparticles resulting from the enzymatic polymerization are compared to those obtained by traditional ways of polymerizations.

**Chapter III** describes and discusses experimental work on enzyme immobilization on glass beads, followed by polymerization in order to obtain hydrogels without any radical source. The different steps of the immobilization were optimized and characterized. The immobilized enzyme-catalyzed synthesis of nanoparticles was investigated in terms of polymerization efficiency and particle size using an experimental design approach to study the effect of the enzymatic system and the polymer formulation and to determine the optimal conditions for nanoparticle synthesis.

**Chapter IV** is dedicated to the production of green MIPs by enzyme-catalyzed free radical polymerization. MIPs specific for two small molecules and the protein trypsin were synthesized by using either the free or the immobilized enzyme as biocatalyst for enzymatically initiated free radical polymerization. The polymer morphology and the molecular recognition properties of the MIPs are compared to those of traditionally synthesized MIPs. The reusability of the immobilized enzyme for subsequent MIPs synthesis of different batches was also examined in this chapter.

## *Chapter I*

### *Literature Review*

## I.1. Enzymatic polymer synthesis

Since the first discovery of the diastase enzyme (amylase) by A. Payen *et al.* (1833), researchers have put great efforts on finding new enzymes and new enzymatic reactions for their wide applications in many products of daily use (food, cleaning products) as well as in advanced technology (industrial applications) [1]. In fact, the application of enzymes in food technology had been known for centuries, primarily in the production of alcoholic drinks such as beer and wine. Indeed, the term *enzyme* itself comes from Greek, *en* and *zýmē*, which means “in yeast”. It was used by Wilhelm Friedrich Kühne in 1867 to describe the process of fermentation within the yeasts. At first, all ferments and other biocatalysts were combined in one group [2]. It was only in the early 20<sup>th</sup> century that Fisher first introduced the theory of “key and lock”, to describe the relation between the enzyme and a natural substrate [3]. Later, a second fundamental characteristic was proposed by Pauling: an enzymatic reaction progresses under mild conditions, as the activation energy is much lowered by a stabilized enzyme-substrate complex [4, 5]. Since then, enzymes are known as a specialized group of proteins that catalyze metabolic reactions within living organisms.

Nowadays, enzymes are classified into six main groups, according to the Enzyme Commission (EC): oxidoreductases (EC 1), transferases (EC 2), hydrolases (EC 3), lyases (EC 4), isomerases (EC 5), and ligases (EC 6) [6].

Enzymes were established over the last decades as biocatalysts in a wide range of fields such as biochemistry, organic chemistry, medicinal chemistry, pharmaceutical chemistry, and polymer chemistry, due to their excellent features, such as efficiency, selectivity, and specificity. **Figure I-1** shows for example the wide application of enzymes in materials science [2, 7, 8]. They constitute an emerging area and a very promising technology in white biotechnology due to their wide distribution among living organisms and their multiple physiological roles [9, 10].

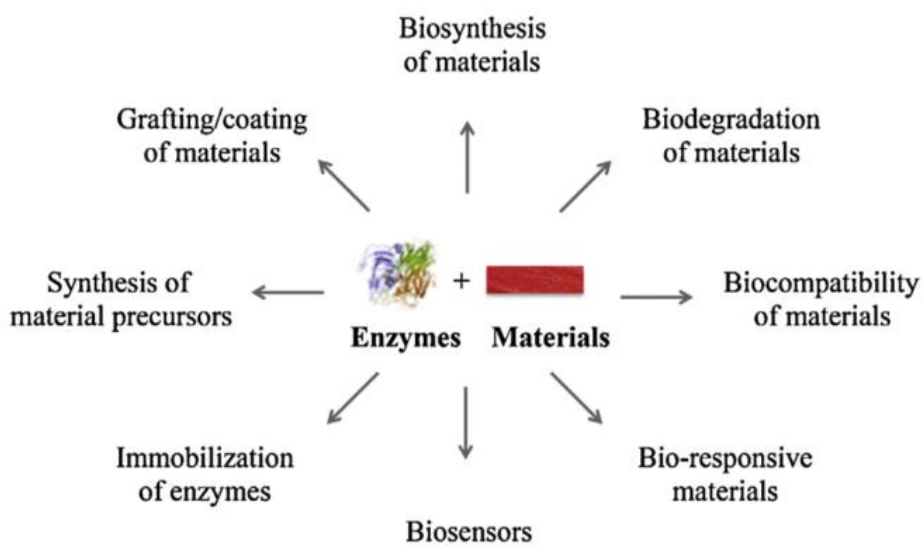


**Figure I-1: Enzyme applications in Materials Science. [2]**

As shown, enzymes have been used in the biosynthesis of materials in order to enhance their biocompatibility. In general, polymers are large molecules, built up in a repetition of many identical, similar, or complementary subunits, known as monomers. Natural polymers are harvested from living organisms. They include DNA (polynucleotides), proteins (polypeptides), polysaccharides, polyesters etc...They are constantly produced for organism survival by complex metabolic pathways involving *in vivo* enzyme-catalyzed reactions.

The *in vitro* enzyme-catalyzed polymerization of natural and synthetic polymers was introduced three decades ago. This polymerization using renewable resource is an eco-friendly alternative to the conventional methods traditionally involving harsh experimental conditions and much energy. Accordingly, it provides a great opportunity to green chemistry [1, 9, 11-13]. Polymer synthesis involving enzymes in the process was extensively investigated [1]. They have been applied either directly for the polymerization of monomers or for the modification of polymer to introduce specific functionality or properties. As shown in **Table I-1**, enzymes are able to catalyze different polymerizations methods leading to typical polymers. This review discusses, in detail, the *in vitro* enzymatic catalysis for both polymerization and modification of natural and synthetic polymers. Special attention is given to enzyme-catalyzed radical polymerization since it is the method of interest in MIP synthesis through this work. Enzymes that are implicated in

the catalysis are studied with emphasis on their catalytic mechanisms. The effect of different experimental conditions on the final polymers is also highlighted. Finally, the potential applications of the enzymatic polymerization are reviewed.

**Table I-1: Classification of the polymerization types, the enzymes that are incorporated in their catalysis, as well as the typical polymers synthesized. Modified from [1, 9, 14].**

Polymerization type	Enzyme	Polymer
Polycondensation	Glycosidases (cellulase, amylase)	Polysaccharides (cellulose, xylan, amylose)
	Lipases	Aliphatic polyesters
Ring-Opening Polymerization	Glycosidases (chitinase, hyaluronidase)	Polysaccharides (chitin, hyaluronan)
	Lipases	Polyesters (lactones, polythioesters)
Radical polymerization	Peroxidases, laccases, oxidase, lipoxygenases	Polyaromatics, Vinyl polymers (polyacrylates and polystyrenes)
Polymer modification	Cellulase, peroxidase, laccase, protease, lipase	Cellulose, dextran conjugates, lignin

### I.1.1. Polymer synthesis by enzyme-mediated polymerization

Enzymatic polymerization is referred to as *in vitro* polymerization of artificial substrate monomers catalyzed by an isolated enzyme via a non metabolic pathway. Actually, it is now proven an efficient method of synthesizing various polymers under a wide range of experimental conditions. In literature, the major target macromolecules formed via the enzymatic polymerizations are polysaccharides, polyesters, polyaromatics and vinyl polymers. The following part describes in detail the synthesis of these polymers with emphasis on the enzymes implicated in the processes [1, 9, 12, 15].

### I.1.1.1. Synthesis of Polysaccharides

Polysaccharides form with nucleic acids (DNA, RNA) and proteins, the three classes of natural biopolymers found in living organisms. As a source of energy, they are essential biomacromolecules to ensure the survival of the body. Polysaccharides are polymeric carbohydrate molecules composed of long chains of monosaccharide units bound together by glycosidic linkages. They are formed *in vivo* by repeated glycosylations between a donor sugar and a acceptor sugar. Polysaccharides are well-known for their broad range and complexity of structures, not only because of the wide variety of monosaccharides, but also of the many different stereo and regio types of the glycosidic linkages. The stereoselectivity is due to  $\alpha$ - and  $\beta$ - isomers, while regioselectivity is due to possible glycosidic linkages between the donor's anomeric carbon and the different hydroxyl groups in the acceptor [1, 16-18].

Due to the polysaccharides' importance in many fields such as their use as drugs or as advanced materials in technology, there is a high demand for efficient synthetic protocols for their preparation [18, 19]. There has been great progress in their *in vitro* chemical synthesis during the last decades but much remains to be achieved. The difficulty resides mainly in the control of the stereochemistry of the anomeric carbon and the regioselectivity of the many hydroxyl groups [1, 16, 17]. Enzyme catalysis of polysaccharides offers thus many advantages over the chemical synthesis. It shows high reaction control from a regio and stereoselectivity point of view, and may rely on renewable resources and catalyst recycling [1, 9, 12, 15, 20].

For enzymatic polymerization, two classes of enzymes are predominately applied: hydrolases [21] and glycosyltransferases [22]. Indeed, the *in vivo*, biosynthetic pathway involves the formation of glycoside linkages catalyzed by glycosyltransferases. However, these enzymes are unstable, difficult to isolate and purify, and thus expensive. Therefore, since the 1980s, the *in vitro* synthesis of polysaccharides has been then performed with glycoside hydrolases (EC 3.2.1) as biocatalyst [1, 12, 17, 23]. For enzymatic polymerization, synthetic monomers should be designed according to a "transition-state analog substrate" (TSAS), leading to chemical structure close to that of *in vivo* enzymatic reactions. In that way, they readily form an enzyme-substrate complex and the reaction is induced to give the product as shown in **Figure I-2**.

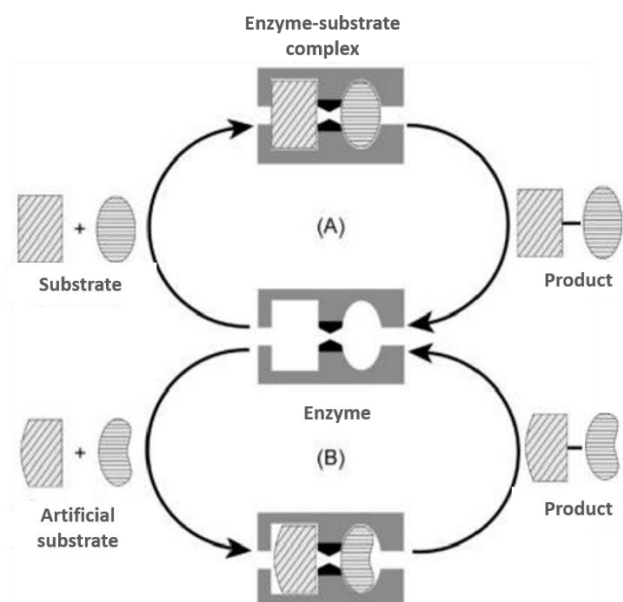


**Figure I-2: Enzyme-substrate relationship for enzymatic reactions: (A) an in vivo reaction obeying the “key and lock” theory and (B) an in vitro reaction involving an enzyme-artificial substrate complex leading to a product with bond formation, where the artificial substrate desirably possesses a close structure of the natural substrate at the active site vicinity. The black part in the enzyme indicates the active site. Reprinted from [1, 24].**

The anomeric carbon of the glycosidic monomer is activated by introducing a fluorine or an oxaline group (**Figure I-3**), which have structures close to TSAS resulting in an efficiently formation of the enzyme-substrates complexes. Following this principle, two types of monomers, efficiently recognized by hydrolases, have been synthesized in the literature : glycosyl fluorides [25] and sugar oxazolines [26]. According to the monomer, the hydrolase catalysis involved in glycosidic polymerization followed two different pathways. For glycosyl fluoride monomers, cellulose and its derivatives, xylan and related unnatural polysaccharides are synthesized by polycondensation. When sugar oxazoline monomers are used, polymerization occurs by ring-opening polyaddition and leads to chitin, hyaluronan, chondroitin, and related aminopolysaccharides.



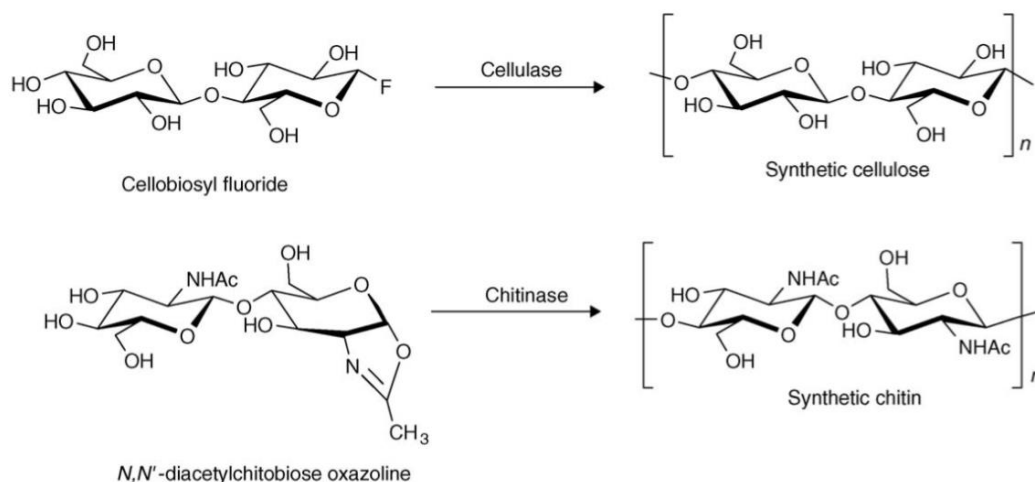


**Figure I-3: Typical enzymatic polymerization of cellobiosyl fluoride and *N,N'*-diacetylchitobiose oxazoline catalyzed by cellulase and chitinase, respectively [15].**

#### A. Synthesis of polysaccharides via polycondensation

As shown, the synthesis of polysaccharides by polycondensation is usually performed using glycosyl fluoride to form a glycosidic linkage between two mono- or oligosaccharides with elimination of HF.

#### ❖ *In vitro* synthesis of cellulose

The main example of hydrolase-catalyzed polycondensation is in the synthesis of cellulose. Cellulose, composed of  $\beta(1-4)$  linked glucoses, is the most abundant naturally occurring polymer. It is one of the three major components in the plant cell wall (60-80%) with hemicellulose (10-20%) and lignin (10-30%). Their renewability, low price, high availability and fibrous and crystalline structure make these biopolymers very attractive for many applications. First attempts of cellulose synthesis were performed by chemical synthesis using activated glucose derivatives and harsh experimental conditions, especially for temperature and solvent. However, region- and stereoselectivity are difficultly controlled by chemical synthesis [17, 27].

Since none of the conventional methods was effective for *in vitro* synthesis of cellulose, enzymes were introduced as catalysts. Kobayashi *et al.* (1991) proposed the polymerization of  $\beta$ -

Cellobiosyl fluoride ( $\beta$ -CF) using cellulase from *Trichoderma viride* in 5:1 acetonitrile: acetate buffer pH 5 under mild conditions (**Figure I-3**). High yield of cellulose (64%) was obtained with a degree of polymerization (DP) of crystalline cellulose II around 22 [28]. Another approach has been derived from the first one for the enzymatic synthesis of cellulose by using a cellulase/surfactant (CS) complex in order to improve the degree of polymerization [29]. The CS complex was a mixture of cellulase (isolated from *Trichoderma viride*) and a specific nonionic surfactant (dioleyl-*N*-D-glucona-L-glutamate). The polymerization of a disaccharide monomer (cellobiose) had been thus achieved by a dehydration polycondensation, resulting in a high polymerization degree (over 100) but with a very low polymerization yield (up to 5%). Recently, cellulose synthesis by the catalysis of enzymes other than cellulase has also been reported. Crystalline cellulose II with a DP of 9 has been obtained by the cellodextrin phosphorylase using glucose and  $\alpha$ -glucose 1-phosphate as monomer [30].

Various kinds of cellulose derivatives have been synthesized by enzymatic polymerization, which allowed the synthesis of well-defined polymeric structures, based on designing the right saccharide fluoride derivative [17, 23]. Since xylan is abundant as well as cellulose in the plant cell wall, its enzymatic synthesis has been also studied. As xylan is a polysaccharide of xylose, xylobiosyl fluoride had been designed as monomer. The polymerization was catalyzed by cellulase from *Trichoderma viride*, in acetonitrile/acetate buffer pH 5 with 72 % and 23 as polymerization yield and degree, respectively. [31].

However, one drawback of the hydrolase enzymes for the polymer synthesis is their capacity to catalyze also the reverse reaction, *i.e.* the hydrolysis of the glycosidic bonds between two saccharidic units. Therefore, partial hydrolysis of the final product is often observed leading to a polymer with lower DP. An inhibition of this reaction was highly required. For this, mutation of cellulase has been investigated. For the synthesis of cellulose and celooligosaccharides, different endo- and exo- types of mutated glycoside hydrolases indeed prevented the hydrolysis of the crystalline structure of the final product. [1, 17]. Other catalysts such as transglycosylase and mutated xylanases were also tried, but less degree of polymerization was obtained [1, 17, 23].

❖ *In vitro* synthesis of amylose

Amylose, a polymer of glucose units linked to each other through  $\alpha(1-4)$  glycoside bonds, is one of the two components of starch, making approximately 20-30% of the structure. The enzymatic synthesis of amylose by polycondensation was investigated using as catalyst not only hydrolase ( $\alpha$ -amylase), but also glycosyltransferases, which are either phosphorylase [32], or glycosyl transferases of Leloir (Amylosucrase). Amylose oligomer (DP about 7) was obtained by  $\alpha$ -amylase-catalyzed polycondensation of  $\alpha$ -D-maltosyl fluoride in methanol-phosphate buffer pH 7 [1, 12]. The synthesis of  $\alpha$ -amylase was also investigated by phosphorylase-catalysis in the presence of a hydrophobic polymer (polyTHF) to favor the formation of polymer with higher DP [32, 33]. Phosphorylase allowed the polymerization of  $\alpha$ -D-glucose 1-phosphate (Glc-1-P) monomer. Amylose with an higher DP value (75-90) than that synthesized by amylase was formed within an inclusion complex due to the presence of the polyTHF. Amylose synthesis was also studied using recombinant amylosucrase from *Neisseria polysaccharea*. This enzyme belongs to the glycotransferases, which catalyze the transfer of a glucose unit to an acceptor molecule. The average degree of polymerization (DP) varied from 58 for the lowest initial sucrose concentration to 45 and 35 for higher sucrose concentrations. The shorter chains (DP 35 and 45), produced in high yields (54 and 24 g/L respectively). The longer chains (DP 58), produced in lower amount (2.9 g/L) [34]. Amylose-based dendritic nanoparticles have also been obtained when glycogen particles were used as primer [35].

*B. Polysaccharides synthesis via ring-opening polyaddition (ROP)*

Polysaccharides synthesis can also proceed by ring-opening polyaddition when sugar oxazoline derivatives are used as monomers [1]. These synthetic monomer acts as a glycosyl donor as well as an acceptor. After protonation of the oxazoline nitrogen by a residue of the catalytic site to form an oxazolinium ion, the oxazoline ring of this intermediate is opened by nucleophilic attack of a second oxazoline derivative, which provides a new glycosidic linkage.

#### ❖ *In vitro* synthesis of chitin

The synthesis of chitin is an interesting example of the ring-opening polyaddition. Chitin is a long-chain polymer of *N*-acetylglucosamine, a glucose derivative applied in many fields, due to its multifunctional properties [36-39]. It is a characteristic component of the cell walls of fungi, and of the exoskeletons of arthropods and insects. Chitin was synthesized *in vitro* for the first time by Kobayashi *et al.* (1995), using a ring-opening polyaddition of chitiobiose oxazoline (disaccharide unit of *N*-acetylglucosamine) catalyzed by chitinase (EC 3.2.1.14) in buffer at room temperature. **Figure I-3** illustrates this polyaddition leading to the formation of  $\beta(1-4)$  glycosidic linkage between two chitiobiose units. It should be mentioned that using *N*-acetylglucosamine oxazoline as TSAS monomer instead of chitiobiose oxazoline lead only to a mixture of chito-oligomers up to pentamers [40, 41]. Nevertheless, many chitiobiose oxazoline derivatives were designed, recognized and polymerized by chitinase [26, 42-45]. Hence, to suppress the undesired chitinase-catalyzed hydrolysis of resulting polymers, mutation of chitinase were also performed [46, 47]. Apart from chitinase-catalyzed ring-opening polyaddition, the synthesis of  $\alpha$ -chitin was achieved, recently, via lysozyme-mediated transglycosylation [38]. Hattori *et al.* used ammonium sulfate to activate  $(\text{GlcNAc})_2/(\text{GlcNAc})_4$ , but the final product was an oligochitinoligomer only up to DP 7.

#### ❖ *In vitro* synthesis of Glycosaminoglycanes

Glycosaminoglycanes (GAGs) are also synthesized by enzyme-catalyzed ring opening polyaddition. Since they are polysaccharides linked to various proteins, playing an important role in living organisms, and used as therapeutic materials and food supplements [19, 48-50], an eco-friendly synthesis was highly required, and was considered one of the most difficult strategies for keeping the GAG functions at the molecular level. Hyaluronidase (Ec 3.2.1.35) is an endotype glucoside hydrolase and had shown a wide use for enzymatic synthesis of the main components of GAGs including hyaluronan, chondroitin, and their derivatives [51-54]. It shows good catalytic activity with various monomers, with respect to stereo and regioselectivities. As the hexoamine unit of GAGs can be either *N*-acetyl-D-glucosamine (GlcNAc) or *N*-acetyl-D-galactosamine (GalNAc), oxazoline sugar monomers used for the chitin synthesis have been

adapted for the production of GAG by hyaluronidase catalysis [55]. **Figure I-4** represents the different oxazoline monomers used for the hydrolase-catalyzed ring-opening polyaddition of several glycoaminoglycans. The structural difference among hyaluronan and chondroitin main chains is only in the stereochemistry of carbon C<sub>4</sub>. For keratan sulfate, which is also one of the main classes of GAGs, the enzymatic synthesis was recently reported by Kobayashi *et al.* (2007) using the keratanase II-catalyzed polymerization of sugar oxazolines through the formation of  $\beta(1-3)$  glycosidic bond [56].

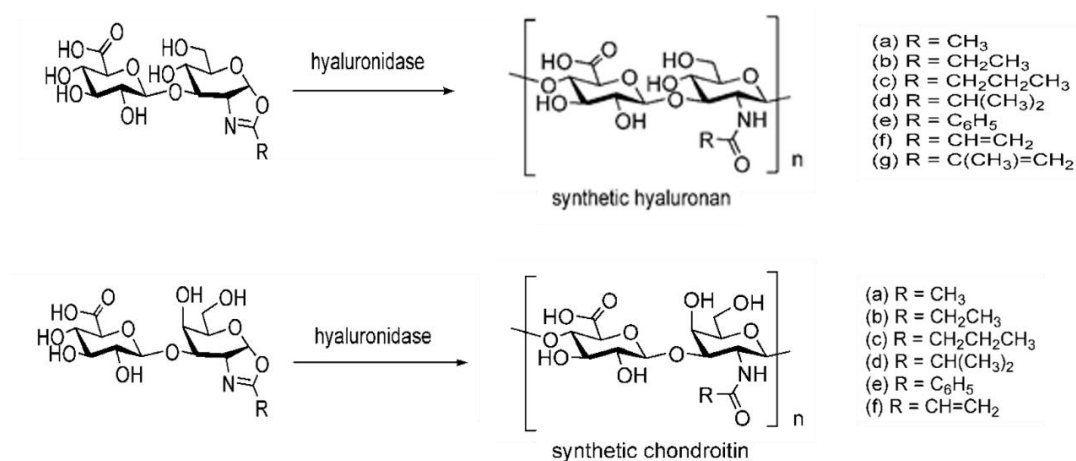


**Figure I-4: Examples of hyaluronidase multi-catalyses for enzymatic polymerizations of sugar oxazoline monomers. Adapted from [1, 17]**

### C. Synthesis of hybrid polysaccharides

As the hydrolases and other enzymes usually applied in the enzymatic synthesis of polysaccharides have a broad spectrum of activity, hybrid polysaccharides had been synthesized based on two different sugar units. In literature, “hybrid” meant the unnatural polysaccharides composed from two different polysaccharide components such as cellulose-xylan, cellulose-chitin, chitin-xylan, etc. [18, 24]. It must be mentioned that the synthesis of such polysaccharides is very difficult by conventional chemical syntheses, and only achieved by enzyme-catalyzed polymerization. Kobayashi *et al.* (1998) successfully synthesized the first unnatural cellulose-xylan polysaccharide using xylanase purified from *Trichoderma viride* in 5:1 acetonitrile/buffer

(pH 5) mixture. The product was obtained by polycondensation of fluoride-based monomers [57]. The synthesis of cellulose-chitin and chitin-xylan was also studied [58, 59]. For cellulose-chitin, the polymerization was possible using either cellulase by polycondensation of fluoride sugars or chitinase by ring-opening polyaddition of oxazolines. However, for preparing chitin-xylan, the reaction was carried out using chitinase as catalyst by ring-opening polymerization of oxazolines. Other hybrid polysaccharides were synthesized such as glucosaminoglycan hybrid polysaccharides [60].

#### I.1.1.2. Synthesis of polyesters

Polyesters are polymers that contain ester functional group within their main chains. According to the composition of their main chain, polyesters can be aliphatic, semi-aromatic or aromatic. They include naturally occurring materials, such as cutin, as well as synthetic polymers such as the polyesters used in clothing. They are widely applied in the biomedical field, for example for drug delivery, cosmetics and tissue engineering and are considered the most competitive biodegradable polymers commercialized up to now. Some polyesters, especially aliphatic ones, have shown biodegradable properties, and thus can be an eco-friendly alternative to the non-degradable polymers for limiting the environmental pollution concerns [61-64].

Among enzymes, lipases proved to be the most efficient catalysts for the *in vitro* synthesis of polyesters. Normally, this enzyme catalyzes the hydrolysis of fatty acid esters in the aqueous environment of living systems. They are ubiquitous enzymes with considerable physiological significance due to their crucial roles in the digestion, transport, and processing of dietary lipids in most of living organisms [65]. The broad synthetic potential of lipases results from their capacity to accept a wide range of substrates and from their stability in organic solvents contrary to most other enzymes.

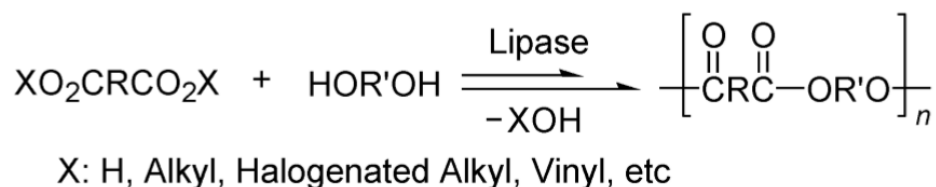
The *in vitro* polyester synthesis can proceed via two major polymerization modes: the polycondensation or the ring-opening polymerization [9].

### A. Enzyme-catalyzed polycondensation of esters

Aliphatic polyesters are among the most used biodegradable polymers in environmental and medical fields. Already decades ago, enzymatic approaches to synthesizing biodegradable polyesters have been developed by lipase-catalyzed polycondensation by using various polymerization modes including esterification and transesterification [66]. As these reactions are all reversible, the co-products of the esterification (water or alcohol) have to be often removed or reduced from the reaction mixture to shift the reaction equilibrium towards the formation of polyesters [1].

Interestingly, complex monomers can be employed in enzymatic polycondensation, and thus the latter has attracted increasing attention in recent years [67]. So far, various dicarboxylic acid derivatives, dicarboxylic acids, their activated and non-activated esters, cyclic and anhydrides have been polymerized with glycols through lipase catalysis to produce polyesters [68-70]. The different polycondensation reactions that are catalyzed by lipase are summarized in the following **Figure I-5**.

#### Polycondensation of Dicarboxylic Acids or Their Derivatives with Glycols



#### Polycondensation of Oxyacids or Their Esters

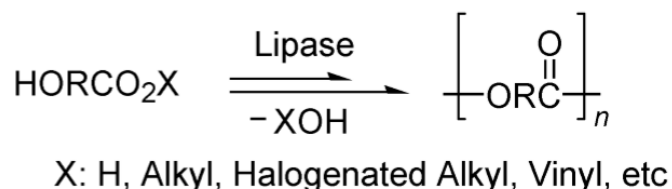


**Figure I-5: Lipase-catalyzed synthesis of aliphatic polyesters via polycondensation. Reprinted from [66]**

Compared to the conventional methods, lipase-catalyzed polycondensations are an easier way for enantio- and region-selective polymerizations in order to prepare chiral polyesters [67]. Using lipase catalysis, biodegradable polyesters have been obtained for environmental, biomedical and cosmetic applications. [11, 64, 71].

### B. Enzyme-catalyzed ring-opening polymerization of esters

Enzyme-catalyzed polymerization has been quickly accepted as a novel methodology of polyester synthesis since the lipase-catalyzed ring-opening polymerization of lactones reported first by Kobayashi *et al.* [72] and Kinani *et al.* [73]. Lactones have been polymerized by a lipase-catalyzed ring-opening polyaddition as shown in **Figure I-6**. Small-, medium-sized (4, 6, and 7-membered ring), large-sized (12 or 16 membered ring) lactones as well as cyclic oligomers were found to be efficiently polymerized by lipase-catalysis [74], though their reactivity varied according to ring size. In contrast to polycondensation reactions, no water or alcohol is co-produced in enzymatic ROP, and thus higher yields can readily be obtained with this method [75].

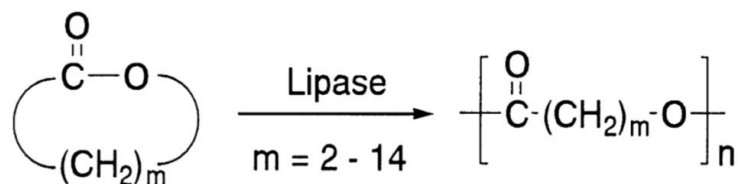


**Figure I-6: Lipase-catalyzed synthesis of polyesters via ring-opening polymerization. Reprinted from [75].**

Polyphosphate and polythioester' syntheses by lipase catalysis are also reported. Enzymatic polyphosphate synthesis has been achieved by lipase-catalyzed ROP of cyclic phosphates or copolymerization with other lactones. **Figure I-7** shows two examples for such enzymatic synthesis based on the polymerization of ethylene isopropyl phosphate (a) and ethylene isobutyl phosphate (b). However, the resulting polymers were of low molecular weights ( $M_n < 10,000$  g/mol) [75].



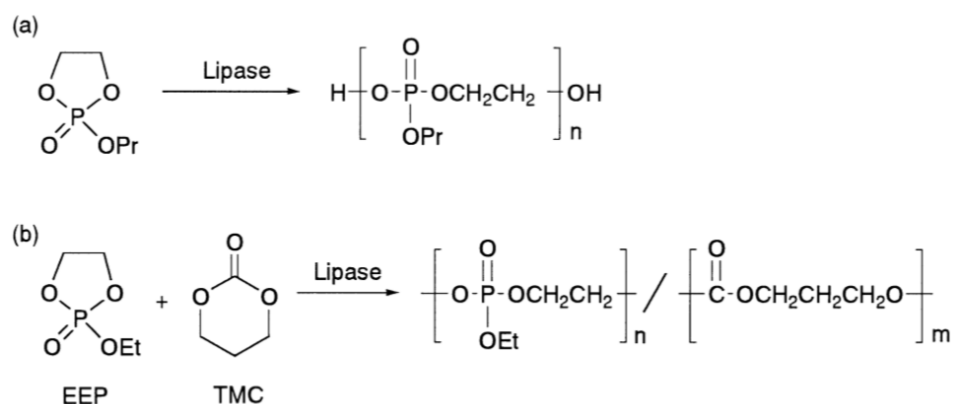


**Figure I-7: Lipase-catalyzed ring-opening polymerization of phosphates. Reprinted from [75]**

Polyesters containing thioester are usually prepared by enzymatic ROP of lactones. The most recent example of such polymerization is reported by Wu *et al.* that described the lipase-catalyzed synthesis of poly( $\beta$ -thioether ester) and poly( $\beta$ -thioether ester-co-lactone) with the optimization of the reaction temperature and time. Immobilized lipase B from *Candida Antarctica* (Novozym 435) was used as biocatalyst. Both homo- and co-polymers were thermally stable up to at least 220°C with high molecular weights ranging from 26300 to 96000 KDa [76].

### I.1.1.3. Oxidative polymerization of polyaromatics and vinyl monomers

In the literature, enzymatic polymerization has been mainly developed for polymers synthesized by polycondensation, ring-opening polymerization, and ring-opening polyaddition. However, some enzymes can also be implicated in radical polymerization due to their capacity to produce radical intermediate species from a variety of substrates by an oxido-reduction mechanism.

In general, radical polymerization is an important technological area. As a synthetic process, it has enabled the production of materials that have enriched the lives of millions of people on a daily basis. Free radical polymerization proceeds *via* a chain mechanism, which basically consists of four different steps involving free radicals: (1) radical generation from non-radical species (initiation), (2) radical addition to a substituted alkene (propagation), (3) atom

transfer and atom abstraction reactions (chain transfer and termination by disproportionation), and (4) radical–radical recombination reactions (termination by combination). The following **Figure I-8** illustrates well the basis of the free radical polymerization.

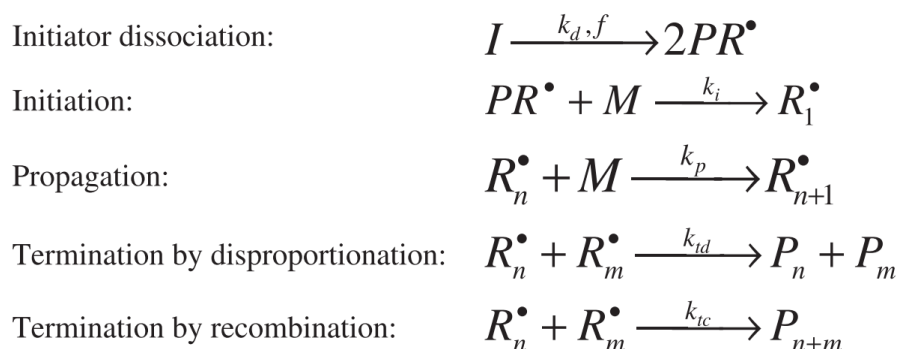


**Figure I-8: Detailed reaction scheme applied for Free radical polymerization. I: Initiator; PR<sup>•</sup>: Primary radical; R<sup>•</sup><sub>1</sub>; M: monomer molecule. Reprinted from [77].**

Mainly, peroxidases and laccases have shown remarkable utility towards the polymerization of aromatics and vinyl monomers. They catalyze the oxidation of compounds such as phenols, and aromatic amines, which leads to their polymerization. They also catalyze the oxidation of mediators, which play the role of initiators in vinyl polymerization. Both polymerization reactions can be summarized in the following **Figure I-9**.

A full description of the implicated enzymes, their mechanisms, as well as the parameters that influence the polymerization are detailed in the next part of **I.1.3**. The synthesis of different polymers based on aromatic compounds and vinyl monomers is described as follows.

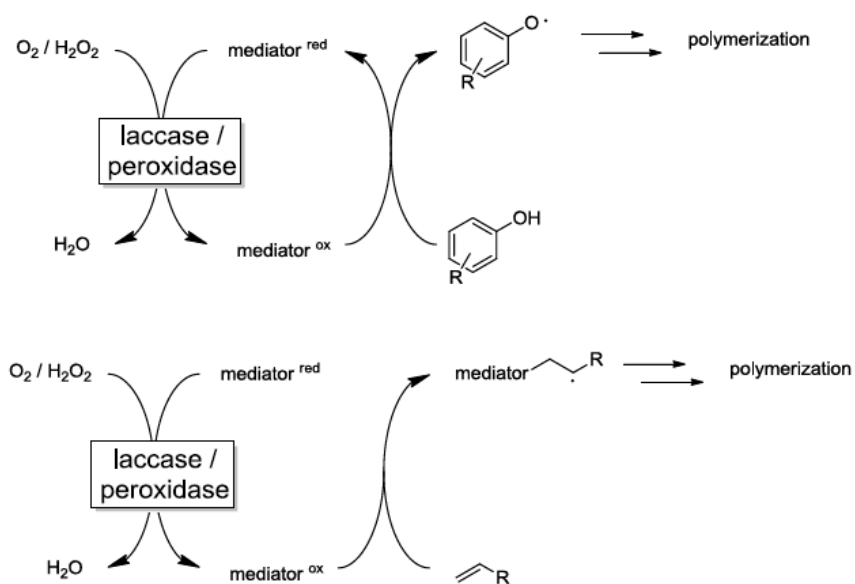


**Figure I-9:** Schematic representation of laccase and peroxidase mediator systems-initiated polymerization reactions. Upper: the mediator is used as true catalyst transferring the radical to a monomer; Lower: the oxidized mediator radical itself initiates the polymerization process and hence is incorporated into the polymer. Reprinted from [79]

#### A. Enzymatic polymerization of aromatic compounds

Polyphenols are abundant micronutrients in our diet. There is evidence for their role in the prevention of cancer and cardiovascular diseases. Over the past 10 years, researchers and food manufacturers have become increasingly interested in these polyaromatics for their antioxidant properties [78]. For this reason, in the past decades, the *in vitro* enzymatic synthesis of polyphenols has been extensively investigated. Several enzymes, such as peroxidases, laccases, and bilirubin oxidases have been reported as efficient biocatalysts in the oxidative polymerization of phenol and phenolic derivatives. Among these enzymes, horseradish peroxidase is most often used for its ability to catalyze the radical reaction. [79]. The enzyme function is to produce phenoxy radicals under mild conditions. The resulting radical species are able to form polymers via recombination process. Thus, the enzyme-catalyzed oxidation of phenols is the only step that is controlled by the enzyme. **Table I-2** gives an overview over some of the polymeric products synthesized by enzymatic polymerization.

**Table I-2: Polyphenols polymerized for improved antioxidant activity**

<b>Monomer</b>	<b>Catalyst</b>	<b>Reference</b>
<b>Phenol</b>	HRP	[80, 81]
<b>Quercetin</b>	HRP	[82]
	Laccase	[83]
<b>Esculin</b>	Laccase	[84, 85]
<b>Rutin</b>	HRP	[86]
	Laccase	[83, 85]
<b>Kaempferol</b>	Laccase	[83]
<b>Epicatechin</b>	HRP	[87]
<b>Catechol</b>	HRP	[88]

Four systems were identified in literature for the enzymatic polymerization of phenolic compounds: monophasic system, biphasic system, micelle system and Langmuir Blodgett system. In the monophasic system, the polymerization reaction is operated in semi-aqueous or nearly anhydrous conditions. Then, many parameters can affect the polymer characteristics such as solvent nature, solvent amounts, pH values, and others. For reactions performed with phenol as substrate, the polymer formed precipitates in water/organic solvents, which facilitates its extraction. For more complex phenolic compounds, such as flavonoids, the polymer formed could be water-soluble [81]. Biphasic systems consist of two phases mutually non-miscible. The aqueous phase contains the enzymatic system and the organic phase contains the monomer. These two phases are stirred to form a micro-emulsion. In the case of peroxidase, hydrogen peroxide is gradually added to start the polymerization reaction. The use of such systems helps to prevent peroxidase denaturation by excess of H<sub>2</sub>O<sub>2</sub> (as it will be explained in **I.1.3**) [79], [89]. In the case of laccases, it was previously reported that low oxidation rates are obtained in biphasic systems, which can be attributed to insufficient mass transfer of the reactants between the two phases [83]. In reversed micelles systems, surfactants are used. It was observed that enzymes have been maintaining their tridimensional structures as well as their activities, which results in better yields of polymerizations [80, 90]. Finally, Langmuir–Blodgett is an operation that consists in orienting amphiphilic molecules at the water–air interface in order to obtain a

structured monolayer. Such organization allows controlling the link type between monomers and preventing the formation of para–para structures. The synthesized polymers have better thermal stability and electronic properties than monomers [89].

### **B. Enzymatic polymerization of vinyl monomers**

Vinyl monomers that are investigated for enzymatic polymerization are roughly classified into acrylic and styrene type. **Figure I-10** illustrates the chemical structures of the vinyl monomers that were mostly used for enzymatic polymerizations.

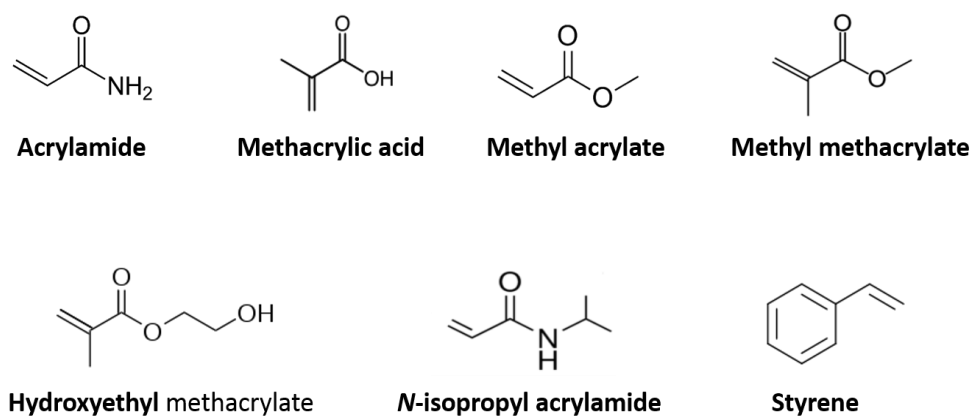


**Figure I-10: Chemical structures of the tested vinyl monomers in the enzyme-initiated polymerization**

The enzymatic polymerization of vinyl monomers was first described by Derango *et al.* [91]. The polymerization of acrylamide, methyl acrylate, hydroxyethyl methacrylate, acrylic acid, and methyl methacrylate was reported with various enzymes such as peroxidases. The polymerization was carried out in buffers pH 6-7. Different substrates were used such as hypoxanthine, hydrogen peroxide, t-butyl-hydroperoxide and methanol according to the enzymes being xanthine oxidase, horseradish peroxidase, chloroperoxidase and alcohol oxidase,

respectively. However, the study did not include any information about the underlying mechanism of enzyme-catalyzed radical generation.

Compared to the polymerization of polyaromatic compounds, vinyl polymerization affords better control of polymer characteristics. Lalot *et al.* showed in a series of publications (1997-2001) that the linear polymerization of acrylamide by HRP-catalysis could result in a wide variation of polymerization yields and molecular weights depending on the concentration of enzyme, hydrogen peroxide, as well as the type and concentration of the reducing species [92-96]. A full description of the generally accepted mechanism of radical generation (as will be detailed in the following part of **I.1.3.2**) was also provided. It included the HRP catalytic cycle in which HRP catalyzes the oxidative formation of two radical molecules and the formation of one water molecule from hydrogen peroxide. In another study, HRP-mediated linear co-polymerization of acrylamide is reported in the presence of starch. The classical enzymatic ternary system including HRP/H<sub>2</sub>O<sub>2</sub>/Acac is used to yield starch-polyacrylamide graft co-polymers [97]. Moreover, linear polymerization of acrylamide by laccase-mediated generation of radicals was reported as well [13, 98].

Peroxidase-mediated free radical polymerization of methyl methacrylate was investigated in water and water-miscible organic cosolvents (DMF, acetone, dioxane, and THF). In aqueous media, poly(methyl methacrylate) (PMMA) was obtained from the reaction mixtures of soybeans peroxidase and HRP II, in 48 and 45% as polymerization yields, respectively. The influence of the experimental parameters such as solvents, type of the reducing molecule, ratio of Acac/H<sub>2</sub>O<sub>2</sub>, and the ternary system concentrations are studied with emphasis on the polymerization yield and the polymer molecular weight [99].

Enzyme-mediated radical polymerization of hydrophobic monomers of styrene and its derivatives at mild polymerization conditions was reported decades ago. Polystyrene synthesis by HRP-catalysis was described in details in the presence of hydrogen peroxide, and extended to different initiators to assess the reaction efficiency and mechanism. Cyclic  $\beta$ -diketones generated polymers in good yields, up to 60%, and it was experimentally observed that the polymer characteristics in terms of yield and molecular weight were depending on the type of the used initiator. Moreover, for the efficient progress of the polymerization, the reaction solvent was very

important to from a homogeneous solution. Best results were obtained using H<sub>2</sub>O/THF (3:1 v/v) as solvent leading to 21.2% increase of polymerization yield [100].

Enzymatic catalysis has received attention not only in free radical polymerization, but it has also been shown that laccase and horseradish peroxidase can induce controlled radical polymerization of vinyl monomers. Enzyme-mediated atom transfer radical polymerization (ATRP) of different monomers has been largely investigated. HRP-catalyzed ATRP of *N*-isopropylacrylamide was studied with emphasis on the polymer molecular weight and the polydispersity index in different experimental conditions. “Activators regenerated by electron transfer” (ARGET) ATRP was investigated by using an alkyl halide (2-hydroxyethyl-2-bromoisobutyrate) as initiator. The commonly accepted mechanism of HRP-mediated ATRP is illustrated in **Figure I-11**. HRP catalyzed the ATRP in absence of any peroxide and the yielded polymers were of low polydispersity indices emphasizing the controlled radical polymerization. However, poorer PDIs with low yields were obtained under some experimental conditions suggesting that the control of polymer characteristics in ATRP depends on the concentration of the reducing agent, as well as the solution pH [101]. In another recent study, emulsion and surface-initiated polymerization of vinyl monomers was also performed by ATRP using laccase and alkyl halides as catalyst and initiator, respectively. Polymerizations of different monomers such as styrene, MMA, and others are investigated. The polymerization required the presence of a reducing agent such as ascorbic acid to be effective. Better control of the polymer molecular weight was achieved in presence of chain transfer agents in a RAFT process [102].

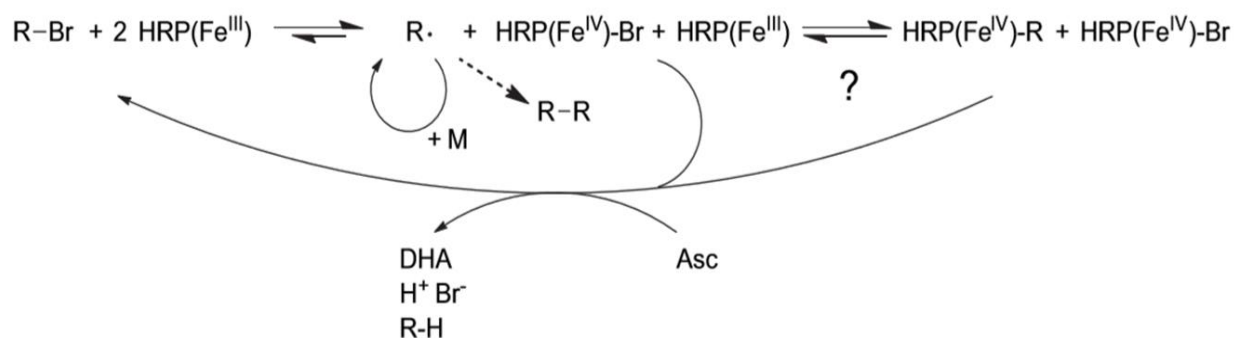


**Figure I-11: Mechanism of HRP-catalyzed polymerization under ARGET ATRP conditions. (Asc=ascorbate, DHA=dehydroascorbic acid). Reprinted from [101].**

In a very recent study, the same enzymes have been actively also engaged in the Reversible-Addition-Fragmentation Chain Transfer (RAFT) polymerization of a wide range of acrylic monomers such as dimethacrylamide, 2-hydroxyethylacrylate, 2-methoxyethylacrylate, poly(ethylene glycol) methyl ether acrylate, and others. HRP-initiated RAFT polymerization was reported, using the ternary system HRP/ACAC/H<sub>2</sub>O<sub>2</sub>. RAFT polymerization initiated by Glucose oxidase-HRP cascade catalysis was also studied in order to initiate facile and well-controlled RAFT polymerization in open air, representing a good progress toward overcoming the oxygen-free restriction of reversible radical polymerization [103]. The following **Figure I-12** shows the schematic mechanism of GOx-HRP cascade catalysis for radical generation in the RAFT polymerization.

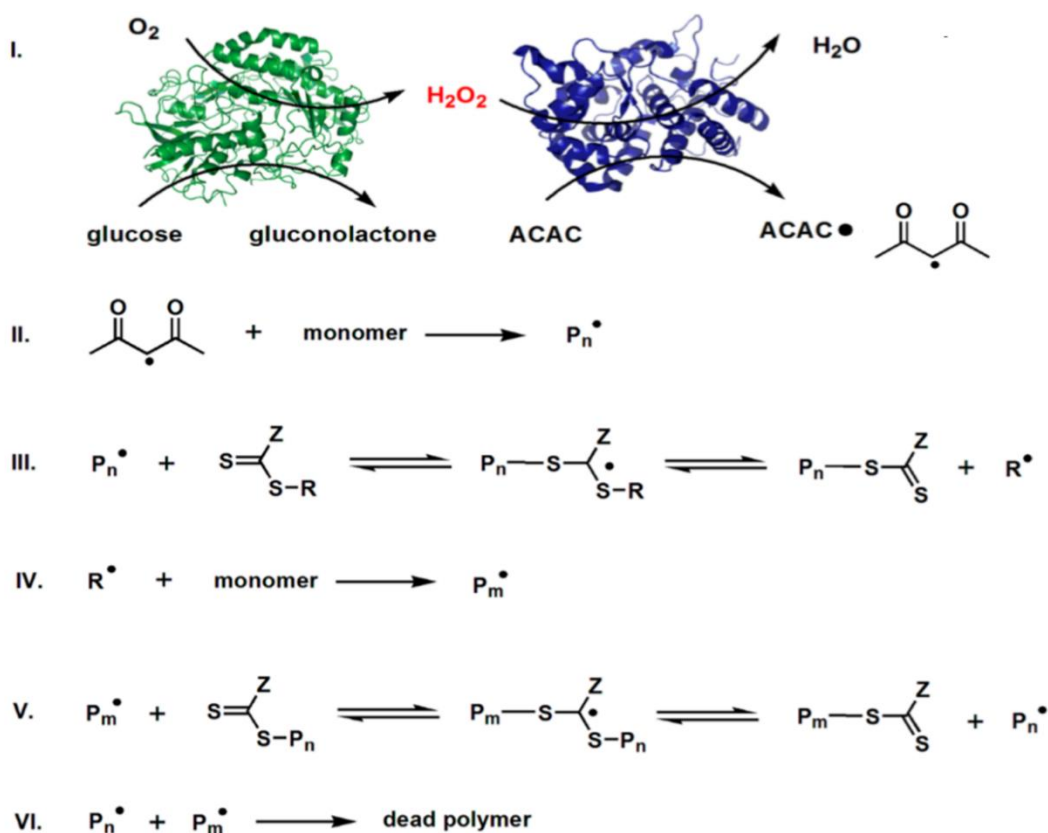


**Figure I-12:** Schematic representation of glucose oxidase (GOx)-HRP cascade catalyzed radical generation in air for the initiation of RAFT polymerization of dimethylacrylamide. Modified from [103].



### I.1.2. Polymer synthesis via Enzymatic Polymer Modification

As mentioned in the beginning of this chapter, enzymatic catalysis in the research field of polymer chemistry is not only limited to polymerization but can also be applied to the modification (functionalization) of the polymers. Enzymes catalyze the modification of a polymer through functional groups located at the polymer terminal, in the main chain or in the side chain. The catalysis is achieved in a specific manner, controlling chemo-, and regio-selectivity, as well as stereochemistry in mild reaction conditions.

Most of the investigations in enzymatic polymer modification have dealt with natural polymers. It is studied for the functionalization of such polymers in order to produce amphiphilic, biodegradable and biocompatible compounds for use as emulsifiers, compatibilizers, detergents and drug-delivery systems. For instance, the formation of polysaccharide-based hydrogels by HRP-catalyzed enzymatic reaction has been reported. Dextran-Tyramine conjugates were synthesized by thermo-initiated radical polymerization. Then, hydrogels were prepared by HRP-coupling reaction of phenol moieties in the Dextran-Tyramine conjugates in presence of hydrogen peroxide [104]. Other example is the use of laccase in combination of mediators for the lignification of pulps. The potential of this enzyme in cross-linking and functionalizing lignocellulose materials has also been examined in order to replace traditional adhesives such as urea-formaldehyde adhesive. Laccase-catalyzed modification has successfully been applied by using various phenolic compounds. Such modifications are usually needed to improve the surface functionality [105].

Enzymatic modification has also been performed with synthetic polymers, especially in the functionalization of bulk materials. For instance, the application of cellulase to improve cellulose fiber properties (textile and paper) is already used in industry. A review of Paulo *et al.* (2003) summarizes the most relevant examples for the enzymatic modification of polyesters, polyamides, polyacrylonitrile, and others by the catalysis of lipases, peroxidases and laccases, hydrolases and esterases, as well as tyrosinases, respectively [105]. **Figure I-13** summarizes the most important enzymes implicated in the polymer modification achieved in literature.

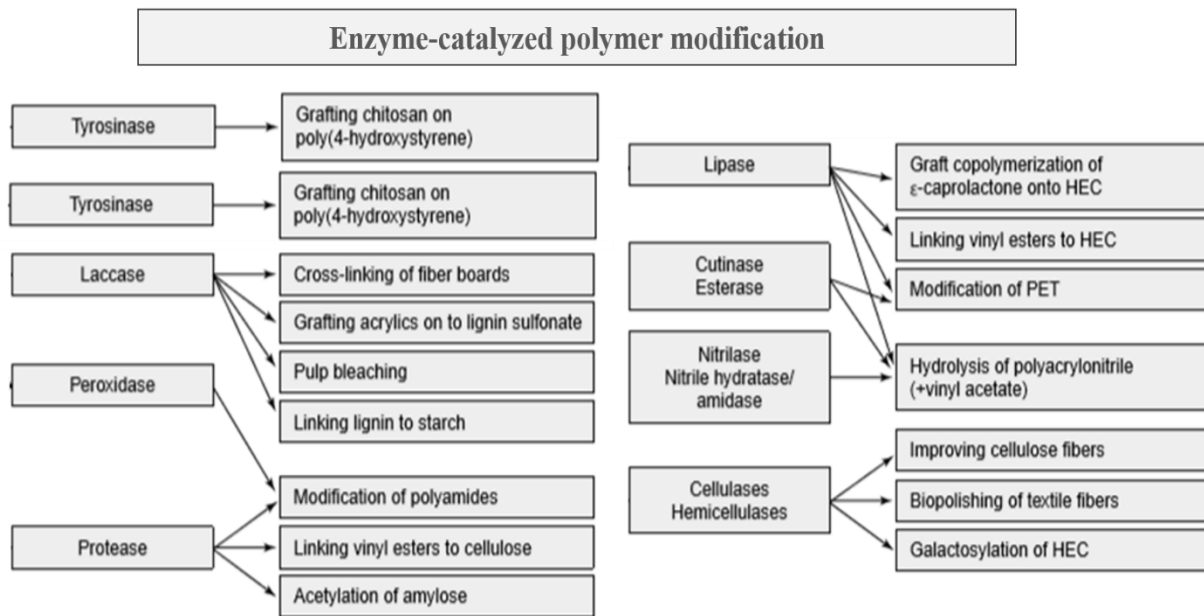


**Figure I-13: Schematic representation of enzymes involved in the enzymatic modification. HEC: Hydroxyethylcellulose; PET: Polyethylene terephthalate. Modified from [105].**

### I.1.3. Enzyme-initiated radical polymerization

Radical polymerization is a universal technique adopted at both industry and laboratory scale for the *in vitro* synthesis of a wide range of polymers. It can be applied for the polymerization of different kinds of monomers with versatile structure. Since the early stage of polymer chemistry, radical generating compounds have acquired great importance among the catalysts to initiate the polymerization. Azo or peroxide radical initiators are commonly used to initiate the free radical polymerization. Compared with peroxides, azo initiators generate carbon-centered radicals, known to be less reactive with respect to hydrogen abstraction than are the oxygen-centered radicals generated by peroxides. This difference has an effect on the branch grafting and preliminary chain termination that are reduced in the case of azo initiators, resulting thus in an efficient polymer chain growth. In contrast to peroxides, most commercial azo initiators are not affected much by solvents, acids, bases, etc [106].

Traditionally, organic polymers are produced in large annual amounts. However, the resulting wastes in the industry are enormous, leaving room for white biotechnology to reduce the toxic effects and waste generation. Indeed, using biocatalysts as enzyme for polymer synthesis has become very popular in the past two decades, and the following part summarizes some of the examples that have impressively demonstrated the potential of enzymes in making the chemical industry environmentally safer and more sustainable.

#### I.1.3.1. Enzymes

Enzyme-initiated radical polymerization has expanded tremendously in the past two decades and polymerization of different aromatic and vinyl monomers has been reported [15]. In this field, two major enzymes have been applied: Peroxidases (EC 1.11.1) and to a lesser extent, Laccases (EC 1.10.3.2). With respect to their structures and catalytic cycles, both enzymes catalyze the hydrogen atom transfer reactions in order to generate radical species that are potential initiators of the polymerization. Other enzymes have also been reported but are of minor importance [79].

### A. Peroxidases

Discovered early in 19<sup>th</sup> century, peroxidases are widely distributed in nature and can be easily found and extracted from plant and some animal cells. They are mainly divided into two superfamilies: plant peroxidases and animal peroxidases. These enzymes belonging to oxidoreductases are heme proteins and contain iron (III) with protoporphyrin IX as a prosthetic group. They catalyze various oxidative reactions in which electrons are transferred to peroxide species (often H<sub>2</sub>O<sub>2</sub>) and substrate molecules are oxidized [107]. Peroxidases have recently conquered a great position in a wide range of biotechnology fields, including biosensors and analytical devices, medicine, in addition to polymer synthesis.

Among all these peroxidases, horseradish peroxidase and cytochrome c are the most intensively studied peroxidases. Soybean peroxidase is also used, but to a lesser extent [108].

Horseradish peroxidase has been studied for more than a century. It emerged as a great tool in biotechnology, where it is applied in a wide range of areas such as enzymology, biochemistry, medicine, genetics, physiology, histo- and cytochemistry [108]. HRP is mainly found in the cell wall, vacuoles and transport organelles, and in the endoplasmic reticulum. It plays an important role in physiological processes including catabolism, pathogen defense, and wound healing.

They have a globular structure with an  $\alpha$ -helical secondary structure with the exception of one short  $\beta$ -sheet region. The HRP protein is separated into a distal and a proximal region by an iron protoporphyrin IX cofactor, commonly named Heme group. These enzymes also contain two conserved calcium ions, and four conserved disulphide bridges [108, 109]. **Figure I-14** shows the three-dimensional structure of HRP.

It is well accepted that HRP occurs in a large family of isoenzymes, which catalyze the same biochemical reactions but have distinct physico-chemical and kinetic properties, and differences at the molecular level such as in their amino acid sequences. Before the development of chromatographic techniques, Theorell (1942) was the first to isolate two forms of peroxidases from horseradish roots. They had different physico-chemical properties. HRP I was basic and contained low carbohydrate content, whereas HRP II was neutral and highly glycosylated. These forms were recognized later on as isoenzymes. Until recently, more than twenty isoenzymes of

HRP have been identified with isoelectric points (pI) ranging from 3.5 to 9. The sequences of the isoenzymes are available in public databases [109]. HRP C dominates quantitatively among all the isoenzymes of HRP, and has an pI close to 9 [110]. The isoenzymes containing most of the peroxidase activity have isoelectric points between 5.5 and 7.6 [111].

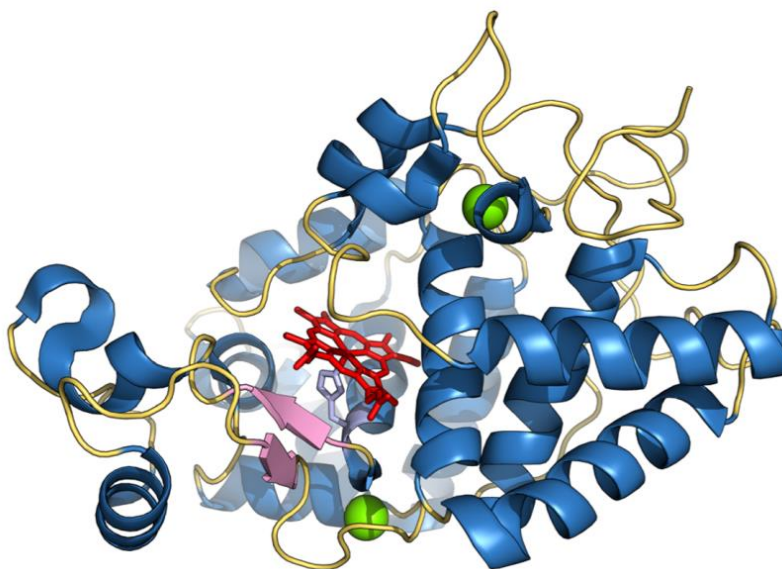


**Figure I-14:** Three-dimensional representation of Horseradish peroxidase (HRP); helices are shown in blue and loops in yellow. One short  $\beta$ -sheet region is shown in pink. The two calcium ions are shown as green spheres. The heme group is shown in red and stands between the distal and the proximal domains; the proximal His170 residue (light blue) coordinates to the heme. [109]

Most reactions catalyzed by HRP involve the conversion of hydrogen peroxide to water and the concomitant oxidation of a reducing substrate. Interestingly, HRP is well-known for its broad specificity.  $\text{H}_2\text{O}_2$  is the natural substrate of the enzyme. Indeed, a very wide range of reducing molecules can be oxidized by horseradish peroxidase. **Table I-3** summarizes some of the most relevant and commonly used substrates for this enzyme. Many of the substrates in **Table I-3** are chromogenic and can be used in colorimetric and fluorimetric assays. These molecules are hydrogen donors, and form, upon oxidation, a colored product that can be monitored by spectrophotometric methods. Therefore, HRP is widely used in labelling systems. A large number of procedures have been developed based on HRP, in histochemical staining and diagnostic assays such as enzyme-linked immunosorbent assays (ELISA), and Western-blotting

[108, 109, 112]. Since HRP is capable of reducing hydrogen peroxide and other peroxides, HRP-based biosensors had been developed to control and monitor these peroxides in pharmaceutical, environmental, and dairy industries.

**Table I-3: Common substrates for horseradish peroxidase. [108]**

Common name	Synonym
<b>ABTS</b>	2,2'-Azino-di(3-ethylbenzothiazolin-6-sulfonate)
<b>Benzidine</b>	4,4'-Diaminobiphenyl
<b>TMB</b>	3,3',5,5'-Tetramethylbenzidine
<b>DAB</b>	3,3'-Diaminobenzidine
<b>Guaiacol</b>	2-Methoxyphenol
<b>Pyrogallol</b>	1,2,3-Trihydroxybenzene
<b>Phenol</b>	Hydroxybenzene
<b><i>p</i>-Cresol</b>	4-Methylphenol
<b><i>o</i>-Dianisidine</b>	3,3'-Dimethoxybenzidine
<b><i>p</i>-Toluidine</b>	1-Amino-4-methylbenzene
<b>Tolidine</b>	3,3'-Dimethylbenzidine
<b>Hydroquinone</b>	1,4-Dihydroxybenzene
<b>Resorcinol</b>	1,3-Dihydroxybenzene
<b>Catechol</b>	1,2-Dihydroxybenzene
<b>4-Aminoantipyrine</b>	4-Amino-2,3-dimethyl-1-phenyl-3-pyrazolinone
<b><i>p</i>-Anisidine</b>	1-Amino-4-methoxyphenol
<b><i>o</i>-Phenylenediamine</b>	1,2-Diaminophenol
<b>Luminol</b>	3-Aminophthalhydrazide
<b>Ferulic acid</b>	4-Hydroxy-3-methoxycinnamic acid
<b>Caffeic acid</b>	3,4-Dihydroxycinnamic acid

HRP has also been studied in enzyme/prodrug systems for cancer treatment. HRP and the prodrug indole-3-acetic acid constitute one of the most frequent combinations for such systems, which are applied to tumor cells labeled with HRP-antibody conjugates in order to kill the cancer

cells selectively [113]. Other combinations including HRP and methylglyoxal have also been used for the same kind of treatment [114]. On the polymer side, Lalot *et al.* proved that  $\beta$ -diketones can also be substrates that are oxidized by HRP. They have been shown key compounds in the HRP catalytic cycle in enzyme-mediated synthesis of linear polyacrylamides, where they act as reducing molecules [93].

### **B. Laccases**

Laccases are oxidative enzymes, belonging to multi-nuclear copper-containing oxidases. They are found in many plants, fungi and microorganisms. They catalyze the oxidation of a wide range of compounds coupled with the reduction of oxygen to water [115]. Laccases play diverse biological roles according to the nature and the life stage of the organism that produces them. For instance, they participate in morphogenesis, pigmentation, oxidation of toxic compounds and protection against oxidizing agents, within bacteria. They play a role in lignin polymerization within the plants, and they are involved in morphogenesis and stress defense in fungi [116].

From a structural point of view, the molecular architecture of laccases is common for all multi-copper oxidases, despite their wide taxonomic distribution. These enzymes are dimeric or tetrameric glycoproteins and contain copper atoms. The copper sites within laccases are categorized into three groups. The Type-1 (T1) copper, so-called blue copper center, shows an intense electronic absorption band near 600 nm, which is responsible for the blue color of laccases. The Type 2 (T2) copper forms with the two type 3 (T3) a trinuclear cluster in which molecular oxygen is reduced to two molecules of water [117, 118]. **Figure I-15** shows the laccase three-dimensional structure. Due to its ability to oxidize a broad range of organic substrates, laccase was found very useful in many applications in the biotechnology field. They are included in the detoxification of industrial effluents, bioremediation of contaminated soils, and in the manufacture of anti-cancer drugs and cosmetics ingredients in addition to polymer synthesis [116, 119].

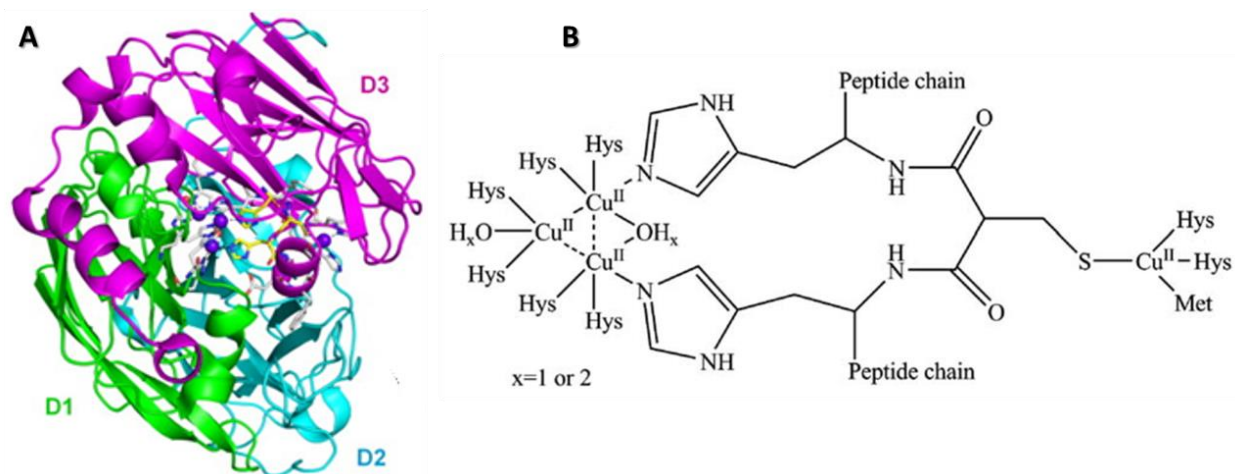


**Figure I-15: A: General 3D structure of laccase (*Trametes Trogii* laccase). The three cupredoxin-like domain (D1, D2, and D3) are shown in green, cyan, and magenta, respectively. B: Schematic representation of the active site of laccase (from *T. versicolor* laccase). It represents the copper ions from T1 Cu to the T2/T3 trinuclear cluster. Residues involved in the coordination sphere of the catalytic coppers are also represented. Modified from [102, 118]**

### C. Other enzymes

In enzyme-initiated radical polymerization, enzymes classes other than peroxidases and laccases play only a minor role. Enzymatic polymerization of phenolic compounds, such as dihydroquercetin, is achieved with bilirubin oxidase. The physicochemical properties of the final product were investigated showing a conservation of the chemical and thermal stabilities and a higher antioxidant activity for the polymer [120]. Enzymatic polymerizations were also reported by using glucose oxidase [121] and cholesterol oxidase [122]. Lipoxygenase was found to catalyze the oxidative polymerization of phenolic lipids. *In vitro* polymerization of different lipophilic phenolic compounds by lipoxygenase-catalyzed oxidation was reported, providing a new explanation for the mechanism of allergic contact dermatitis which is induced by plants allergens [123].



### I.1.3.2. Catalytic mechanism

Since the study of the enzyme-mediated synthesis of polymers begins by understanding the method in which the radicals are generated, the catalytic cycles of both horseradish peroxidase and laccase with their generally accepted mechanisms will be highlighted below.

#### A. Peroxidases-mediated initiation

The mechanism of HRP catalysis has been extensively investigated. It can be roughly described by three consecutive elementary reactions including the enzyme resting state, and two intermediates, which are so-called compounds I and II. The important features of this catalytic cycle are illustrated in **Figure I-16**.

The first step consists of the Compound I formation. This species is characterized by an [Fe(IV)=O] ferryl species coupled with a porphyrin radical cation. This step of peroxidase catalysis involves binding of the peroxide, usually H<sub>2</sub>O<sub>2</sub>, to the heme iron atom to produce the ferric hydroperoxide intermediate [Fe(III)-OOH]. Then, a protonation of the distal oxygen of the ferric hydroperoxide complex takes place so that the formation of the ferryl species can be linked to the elimination of the distal oxygen as a molecule of water. It is thought that the distal histidine residue in the peroxidase active site is the base that deprotonates the peroxide. This proton is then delivered by the imidazole to the terminal oxygen of the ferric hydroperoxide complex, catalyzing the O-O bond cleavage that produces the Compound I.

Thereafter, several reducing substrates, already mentioned above, are liable to interact with compound I. This second step involves a single-electron transfer, in which the  $\pi$ -cation radical is discharged. The porphyrin ring gets back one electron from the reducing species, leading to the formation of compound II, which contains an oxoferryl group (Fe<sup>IV</sup>=O). The deprotonation of the oxidized substrates by this oxido-reduction step results in the radical formation.

Finally, compound II is reduced by one more substrate molecule, and the enzyme goes back to its native resting state. This one-electron reduction of HRP-II transforms the ferryl iron to its ferric state (Fe<sup>III</sup>), whereas the oxygen accepts two protons to form a water molecule and it is released from the heme. A free radical is generated in this step as well. [94, 108, 112]. Globally, HRP

catalyzes the oxidation of one hydrogen peroxide molecule and the whole catalytic cycle leads to the formation of two radical molecules.

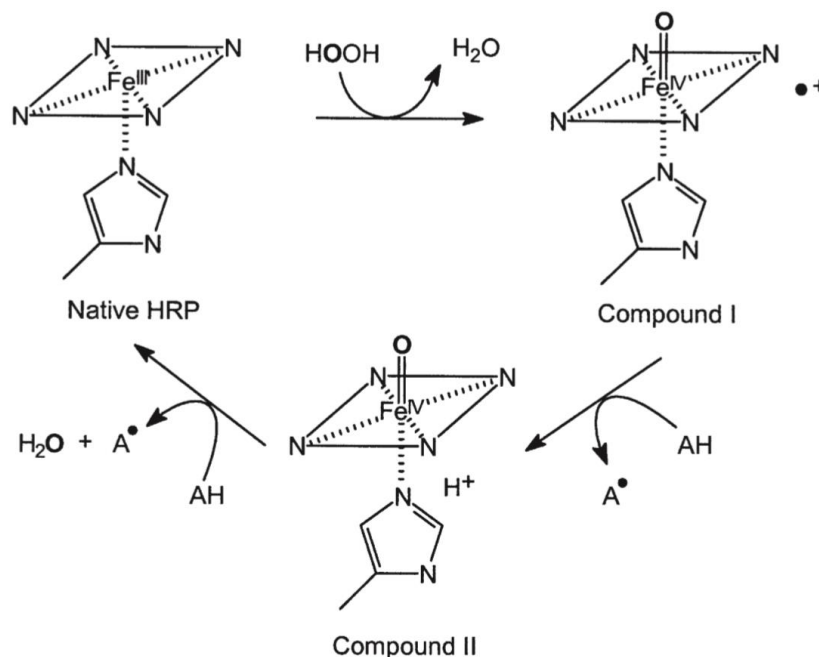


**Figure I-16: Mechanism of the HRP catalytic cycle, showing compounds I and II as enzyme intermediates. Reprinted from [108].**

This generally accepted mechanism depends on hydrogen peroxide or other organic hydroperoxides. However, oxidation of substrates by HRP catalysis has been described in a reaction independent of hydrogen peroxide. In such cases, dihydroxyfumarate, and indole-3-acetic acid were the reducing species [113]. The possibilities of acetylacetone oxidation by HRP catalysis in presence or absence of hydrogen peroxide are both emphasized [93, 114]. All the possible pathways in the HRP catalytic mechanism can be summarized as represented in **Figure I-17**. HRP-catalyzed oxidation of several molecules without any prior intervention of hydrogen peroxide can be possibly explained by the fact that native ferric enzyme might be able to oxidize the substrate directly leading to the ferrous form (Reaction 4, **Figure I-17**). This ferrous form is unstable, and is liable to react with oxygen to form the so-called compound II, which is the combination of ferric form with superoxide anion (Reactions 5). The same compound III can be obtained throughout two other pathways. The first one is a reaction between the native form of

the enzyme and the superoxide anion (reaction 6) and the second one is between compound III and an excess of hydrogen peroxide in the media (reaction 7) [113, 114]. It is already well known that the formation of compound III leads to an irreversible inactivated state of the enzyme [95, 109]. In summary, beside the three described HRP states in the classical catalytic cycle, two more oxidation states can be formed: a ferrous form ( $\text{Fe}^{\text{II}}$ ) and compound III.

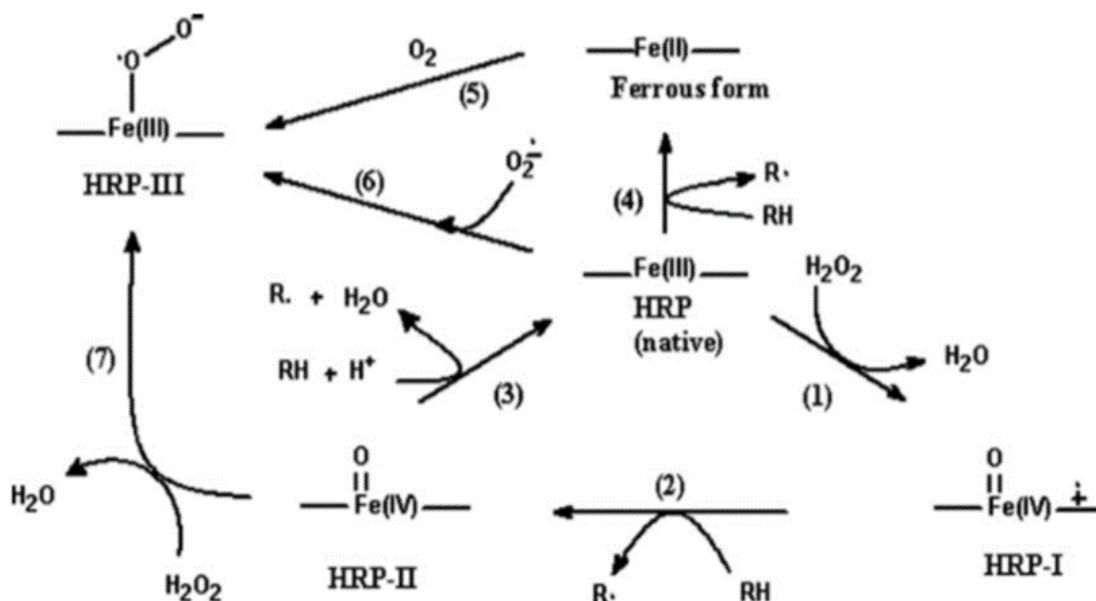


**Figure I-17: The classical peroxidase cycle and the pathways for the production of the redox forms ferrous and compound III (HRP-III). Reactions 1-3: classical cycle; Reaction 4: reduction of the ferric enzyme to the ferrous form; Reactions 5, 6, and 7: possible pathways for the formation of compound III. Reprinted from [114].**

In the absence of reducing substrates, excess of peroxides reacts with the enzyme, and gives rise to distinct species, compound III. Upon formation of compound I, excess of  $\text{H}_2\text{O}_2$  can act on this compound *via* several pathways: a catalase-like two-electron reduction reaction that restores the enzyme resting state, or a competing pathway that leads to the irreversible inactivation of the enzyme [109, 124]. The presence of reducing molecule in the medium plays an important role in preventing enzyme inactivation by  $\text{H}_2\text{O}_2$ .

### B. Laccases-mediated initiation

From a mechanistic point of view, the reaction catalyzed by laccase depends on the Cu atoms as summarized by the scheme in **Figure I-18**. These various copper centers drive electrons from a reducing substrate to molecular oxygen without releasing toxic peroxide intermediates.

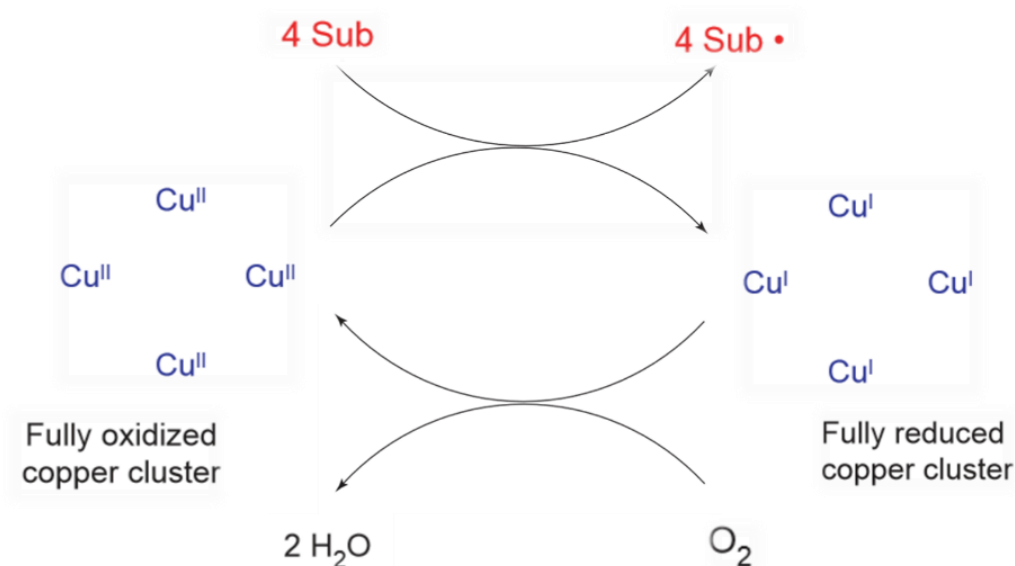


**Figure I-18: Schematic representation of a laccase catalytic cycle producing two molecules of water from the reduction of one molecule of molecular oxygen and the concomitant oxidation (at the T1 copper site) of four substrate molecules to the corresponding radicals. Sub: substrate molecule; Sub•: oxidized substrate radicals. Adapted from [125].**

A minimum of four Cu atoms per active protein is required. Three major steps can be recognized in the laccase catalysis of radical generation. First, the Type 1 (T1) copper atom is reduced by a reducing substrate, which therefore is oxidized. Then, the electron is internally transferred to the trinuclear cluster of T2 and T3 copper atoms. The last step is the reduction of a dioxygen molecule to water at the molecular level of the cluster, and the enzyme returns to its fully oxidized form [125].

In summary, laccases use oxygen as the electron acceptor to remove protons from the substrate. The overall outcome of such catalytic cycle is the reduction of one molecule of oxygen to two water molecules, and the oxidation of four substrate molecules. Then, this reaction produces

radicals that can spontaneously rearrange or can form dimers, oligomers, or even polymers. However, when the substrate cannot be directly oxidized by laccases, because they cannot penetrate easily in the enzyme active site or they have higher or lower redox potential, it is possible to use “chemical mediators”. These compounds act as intermediate substrates to interact or to react with the redox-potential targets [115, 117, 125]. **Figure I-19** shows the most common mediators incorporated in the laccase catalytic cycle.

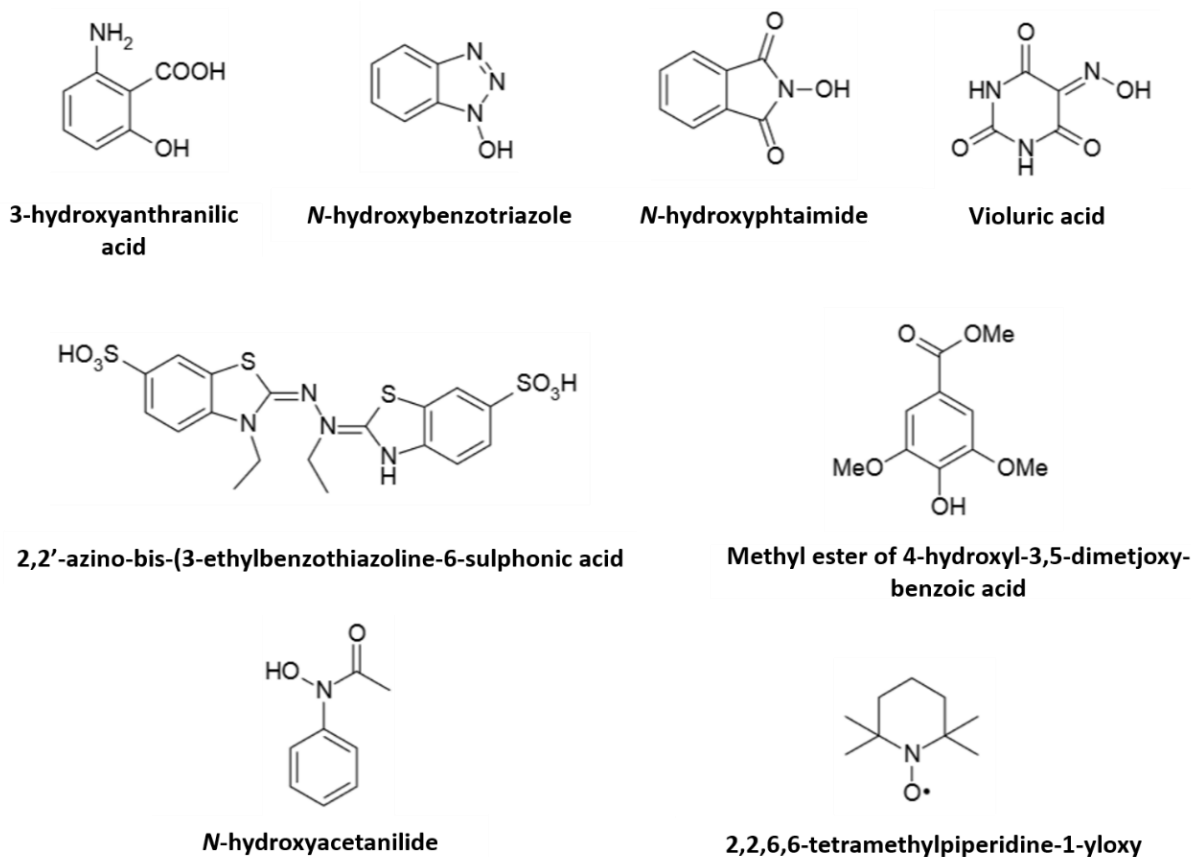


**Figure I-19:** Chemical structures of the most common laccase mediators.

### I.1.3.3. Influence of different parameters on the polymerization

*In vitro* enzyme-mediated polymerization of vinyl and aromatic monomers has been extensively studied for more than twenty years. Peroxidases and laccases have been used for the polymerization of styrene, acrylates and acrylamides, as well as polymerization of phenols and

anilines. Kinetic and mechanistic studies revealed that the enzymatic system, including the biocatalyst and its corresponding substrates plays a major role in obtaining an efficient polymerization. The effect of the experimental conditions on the polymer characteristics are reviewed in this part.

#### A. Enzyme-initiated radical polymerization of vinyl monomers

Enzyme-catalyzed radical polymerization of vinyl monomers such as acrylates, acrylamide, and styrene has been demonstrated in recent years, using mostly the ternary system including the enzyme and the oxidant and reducing species. The main current efforts within enzymatic approaches to vinyl polymerization aim at a significant control of polymer molecular weight and yield [126, 127].

Enzyme-mediated polymerization of acrylic monomers, including acrylamide, methacrylate, and hydroxyethyl methacrylate, was first reported by Derango *et al.* [91]. The polymerization occurred in the presence of enzyme and a large excess of oxidant without any mediator. The polymerization mechanism was not elucidated and no information was provided on the polymer characteristics or on the influence of the initiator system components.

Starting from this work, there is an ongoing discussion about the necessity of the reducing species (called mediator or initiator) to initiate the polymerization reaction. Earlier reports on mediator-free polymerization of acrylamide was performed using HRP as catalyst [91], but could not be reproduced by others [92]. One potential hypothesis of this apparent condition may be due to a very high concentration of hydrogen peroxide resulting in “unusual” heme-iron species [91], [109]. Indeed, oxidative degradation of heme resulting of Fe-release into the reaction medium might account for the Fenton-like generation of reactive oxygen species (ROS), which can be a potential initiator of acrylamide polymerization [79].

Kobayashi *et al.* (1998) reported enzymatic polymerization of acrylamide in water using laccase derived from *Pycnoporus coccineus* [13]. Without any initiator, laccase-catalyzed polymerization has been studied to produce polyacrylamide at temperatures from 50 to 80°C.

Polymers with  $M_n = 9,2-10 * 10^5$  g/mol were obtained with the highest yield of 70% at 65°C. However, the same reactions, but in presence of 2,4-pentanedione at room temperature, were more efficient, leading to 97% yield ( $M_n = 2,3 * 10^5$  g/mol).

In the presence of moderate oxidant concentration at room temperature, the nature and the concentration of the mediator has shown a major impact on the resulting polymer properties. For enzymatic vinyl polymerization, the authors used a ternary system including HRP, hydrogen peroxide and  $\beta$ -diketones to generate radicals in the oxidoreductive pathway. **Figure I-20** illustrates the chemical structures of the  $\beta$ -diketones that have been investigated for the enzyme-mediated radical polymerization of vinyl monomers. The influence of the  $\beta$ -diketones on the radical polymerization of acrylamide was studied by Teixeira *et al.* (1998) [93]. The results demonstrated that  $\beta$ -diketones are key compounds in the reactions. In details, regardless of the molecular structure, the yield and the molecular weight of polyacrylamide are the highest when acetylacetone (2,4-pentanedione) are used as mediator. The effect of  $\beta$ -diketones was also tested in the HRP-catalyzed polymerization of styrene and derivatives by Singh *et al.* (2000) [100]. They showed polymers with higher molecular weight are obtained when the methyl groups of 2,4-pentanedione were replaced by bulky phenyl groups, with no significant variation in yield. Good polymerization yields were obtained by using cyclic  $\beta$ -diketones. Detailed studies on the influence of the mediator structure on the enzyme activity are missing in both studies.

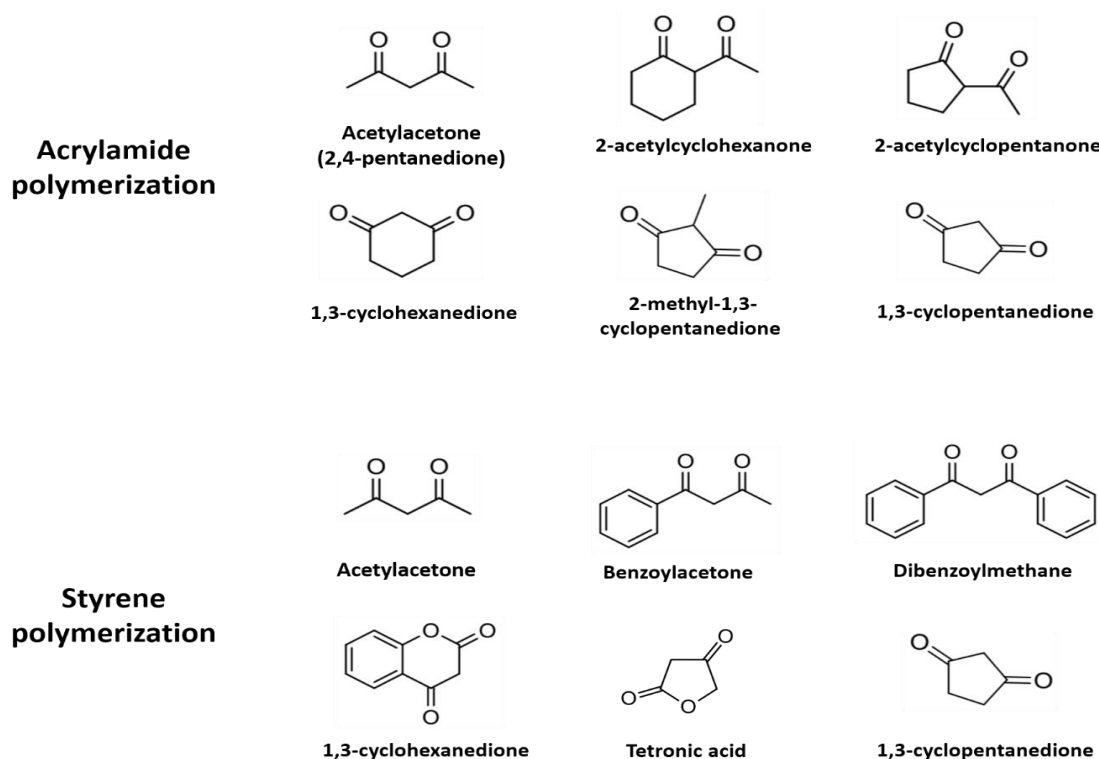


**Figure I-20: Chemical structures of the  $\beta$ -diketones that have been mostly investigated for the enzyme-mediated initiation of the acrylamide and styrene polymerization. Modified form [93, 100].**

The acetylacetone initial concentration affects also the molecular weight of the polymer in the HRP-catalyzed synthesis of acrylamide [96]. The results showed that increasing Acac concentrations lead to a lower viscosity and an increase of the polymerization yields. Obviously, the ratio of monomer to initiator  $[\text{Monomer}]_0/[\text{Initiator}]_0$  has a strong influence on the average size of the polymer. When this ratio was varied from about 1 to  $10^3$ ,  $M_n$  increases from  $10^4$  to  $10^6$  g/mol. The number of growing polymer chains increases with the initial Acac concentration [96]. Moreover, for a given acetylacetone concentration, it was also observed that monomer concentration has also an influence on the polymerization. The ratio of initiator to monomer  $[\text{Initiator}]_0/[\text{Monomer}]_0$  is also an essential parameter to favor the polymer propagation (Equation 2) instead of Acac dimerization (Equation 3) as shown in **Figure I-21** [92, 95]. Its value ranges in literature between 0.0034 and 0.033. It should be mentioned that all the above-mentioned effects and dependencies effects have also been observed for free radical polymerizations with traditional initiators.



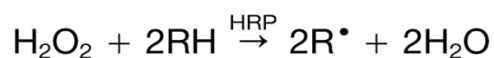


**Figure I-21: Commonly accepted reaction scheme of HRP catalytic cycle. Adapted from [92].**

Beyond the effect of mediators, many studies showed that biocatalysts and oxidant concentrations affect the polymer characteristics. HRP-catalyzed polymerization of linear acrylamide was carried out with different enzyme concentrations. Increased HRP concentration caused reduced average molecular weight of the polymer but an increase in polymerization yield [96]. **Figure I-22** shows the variation of the polyacrylamide molecular weight according to the initial concentration of HRP. A regular decrease of the polymer molecular weight was evidenced through the evolution of the reduced viscosity. Moreover, the authors noticed in this study that the molecular weight did not vary anymore with HRP concentrations higher than 2 g/l. Generally, increased yields of polyacrylamides are also obtained by increasing concentrations of laccases [98]. As a rule of thumb, increased yields of polyacrylamides are also obtained by increasing concentrations of laccases [98].

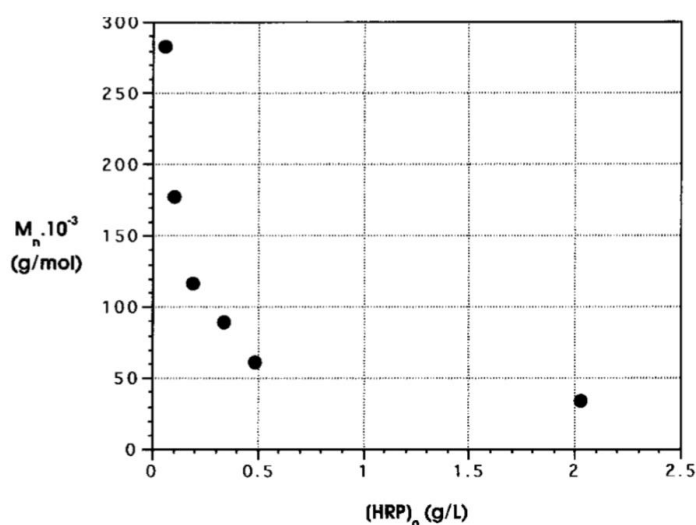


**Figure I-22: Variation of the polymer molecular weight depending on the initial concentration of horseradish peroxidase. [AAM]<sub>0</sub> = 0.64 mol/l; [Acac]<sub>0</sub> = 0.02 mol/l; [H<sub>2</sub>O<sub>2</sub>]<sub>0</sub> = 7 · 10<sup>-4</sup> mol/l. Reprinted from [96].**

Oxidant compounds involved in the enzyme catalytic cycle play also an important role in regulating the biocatalyst activity. For instance, polymerizations of acrylamides were studied with different hydrogen peroxide concentrations in order to determine its role in the catalysis. Durand *et al.* (2000) showed that H<sub>2</sub>O<sub>2</sub> concentration has no great influence on the molecular weight and on the polymerization yield, except at high concentration. Indeed, an excess of hydrogen peroxide can lead to the formation of compound III, the irreversibly inactive form of HRP [95, 96]. Particularly, when laccases are used as catalyst, molecular oxygen plays an important role. O<sub>2</sub> serves as stoichiometric oxidant to initiate the polymerization reaction. However, an excess of O<sub>2</sub> can also efficiently quench the radical polymerization. The polymer properties can thus easily be optimized by the control over the oxygen content in the polymerization reaction [98].

### ***B. Aromatics radical polymerization***

As for vinyl polymerization, the effects of the enzymatic components, biocatalyst and hydrogen peroxide, as well as the reaction temperature were investigated for the polymerization of both phenols and anilines [128].

In contrast to the above-mentioned polymerization of vinyl monomers, polymerization of phenols and anilines has been studied in detail in order to control the polymer structure, especially its molecular weight. Therefore, more parameters in addition to the components of the enzymatic process have been examined. Hence, many efforts have been made towards gaining control over the polymer characteristics by optimizing experimental conditions such as solvents, the addition of templates, and others. [79]

Due to the poor aqueous solubility of most aromatic compounds, the influence of co-solvents is frequently studied. Solvent compositions, such as type of organic solvent, buffer pH, and the mixed ratio greatly affected the yield, molecular weight and the solubility of the polymer. The polymerization of cardanol, a phenol derivative, has been examined in a range of hydro-organic mixtures based on phosphate buffer pH 7.0 or distilled water at room temperature using Soybean peroxidase (SBP) as catalyst [129]. With 1,4-dioxane as co-solvent, no polymer can be

recovered, whereas in a mixture of isopropanol/buffer (70:30 vol%) an insoluble powdery product was produced. Instead of buffer, distilled water yielded a mixture of oily soluble polymer and powdery product. SBP-catalyzed polymerization in acetone/buffer (75/25 vol%) led to 21% as polymerization yield, whereas HRP-catalyzed polymerization of cardanol could not proceed under the same experimental conditions. However, the HRP-catalyzed polymerization of phenol in 1,4-dioxane/buffer (80:20 vol%) produced a powdery polymer, suggesting the solvent selection is depending on the polyphenol monomer and on the enzyme. [130]

Experimental parameters other than the solvents can take part in the control of the polymer characteristics. A large number of oxidoreductase-initiated polymerizations of phenols and anilines have been investigated in the presence of templates. Poly(styrenesulfate) represents one of the widely applied templates in the polymerization of aniline to the conducting polymer form (emeraldine). In the absence of the template, aniline polymerizes with poor regioselectivity, yielding an insoluble and non-conducting polymer [79].

Other templates such as polymeric stabilizers have also been screened for the dispersion polymerization of phenol in order to improve the degree of polymerization [130]. The polymerization was performed using HRP as a catalyst in a mixture of 1,4-dioxane and phosphate buffer pH 7 60:40 vol.%. Water-soluble polar polymers, such as poly(acrylic acid) (PAA), poly(ethylene glycol) (PEG), poly(vinyl alcohol) (PVA), and poly(vinyl methyl ether) (PVME) were used as a stabilizer. In the presence of the stabilizers, the polymerization gave a stable dispersion of particles formed by a blend of the stabilizer and the polyphenolic polymer, except for PAA. The absence of the corresponding polymerization with PAA might be due to the loss of the HRP activity by its interaction with this stabilizer. The nature of the stabilizers also affects the yield and the particles size. Moreover, the enzymatic polymerization of phenols was also investigated in the presence of poly(ethylene glycol)-poly(propylene glycol)-poly(ethylene glycol) triblock copolymer (Pluronic) in water [131]. Micellar aggregates of phenol and Pluronic were achieved by hydrogen bonding interactions. This phenomenon greatly affected the polymerization behaviors by improving the regio-selectivity of the phenol polymerization. When Pluronic F68 was used as additive, homogenous polymerization proceeded leading to the formation of phenolic polymer with molecular weight higher than  $10^6$  g/mol. This is considered

an interesting advantage compared to the traditional enzymatic phenols polymerizations where the resulting product was precipitating immediately with an average molecular weight of only thousands.

In addition to the different templates and stabilizers, surfactants forming micelles were also used in the literature. An aqueous system using sodium dodecyl benzene sulfonate (SDBS) as surfactant, was tested for the HRP-catalyzed polymerization of phenol. The addition of 0.1 g of SDBS greatly improved the polymerization yield from 5% to 35%. Nevertheless, due to the solubilization effect of the micelles, increasing the SDBS amount led also to high yields up to 95%, but with moderate molecular weight [90]. In the same context, HRP-catalyzed polymerization of phenol was, recently, studied in the presence of an environmentally friendly system containing sodium dodecyl sulfate (SDS). The phenolic polymer was partially soluble in common solvents. High polymerization yields, from 85% to 97% were obtained in phosphate buffer with SDS concentrations ranging from 0.1 to 0.4 g [80].

#### **I.1.4. Potential applications of enzymatic polymerization**

During the last three decades, the scope of biocatalysis has been expanding thus improving biotransformation and new products synthesis. While many processes are at the laboratory scale, a subset of biocatalytic reactions has progressed beyond. The availability and application of enzymes at pilot and large scale opens up possibilities for further improvements at industrial level [132]. The use of enzymes for industrial synthetic chemistry is on the verge of significant growth, and biocatalytic processes can be carried out in organic solvents as well as in aqueous environments. The fact that the enzymes are the most effective catalysts, offering much more competitive processes compared to chemical ones, has resulted in different commercial enzyme-based processes in application areas such as medicine, pharmaceuticals, dairy industries, and others.

#### **I.1.4.1. Biocatalysts in fine and bulk chemical industries**

In industrial systems, synthetic materials are prepared by using basic materials from fossil resources such as coal, petroleum, and others. However, the increased consumption of such resources has led to an increase of atmospheric pollution, as well as depletion of these resources. Therefore, development of environmentally benign alternatives becomes urgently desired to synthesize polymers [133]. For instance, enzymatic methods for the synthesis of conducting polymers are well recognized. Peroxidases and laccases were mainly investigated for the synthesis of polyaniline, polypyrrole and other polymers [134].

#### **I.1.4.2. Biocatalysts in food industry**

In food industries, enzymatic polymerization has been used since long time to prepare raw materials. Moreover, a recent trend is to synthesize functional foods by enzyme-catalyzed syntheses, like low-calorie sweeteners and sugars. Enzyme-catalyzed synthesis of prebiotics is now acquiring an interesting place in food industry. They are dietary substances composed of non-starch polysaccharides and oligosaccharides which offer many health benefits including improvement in the digestion stimulation, the enhancement of mineral absorption and the protection against certain pathogenic bacterial infections [135]. The use of enzymes in the synthesis of such polymers has provided the benefits of high-production yields at low cost and using simple processes. By this approach, different polysaccharides such as difructose anhydride, fructo-oligosaccharides, galacto-oligosaccharides have been synthesized by using inulin fructotransferase, fructosyltransferase,  $\beta$ -galactosidases, respectively [136].

#### **I.1.4.3. Application of biocatalysts in biomedical and pharmaceutical fields**

Application of enzymes for producing diverse types of chemical and biological substances has become a proven technology in pharmaceutical industries. Indeed, the biocatalysts provide a powerful tool for producing enantiomeric compounds with high stereo- and regioselectivity, by reducing the process and the waste. In this context, the biotransformation field has emerged as a real alternative to traditional routes. Enzymatic modification is widely used at industrial scale in order to synthesize building blocks for the synthesis of enantiopure drugs. Hydrolases, such as

lipases, serine endopeptidases, and penicillin G acylases are the most employed enzymes, as well as oxido-reductases including peroxidases and dehydrogenases [137, 138].

Enzymatic modification is also well-known in biomedical fields. An important application is worth to be highlighted in this context. Vitamin C-functionalized poly(methyl methacrylate) is prepared by enzyme-catalyzed synthesis and modification for the osteogenic differentiation of bone marrow-derived stem cells [139]. L-ascorbyl methyl methacrylate was synthesized by lipase-catalyzed transesterification reaction. The polymerization of the corresponding product was accomplished by HRP-catalysis in presence of hydrogen peroxide and 2,4-pentanedione as oxidant and reducing species, respectively. The polymer showed antioxidant properties as the structure of ascorbic acid was maintained [140]. The proliferation and the osteogenic differentiation of bone marrow-derived mesenchymal stem cells were investigated in the presence of the functionalized polymer. The results showed that the AA-PMMA films established, at optimal concentrations of covalently coupled ascorbic acid, a good microenvironment that preserved the capacity of stem cells to undergo osteogenic differentiation *in vitro* [139].

## I.2. Molecularly imprinted polymers

Molecular recognition became a popular term since the early 1980s, covering a set of phenomena that are crucial in biological systems. It refers to the specific interaction among two or more molecules through different mechanisms. For instance, molecular recognition is referred to when interactions are observed between receptor-ligand, enzyme-substrate, antigen-antibody [141]. The ability of biological hosts to strongly and specifically bind to a particular structure has inspired chemists and biochemists. Much modern chemical research has been developed since decades, motivated by the prospect to design new artificial molecular recognition systems for various applications. For instance, stable recognition elements can be used in robust analytical devices for the detection of trace levels of compounds in complex matrices. Alternatively, similar recognition elements can play a major role in the separation of toxic or other compounds from food and biological fluids, and even in targeted delivery of drugs. If the sites can be made to catalyze chemical reaction, the resulting 'enzyme mimics' can provide a prominent tool to achieve efficient catalysis.

Inspired by the natural molecular recognition phenomena, molecular imprinting technology has been extensively developed since the first well-known works of Mosbach (1981) and Wulff (1972). This technology is thus a simple way to create tailor-made receptor sites within a synthetic polymer. Molecularly imprinted polymers (MIPs) are synthetic bio-mimetic materials capable to specifically recognize and bind target molecules with the same affinity as natural receptors. These imprinted polymers, due not only to their specificity and selectivity, but also to their physical and chemical stabilities, have been applied in many areas [142, 143] such as in immunoassays [144-146], separation [147], sensors [148-151], and catalysis [152-153]. More recently, the MIPs application in physiological systems is increasingly investigated with the development of these materials in drug discovery and as delivery system [154-158].

### I.2.1. Principle of molecular imprinting

Molecularly imprinted polymers (MIPs) are robust molecular recognition elements with antibody-like ability to bind and discriminate between molecules, inspired by the natural phenomena of molecular recognition [159]. The synthesis of such materials includes the copolymerization of functional monomers and cross-linker in the presence of the target molecule, which serves as template to create specific cavities in the polymeric matrix (**Figure I-23**). The template may be small molecules such as amino acids [160], drugs [155], metabolites [161], herbicides [162], biological macromolecules proteins [163, 164], microorganisms, crystals [165] etc.

**Figure I-23** illustrates the concept of the molecular imprinting based on the formation of a complex between the template and the functional monomer prior to polymerization, through covalent or non-covalent interactions. This complex is then fixed in space by copolymerization with a cross-linker by photo or thermal initiation. After polymerization, the template is extracted using an appropriate solvent selected to disrupt the interactions between the template and the functional monomer. Removal of the target molecule from the polymeric matrix leaves cavities that are complementary to the target molecule in size, shape, and chemical functionality. In this way, a molecular memory is formed within the polymeric matrix, capable of specifically and selectively rebinding the target molecule [166].



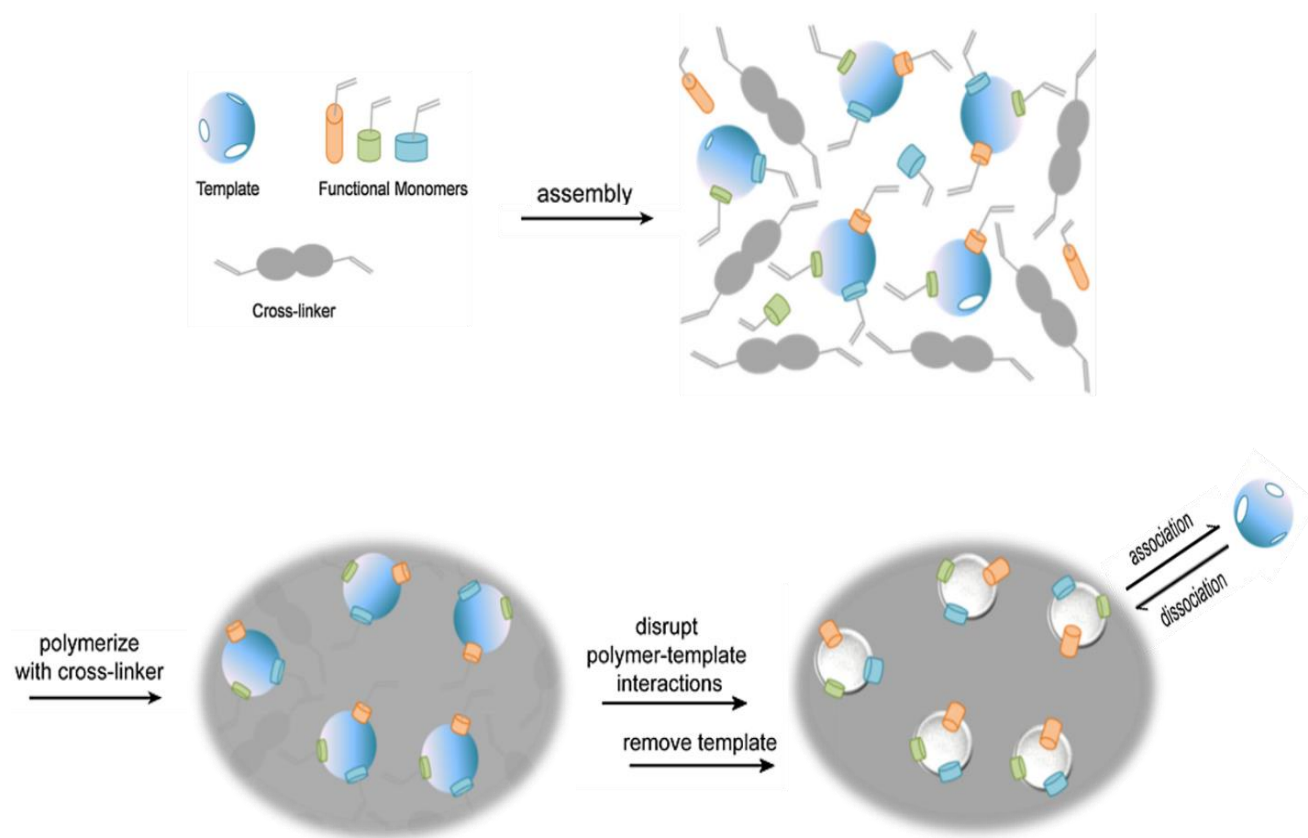


**Figure I-23: Highly schematic representation of the molecular imprinting process. Adapted from [167]**

### I.2.1.1. Background of the molecular imprinting technique

In 1931, M.V. Polyakov introduced firstly the concept of molecular imprinting in silica materials for chromatography application. Briefly, he studied the effects of small molecules as benzene, toluene, or xylene on the silica pore structures. The extent of silica adsorption of the different additives was shown to be dependent on the structure of additive present during the drying process of the silica. This selectivity was suggested to arise from structural changes within the silica induced by the chemical nature of the additive.

However, the 1970's marked really the beginning of molecularly imprinted technology when Wulff and Klotz independently reported the preparation of organic polymers with predetermined

ligand selectivities. Klotz and Takagishi developed the synthesis of methyl orange-templated poly(ethyleneimine) polymers. The cross-linking was achieved via the formation of disulphide bridges in presence of the methyl orange, and the yielding MIPs showed enhanced adsorption in comparison to the polymers which were cross-linked in absence of the template [168].

In the same year, Wulff and Sarhan described the synthesis of an imprinted polymer for the chiral recognition of D-glyceric acid. The synthesis was achieved using a reversible covalent approach by the co-polymerization of divinylbenzene in presence of a polymerizable template, D-glyceric-(*p*-vinylanilide)-2,3-O-*p*-vinylphenylboronate, which was hydrolyzed after polymerization. This covalent approach for MIP synthesis required the formation of a covalent bond between the template and one or more monomers prior to polymerization. The template had to be removed by chemical cleavage, leaving the functional groups that could form again the covalent bond upon binding of the target [169].

The concept of molecular imprinting was later reconsidered from a biochemist point of view by Mosbach in the 80s. The introduction of the general non-covalent approach by the group of Mosbach was a great development that broadened significantly the scope of molecular imprinting. In this approach, the complex template-monomer is formed by interactions such as hydrogen bonds, ionic bonds, van der Waals forces, and hydrophobic effect [170]. These MIPs are analogous to antibodies. They are referred to as antibody mimics or 'plastic antibodies' since they share the most important feature of the natural receptor molecules: the capability to bind specifically to a target molecule. However, MIPs are larger than antibodies in size, rigid and insoluble [166].

### **1.2.1.2. Imprinting matrix**

Generally, MIPs are synthesized using three approaches: covalent, non-covalent and semi-covalent. Currently, the non-covalent approach became the most widely applied technique to prepare molecularly imprinted polymers due to the easy complexation step which consists of the self-assembly between template and functional monomers and to the large variety of available

commercial functional monomers. This approach has been selected for the work developed in this thesis. It allows to generate molecular recognition materials for a diverse range of analytes [143]. However, one of the disadvantages with this method is that the interaction between template and functional monomers is generally weak, as compared to covalent binding. Generally, the MIPs synthesis based on non-covalent approach needed an excess of functional monomers to drive the equilibrium towards the formation of the monomer-template complex. Thus, some excess functional monomers are randomly incorporated in the polymer matrix increasing the non-specific interactions. Another important feature of MIP is the polymeric matrix rigidity to maintain the structure of binding sites and preserve chemical and physical stabilities of the polymer. However, a high flexibility is also required to ensure a fast equilibrium between the binding and the release of the template within the cavities. These features are contradictory and require a careful optimization during the synthesis. MIPs design is still challenging and complex and several experimental conditions have to be carefully selected in order to obtain MIPs with high selectivity and specificity. In the following, we have focused our review on such parameters as the template, the functional and cross-linking monomers, as well as the solvents and the polymerization methods [171].

### A. Template

The target molecule is of central importance in all molecular imprinting processes. It directs the arrangement of the monomers functional groups prior to polymerization. Different criteria should be taken into consideration for the template selection. The target molecule should be chemically inert under polymerization conditions, such as heat, or U.V lights. Template with any polymerizable or radical inhibitor functional groups can inhibit or retard the polymerization and affects the polymerization yield or the recognition properties of the MIP. In these specific cases, a structural analogue of the target molecule can be used as template during the polymerization [172]. MIPs have been prepared for the specific and selective recognition of a wide range of target molecules. Small analytes such as amino acids, drugs, and pollutants and herbicides are imprinted as well as macromolecules such as polypeptides, whole proteins, bacteria, and viruses, and the established polymers are considered almost as routine.

### B. Functional monomer

Functional monomers have to be carefully chosen for the MIPs synthesis based on the complementarity of their functional groups with target molecule [173]. Indeed, the complex formed between functional monomer and template has to be strong enough, in order to bind efficiently and specifically the template.

In non-covalent approach, an equilibrium reaction between the free and the complex template is usually observed. Thus, in order to drive this reaction toward the complex formation, an excess of functional monomers have to be added in the polymerization mixture. Generally a ratio monomer to template used is from 4:1 to 10:1, but it can go up to 500:1. A large number of commercially available functional monomers, or a combination of them, have been used to synthesize MIPs via this approach [173]. Examples of monomers used for non-covalent imprinting are shown in **Figure I-24**.

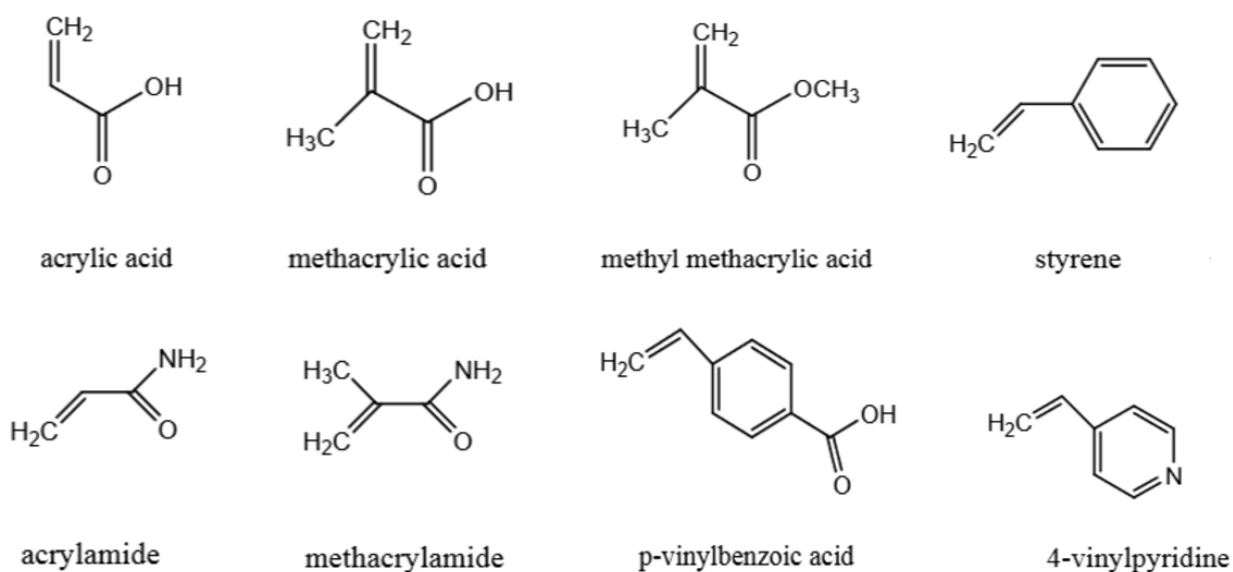


**Figure I-24: Functional monomers commonly used in the non-covalent molecular imprinting.**

Monomers can carry basic (e.g. vinylpyridine), acid (methacrylic acid), hydrogen bonding (methacrylamide), or hydrophobic (styrene) functionalities [174]. The functional monomers can

provide ionic, hydrophobic, van der Waals and hydrogen bonding to interact with the template molecule. AA and MAA are often employed as functional monomers, since the carboxyl group is a hydrogen donor and a hydrogen acceptor at the same time, and an ion pair interaction can be established with a basic template.

### C. Cross-linker

The cross-linkers play a major role in stabilizing the binding sites and providing the mechanical stability of the polymer, as well as controlling the polymer morphology and solubility. A large number of cross-linkers have been used in MIP synthesis. Some of the commonly used cross-linkers are presented in **Figure I-25**. Generally, cross-linkers are usually multi-functional monomers bearing two or more vinyl groups. Their co-polymerization with the functional monomers results generally in non-linear polymer architectures, which can be conventionally classified into branched polymers, micro- or nanogels, and microscopic tridimensional networks.

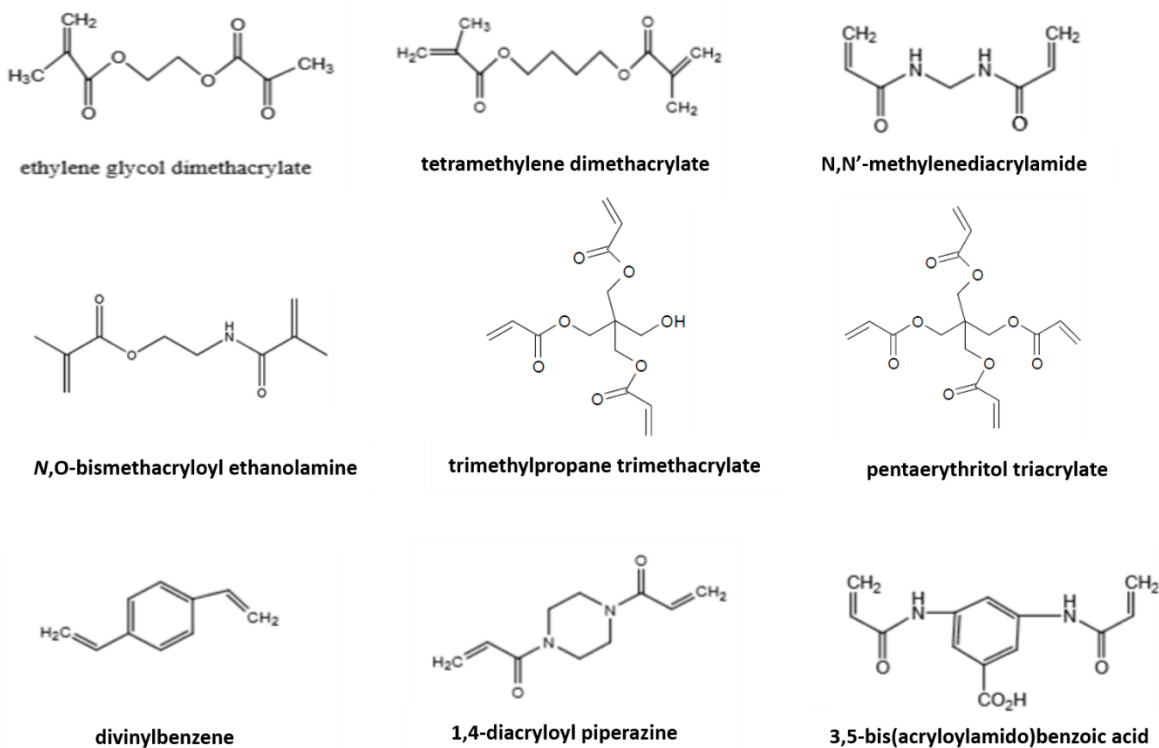


**Figure I-25:** Cross-linkers most commonly used in the non-covalent imprinting.

Some of the cross-linkers can also act as functional monomers at the same time such as N,O-bismethacryloyl ethanolamine (NOBE).

The types and amounts of cross-linkers have an impact on the selectivity and binding capacity of the MIPs by affecting the rigidity and the flexibility of the polymeric matrix, as well as by forming non-covalent interactions with the template molecules. The cross-linker that exhibits a lower interaction with template generates MIPs with lower non-specific binding. Philip *et al.* studied the effect of cross-linker for *S*-propranolol imprinting on MIP binding properties. Non-specific binding was lower for MIP prepared using DVB as cross-linker compared to cross-linker (EDMA) forming hydrogen bond with template [175]. Similar phenomenon was observed for the drug zidovudine (AZT)-imprinted polymer, which was prepared three cross-linkers (EDMA, TRIM and DVB). A higher imprinting factor (IF=1.85) was obtained with DVB cross-linked MIPs compared with other tested cross-linked polymers [176].

Cross-linker density affects the polymer rigidity, impacts on the capability of holding the cavities and the diffusion efficiency of the target molecules. A proper amount of cross-linking, generally ranged from 25% to 83% needs to be chosen, depending on the MIP application. Fortunately, it is possible to rationally predict how this variable impacts the performance of MIPs, using experimental design. For instance, Rossi and Haupt reported a Doehlert's design approach that shows the influence of the kind and the degree of cross-linking on the molecular recognition. The model system allows then to screen the evolution of MIP binding capacity as a function of different parameters, and appears to be a powerful tool to seek for the best MIP composition [177].

#### ***D. Solvent***

The majority of molecularly imprinted polymers are synthesized in aprotic and low polarity organic solvents such as chloroform, or toluene, in order to maintain the recognition between template and functional monomer by electrostatic interactions and hydrogen bonding [178]. Polar protic solvents such as alcohol and water are generally excluded. However, more polar solvents like acetonitrile or water-containing mixtures have been used as porogen to solve the

solubility problems when the template or other reagents are polar compounds insoluble in organic solvents [179]. Such porogens are also used when the interaction template-monomer can be achieved better in polar environment. For instance, the herbicide 2,4-dichlorophenoxyacetic acid, bearing an acidic group with aromatic ring, was imprinted by Haupt *et al.* in a mixture of methanol/water (4:1, % v/v) using a basic monomer, 4-vinylpyridine [180]. The interactions are ionic with the carboxylic group and  $\pi$ - $\pi$  stacking with the aromatic ring. These strong interactions allow the formation of the complex with specificity in a polar environment. NMR titration experiments confirmed these observations [181]. Nevertheless, a few exceptions of MIP synthesis for small molecules in water systems do exist [182].

### ***E. Methods of polymerization***

Most of the MIPs are synthesized by free radical copolymerization of vinyl monomers with an excess of cross-linking divinyl monomer in the presence of solvent acting as porogen. The polymerization reaction conditions impact on the binding affinity, selectivity, and number of binding sites within the polymer matrix.

Free radical polymerization (FRP) had been adopted in the molecular imprinting community as a conventional method for MIP synthesis, known for its universality and flexibility, as well as its application to a wide range of commercially available monomers. Free radical polymerization (FRP) can be fine-tuned with respect to the type and amount of solvent, the concentration of monomers, cross-linkers and initiators, as mentioned in the previous sections. However, in order to obtain a more homogeneous polymer matrix, controlled/living radical polymerization (CRP) including ATRP, RAFT and iniferters, may be used [167]. CRP methods allow having a controlled molecular weight and molecular weight distribution from an expanded range of monomers [173], and have been used for the synthesis of MIPs. For instance, a bulk polymer for covalent imprinting of bisphenol A (BPA) was prepared by ATRP and was found to have a higher specificity as compared to conventional MIPs [183]. Additionally, bulk polymer for *S*-propranolol was synthesised by both RAFT and FRP; the RAFT-polymers showed higher affinity towards the template [184].

Depending on the desired applications, these materials can be synthesized in a variety of physical forms through radical polymerization in a free or controlled state by different polymerization methods. Traditionally, MIPs have been usually prepared as monoliths by bulk polymerization. Nowadays, most efforts are directed towards the preparation of uniformly spherical micro- or nanoparticles and other more sophisticated MIP forms such as membranes, nanocapsules, core-shell, and nanogels as shown in **Figure I-26**. These formats are obtained by different strategies for the polymerization including suspension or precipitation polymerization, multi-step swelling, surface or grafting from-polymerizations.

#### ❖ Bulk polymerization

Bulk polymerization is a conventional method for preparing MIPs. Template, monomers, cross-linkers as well as initiator are mixed in a small volume of porogen. Polymerization is then followed by mechanical grinding of the resulting polymer, yielding irregularly shaped micrometer-sized particles. In fact, it is fast and simple in its practical execution and it does not require particular operator skills or sophisticated instrumentation. The main disadvantages are that the process is time-consuming since grinding is needed after polymerization and the polymerization often results in polymers with a random shape and a broad size distribution, hence limiting their applications. Moreover, the overall yield of bulk polymerization is relatively low, from 50% to 75% of the initial amount of bulk polymer caused by the loss of substantial loss of useful polymer upon grinding [171].

#### ❖ Polymerization for micro/nanoparticle synthesis

Recently, there is a growing demand for MIPs tailored in specific physical forms. These kinds of materials are needed nowadays in a wide range of applications such as high-performance-chromatographic columns, capillaries for electrophoresis, solid-phase extractions, drug delivery, biosensors and many others. As will be discussed in the following section, many different polymerization methods have been developed moving from traditional to more original approaches in order to obtain predetermined micro/nano scaled physical forms of MIPs.



- *Suspension polymerization*

Suspension polymerization is by far the simplest and the most common method for MIP preparation in the form of particles. A monomer or a mixture of monomers is dispersed by strong mechanical agitation into droplets suspended in a second liquid phase in which both monomer and polymer are essentially insoluble. The monomer droplets, which are larger than those in a true emulsion, are then polymerized while dispersion is maintained by continuous agitation [185]. Highly cross-linked polymers in form of regular spheres are obtained. However, the limitations of this technique arise from the use of water which is an immiscible phase for the most commonly used monomers. Its polarity and high hydrogen bonding capability is well-known to be unsuitable for MIP and greatly affect the monomer-template interactions [173]. Despite this drawback, many MIPs have been prepared in literature with high selectivity and specificity. For instance, in a very recent study, efficient magnetic MIP beads were obtained by suspension polymerization using methacrylic acid (MAA) as functional co-monomer, 2,2'-azobisisobutyronitrile (AIBN) as a initiator and ethylene glycol dimethacrylate (EGDMA) as a cross-linker. The MIP was applied for the removal of dibenzothiophene, a sulphur compound, from fuels. Relatively high specificity and selectivity towards the template have been obtained [186]. Nevertheless, in order to avoid the use of water that often hinders the formation between template and functional monomers, liquid perfluorocarbons have been used as a more compatible continuous phase [187]. Other dispersants, including silicon oil [188] or mineral oil [189] can be used as well.

- *Emulsion polymerization*

Emulsion polymerization is related to the previous methodology. The monomer phase is dispersed in a continuous phase of immiscible solvent. In emulsion polymerization, the resulting dispersion is stabilized by the addition of surfactant, which forms micelles around the monomer droplets and allows to reach smaller particle sizes from tens to hundreds of nanometers. Moreover, there are different methods for achieving emulsion polymerization such as mini-emulsion and micro-emulsion [190], inverse emulsion [191], and core-shell emulsion [192].

- *Precipitation polymerization*

Precipitation polymerization is a surfactant-free and easy method to prepare spherical MIP particles with high polymerization yield in a homogenous phase. Particles grow and precipitate once they insoluble become due to their size. This method became the most commonly employed method for MIP preparation in many applications [190]. However, there is just one drawback of this technique, which is low monomer concentration and an excess of solvent. Such high dilution conditions negatively affect the stability of the template-monomer complex. This problem is usually overcome in literature by the careful choice of suitable monomers that can establish strong interactions with the template [193].

- *Micro/Nanogel synthesis*

Micro- or nano-sized imprinted polymers are of great importance in many biomedical applications including biosensors for diagnosis, separation and most interestingly in drug delivery as potential carriers for bioactive molecules. They could be prepared by post-dilution, early termination or high dilution methods [190]. Post-dilution method is used to prepare homogenous nanogels with high yield. It involves polymerization at high monomer concentration in a suitable solvent, while macrogelation is avoided by diluting the solution [194]. Although the post-dilution method provides high yields, it often relies on thermal polymerization, which might interfere with the imprinting process [195]. Also, it is difficult to scale up since the exact moment in time needs to be found to dilute the system before macrogelation occurs. To overcome this problem, early termination can be used to prepare nanogels using a CRP initiator like an iniferter. For example, a dendritic multi-iniferter allowed the synthesis of MIPs of approximately 50 nm with very high imprinting factor (>20) [196]. One drawback for this method is the very low yield of nanogels (often less than 1%), since the early termination after the initial formation of seed particles leaves much unreacted monomer. The high dilution is the most used strategy to prepare micro or nanogel, especially in proteins imprinting. An example of MIPs microgels prepared in high dilution polymerization showed ability to inhibit the enzyme activity of trypsin MIPs were prepared by testing a wide range of

functional and cross-linking monomers and relatively high affinity and selectivity for trypsin were obtained [164].

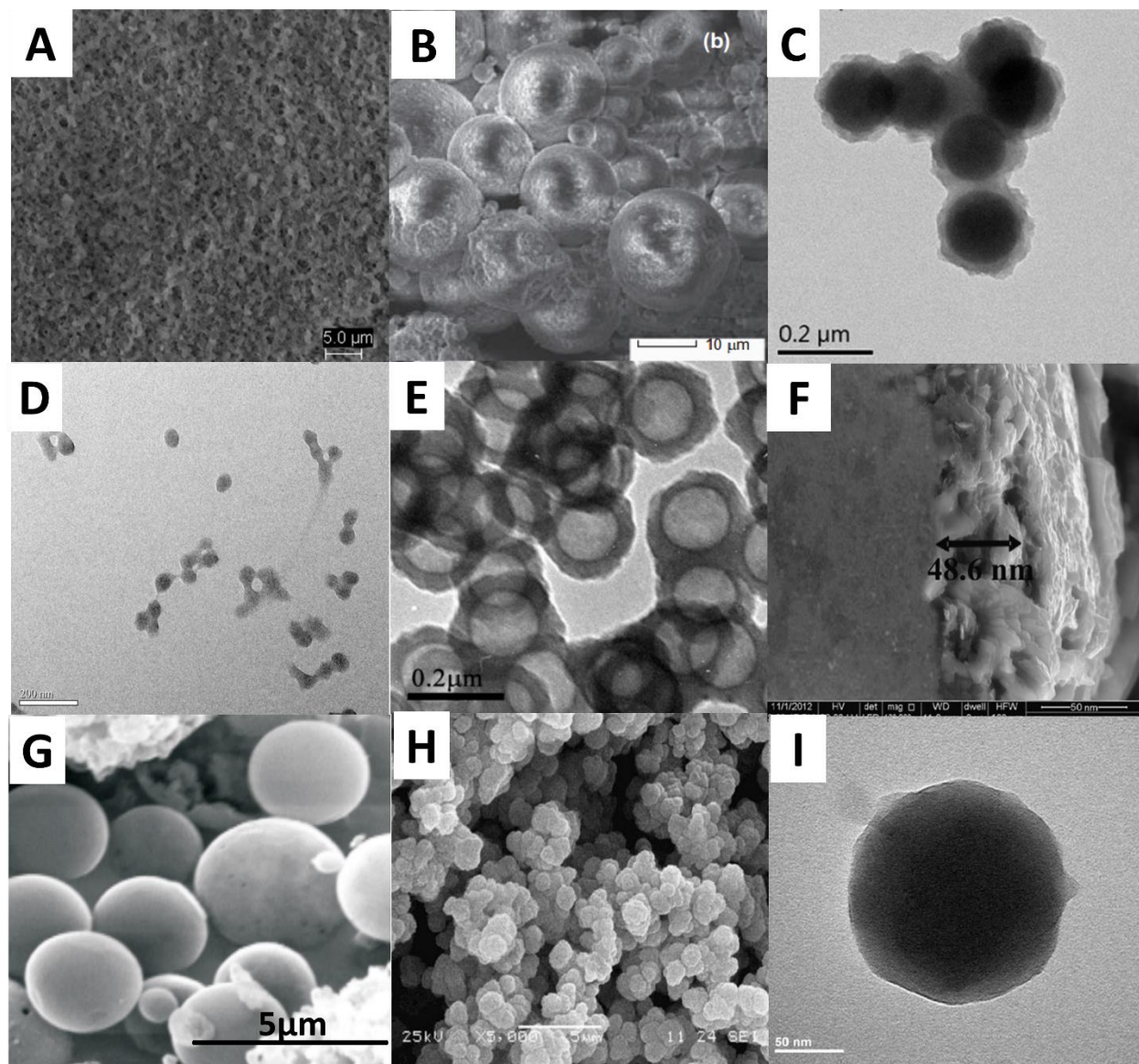


**Figure I-26: Characterization of different physical forms for molecularly imprinted polymers synthesized by different strategies: (A) SEM photos for MIP membrane prepared by immersion polymerization [197]; (B): SEM photos for magnetic MIP beads prepared by suspension polymerization [185]; (C): TEM photos for MIP silica beads [198]; (D): TEM photos for MIP nanoparticles (43 nm) prepared by precipitation polymerization [199]; (E): TEM photos for MIP nanocapsule prepared by emulsion polymerization [198]; (F): TEM photo for a side view of MIP nanofilm [162]; (G): SEM photos for MIP microspheres prepared by two-step seed swelling polymerization [200]; (H): SEM photo for monolithic MIP prepared by *In situ* polymerization [201]; (I): TEM photos for core-shell MIP prepared by emulsion polymerization [192].**

## **I.2.2. Development of water-compatible molecularly imprinted polymers**

The majority of molecularly imprinted polymers are prepared by non-covalent approach in aprotic and low polarity organic solvents. However, these MIPs for small organic molecules failed to show specific bindings in aqueous solutions, where template binds non-specifically to the MIP matrix due to hydrophobic effects. This is in contrast to biological receptors, and limits the use of MIPs in many important applications in biomedical and environmental fields, since the most of the target molecules are present in aqueous media, such as bodily fluids, drinking water, and wastewater.

Therefore, it is important to develop water-compatible MIPs that can bind their target molecules in a specific and selective manner in an aqueous phase. In addition, problems with the solubility of the ingredients or their structural integrity sometimes require achieving the imprinting directly in aqueous media.

### **I.2.2.1. Synthesis of water-compatible MIPs in organic solvents**

Recent developments in the field of water-compatible MIPs are the development of novel systems for the controlled delivery of a wide range of drugs. Delivery drug systems are generated for anti-inflammatory molecules such as *p*-acetaminophen (paracetamol) [202], and diclofenac [203, 204], as well as anti-cancer therapeutic agents such as 5-fluorouracil [155], aminoglutethimidine [205], and paclitaxel [206]. A MIP-based nicotine transdermal delivery system is also developed as an aid to smoking cessation therapy [207].

As a new class of synthetic receptors, molecularly imprinted polymers have shown a great potential in many applications such as biomimetic assays and sensors [208]. For sensor purposes, hydrophobic effect is a considerable problem which can largely limit the MIP application, since only specific binding is of interest in this field. Interestingly, many efforts have been devoted for

the development of improved procedures towards water-compatible MIPs, with an emphasis on tuning the polarity of the pore wall of the MIPs [209]

In a particular MIP synthesized in organic solvents or mixtures, binding sites are optimized to bind the template in similar solvents and will not necessarily bind this target in water. This results from the fact that MIP characteristics in polar solvents differ significantly from those in apolar media. Many efforts have been devoted to address this issue in the past two decades and various strategies have been developed as will be subsequently detailed. **Table I-4** summarizes some of the prominent examples water-compatible molecularly imprinted polymers with emphasis on the target molecule, MIP formulation, and the strategy for the improvement of the MIP behavior in aqueous media.

❖ *Use of conventional imprinting approaches and optimization of the binding conditions*

In 1995, Mosbach and colleagues presented their work about the application of MIPs as plastic antibodies. Non-covalent imprinting was used to synthesize MIPs for the recognition of enkephalin and morphin by using methacrylic acid (MAA) and ethylene glycol dimethacrylate (EGDMA) as functional and cross-linking monomers in acetonitrile. The radioactivity ligand binding analyses were assessed in different organic and aqueous solvents. In particular, the MIPs proved to be applicable in buffer (+10% of ethanol) despite their weaker affinity and cross reactivity in aqueous media compared to toluene or acetonitrile [210].

Following these encouraging results, Haupt *et al.* reported the synthesis of water-compatible MIPs for the recognition of an herbicide, 2,4-dichlorophenoxyacetic acid (2,4-D), by using the functional monomer 4-vinylpyridine (4-VP) and EGDMA as cross-linker. The synthesis was achieved in a hydro-organic mixture of methanol/water (4:1). As the polymers were prepared to be used in aqueous media and involved charged species, the right pH was important. It was found that the obtained MIP had good affinity and high template selectivity in 20 mM phosphate buffer pH 7.0 containing 0.1% Triton X-100 as nonionic surfactant [180].

Extensive studies have been carried out that showed that some MIPs could be used in aqueous media for the recognition of small analytes despite their preparation by non-covalent approach in

organic solvents. Different optimizations aminoglycanes were necessary to improve the binding conditions such as the kind of buffer used and their pH values [178, 211], as well as the amount of the added organic solvent [212].

❖ *Use of specially designed functional monomers*

One of the strategies developed before to obtain water-compatible MIPs was the use of special functional monomers bearing strong interacting groups towards the template. For this, a series of such monomers have been rationally designed and synthesized. The following **Figure I-27** their chemical structures. For instance, styryl amidines (**A**) were used in the preparation of water-compatible MIPs for the recognition of phosphate templates in aqueous media. Polymerizable ureas (**C and F**) showed very strong non-covalent interaction with a series of templates such as antibiotics, such as riboflavin. Similar results were obtained with **D** and **G** for the recognition of ampicillin [209].

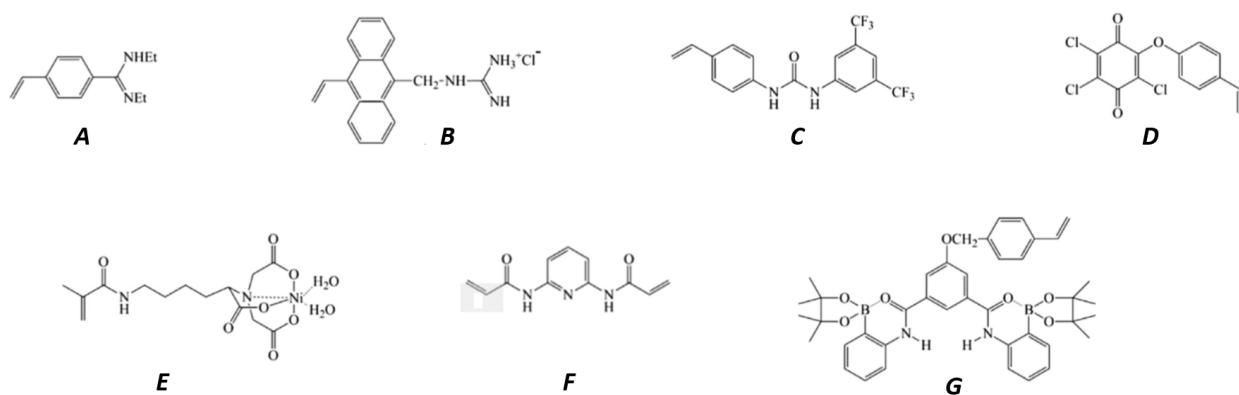


**Figure I-27:** Chemical structures of the specially designed functional monomers for the preparation of water-compatible MIPs. **A:** *N,N'*-diethyl(4-vinylphenyl)amidine; **B:** 9-(guanidinomethyl)-10-vinylanthracene; **C:** 1-(3,5-bis(trifluoromethyl)phenyl)-3-(4-vinylphenyl)urea); **D:** 2,6-bis(acrylamide)pyridine; **E:** 2,2'-((1-carboxy-5-methacrylamidopentyl)azanediyl)diacetic acid-Nickel(II); **F:** 2-(4-vinylphenoxy)-3,5,6-trichlorobenzoquinone; **G:** 5-(4''-vinyl)benzyloxy-1,3-bis[2'-(3''',3''',4'',4''-tetramethyl-2'',5''-dioxaborolanyl)phenylcarbomoyl]benzene. Reprinted from [209]



❖ *Use of hydrophilic functional and cross-linking monomers or comonomers*

One approach among the others, which have been studied, has to overcome the non-specific hydrophobic bindings of the target, which are often induced in water, by the synthesis of a more hydrophilic MIP [213]. To this end, many hydrophilic functional monomers (or comonomers) such as acrylamide and 2-hydroxyethyl methacrylate, as well as cross linkers (*N,N'*-ethylene bisacrylamide, *N,N'*-methylene bisacrylamide, have been introduced to the MIP formulation in order to enhance the MIP surface hydrophilicity [209]. For instance, MIP as solid-phase extraction have been developed for the selective removal of sildenafil from plasma samples. MAA and EGDMA were used as functional and cross-linking monomers, respectively. HEMA was also introduced as hydrophilic comonomer. The synthesis was achieved in trichloroethane. Binding properties were evaluated in acetonitrile, water, as well as spiked plasma. The obtained results proved that the resulting MIP could be a very efficient material for the selective extraction of sildenafil from aqueous solutions as well as plasma. The polymer compatibility in aqueous samples was improved significantly by using HEMA compared to what has been done in literature before, especially for solid phase extraction [214]. In another recent study, MIPs for the recognition of 2,4-D were synthesized. Different functional monomer have been tested such as 4-VP, acrylamide and styrene. The results showed that acrylamide and styrene mixed together led to best imprinting factor (IF=2.41), compared to the use of only one monomer like styrene (IF=1.35), acrylamide (IF=1.55) and 4-VP (IF=1.22) [215], although these IF are typically much lower than those obtained with the original (less hydrophilic) MIP composition for 2,4-D [180].

❖ *Surface post-modification approaches by controlled radical polymerization (CRP)*

Grafting hydrophilic polymer layer onto the surfaces of materials was shown to readily improve their hydrophilicity. This strategy had been used in literature for the preparation of more water-compatible MIPs. Controlled radical polymerization depends on creating a dynamic equilibrium between active and dormant species, which leads to very low radical concentrations in the polymerization systems and thus negligible radical termination and eventually controlled polymerizations. Normally, these polymerizations have a 'living' character, that is, once stopped by shifting to the dormant state, they can be re-activated to proceed polymerization with new, for

example hydrophilic monomers. In a study by Pan *et al.*, water-compatible MIPs for the recognition of 2,4-D was obtained by RAFT-polymerization of 4-VP and EGDMA in (methanol/water 4:1 v/v). Polymer brushes were grafted onto the resulting MIP/NIP microspheres via surface-initiated RAFT-polymerization of *N*-isopropylacrylamide. Binding properties of both MIPs and NIPs were assessed in both methanol/water and pure water. Both the ungrafted MIP and NIP showed high binding, mainly due to their rather high surface hydrophobicity. Interestingly, MIPs with the polyNIPAM showed reduced nonspecific binding in water, thereby enhancing the water-compatibility of the MIPs [216].



Table I-4: Summary for water-compatible MIPs applied as analytical devices.

Application	Template	Functional monomer	Solvent of synthesis	Solvent of binding	Strategy	Ref
Selective extraction of therapeutics from plasma, urine, or other biological fluids	Tramadol	MAA	Chloroform	Buffer pH 8.0	Optimizing the binding conditions	[178]
	Amiodarone	4-VP	Chloroform	Buffer pH 4.5	Molecular modeling, optimization of the binding conditions	[211]
	Quinolones	MAA	MeOH:H <sub>2</sub> O (9:1 v/v)	ACN-Buffer	Optimization of the elution solvent	[212]
	Paracetamol	Aniline	DMF then water	Phosphate buffer pH 7.0	Use of polymeric micelle to increase the hydrophilicity	[217]
	Sildenafil	MAA/HEMA	trichloroethane	H <sub>2</sub> O/ACN	Use of HEMA as hydrophilic monomer	[214]
Quantitative analysis of biomarkers engaged in diseases in plasma	Norepinephrine	Phenyl TMS	Ethanol	Phosphate buffer pH 7.0	Synthesis by sol-gel method	[218]
	Estrogens	MAA	Toluene	Buffered solution	Optimization of porogen and T°C	[219]
	Serotonin	MAA	Chloroform-DMSO (1:1)	Buffered solution	Multivariate optimization	[220]
	3-nitro-L-tyrosine	MAA	ACN	Buffer saline	Use of trace of acidic compounds	[221]
Detection of toxic molecules from water and food	Benzylpenicillin	MAA	ACN	ACN/H <sub>2</sub> O	Optimization of cross-linker	[179]
	Nicosulfuron	APTES	Ethanol	Aqueous alkaline solution	Surface coating of quantum dots	[222]
	2,4-dichlorophenoxyacetic acid	4-VP	MeOH:H <sub>2</sub> O (8:2 v/v)	Phosphate buffer	Optimization of binding conditions	[180]
		Styrene / Acrylamide	ACN	H <sub>2</sub> O/ACN	Use of acrylamide as hydrophilic monomer	[215]
		4-VP	MeOH:H <sub>2</sub> O (8:2 v/v)	MeOH:H <sub>2</sub> O	Grafting of NiPAm as hydrophilic monomer/controlled RAFT polymerization	[216]

### I.2.2.2. Synthesis of water-compatible MIPs in aqueous media

Although most of the MIPs are synthesized in organic solvents or hydro-organic mixtures, a few exceptions of imprinting in pure water or buffered media do exist.

In 1982, Takagishi *et al.* were the first to study the imprinting of small molecules in a polar solvent. The preparation of polyvinylpyrrolidone (PVP) with various cross-linking degrees was achieved by free radical polymerization in presence of methyl or butyl orange as template in phosphate buffer pH 7.0. The different MIPs exhibit high affinities towards the target molecular compared to the cross-linked PVP in absence of the dye, as well as good selectivity [223].

In the same context, molecularly imprinted bulk polymers were synthesized in distilled water as adsorbents in ligand-exchange chromatography for the chiral separation of underivatized amino acids. The report highlighted the affinity and cross-selectivity of the MIPs and discussed the mechanism underlying the observed enantioselectivity in light of the interaction model for conventional chiral ligand-exchange separations [160].

Another example of MIPs synthesized in water was introduced by Asanuma *et al.* who synthesized acryloyl-cyclodextrins as functional monomers for the preparation of MIPs in water for nanoscaled biologically important molecules, such as steroids, peptides, antibiotics. These cyclodextrins have hydrophilic exterior and hydrophobic interior. These characteristics provide a good tool not only to improve the hydrophilicity of the MIP, but also to maintain the hydrophobic interactions with the template. Stronger complex formation between cyclodextrin and the template are promoted in water rather than DMSO [224]. Moreover, MIPs for peptide has been developed by using a strong Ni(II)-histidine binding with the imidazole group of the N-terminal histidine. Water soluble acrylamide-based monomers were used in addition to Ni(II)-nitrilotriacetic acid (NTA) complex. Nickel has been selected over other divalent metals such as copper and zinc due to its highest association constant with N-terminal histidine of the peptides and the higher polymerization yields than that obtained with Cu(II) complexes in the polyacrylamide networks [225].

Water-compatible MIPs have been produced for biomedical applications to remove toxic compounds from the body. MIPs have been synthesized in only distilled water for the removal of

bilirubin directly from the plasma of patients suffering from uremic syndrome or hepatic failure. Bilirubin imprinted supermacroporous cryogels were generated by free-radical polymerization in water. A good affinity with an imprinting factor of 6 and an excellent specificity for bilirubin have been obtained for MIPs. Finally, the polymeric materials had shown a good reusability for 10 cycles of adsorption-desorption [161].

In 2012, Henry *et al.* reported the synthesis of MIPs in water for the molecular recognition of flavoring agents such as fructosazine and 2,5-deoxyfructosazine. These agents are used in food and tobacco industries and showed also anti-diabetic and anti-inflammatory activities. MIPs had significant affinity with an imprinting factor of 3 for both templates. The specificity and selectivity of the MIPs result to the efficient extraction and purification of these two molecules from plants and food samples, with respect of the eco-friendly parameters used for the synthesis [182].

### **I.2.3. Molecular imprinting of macromolecules**

Motivated by the fact that the most exciting features of the natural molecular mechanism relies on the biorecognition of macromolecules such as enzymes, receptors, and antibodies, polymer chemists working on molecular imprinting have devoted their efforts to design artificial recognition elements for biological macromolecules, with applications in medicine, diagnostics, proteomics, biosensor, and drug delivery. Hence, there is a strong demand essentially for molecularly imprinted polymers due to their low cost, robustness, and their high level of selectivity and selectivity [142]. Review of the current status of the research in the area of macromolecules imprinting is the scope of this part.

#### **I.2.3.1. Limitations of the protein imprinting**

The synthesis of molecularly imprinted polymers, by non-covalent approach, for small molecules as templates is now almost routine. Short peptides can still be imprinted via the conventional protocol [225]. However, preparing MIPs for biomacromolecules, such as proteins, is remaining as a challenge, and progress in the preparation of such materials has until recently been relatively modest. Nevertheless, the number of research papers using proteins, DNA, and whole cells and viruses is increasing. When dealing with proteins, a number of key issues need to be addressed related to the molecular size and complexity of the targeted macromolecule, as well as its conformational flexibility and solubility [226].

Generally, in the molecular imprinting of low molecular weight molecules, highly cross-linked polymers are used to ensure the preservation of the binding sites upon the template removal. However, for large molecules, high cross-linking densities lead to mass transfer limitations for template reaching or leaving the binding sites. This results in a slow binding kinetics. In the worse case, the removal of the template after imprinting will be difficult due to the physical entrapment of the protein within the polymeric matrix. The extraction of the protein necessitates then the use of detergents which, if it remains in the material, may lead to artifacts. In literature, several solutions have been proposed such as electromigration where protein migrates due to the

effect of an electric field [164], or even template immobilization on a solid carrier in order to facilitate the protein elimination from the resulting MIP [163].

Moreover, biomacromolecules are highly complex, and have a large number of potential recognition sites over a relatively large surface area, unlike smaller templates. Physicochemical properties such as charge or hydrophobicity can strongly vary according to different regions, which can hence arise problems of specificity and selectivity [227]. In particular, proteins have a complex organization, with primary (sequence), secondary (folding,  $\alpha$ -helix,  $\beta$ -sheet, loops, etc.), tertiary (disulphide bonds), and quaternary (multi-subunits complex) structures. The protein flexibility could be affected by the non-physiological conditions that may denature the protein or force it to change its conformation or to aggregate, which is not suitable for the imprinting, especially when dealing with proteins where conformation is needed to site-directed activity [226, 228].

Perhaps, the greatest challenge of all in protein imprinting is the limited choice of the solvent for the polymerization step. Due to the solubility properties of the proteins, as well as their sensitive structure, imprinting should generally be performed in water or buffered media. However, in such polar solvents, hydrogen bonding and electrostatic interactions are hampered as seen in the previous section. This will affect the MIP behavior which relies on this type of interaction between functional monomer and the template, and may lead to high non-specific binding and cross-reactivity of the imprinted polymer [213]. It must be added that performing the imprinting in water will greatly limit the choice of the functional monomer and cross-linker, since most of the available popular monomers are insoluble or partially soluble in water [229].

### **I.2.3.2. Imprinting in hydrogels and sol-gels**

When dealing with protein imprinting strategies, control of porosity and pore size is a major design criterion that should be considered in order to ensure that the protein can freely be removed and reintroduced into the imprinted site. For this, a number of different polymeric matrices have been developed and used for the protein imprinting such as hydrogels, sol-gels. Their flexible networks may greatly facilitate macromolecular transfer and recognition.

In fact, hydrogels are known for their loose networks and for their aqueous environment, which enables the diffusion of the proteins. They are, then, compatible with the molecular imprinting of biomacromolecules [230]. Since proteins are largely insoluble in the most common solvents used for the imprinting, a major limitation of molecular imprinting is the choice of the appropriate functional monomer. This may have implications for the efficacy of the resulting MIP in aqueous environments. Therefore, different groups have started to use water-soluble acrylic monomers to prepare bulk or hydrogel MIPs. Cutivet *et al.* used different functional and cross-linking monomers to imprint trypsin. A complex of this enzyme and a polymerizable inhibitor, methacryloylaminobenzamidine used as anchoring monomer, is used to prepare MIPs based on a number of selected functional monomers, such as acrylamide, methacrylamide, hydroxyethyl methacrylate, *N*-isopropyl acrylamide, as well as water-soluble cross-linking monomers as ethylene bisacrylamide, methylenebisacrylamide, and bis(acryloyl)piperazine. They found that the best imprinting factors were obtained with hydroxyethyl methacrylate and methacrylamide as functional monomers. Moreover, the MIP microgels bound selectively trypsin over other serine-protease family proteins [164]. Similarly, different monomers have been studied to prepare MIPs for the imprinting of serum albumin. Better protein recognition had been obtained with methacrylamide or its analogs as the functional monomer. Additionally, bis(acryloyl)piperazine instead of the common acrylamide-based cross-linking monomers was used to ensure the good hydrophilicity and the mechanic stability of prepared polymers [231]. For the same template protein (BSA), used in this study as a model protein, Zhao *et al.*, recently introduced the synthesis for calcium alginate/polyacrylamide hydrogel film for the molecular recognition of bovine serum albumin [232]. Molecularly imprinted polyacrylamide-based gels were recently prepared for the recognition of maltose binding protein. Influence of the cross-linking and functional monomers concentrations was also investigated in this work [233].

Novel “smart” polymers have been used for proteins imprinting. Recently, several research groups have focused on stimulus-responsive gels that can undergo volume phase transition in response to environmental changes, for instance pH, temperature. Moreover, these gels have flexible binding sites and controllable binding characteristics, due to their low crosslinking density and porous structure. For example, Pan *et al.* reported the synthesis of thermo-responsive nanogels for the recognition of lysozyme, which showed a dramatic temperature-dependence,

with clear on-off transition characteristics around 33°C. Moreover, compared to the control counterparts, lysozyme-imprinted intelligent nanogels possessed a higher binding capacity (imprinting factor of 2.3), more rapid rebinding kinetics, and much higher specificity toward the template [234].

Qin *et al.* provided the synthesis of molecularly imprinted beads coated by thermo-responsive poly(*N*-isopropyl acrylamide) layer for the recognition of lysozyme. In this original study, mesoporous chloromethylated polystyrene beads (MCP beads) were modified and used as a solid support for the grafting of lysozyme-imprinted polymers using NIPAM as thermosensitive monomer, acrylamide and methacrylic acid as functional monomers for protein recognition. **Figure I-28** illustrates the strategy for the preparation of molecularly imprinted beads. The carboxyl groups of the MAA were negatively charged on the polymer chains, and the template protein was positively charged (pI 11.2) when the pH of the imprinting buffer was set at 7.0. Therefore, electrostatic attraction existed between the protein and the imprinting cavities. In order to improve the thermosensitive recognition ability, a layer of poly(NIPAM) was coated in a second polymerization step and acted as a selective thermo-responsive “gate”. At 43 °C, the outer PNIPAM layer and the inner imprinting layer all shrunk. The PNIPAM was therefore more hydrophobic and the spatial arrangement of the imprinting cavities also changed. The template and non-template proteins were all accumulated on the surface of the PNIPAM layer. The interaction between the PNIPAM and the proteins is mainly a hydrophobic effect at temperatures higher than the  $T_{vpt}$  (volume phase transition temperature). The hydrophobic interaction is non-specific, so the coated MIP beads could randomly adsorb both the template lysozyme and the reference proteins on the outer PNIPAM layer. When the temperature changed nearly to 38 °C, because of shape transformations of the inner and outer layers, the adsorption properties of the coated MIP beads also improved, resulting in the squeezing out of the reference proteins. When the temperature decreased to 23 °C, the coated MIP beads returned to the swollen state and released the adsorbed template lysozyme. The coated NIP beads could not release the reference proteins and the template lysozyme at different temperatures in the same way as the coated MIP beads. The behavior of the coated MIP beads toward the mixture of proteins further indicated that the coated MIP beads have a thermosensitive “gate” to the template lysozyme and reference proteins [235].

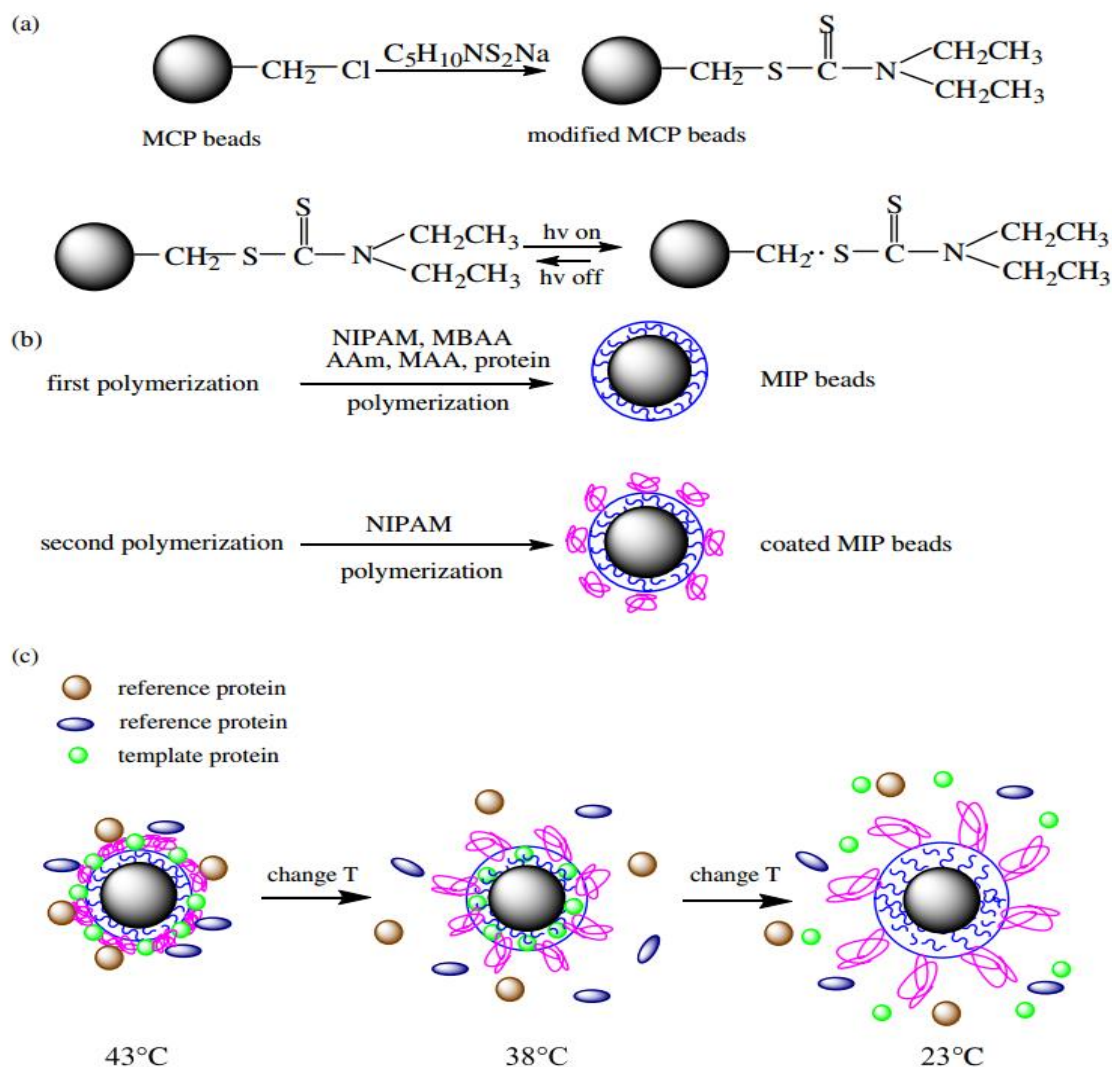


**Figure I-28: Strategy for preparation of protein-imprinted beads with double thermo-responsive gates by surface-initiated living radical polymerization. (a) Generation of mesoporous chloromethylated polystyrene beads (MCP beads) modified. (b) Use of the supports (modified MCP beads) for the grafting of lysozyme-imprinted polymers (MIP beads) and then coating with poly(*N*-isopropylacrylamide) (coated MIP beads) by two-step polymerization. (c) Schematic illustration of coated MIP beads with thermosensitive swelling/collapse phase transitions for selective adsorption of proteins. Reprinted from [235].**

The resulting MIP beads acquired a specific selectivity to the template lysozyme (IF between 2 and 2.5), and could release the template separately at 38°C and 23°C. In fact, the volume phase transition temperatures of the outer PNIPAM layer and the inner imprinting layer were different.



More recently, covalent immobilization of the template on glass beads for solid-phase synthesis of molecularly imprinted polymer nanoparticles (MIP-NPs) specific for proteins was described. Thermoresponsive MIP-NPs were molded around immobilized trypsin by using NIPAM as the major component in the polymerization mixture, a thermoresponsive polymer was obtained. The MIP-NPs could then be released by a simple temperature change, resulting in synthetic antibody mimics exhibiting high specificity and selectivity for trypsin [163]. As an extension of this work and based on the same solid-phase approach, Xu *et al.* used non-covalent immobilization of the template trypsin via a metal chelate acting as a general affinity ligand for accessible surface histidine residues present on some proteins. This strategy is illustrated in **Figure I-29**. The resulting MIP-NPs were endowed with improved binding site homogeneity, since all binding sites have the same orientation. Moreover, the MIPs exhibited apparent dissociation constants in the nanomolar range, with little or no cross-reactivity toward other proteins [236]. Similar work of MIP solid-phase synthesis for the recognition of trypsin was achieved by Poma *et al.* [237].

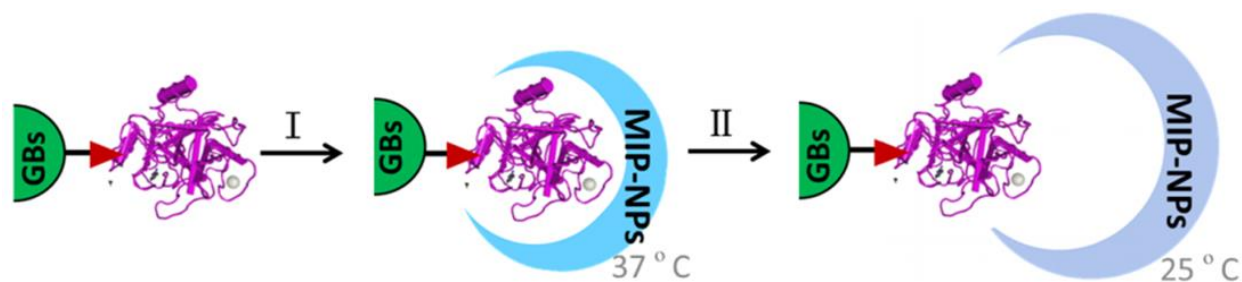


**Figure I-29: Schematic representation of the solid-phase synthesis of MIP-NPs. 1: Polymerization; 2: Release of thermoresponsive MIP-NPs (temperature change from 37 °C to room temperature, 25 °C). Modified from [236]**

Sol-gels have also proved to be able to specifically interact with a variety of proteins for encapsulation. This has been adapted to protein imprinting, by using the benefits of working with sol-gels such as mild polymerization conditions, neutral buffers, ionic strengths, favorable for aqueous solutions. A very recent example of molecularly imprinted polysiloxane was synthesized by Feng *et al.* for the recognition of Bovin serum albumin (BSA) as a model protein. The binding capacity of imprinted polysiloxane for BSA reached 81.31 mg/g, which was 2.25 times more than the control (NIP) [238].

### I.2.3.3. Surface imprinting

In general, surface imprinting is achieved by either synthesizing a thin polymer films using approaches similar to those applied in bulk imprinting, or by attaching the protein template to the surface of a substrate with subsequent polymerization around it. The imprinted binding sites will then be located at or very near to the surface of the polymer layer, which solves the problems of restricted mass transfer and the permanent entrapment of the template after washing.

One of the strategies that have been investigated for the surface imprinting of the whole protein was to use procedure based on metal coordination. Selective adsorbents for high performance liquid chromatography (HPLC) separation of lysozyme and RNase was developed by the polymerization of *N*-(4-vinyl)-benzyl iminodiacetic acid onto methacrylate-derivatized silica particles in the presence of RNase and Cu (II) metal ions. This monomer was then allowed to form a complex with the metal ions and the imidazole groups of the protein surface-exposed histidines. The protein was subsequently removed by a treatment with EDTA [239].

Another approach for surface imprinting was to cast a continuous polymer film on a surface with immobilized proteins. Forming imprinted thin polymeric films solve in a simple and effective manner the diffusion problems associated with the bulky templates. One of the first examples is the work by Ratner and colleagues [240]. They spin-coated a thin oligosaccharide layer on a surface with immobilized proteins, which was then cross-linked by plasma deposition of polymer, and glued to a glass support. After unmolding, the imprints of the protein could be visualized by AFM imaging. Later, Chuan Chou *et al.* used also this approach and developed a MIP thin film for the recognition of C-reactive protein (CRP) by surface-imprinting. **Figure I-30** summarizes the underlying mechanism behind the preparation of such MIP films. In this study, they have formed a single layer of protein on a microscope cover glass, together with a functional monomer, and then contacted this onto a glass support carrying the cross-linking agent. An analogue, *O*-(-4-nitrophenylphosphoryl)choline, of the templates natural ligand, phosphorylcholine, was used as the functional monomer. After UV induced polymerization, the cover glass can be easily removed to allow washing of the polymer and evaluation of its affinity in subsequent rebinding protocols [241].

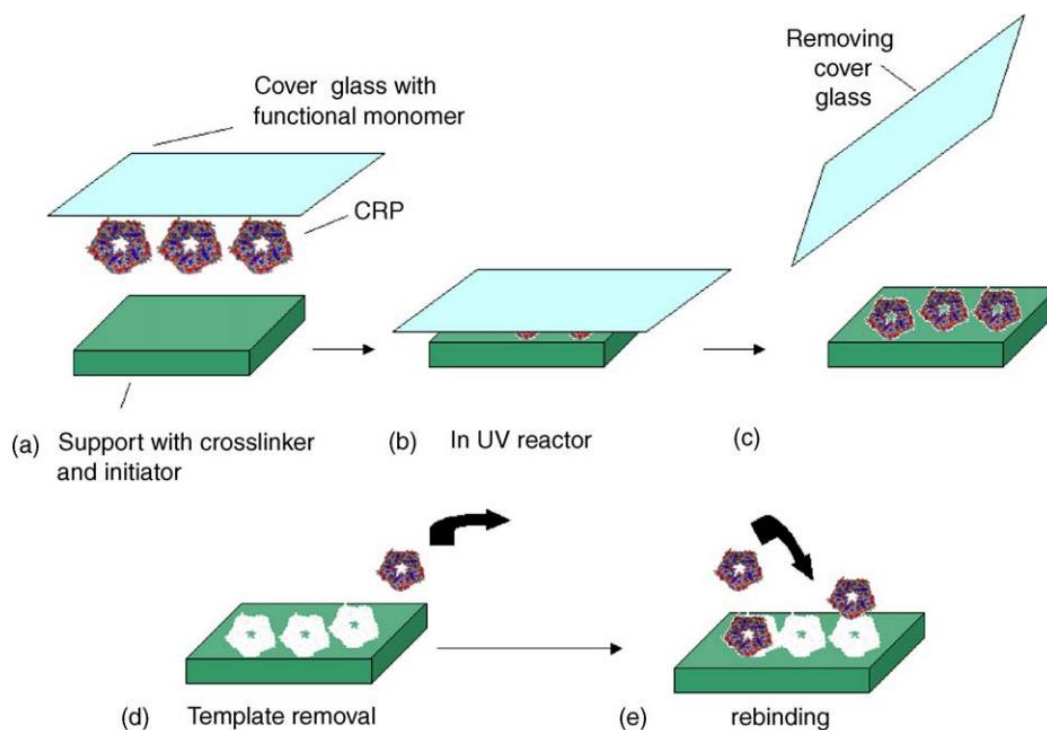


**Figure I-30: Outline of CRP micro-contact imprinting and re-binding:** (a) protein is adsorbed onto the microscope cover glass together with the functional monomer; (b) the cover glass is brought into contact with the support carrying the cross-linker and initiator and then placed in UV reactor; (c) the cover glass is removed; (d) template protein is extracted by washing; (e) rebinding of template or competitor proteins. Reprinted from [241].

In a recent work, Haupt and colleagues have used AFM and force spectroscopy by AFM (with the template protein attached to the AFM cantilever) to reveal binding sites for proteins molded into thin polyacrylamide layers on glass slides [242].

Surface-imprinting with immobilized template can also be done in hierarchically structured support materials. **Figure I-31** illustrates well this principle. It was first described by Mosbach and colleagues for the recognition of small molecule as theophylline [243]. This approach was later used for imprinting of proteins such as human serum albumin [231], immunoglobulin G [244] and transferrin [245], for instance. In this technique, porous silica particles several  $\mu\text{m}$  in size containing protein templates immobilized onto the inner pore surface are used for the generation of imprinted polymers. The pores of the silica mould were filled with the MIP

precursors mixture, which is polymerized, followed by dissolution of the silica support. This method leaves behind the imprinted polymers in the form of a negative image (the pore network) of the silica particles, with binding sites located at the surface of the polymer, which are capable of recognizing with the target protein [246, 247].

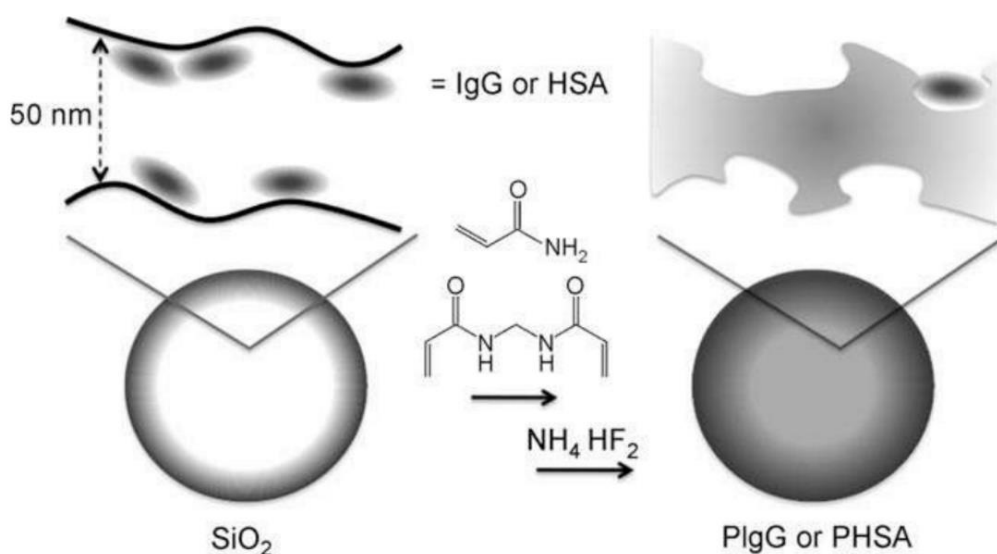


**Figure I-31: Protein imprinting using a sacrificial wide-pore silica support modified with a submonolayer of adsorbed protein (IgG or HSA), filling of the pores of the protein–silica template with a monomer solution, polymerization, and subsequent removal of the protein and silica porogen by fluoride etching and washing. The last step leaves behind an inverse replica of the silica template that features highly accessible protein-complementary binding sites at the pore walls of the polymeric beads. Reprinted from [247]**

In the attempt to increase the surface area of the protein-imprinted polymer, as well as the accessibility of the binding sites, the development of surface-imprinted nanomaterials has been achieved. Different nanomaterials are used for the surface-imprinting of proteins such as magnetic and silica nanoparticles, nanowires, carbon nanotubes, quantum dots, and others. The application of such materials for the protein recognition was, recently, summarized and reviewed by Svec *et al.* [248].

#### I.2.3.4. Imprinting by epitope approach

Inspired by the way antibodies function, where they recognize their target via certain sequential or conformational epitopes, MIPs have also been synthesized by an 'epitope approach'. In this approach, only a part of the protein is imprinted, a surface accessible oligopeptide, for instance. The resulting MIP will be then able to specifically bind the target via this epitope. This concept was applied by Rachkov and Minoura for the synthesis of MIPs, and was proved using as template a short sequence of a bioactive peptide (3-4) residues) [249], as shown in **Figure I-32**.

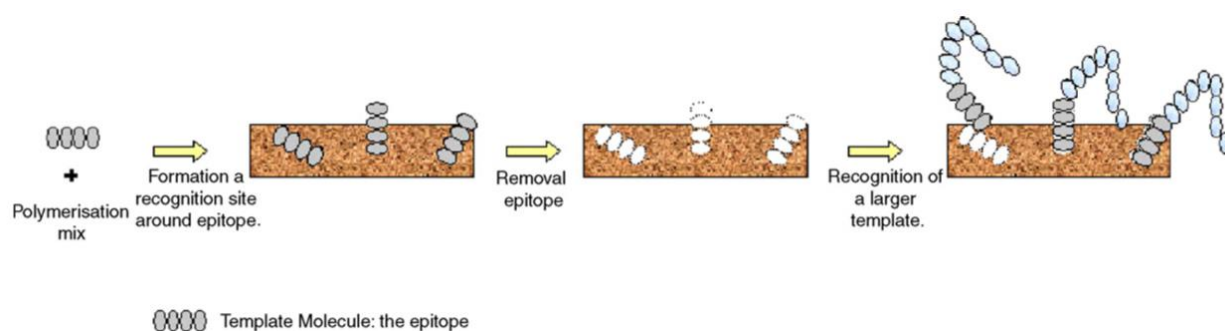


**Figure I-32: Schematic representation of the epitope approach for MIP synthesis. Reprinted from [228].**

In their studies, Rachkov *et al.* used a tetrapeptide, Tyr-Pro-Leu-Gly-NH<sub>2</sub> (YPLG), as template for the preparation of MIPs by epitope approach. It was shown that the MIP can recognize not only the template, but also some other peptides possessing Pro-Leu-Gly-NH<sub>2</sub> sequence at the C-terminus, including the neurohypophyseal hormone oxytocin. The polymer was made of methacrylic acid (MAA) and ethylene glycol di-methacrylate (EGDMA) as functional and cross-linking monomers, respectively [249]. In the same context, the authors studied the synthesis of a MIP for the recognition of the octa-peptide hormone angiotensin II [106].

The epitope approach was, subsequently, nicely also used by Shea *et al.* to prepare MIPs for the nonapeptides recognition of many proteins such as cytochrome *c*, alcohol dehydrogenase, and bovine serum albumin [250]. More recently, MIPs are synthesized, by this approach, for the tyrosine phosphopeptide [251] and angiotensin I and II [252]. An interesting study conducted by Bossi *et al.* provided a novel method for the rational preparation of MIPs for proteins recognition by fingerprint-imprinted polymers. The choice of the epitope was done based on an *in silico*

cleavage of the protein sequence, followed by the selection of the resulting peptide fragments that have the appropriate length and hydrophilicity. The last step was the screening of each peptide candidate against the entire protein databank. This fingerprint was used to prepare MIPs for the efficient recognition of many proteases [253]. This method of epitope selection was also used in a very recent study by Cenci *et al.* in order to prepare MIPs suitable for medical diagnosis of myocardial infarctions. For this purpose, specific and selective MIPs for cardiac troponin I peptide by fingerprint-imprinting approach [254].

### **I.2.3.5. Microorganisms and cells imprinting**

A recent extension of the work in the molecular imprinting is targeting large biomolecules such as viruses and cells. Several studies demonstrated the possibility of preparing micro-organisms-imprinted polymers for the rapid detection of bacteria and viruses in the clinical diagnosis of the infection diseases [255]. In essence, all strategies for imprinting such entities rely on of the two different approaches: bulk polymerization or surface polymerization.

Pioneering work on the imprinting of bacteria by surface polymerization was performed by Vulfson and colleagues [256, 257]. They provided microparticles with functional hollows on the surface for the recognition of *Listeria monocytogenes*. In another study, Tokonami *et al.*, effectively developed a label free and selective *E. coli* identification by surface imprinting the whole bacteria cell in a surface layer of overoxidized polypyrrole, which could detect the bacteria within the range of 10<sup>3</sup>–10<sup>9</sup> CFU/mL [258]. In a study conducted by Dickert and Hayden, a selective detection of *Saccharomyces* was emphasized using cell imprinted polymers with a detection ranges within 10<sup>4</sup>–10<sup>9</sup> cells/mL in a quartz crystal microbalance (QCM) system [259]. More recently, molecular imprinting based bacteria sensor via whole cell imprinting is described by Yilmaz *et al.* for biosensors based on surface plasmon resonance (SPR), and QCM [260]. Amino acids were used as recognition elements for the biomimetic sensor surface. During this study produced sensors used for at least 10 equilibration–adsorption–regeneration cycles with both aqueous and apple juice solutions at different concentrations for both SPR and QCM sensors.

Further successes involved the application of polymer imprinting to viruses. The latest developments in molecular imprinting has shown a big potential in producing sensor surfaces based on synthetic materials and achieving low detection limits for virus sensing. Recently, different examples of viruses are used as templates to prepare corresponding MIPs such as waterborne virus [261], Adenovirus [262], Human immunodeficiency virus (HIV) [263] and many others [229, 255].



## References

- [1] S. Kobayashi and A. Makino, “Enzymatic polymer synthesis: an opportunity for green polymer chemistry,” *Chem. Rev.*, vol. 109, no. 11, pp. 5288–5353, 2009.
- [2] M. Richter, C. Schulenburg, D. Jankowska, T. Heck, and G. Faccio, “Novel materials through Nature ’ s catalysts,” *Mater. Today*, vol. 00, no. 00, 2015.
- [3] E. Fischer, “Einfluss der Configuration auf die Wirkung der Enzyme,” *Ber Dt Chem Ges*, vol. 27, pp. 2985 – 2293, 1894.
- [4] L. Pauling, “Nature of forces between large molecules of biological interest,” *Nature*, vol. 191, pp. 707–709, 1948.
- [5] P. a. Kollman, B. Kuhn, O. Donini, M. Perakyla, R. Stanton, and D. Bakowies, “Elucidating the nature of enzyme catalysis utilizing a new twist on an old methodology: Quantum mechanical-free energy calculations on chemical reactions in enzymes and in aqueous solution,” *Acc. Chem. Res.*, vol. 34, no. 1, pp. 72–79, 2001.
- [6] J. Berg, J. Tymoczko, and L. Stryer, *Biochemistry*, 5th ed. New York: W.H. Freeman and Company.
- [7] a Schmid, J. S. Dordick, B. Hauer, a Kiener, M. Wubbolts, and B. Witholt, “Industrial biocatalysis today and tomorrow.,” *Nature*, vol. 409, no. 6817, pp. 258–268, 2001.
- [8] A. Rajagopalan and W. Kroutil, “Biocatalytic reactions: Selected highlights,” *Mater. Today*, vol. 14, no. 4, pp. 144–152, 2011.
- [9] R. a Gross, A. Kumar, and B. Kalra, “Polymer synthesis by in vitro enzyme catalysis,” *Chem. Rev.*, vol. 101, no. 7, pp. 2097–2124, 2001.
- [10] U. T. Bornscheuer, G. W. Huisman, R. J. Kazlauskas, S. Lutz, J. C. Moore, and K. Robins, “Engineering the third wave of biocatalysis,” *Nature*, vol. 485, no. 7397, pp. 185–194, 2012.
- [11] H. Uyama and S. Kobayashi, “Enzyme-catalyzed polymerization to functional polymers,” *J. Mol. Catal. B Enzym.*, vol. 19–20, pp. 117–127, 2002.
- [12] S. Kobayashi, S. Kobayashi, H. Uyama, H. Uyama, S. Kimura, and S. Kimura, “Enzymatic Polymerization,” *Chem. Rev.*, vol. 101, no. 12, pp. 3793–3818, 2001.
- [13] R. Ikeda, H. Tanaka, H. Uyama, and S. Kobayashi, “Laccase-catalyzed polymerization of acrylamide,” *Macromol. Rapid Commun.*, vol. 19, no. 8, pp. 423–425, 1998.
- [14] S. Sen and J. Puskas, “Green Polymer Chemistry: Enzyme Catalysis for Polymer Functionalization,” *Molecules*, vol. 20, no. 5, pp. 9358–9379, 2015.
- [15] J. Kadokawa and S. Kobayashi, “Polymer synthesis by enzymatic catalysis.,” *Curr. Opin. Chem. Biol.*, vol. 14, no. 2, pp. 145–153, 2010.
- [16] J. I. Kadokawa, “Precision polysaccharide synthesis catalyzed by enzymes,” *Chem. Rev.*, vol. 111, no. 7, pp. 4308–4345, 2011.
- [17] S. Kobayashi and M. Ohmae, “Enzymatic polymerization to polysaccharides,” *Adv. Polym. Sci.*, vol. 194, no. 1, pp. 159–210, 2006.
- [18] M. Faijes and A. Planas, “In vitro synthesis of artificial polysaccharides by glycosidases and glycosynthases,” *Carbohydr. Res.*, vol. 342, no. 12–13, pp. 1581–1594, 2007.
- [19] D. D. Allison and K. J. Grande-Allen, “Review. Hyaluronan: a powerful tissue engineering tool.,” *Tissue Eng.*, vol. 12, no. 8, pp. 2131–2140, 2006.
- [20] S. Kobayashi, S. Shoda, and H. Uyama, “Enzymatic polymerization and oligomerization,” *Polym. Synth. Eng.*, vol. 121, pp. 1–30, 1995.
- [21] K. G. I. Nilsson, “Enzymatic synthesis of oligosaccharides,” *Trends Biochem. Sci.*, vol. 6, pp. 256–264, 1988.
- [22] M. Kitaoka and K. Hayashi, “Carbohydrate-Processing Phosphorolytic Enzymes.,” *Trends Glycosci. Glycotechnol.*, vol. 14, no. 75, pp. 35–50, 2002.



- [23] S. Kobayashi, J. Sakamoto, and S. Kimura, *In vitro synthesis of cellulose and related polysaccharides*, vol. 26, no. 9. 2001.
- [24] M. Ohmae, S. I. Fujikawa, H. Ochiai, and S. Kobayashi, "Enzyme-Catalyzed Synthesis of Natural and Unnatural Polysaccharides," *J. Polym. Sci. Part a-Polymer Chem.*, vol. 44, pp. 5014–5027, 2006.
- [25] S. J. Williams and S. G. Withers, "Glycosyl fluorides in enzymatic reactions," *Carbohydr. Res.*, vol. 327, no. 1–2, pp. 27–46, 2000.
- [26] A. Makino and S. Kobayashi, "Chemistry of 2-Oxazolines: A Crossing of Cationic Ring-Opening Polymerization and Enzymatic Ring-Opening Polyaddition," *J. Polym. Sci. Part a-Polymer Chem.*, vol. 48, pp. 1251–1270, 2010.
- [27] K. Nk, "Synthesis of polysaccharides with a regular structure," *Tetrahedron*, vol. 43, pp. 2389–2436, 1987.
- [28] S. Kobayashi, K. Kashiwa, J. Shimada, T. Kawasaki, and S. Shoda, "THE FIRST IN VITRO SYNTHESIS OF CELLULOSE VIA NONBIOSYNTHETIC PATH CATALYZED BY CELLULASE," *Makromol. Chem.*, vol. 54/55, pp. 509–518, 1992.
- [29] S. Egusa, T. Kitaoka, M. Goto, and H. Wariishi, "Synthesis of cellulose in vitro by using a cellulase/surfactant complex in a nonaqueous medium," *Angew. Chemie - Int. Ed.*, vol. 46, no. 12, pp. 2063–2065, 2007.
- [30] M. Hiraishi, K. Igarashi, S. Kimura, M. Wada, M. Kitaoka, and M. Samejima, "Synthesis of highly ordered cellulose II in vitro using cellodextrin phosphorylase," *Carbohydr. Res.*, vol. 344, no. 18, pp. 2468–2473, 2009.
- [31] S. Kobayashi, X. Wen, and S. I. Shoda, "Specific preparation of artificial xylan: a new approach to polysaccharide synthesis by using cellulase as catalyst," *Macromolecules*, vol. 29, no. 7, pp. 2698–2700, 1996.
- [32] E. Samain, C. Lancelon-Pin, F. Férido, V. Moreau, H. Chanzy, A. Heyraud, and H. Driguez, "Phosphorolytic synthesis of cellodextrins," *Carbohydr. Res.*, vol. 271, no. 2, pp. 217–226, 1995.
- [33] B. Pfannemüller, "Influence of chain length of short monodisperse amyloses on the formation of A- and B-type X-ray diffraction patterns," *Int. J. Biol. Macromol.*, vol. 9, no. 2, pp. 105–108, 1987.
- [34] G. Potocki-Veronese, J. L. Putaux, D. Dupeyre, C. Albenne, M. Remaud-Siméon, P. Monsan, and A. Buleon, "Amylose synthesized in vitro by amylosucrase: Morphology, structure, and properties," *Biomacromolecules*, vol. 6, no. 2, pp. 1000–1011, 2005.
- [35] J. L. Putaux, G. Potocki-Véronèse, M. Remaud-Simeon, and A. Buleon, "α-D-glucan-based dendritic nanoparticles prepared by in vitro enzymatic chain extension of glycogen," *Biomacromolecules*, vol. 7, no. 6, pp. 1720–1728, 2006.
- [36] a. Anitha, S. Sowmya, P. T. S. Kumar, S. Deepthi, K. P. Chennazhi, H. Ehrlich, M. Tsurkan, and R. Jayakumar, "Chitin and chitosan in selected biomedical applications," *Prog. Polym. Sci.*, vol. 39, no. 9, pp. 1644–1667, 2014.
- [37] R. Muzzarelli, M. Mehtedi, and M. Mattioli-Belmonte, "Emerging Biomedical Applications of Nano-Chitins and Nano-Chitosans Obtained via Advanced Eco-Friendly Technologies from Marine Resources," *Mar. Drugs*, vol. 12, no. 11, pp. 5468–5502, 2014.
- [38] T. Hattori, Y. Sakabe, M. Ogata, K. Michishita, H. Dohra, H. Kawagishi, K. Totani, M. Nikaido, T. Nakamura, H. Koshino, and T. Usui, "Enzymatic synthesis of an ??-chitin-like substance via lysozyme-mediated transglycosylation," *Carbohydr. Res.*, vol. 347, no. 1, pp. 16–22, 2012.
- [39] M. Rinaudo, "Chitin and chitosan: Properties and applications," *Prog. Polym. Sci.*, vol. 31, no. 7, pp. 603–632, 2006.

- [40] H. Sato, S. Mizutani, S. Tsuge, H. Ohtani, K. Aoi, a Takasu, M. Okada, S. Kobayashi, T. Kiyosada, and S. Shoda, "Determination of the degree of acetylation of chitin/chitosan by pyrolysis-gas chromatography in the presence of oxalic Acid.," *Anal. Chem.*, vol. 70, no. 1, pp. 7–12, 1998.
- [41] S. Kobayashi, T. Kiyosada, and S. I. Shoda, "Synthesis of artificial chitin: Irreversible catalytic behavior of a glycosyl hydrolase through a transition state analogue substrate," *J. Am. Chem. Soc.*, vol. 118, no. 51, pp. 13113–13114, 1996.
- [42] H. Ochiai, M. Ohmae, and S. Kobayashi, "Enzymatic glycosidation of sugar oxazolines having a carboxylate group catalyzed by chitinase," *Carbohydr. Res.*, vol. 339, no. 17, pp. 2769–2788, 2004.
- [43] A. Makino, K. Kurosaki, M. Ohmae, and S. Kobayashi, "Chitinase-catalyzed synthesis of alternatingly N-deacetylated chitin: A chitin-chitosan hybrid polysaccharide," *Biomacromolecules*, vol. 7, no. 3, pp. 950–957, 2006.
- [44] A. Makino, H. Nagashima, M. Ohmae, and S. Kobayashi, "Chitinase-catalyzed synthesis of an alternatingly N-sulfonated chitin derivative," *Biomacromolecules*, vol. 8, no. 1, pp. 188–195, 2007.
- [45] M. R. Langlois and J. R. Delanghe, "Biological and clinical significance of haptoglobin polymorphism in humans," *Clin. Chem.*, vol. 42, no. 10, pp. 1589–1600, 1996.
- [46] T. Watanabe, K. Suzuki, W. Oyanagi, K. Ohnishi, and H. Tanaka, "Gene cloning of chitinase A1 from *Bacillus circulans* WL-12 revealed its evolutionary relationship to *Serratia* chitinase and to the type III homology units of fibronectin," *J. Biol. Chem.*, vol. 265, no. 26, pp. 15659–15665, 1990.
- [47] T. Watanabesq, K. Koboris, T. Fujiin, H. Sakaiiii, M. Uchidas, and H. Tanakas, "Bacillus circulans," no. 12, pp. 18567–18572, 1993.
- [48] K. Prydz and K. T. Dalen, "Synthesis and sorting of proteoglycans.," *J. Cell Sci.*, vol. 113 Pt 2, pp. 193–205, 2000.
- [49] M. S. G. Pavãõ, "Glycosaminoglycans analogs from marine invertebrates: structure, biological effects, and potential as new therapeutics," *Front. Cell. Infect. Microbiol.*, vol. 4, no. September, pp. 1–6, 2014.
- [50] R. J. Linhardt and T. Toida, "Role of glycosaminoglycans in cellular communication," *Acc. Chem. Res.*, vol. 37, no. 7, pp. 431–438, 2004.
- [51] S. Kobayashi, H. Morii, R. Ito, and M. Ohmae, "Enzymatic polymerization to artificial hyaluronic acid using a transition state analogue monomer," *Macromol. Symp.*, vol. 183, no. 16, pp. 127–132, 2002.
- [52] R. Stern and M. J. Jedrzejas, "Hyaluronidases: Their genomics, structures, and mechanisms of action," *Chem. Rev.*, vol. 106, no. 3, pp. 818–839, 2006.
- [53] S. Kobayashi, M. Ohmae, S. I. Fujikawa, and H. Ochiai, "Enzymatic precision polymerization for synthesis of glycosaminoglycans and their derivatives," *Macromol. Symp.*, vol. 226, pp. 147–156, 2005.
- [54] S. I. Fujikawa, M. Ohmae, and S. Kobayashi, "Enzymatic synthesis of chondroitin 4-sulfate with well-defined structure," *Biomacromolecules*, vol. 6, no. 6, pp. 2935–2942, 2005.
- [55] S. Kobayashi, M. Ohmae, H. Ochiai, and S. I. Fujikawa, "A hyaluronidase supercatalyst for the enzymatic polymerization to synthesise glycosaminoglycans," *Chem. - A Eur. J.*, vol. 12, no. 23, pp. 5962–5971, 2006.
- [56] M. Ohmae, K. Sakaguchi, T. Kaneto, S. I. Fujikawa, and S. Kobayashi, "Keratanase II-catalyzed synthesis of keratan sulfate oligomers by using sugar oxazolines as transition-state analogue substrate monomers: A novel insight into the enzymatic catalysis mechanism," *ChemBioChem*, vol. 8, no. 14, pp. 1710–1720, 2007.

- [57] M. Fujita, S. Shoda, and S. Kobayashi, "Xylanase-Catalyzed Synthesis of a Novel Polysaccharide Having a Glucose-Xylose Repeating Unit, a Cellulose-Xylan Hybrid Polymer," *J. Am. Chem. Soc.*, vol. 120, no. 25, pp. 6411–6412, 1998.
- [58] S. Kobayashi, A. Makino, H. Matsumoto, S. Kunii, M. Ohmae, T. Kiyosada, K. Makiguchi, A. Matsumoto, M. Horie, and S. I. Shoda, "Enzymatic polymerization to novel polysaccharides having a glucose-N-acetylglucosamine repeating unit, a cellulose - Chitin hybrid polysaccharide," *Biomacromolecules*, vol. 7, no. 5, pp. 1644–1656, 2006.
- [59] S. Kobayashi, A. Makino, N. Tachibana, and M. Ohmae, "Chitinase-catalyzed synthesis of a chitin-xylan hybrid polymer: A novel water-soluble (1 → 4) polysaccharide having an N-acetylglucosamine-xylose repeating unit," *Macromol. Rapid Commun.*, vol. 27, no. 10, pp. 781–786, 2006.
- [60] H. Ochiai, S. I. Fujikawa, M. Ohmae, and S. Kobayashi, "Enzymatic copolymerization to hybrid glycosaminoglycans: A novel strategy for intramolecular hybridization of polysaccharides," *Biomacromolecules*, vol. 8, no. 6, pp. 1802–1806, 2007.
- [61] Y. Ikada and H. Tsuji, "Biodegradable polyesters for medical and ecological applications," *Macromol. Rapid Commun.*, vol. 21, no. 3, pp. 117–132, 2000.
- [62] A. Díaz, R. Katsarava, and J. Puiggali, "Synthesis, properties and applications of biodegradable polymers derived from diols and dicarboxylic Acids: From Polyesters to poly(ester amide)s," *Int. J. Mol. Sci.*, vol. 15, no. 5, pp. 7064–7123, 2014.
- [63] A. A. Shah, S. Kato, N. Shintani, N. R. Kamini, and T. Nakajima-Kambe, "Microbial degradation of aliphatic and aliphatic-aromatic co-polyesters," *Appl. Microbiol. Biotechnol.*, vol. 98, no. 8, pp. 3437–3447, 2014.
- [64] B. D. Ulery, L. S. Nair, and C. T. Laurencin, "Biomedical applications of biodegradable polymers," *J. Polym. Sci. Part B Polym. Phys.*, vol. 49, no. 12, pp. 832–864, 2011.
- [65] D. C. Meng, R. Shen, H. Yao, J. C. Chen, Q. Wu, and G. Q. Chen, "Engineering the diversity of polyesters," *Curr. Opin. Biotechnol.*, vol. 29, no. 1, pp. 24–33, 2014.
- [66] H. Uyama and S. Kobayashi, "Enzymatic Synthesis of Polyesters via Polycondensation," *Adv. Polym. Sci.*, vol. 194, pp. 133–158, 2006.
- [67] Z. Jiang and J. Zhang, "Lipase-catalyzed synthesis of aliphatic polyesters via copolymerization of lactide with diesters and diols," *Polym. (United Kingdom)*, vol. 54, no. 22, pp. 6105–6113, 2013.
- [68] J. Zhang, H. Shi, D. Wu, Z. Xing, A. Zhang, Y. Yang, and Q. Li, "Recent developments in lipase-catalyzed synthesis of polymeric materials," *Process Biochem.*, vol. 49, no. 5, pp. 797–806, 2014.
- [69] E. M. Rustoy, Y. Sato, H. Nonami, R. Erra-Balsells, and A. Baldessari, "Lipase-catalyzed synthesis and characterization of copolymers from ethyl acrylate as the only monomer starting material," *Polymer (Guildf.)*, vol. 48, no. 6, pp. 1517–1525, 2007.
- [70] K. a. Barrera-Rivera, L. Peponi, Á. Marcos-Fernández, J. M. Kenny, and A. Martínez-Richa, "Synthesis, characterization and hydrolytic degradation of polyester-urethanes obtained by lipase biocatalysis," *Polym. Degrad. Stab.*, vol. 108, pp. 188–194, 2014.
- [71] K. Greimel, A. Marold, C. Sohar, R. Feola, A. Temel, T. Schoenbacher, E. H. Acero, and G. M. Guebitz, "Enzymatic hydrolysis of polyester based coatings," *React. Funct. Polym.*, vol. 73, no. 10, pp. 1335–1339, 2013.
- [72] S. Kobayashi, H. Uyama, S. Namekawa, and H. Hayakawa, "Enzymatic Ring-Opening Polymerization and Copolymerization of 8-Octanolide by Lipase Catalyst," *Macromolecules*, vol. 31, no. 17, pp. 5655–5659, 1998.
- [73] D. Knani and D. Kohn, "Enzymatic Polyesterification in Organic Media. EnzymeCatalyzed Synthesis of Lateral-Substituted Aliphatic Polyesters and Copolyesters," *Polym. Chem.*, vol. 31, no. 5, pp. 1221–1232, 1993.

- [74] A. C. Albertsson and R. K. Srivastava, "Recent developments in enzyme-catalyzed ring-opening polymerization," *Adv. Drug Deliv. Rev.*, vol. 60, no. 9, pp. 1077–1093, 2008.
- [75] S. Matsumura, "Enzymatic synthesis of polyesters via ring-opening polymerization," *Adv. Polym. Sci.*, vol. 194, no. 1, pp. 95–132, 2006.
- [76] W.-X. Wu, L. Qu, B.-Y. Liu, W.-W. Zhang, N. Wang, and X.-Q. Yu, "Lipase-catalyzed synthesis of acid-degradable poly( $\beta$ -thioether ester) and poly( $\beta$ -thioether ester-co-lactone) copolymers," *Polymer (Guildf)*, vol. 59, pp. 187–193, 2015.
- [77] Y. Mohammadi, A. S. Pakdel, M. R. Saeb, and K. Boodhoo, "Monte Carlo simulation of free radical polymerization of styrene in a spinning disc reactor," *Chem. Eng. J.*, vol. 247, pp. 231–240, 2014.
- [78] C. Manach, A. Scalbert, C. Morand, C. Rémésy, and L. Jiménez, "Polyphenols : food sources and bioavailability," *Am. J. Clin. Nutr.*, vol. 79, no. 5, pp. 727–747, 2004.
- [79] F. Hollmann and I. W. C. E. Arends, "Enzyme initiated radical polymerizations," *Polymers (Basel)*, vol. 4, no. 1, pp. 759–793, 2012.
- [80] L. Zhang, W. Zhao, H. Chen, and Y. Cui, "Enzymatic synthesis of phenol polymer and its functionalization," *J. Mol. Catal. B Enzym.*, vol. 87, pp. 30–36, 2013.
- [81] P. Di Gennaro, A. Bargna, F. Bruno, and G. Sello, "Purification of recombinant catalase-peroxidase HPI from *E. coli* and its application in enzymatic polymerization reactions," *Appl. Microbiol. Biotechnol.*, vol. 98, no. 3, pp. 1119–26, 2014.
- [82] F. F. Bruno, a Trotta, S. Fossey, S. Nagarajan, R. Nagarajan, L. a Samuelson, and J. Kumar, "Enzymatic synthesis and characterization of polyquercetin," *J. Macromol. Sci. Part A Pure Appl. Chem.*, vol. 47, no. 12, pp. 1191–1196, 2010.
- [83] R. M. Desentis-Mendoza, H. Hernández-Sánchez, A. Moreno, E. Rojas del C., L. Chel-Guerrero, J. Tamariz, and M. E. Jaramillo-Flores, "Enzymatic polymerization of phenolic compounds using laccase and tyrosinase from *Ustilago maydis*," *Biomacromolecules*, vol. 7, no. 6, pp. 1845–1854, 2006.
- [84] J. Anthoni, C. Humeau, E. R. Maia, L. Chebil, J.-M. Engasser, and M. Ghoul, "Enzymatic synthesis of oligoesculin: structure and biological activities characterizations," *Eur. Food Res. Technol.*, vol. 231, no. 4, pp. 571–579, 2010.
- [85] L. Chebil, G. Ben Rhouma, L. Chekir-ghedira, and M. Ghoul, "Enzymatic Polymerization of Rutin and Esculin and Evaluation of the Antioxidant Capacity of Polyruutin and Polyesculin," 2015.
- [86] S. Savic, K. Vojinovic, S. Milenkovic, A. Smelcerovic, M. Lamshoeft, and Z. Petronijevic, "Enzymatic oxidation of rutin by horseradish peroxidase: Kinetic mechanism and identification of a dimeric product by LC-Orbitrap mass spectrometry," *Food Chem.*, vol. 141, no. 4, pp. 4194–4199, 2013.
- [87] J. E. Wong-Paz, D. B. Muñiz-Márquez, C. N. Aguilar, H. Sotin, and S. Guyot, "Enzymatic synthesis, purification and in vitro antioxidant capacity of polyphenolic oxidation products from apple juice," *LWT - Food Sci. Technol.*, vol. 64, no. 2, pp. 1091–1098, 2015.
- [88] S. Dubey, D. Singh, and R. a. Misra, "Enzymatic synthesis and various properties of poly(catechol)," *Enzyme Microb. Technol.*, vol. 23, no. April, pp. 432–437, 1998.
- [89] M. Ghoul and L. Chebil, *Enzymatic polymerization of phenolic compounds by oxidoreductases*. 2012.
- [90] L. Zhang, W. Zhao, Z. Ma, G. Nie, and Y. Cui, "Enzymatic polymerization of phenol catalyzed by horseradish peroxidase in aqueous micelle system," *Eur. Polym. J.*, vol. 48, no. 3, pp. 580–585, 2012.
- [91] R. A. Derango, L. Chiang, R. Dowbenko, and J. G. Lasch, "Enzyme-mediated polymerization of acrylic monomers," *Science (80- )*, vol. 6, no. 6, pp. 523–526, 1992.

- [92] O. Emery, T. Lalot, M. Brigodiot, and E. Maréchal, "Free-radical polymerization of acrylamide by horseradish peroxidase-mediated initiation," *J. Polym. Sci. Part A Polym. Chem.*, vol. 35, no. 15, pp. 3331–3333, 1997.
- [93] D. Teixeira, T. Lalot, M. Brigodiot, and E. Maréchal, "β-Diketones as Key Compounds in Free-Radical Polymerization by Enzyme-Mediated Initiation," *Macromolecules*, vol. 32, no. 1, pp. 70–72, 1998.
- [94] T. Lalot, M. Brigodiot, and E. Maréchal, "A kinetic approach to acrylamide radical polymerization by horse radish peroxidase-mediated initiation," *Polym. Int.*, vol. 48, no. 4, pp. 288–292, 1999.
- [95] A. Durand, T. Lalot, M. Brigodiot, and E. Maréchal, "Enzyme-mediated initiation of acrylamide polymerization: reaction mechanism," *Polymer (Guildf.)*, vol. 41, no. 23, pp. 8183–8192, 2000.
- [96] A. Durand, T. Lalot, M. Brigodiot, and E. Maréchal, "Enzyme-mediated radical initiation of acrylamide polymerization: Main characteristics of molecular weight control," *Polymer (Guildf.)*, vol. 42, no. 13, pp. 5515–5521, 2001.
- [97] R. L. Shogren, J. L. Willett, and A. Biswas, "HRP-mediated synthesis of starch-polyacrylamide graft copolymers," *Carbohydr. Polym.*, vol. 75, no. 1, pp. 189–191, 2009.
- [98] F. Hollmann, Y. Gumulya, C. Tölle, A. Liese, and O. Thum, "Evaluation of the laccase from *Myceliophthora thermophila* as industrial biocatalyst for polymerization reactions," *Macromolecules*, vol. 41, no. 22, pp. 8520–8524, 2008.
- [99] B. Kalra and R. a Gross, "Horseradish peroxidase mediated free radical polymerization of methyl methacrylate.," *Amani*, vol. 1, no. 3, pp. 501–5, 2000.
- [100] a Singh, D. Ma, and D. L. Kaplan, "Enzyme-mediated free radical polymerization of styrene.," *Biomacromolecules*, vol. 1, no. 4, pp. 592–596, 2000.
- [101] S. J. Sigg, F. Seidi, K. Renggli, T. B. Silva, G. Kali, and N. Bruns, "Horseradish peroxidase as a catalyst for atom transfer radical polymerization," *Macromol. Rapid Commun.*, vol. 32, no. 21, pp. 1710–1715, 2011.
- [102] Y.-H. Ng, F. di Lena, and C. L. L. Chai, "Metalloenzymatic radical polymerization using alkyl halides as initiators," *Polym. Chem.*, vol. 2, no. 3, p. 589, 2011.
- [103] B. Zhang, X. Wang, A. Zhu, K. Ma, Y. Lv, X. Wang, and Z. An, "Enzyme-Initiated Reversible Addition – Fragmentation Chain Transfer Polymerization," *Biomacromolecules*, 2015.
- [104] R. Jin, C. Hiemstra, Z. Zhong, and J. Feijen, "Enzyme-mediated fast in situ formation of hydrogels from dextran-tyramine conjugates," *Biomaterials*, vol. 28, no. 18, pp. 2791–2800, 2007.
- [105] G. M. Gübitz and A. C. Paulo, "New substrates for reliable enzymes: Enzymatic modification of polymers," *Curr. Opin. Biotechnol.*, vol. 14, no. 6, pp. 577–582, 2003.
- [106] A. Rachkov, M. Hu, E. Bulgarevich, T. Matsumoto, and N. Minoura, "Molecularly imprinted polymers prepared in aqueous solution selective for [Sar1,Ala8]angiotensin II," *Anal. Chim. Acta*, vol. 504, no. 1, pp. 191–197, 2004.
- [107] M. Hamid and Khalil-ur-Rehman, "Potential applications of peroxidases," *Food Chem.*, vol. 115, no. 4, pp. 1177–1186, 2009.
- [108] A. M. Azevedo, V. C. Martins, D. M. F. Prazeres, V. Vojinović, J. M. S. Cabral, and L. P. Fonseca, "Horseradish peroxidase: A valuable tool in biotechnology," *Biotechnol. Annu. Rev.*, vol. 9, no. 03, pp. 199–247, 2003.
- [109] F. W. Krainer and A. Glieder, "An updated view on horseradish peroxidases: recombinant production and biotechnological applications," *Appl. Microbiol. Biotechnol.*, vol. 99, no. 4, pp. 1611–1625, 2015.
- [110] K. G. Welinder, "Amino acid sequence studies of horseradish peroxidase. Amino and carboxyl termini, cyanogen bromide and tryptic fragments, the complete sequence, and some structural



- characteristics of horseradish peroxidase C.," *Eur. J. Biochem.*, vol. 96, no. 3, pp. 483–502, 1979.
- [111] H. G. Rennke and M. a Venkatachalam, "Chemical modification of horseradish peroxidase. Preparation and characterization of tracer enzymes with different isoelectric points.," *J. Histochem. Cytochem.*, vol. 27, no. 10, pp. 1352–1353, 1979.
- [112] N. C. Veitch, "Horseradish peroxidase: A modern view of a classic enzyme," *Phytochemistry*, vol. 65, no. 3, pp. 249–259, 2004.
- [113] L. K. Folkes and P. Wardman, "Oxidative activation of indole-3-acetic acids to cytotoxic species - A potential new role for plant auxins in cancer therapy," *Biochem. Pharmacol.*, vol. 61, no. 2, pp. 129–136, 2001.
- [114] A. P. Rodrigues, L. M. da Fonseca, O. M. de Faria Oliveira, I. L. Brunetti, and V. F. Ximenes, "Oxidation of acetylacetone catalyzed by horseradish peroxidase in the absence of hydrogen peroxide," *Biochim. Biophys. Acta - Gen. Subj.*, vol. 1760, no. 12, pp. 1755–1761, 2006.
- [115] H. Claus, "Laccases: structure, reactions, distribution," *Micron*, vol. 35, no. 1–2, pp. 93–96, 2004.
- [116] A. M. Mayer and R. C. Staples, "Laccase: New functions for an old enzyme," *Phytochemistry*, vol. 60, no. 6, pp. 551–565, 2002.
- [117] U. N. Dwivedi, P. Singh, V. P. Pandey, and A. Kumar, "Structure–function relationship among bacterial, fungal and plant laccases," *J. Mol. Catal. B Enzym.*, vol. 68, no. 2, pp. 117–128, 2011.
- [118] D. M. Mate and M. Alcalde, "Laccase engineering: From rational design to directed evolution," *Biotechnol. Adv.*, vol. 33, no. 1, pp. 25–40, 2015.
- [119] A. Kunamneni, F. J. Plou, A. Ballesteros, and M. Alcalde, "Laccases and their applications: a patent review.," *Recent Pat. Biotechnol.*, vol. 2, no. 1, pp. 10–24, 2008.
- [120] V. A. Chertkov, A. K. Shestakova, A. V. Kisin, and A. I. Yaropolov, "Enzymatic Polymerization of Dihydroquercetin Using Bilirubin Oxidase," vol. 80, no. 2, 2015.
- [121] V. Krikstolaityte, J. Kuliesius, A. Ramanaviciene, L. Mikoliunaite, A. Kausaite-Minkstimiene, Y. Oztekin, and A. Ramanavicius, "Enzymatic polymerization of polythiophene by immobilized glucose oxidase," *Polym. (United Kingdom)*, vol. 55, no. 7, pp. 1613–1620, 2014.
- [122] S. Ahmad and P. Goswami, "Application of chitosan beads immobilized Rhodococcus sp. NCIM 2891 cholesterol oxidase for cholestenone production," *Process Biochem.*, vol. 49, no. 12, pp. 2149–2157, 2014.
- [123] Z. Xia, T. Miyakoshi, and T. Yoshida, "Lipoxygenase-catalyzed polymerization of phenolic lipids suggests a new mechanism for allergic contact dermatitis induced by urushiol and its analogs.," *Biochem. Biophys. Res. Commun.*, vol. 315, no. 3, pp. 704–9, 2004.
- [124] D. Keilin and E. F. Hartree, "Purification of horse-radish peroxidase and comparison of its properties with those of catalase and methaemoglobin," *Biochem. J.*, vol. 49, no. 1, pp. 88–106, 1951.
- [125] S. Riva, R. Molcolare, and V. M. Bianco, "Laccases : blue enzymes for green chemistry," vol. 24, no. 5, 2006.
- [126] A. Singh and D. L. Kaplan, "Enzyme-Based Vinyl Polymerization," vol. 10, no. 3, 2002.
- [127] A. Singh and D. L. Kaplan, "In Vitro Enzyme-Induced Vinyl Polymerization.pdf," *Adv. Polym. Sci.*, vol. 194, pp. 211–224, 2006.
- [128] N. R. Curvetto, D. Figlas, A. Brandolin, S. B. Saidman, E. H. Rueda, and M. L. Ferreira, "Efficiency of enzymatic and non-enzymatic catalysts in the synthesis of insoluble polyphenol and conductive polyaniline in water," *Biochem. Eng. J.*, vol. 29, no. 3, pp. 191–203, 2006.
- [129] R. Ikeda, H. Tanaka, H. Uyama, and S. Kobayashi, "Enzymatic synthesis and Curing of poly(cardanol)," *Polym. J.*, vol. 32, no. 7, pp. 589–593, 2000.

- [130] H. Uyama, H. Kurioka, and S. Kobayashi, "Preparation of Polyphenol Particles by Peroxidase-catalyzed Dispersion Polymerization," *Colloids surfaces A Physicochemical Eng. Asp.*, vol. 153, pp. 189–194, 1999.
- [131] Y. J. Kim, K. Shibata, H. Uyama, and S. Kobayashi, "Synthesis of ultrahigh molecular weight phenolic polymers by enzymatic polymerization in the presence of amphiphilic triblock copolymer in water," *Polymer (Guildf.)*, vol. 49, no. 22, pp. 4791–4795, 2008.
- [132] T. Narancic, R. Davis, J. Nikodinovic-Runic, and K. E. O' Connor, "Recent developments in biocatalysis beyond the laboratory," *Biotechnol. Lett.*, pp. 943–954, 2015.
- [133] T. Hiraishi and S. Taguchi, "Enzyme-catalyzed Synthesis and Degradation of Biopolymers," *Mini. Rev. Org. Chem.*, vol. 6, no. 1, pp. 44–54, 2009.
- [134] G. V. Otrokhov, O. V. Morozova, I. S. Vasil'eva, G. P. Shumakovich, E. a. Zaitseva, M. E. Khlopova, and a I. Yaropolov, "Biocatalytic synthesis of conducting polymers and prospects for its application.," *Biochem. Biokhimiia*, vol. 78, no. 13, pp. 1539–53, 2013.
- [135] I. Figueroa-González, G. Quijano, G. Ramírez, and A. Cruz-Guerrero, "Probiotics and prebiotics-perspectives and challenges," *J. Sci. Food Agric.*, vol. 91, no. 8, pp. 1341–1348, 2011.
- [136] J.-M. Choi, S.-S. Han, and H.-S. Kim, "Industrial applications of enzyme biocatalysis: Current status and future aspects," *Biotechnol. Adv.*, 2015.
- [137] D. Muñoz Solano, P. Hoyos, M. J. Hernáiz, a. R. Alcántara, and J. M. Sánchez-Montero, "Industrial biotransformations in the synthesis of building blocks leading to enantiopure drugs," *Bioresour. Technol.*, vol. 115, pp. 196–207, 2012.
- [138] S. Li and X. Cao, "Enzymatic synthesis of Cephalexin in recyclable aqueous two-phase systems composed by two pH responsive polymers," *Biochem. Eng. J.*, vol. 90, pp. 301–306, 2014.
- [139] Y. Wang, A. Singh, P. Xu, M. a. Pindrus, D. J. Blasioli, and D. L. Kaplan, "Expansion and osteogenic differentiation of bone marrow-derived mesenchymal stem cells on a vitamin C functionalized polymer," *Biomaterials*, vol. 27, no. 17, pp. 3265–3273, 2006.
- [140] A. Singh and D. L. Kaplan, "Vitamin C Functionalized Poly(Methyl Methacrylate) for Free Radical Scavenging," *J. Macromol. Sci. Part A*, vol. 41, no. 12, pp. 1377–1386, 2004.
- [141] S. H. Gellman, "Introduction: Molecular Recognition," *Chem. Rev.*, vol. 95, no. 5, pp. 1231–1232, 1997.
- [142] R. Schirhagl, "Bioapplications for Molecularly Imprinted Polymers," *Anal. Chem.*, vol. 86, pp. 250–261, 2014.
- [143] M. J. Whitcombe, N. Kirsch, and I. a. Nicholls, "Molecular imprinting science and technology: A survey of the literature for the years 2004-2011," *J. Mol. Recognit.*, vol. 27, no. 6, pp. 297–401, 2014.
- [144] R. J. Ansell, "Molecularly imprinted polymers in pseudoimmunoassay," *J. Chromatogr. B Anal. Technol. Biomed. Life Sci.*, vol. 804, no. 1, pp. 151–165, 2004.
- [145] Z. X. Xu, H. J. Gao, L. M. Zhang, X. Q. Chen, and X. G. Qiao, "The Biomimetic Immunoassay Based on Molecularly Imprinted Polymer: A Comprehensive Review of Recent Progress and Future Prospects," *J. Food Sci.*, vol. 76, no. 2, 2011.
- [146] C. Baggiani, L. Anfossi, and C. Giovannoli, "MIP-based immunoassays: State of the Art, limitations and Perspectives," *Mol. Imprinting*, vol. 1, pp. 41–54, 2013.
- [147] X. X. Li, L. H. Bai, H. Wang, J. Wang, Y. P. Huang, and Z. S. Liu, "Preparation and characterization of enrofloxacin-imprinted monolith prepared with crowding agents," *J. Chromatogr. A*, vol. 1251, pp. 141–147, 2012.
- [148] X. A. Ton, B. Tse Sum Bui, M. Resmini, P. Bonomi, I. Dika, O. Soppera, and K. Haupt, "A versatile fiber-optic fluorescence sensor based on molecularly imprinted microstructures polymerized in situ," *Angew. Chemie - Int. Ed.*, vol. 52, no. 32, pp. 8317–8321, 2013.

- [149] N. Atar, T. Eren, and M. L. Yola, "A molecular imprinted SPR biosensor for sensitive determination of citrinin in red yeast rice," *Food Chem.*, vol. 184, pp. 7–11, 2015.
- [150] M. L. Yola, T. Eren, and N. Atar, "A sensitive molecular imprinted electrochemical sensor based on gold nanoparticles decorated graphene oxide: Application to selective determination of tyrosine in milk," *Sensors Actuators B Chem.*, vol. 210, pp. 149–157, 2015.
- [151] P. Bonomi, A. Servant, and M. Resmini, "Modulation of imprinting efficiency in nanogels with catalytic activity in the Kemp elimination," *J. Mol. Recognit.*, vol. 25, no. 6, pp. 352–360, 2012.
- [152] M. Resmini, "Molecularly imprinted polymers as biomimetic catalysts," *Anal. Bioanal. Chem.*, vol. 402, no. 10, pp. 3021–3026, 2012.
- [153] a Katz and M. Davis, "Molecular imprinting of bulk, microporous silica," *Nature*, vol. 403, no. 6767, pp. 286–9, 2000.
- [154] D. L. Rathbone, "Molecularly imprinted polymers in the drug discovery process," *Adv. Drug Deliv. Rev.*, vol. 57, no. 12, pp. 1854–1874, 2005.
- [155] K. Çetin and A. Denizli, "5-Fluorouracil delivery from metal-ion mediated molecularly imprinted cryogel discs," *Colloids Surfaces B Biointerfaces*, vol. 126, pp. 401–406, 2015.
- [156] D. Cunliffe, A. Kirby, and C. Alexander, "Molecularly imprinted drug delivery systems," *Adv. Drug Deliv. Rev.*, vol. 57, no. 12, pp. 1836–1853, 2005.
- [157] Q. Zhao, J. Sun, H. Ren, Q. Zhou, and Q. Lin, "Horseradish Peroxidase Immobilized in Macroporous Hydrogel for Acrylamide Polymerization," *J. Polym. Sci. Part a-Polymer Chem.*, vol. 46, no. 3, pp. 2222–2232, 2008.
- [158] Y. Yu, L. Ye, K. Haupt, and K. Mosbach, "Formation of a class of enzyme inhibitors (drugs), including a chiral compound, by using imprinted polymers or biomolecules as molecular-scale reaction vessels," *Angew. Chemie - Int. Ed.*, vol. 41, no. 23, pp. 4459–4463, 2002.
- [159] K. Mosbach, "Molecular imprinting," *Trends Biochem. Sci.*, vol. 19, no. 1, pp. 9–14, 1994.
- [160] S. Vidyasankar, M. Ru, and F. H. Arnold, "Molecularly imprinted ligand-exchange adsorbents for the chiral separation of underivatized amino acids," vol. 775, pp. 51–63, 1997.
- [161] G. Baydemir, N. Bereli, M. Andac, R. Say, I. Yu, and A. Denizli, "Bilirubin recognition via molecularly imprinted supermacroporous cryogels," *Colloids Surfaces B Biointerfaces*, vol. 68, pp. 33–38, 2009.
- [162] B. B. Prasad, D. Jauhari, and M. P. Tiwari, "Doubly imprinted polymer nanofilm-modified electrochemical sensor for ultra-trace simultaneous analysis of glyphosate and glufosinate," *Biosens. Bioelectron.*, vol. 59, pp. 81–88, 2014.
- [163] S. Ambrosini, S. Beyazit, K. Haupt, and B. Tse Sum Bui, "Solid-phase synthesis of molecularly imprinted nanoparticles for protein recognition," *Chem. Commun. (Camb.)*, vol. 49, no. 60, pp. 6746–8, 2013.
- [164] A. Cutivet, C. Schembri, J. Kovensky, and K. Haupt, "Molecularly imprinted microgels as enzyme inhibitors," *J. Am. Chem. Soc.*, vol. 131, no. 41, pp. 14699–14702, 2009.
- [165] Y.-S. Fang, X.-J. Huang, L.-S. Wang, and J.-F. Wang, "An enhanced sensitive electrochemical immunosensor based on efficient encapsulation of enzyme in silica matrix for the detection of human immunodeficiency virus p24," *Biosens. Bioelectron.*, vol. 64, pp. 324–332, 2015.
- [166] K. Haupt and K. Mosbach, "Plastic antibodies: Developments and applications," *Trends Biotechnol.*, vol. 16, no. 11, pp. 468–475, 1998.
- [167] J. Wackerlig and P. a. Lieberzeit, "Molecularly imprinted polymer nanoparticles in chemical sensing – Synthesis, characterisation and application," *Sensors Actuators B Chem.*, vol. 207, pp. 144–157, 2015.
- [168] T. Takagishi and I. M. Klotz, "Macromolecule-small molecule interactions; introduction of additional binding sites in polyethyleneimine by disulfide cross-linkages," *Biopolymers*, vol. 11, no. 2, pp. 483–491, 1972.



- [169] G. Wulff, a. Sarhan, and K. Zabrocki, "Enzyme-Analogue Built Polymers and Their Use for the Resolution of Racemates," *Tetrahedron Lett.*, vol. 44, no. 44, pp. 4329–4332, 1973.
- [170] R. Arshady and K. Mosbach, "Synthesis of Substrate-selective Polymers by Host-Guest Polymerization," *Makromol. Chem.*, vol. 692, pp. 687–692, 1981.
- [171] H. Yan and K. H. Row, "Characteristic and Synthetic Approach of Molecularly Imprinted Polymer," *Int. J. Mol. Sci.*, vol. 7, no. 5, pp. 155–178, 2006.
- [172] S. A. S. Tabassi, S. V. Hashemi, and S. A. Mohajeri, "Dummy template molecularly imprinted polymer for omeprazole and the study of its drug binding and release properties," *J. Appl. Polym. Sci.*, vol. 130, no. 6, pp. 4165–4170, 2013.
- [173] B. H. karsten, V. L. Ana, B. Marc, and Tse Sum Bui, "Molecularly Imprinted Polymers," *Top Curr Chem*, vol. 325, pp. 1–28, 2012.
- [174] P. a G. Cormack and A. Z. Elorza, "Molecularly imprinted polymers: synthesis and characterisation.," *J. Chromatogr. B. Analyt. Technol. Biomed. Life Sci.*, vol. 804, no. 1, pp. 173–182, 2004.
- [175] J. Y. N. Philip, J. Buchweishaija, L. L. Mkayula, and L. Ye, "Preparation of molecularly imprinted polymers using anacardic acid monomers derived from cashew nut shell liquid," *J. Agric. Food Chem.*, vol. 55, no. 22, pp. 8870–8876, 2007.
- [176] T. Muhammad, Z. Nur, E. V. Piletska, O. Yimit, and S. a. Piletsky, "Rational design of molecularly imprinted polymer: the choice of cross-linker.," *Analyst*, vol. 137, no. 11, p. 2623, 2012.
- [177] C. Rossi and K. Haupt, "Application of the Doehlert experimental design to molecularly imprinted polymers: Surface response optimization of specific template recognition as a function of the type and degree of cross-linking," *Anal. Bioanal. Chem.*, vol. 389, pp. 455–460, 2007.
- [178] M. Javanbakht, A. M. Attaran, M. H. Namjumanesh, M. Esfandyari-Manesh, and B. Akbari-adergani, "Solid-phase extraction of tramadol from plasma and urine samples using a novel water-compatible molecularly imprinted polymer," *J. Chromatogr. B Anal. Technol. Biomed. Life Sci.*, vol. 878, no. 20, pp. 1700–1706, 2010.
- [179] G. Van Royen, P. Dubruel, and E. Daeseleire, "Development and evaluation of a molecularly imprinted polymer for benzylpenicillin detection and clean-up in milk.," *J. Agric. Food Chem.*, 2014.
- [180] K. Haupt, A. Dzgoev, and K. Mosbach, "Assay system for the herbicide 2,4-dichlorophenoxyacetic acid using a molecularly imprinted polymer as an artificial recognition element," *Anal. Chem.*, vol. 70, no. 3, pp. 628–631, 1998.
- [181] K. Haupt, A. G. Mayes, and K. Mosbach, "Herbicide assay using an imprinted polymer-based system analogous to competitive fluoroimmunoassays," *Anal. Chem.*, vol. 70, no. 18, pp. 3936–3939, 1998.
- [182] N. Henry, R. Delépée, J. M. Seigneuret, and L. a. Agrofoglio, "Synthesis of water-compatible imprinted polymers of in situ produced fructosazine and 2,5-deoxyfructosazine," *Talanta*, vol. 99, pp. 816–823, 2012.
- [183] S. Sasaki, T. Ooya, T. Takeuchi\*, and T. Takeuchi, "Highly selective bisphenol A—imprinted polymers prepared by atom transfer radical polymerization," *Polym. Chem.*, vol. 1, no. 10, p. 1684, 2010.
- [184] C. Gonzato, M. Courty, P. Pasetto, and K. Haupt, "Magnetic molecularly imprinted polymer nanocomposites via surface-initiated RAFT polymerization," *Adv. Funct. Mater.*, vol. 21, no. 20, pp. 3947–3953, 2011.
- [185] P. Yu, Q. Sun, Z. Tan, M. Meng, J. Pan, Y. Yan, and C. Li, "Magnetic Molecularly Imprinted Polymer Beads Obtained by Suspension Polymerization for the Adsorption of 2,4,6-

- Trichlorophenol from an Aqueous Solution in a Fixed-bed Column,” *Adsorpt. Sci. Technol.*, vol. 33, no. 3, pp. 321–336, 2015.
- [186] W. Xu, H. Li, X. Ni, N. Wang, and Y. Yan, “Synthesis and Characterization of a Magnetic Molecularly Imprinted Polymer by Suspension Polymerization for Selective Recognition of Dibenzothiophene from Gasoline Samples,” *Adsorpt. Sci. Technol.*, vol. 33, no. 9, pp. 819–831, 2015.
- [187] A. G. Mayes and K. Mosbach, “Molecularly imprinted polymer beads: suspension polymerization using a liquid perfluorocarbon as the dispersing phase,” *Anal. Chem.*, vol. 68, no. 21, pp. 3769–3774, 1996.
- [188] X. Wang, X. Ding, Z. Zheng, X. Hu, X. Cheng, and Y. Peng, “Magnetic molecularly imprinted polymer particles synthesized by suspension polymerization in silicone oil,” *Macromol. Rapid Commun.*, vol. 27, no. 14, pp. 1180–1184, 2006.
- [189] H. Kempe and M. Kempe, “Novel Method for the Synthesis of Molecularly Imprinted Polymer Bead Libraries,” *Macromol. Rapid Commun.*, vol. 25, no. 1, pp. 315–320, 2004.
- [190] A. Poma, A. P. F. Turner, and S. a. Piletsky, “Advances in the manufacture of MIP nanoparticles,” *Trends Biotechnol.*, vol. 28, no. 12, pp. 629–637, 2010.
- [191] Y. K. Lv, C. X. Zhao, P. Li, Y. D. He, Z. R. Yang, and H. W. Sun, “Preparation of doxycycline-imprinted magnetic microspheres by inverse-emulsion suspension polymerization for magnetic dispersion extraction of tetracyclines from milk samples,” *J. Sep. Sci.*, vol. 36, no. 16, pp. 2656–2663, 2013.
- [192] Z. Wang and X. Cao, “Preparation of core–shell molecular imprinting polymer for lincomycin A and its application in chromatographic column,” *Process Biochem.*, vol. 50, no. 7, pp. 1136–1145, 2015.
- [193] S. Boonpangrak, V. Prachayasittikul, L. Bülow, and L. Ye, “Molecularly imprinted polymer microspheres prepared by precipitation polymerization using a sacrificial covalent bond,” *J. Appl. Polym. Sci.*, vol. 99, no. 4, pp. 1390–1398, 2006.
- [194] G. Wulff, B. O. Chong, and U. Kolb, “Soluble single-molecule nanogels of controlled structure as a matrix for efficient artificial enzymes,” *Angew. Chemie - Int. Ed.*, vol. 45, no. 18, pp. 2955–2958, 2006.
- [195] S. Subrahmanyam, A. Guerreiro, A. Poma, E. Moczko, E. Piletska, and S. Piletsky, “Optimisation of experimental conditions for synthesis of high affinity MIP nanoparticles,” *Eur. Polym. J.*, vol. 49, no. 1, pp. 100–105, 2013.
- [196] P. Çakir, A. Cutivet, M. Resmini, B. T. S. Bui, and K. Haupt, “Protein-size molecularly imprinted polymer nanogels as synthetic antibodies, by localized polymerization with multi-initiators,” *Adv. Mater.*, vol. 25, no. 7, pp. 1048–1051, 2013.
- [197] S. Scorrano, L. Mergola, M. Di Bello, M. Lazzoi, G. Vasapollo, and R. Del Sole, “Molecularly Imprinted Composite Membranes for Selective Detection of 2-Deoxyadenosine in Urine Samples,” *Int. J. Mol. Sci.*, vol. 16, no. 6, pp. 13746–13759, 2015.
- [198] H. Shi, R. Wang, J. Yang, H. Ren, S. Liu, and T. Guo, “Novel imprinted nanocapsule with highly enhanced hydrolytic activity for organophosphorus pesticide degradation and elimination,” *Eur. Polym. J.*, vol. 72, pp. 190–201, 2015.
- [199] M. Seifi, M. Hassanpour Moghadam, F. Hadizadeh, S. Ali-Asgari, J. Aboli, and S. A. Mohajeri, “Preparation and study of tramadol imprinted micro- and nanoparticles by precipitation polymerization: Microwave irradiation and conventional heating method,” *Int. J. Pharm.*, vol. 471, no. 1–2, pp. 37–44, 2014.
- [200] J. Chen, L. Bai, Y. Zhang, N. Chen, and Y. Zhang, “Fabrication of Atrazine Molecularly Imprinted Polymer Microsphere by Two Step Seed Swelling Polymerization Method,” *J. Chinese Chem. Soc.*, vol. 59, no. 12, pp. 1493–1499, 2012.

- [201] X. Chen, W. Yang, Y. Zhou, and F. Jiao, "In situ synthesis of monolithic molecularly imprinted stationary phases for liquid chromatographic enantioseparation of dibenzoyl tartaric acid enantiomers," *J. Porous Mater.*, vol. 19, no. 5, pp. 587–595, 2011.
- [202] F. Puoci, F. Iemma, G. Cirillo, M. Curcio, O. I. Parisi, U. G. Spizzirri, and N. Picci, "New restricted access materials combined to molecularly imprinted polymers for selective recognition/release in water media," *Eur. Polym. J.*, vol. 45, no. 6, pp. 1634–1640, 2009.
- [203] S. A. Mohajeri, B. Malaekheh-nikouei, and H. Sadegh, "Development of a pH-responsive imprinted polymer for diclofenac and study of its binding properties in organic and aqueous media," *drug Dev. Ind. Pharm.*, vol. 38, no. 5, pp. 616–622, 2012.
- [204] A. Tieppo, K. M. Pate, and M. E. Byrne, "In vitro controlled release of an anti-inflammatory from daily disposable therapeutic contact lenses under physiological ocular tear flow," *Eur. J. Pharm. Biopharm.*, vol. 81, no. 1, pp. 170–177, 2012.
- [205] L. Tang, C. Zhao, X. Wang, R. Li, J. Yang, Y. Huang, and Z. Liu, "Macromolecular crowding of molecular imprinting: A facile pathway to produce drug delivery devices for zero-order sustained release," *Int. J. Pharm.*, 2015.
- [206] F. A. Ishkuh, M. Javanbakht, M. Esfandyari-Manesh, R. Dinarvand, and F. Atyabi, "Synthesis and characterization of paclitaxel-imprinted nanoparticles for recognition and controlled release of an anticancer drug," *J. Mater. Sci.*, vol. 49, pp. 6343–6352, 2014.
- [207] A. Luís, M. Ruela, E. C. Figueiredo, and G. R. Pereira, "Molecularly imprinted polymers as nicotine transdermal delivery systems," *Chem. Eng. J.*, vol. 248, pp. 1–8, 2014.
- [208] P. S. Sharma, Z. Iskierko, A. Pietrzyk-Le, F. D'Souza, and W. Kutner, "Bioinspired intelligent molecularly imprinted polymers for chemosensing: A mini review," *Electrochem. commun.*, vol. 50, pp. 81–87, 2015.
- [209] H. Zhang, "Water-compatible molecularly imprinted polymers: Promising synthetic substitutes for biological receptors," *Polym. (United Kingdom)*, vol. 55, no. 3, pp. 699–714, 2014.
- [210] L. I. Andersson, R. Mullert, G. Vlatakist, and K. Mosbach, "Mimics of the binding sites of opioid receptors obtained by molecular imprinting of enkephalin and morphine (molecular recognition/synthetic polymers/ligand-receptor interactions/molecularly imprinted sorbent assay)," *Proc. Natl. Acad. Sci. U. S. A.*, vol. 92, no. May, pp. 4788–4792, 1995.
- [211] T. Muhammad, L. Cui, W. Jide, E. V. Piletska, A. R. Guerreiro, and S. a. Piletsky, "Rational design and synthesis of water-compatible molecularly imprinted polymers for selective solid phase extraction of amiodarone," *Anal. Chim. Acta*, vol. 709, pp. 98–104, 2012.
- [212] H. W. Sun and F. X. Qiao, "Recognition mechanism of water-compatible molecularly imprinted solid-phase extraction and determination of nine quinolones in urine by high performance liquid chromatography," *J. Chromatogr. A*, vol. 1212, no. 1–2, pp. 1–9, 2008.
- [213] F. Horemans, a. Weustenraed, D. Spivak, and T. J. Cleij, "Towards water compatible MIPs for sensing in aqueous media," *J. Mol. Recognit.*, vol. 25, no. 6, pp. 344–351, 2012.
- [214] P. Dzygiel, E. O'Donnell, D. Fraier, C. Chassaing, and P. a G. Cormack, "Evaluation of water-compatible molecularly imprinted polymers as solid-phase extraction sorbents for the selective extraction of sildenafil and its desmethyl metabolite from plasma samples," *J. Chromatogr. B Anal. Technol. Biomed. Life Sci.*, vol. 853, no. 1–2, pp. 346–353, 2007.
- [215] W. Yang, F. Jiao, L. Zhou, X. Chen, and X. Jiang, "Molecularly imprinted polymers coated on multi-walled carbon nanotubes through a simple indirect method for the determination of 2,4-dichlorophenoxyacetic acid in environmental water," *Appl. Surf. Sci.*, vol. 284, pp. 692–699, 2013.
- [216] G. Pan, Y. Zhang, X. Guo, C. Li, and H. Zhang, "An efficient approach to obtaining water-compatible and stimuli-responsive molecularly imprinted polymers by the facile surface-grafting of functional polymer brushes via RAFT polymerization," *Biosens. Bioelectron.*, vol. 26, no. 3, pp. 976–982, 2010.

- [217] J. Luo, J. Sun, J. Huang, and X. Liu, "Preparation of water-compatible molecular imprinted conductive polyaniline nanoparticles using polymeric micelle as nanoreactor for enhanced paracetamol detection," *Chem. Eng. J.*, vol. 283, pp. 1118–1126, 2016.
- [218] J. Chen, H. Huang, Y. Zeng, H. Tang, and L. Li, "Novel composite of molecularly imprinted polymer-coated PdNPs for electrochemical sensing norepinephrine," *Biosens. Bioelectron.*, vol. 65, pp. 366–374, 2015.
- [219] B. Buszewski, J. Ričanyová, R. Gadzała-Kopciuch, and M. Szumski, "Supramolecular recognition of estrogens via molecularly imprinted polymers," *Anal. Bioanal. Chem.*, vol. 397, no. 7, pp. 2977–2986, 2010.
- [220] W. D. J. R. Santos, P. R. Lima, C. R. T. Tarley, N. F. Höehr, and L. T. Kubota, "Synthesis and application of a peroxidase-like molecularly imprinted polymer based on hemin for selective determination of serotonin in blood serum," *Anal. Chim. Acta*, vol. 631, no. 2, pp. 170–176, 2009.
- [221] L. Mergola, S. Scorrano, R. Del Sole, M. R. Lazzoi, and G. Vasapollo, "Developments in the synthesis of a water compatible molecularly imprinted polymer as artificial receptor for detection of 3-nitro-L-tyrosine in neurological diseases," *Biosens. Bioelectron.*, vol. 40, no. 1, pp. 336–341, 2013.
- [222] X. Ren and L. Chen, "Preparation of molecularly imprinted polymer coated quantum dots to detect nicosulfuron in water samples," *Anal. Bioanal. Chem.*, vol. 407, no. 26, pp. 8087–8095, 2015.
- [223] T. Takagishi, A. Hayashi, and N. Kuroki, "Cross-Linked Polyvinylpyrrolidones with Increased Affinity and Specificity for Methyl Orange and Its Homologs," *J. Polym. Sci.*, vol. 20, pp. 1533–1547, 1982.
- [224] H. Asanuma, T. Akiyama, K. Kajiyama, T. Hishiya, and M. Komiyama, "Molecular imprinting of cyclodextrin in water for the recognition of nanometer-scaled guests," *Anal. Chim. Acta*, vol. 435, pp. 25–33, 2001.
- [225] B. R. Hart and K. J. Shea, "Molecular Imprinting for the Recognition of N-Terminal Histidine Peptides in Aqueous Solution," *Macromolecules*, vol. 35, pp. 6192–6201, 2002.
- [226] N. Turner and C. Jeans, "From 3D to 2D: a review of the molecular imprinting of proteins," *Biotechnol. ...*, vol. 22, no. 6, pp. 1474–1489, 2006.
- [227] E. Verheyen, J. P. Schillemans, M. Van Wijk, M. A. Demeniex, W. E. Hennink, and C. F. Van Nostrum, "Challenges for the effective molecular imprinting of proteins," *Biomaterials*, vol. 32, no. 11, pp. 3008–3020, 2011.
- [228] A. Bossi, F. Bonini, a. P. F. Turner, and S. a. Piletsky, "Molecularly imprinted polymers for the recognition of proteins: The state of the art," *Biosens. Bioelectron.*, vol. 22, no. 6, pp. 1131–1137, 2007.
- [229] S. Li, S. Cao, M. J. Whitcombe, and S. a. Piletsky, "Size matters: Challenges in imprinting macromolecules," *Prog. Polym. Sci.*, vol. 39, no. 1, pp. 145–163, 2014.
- [230] M. E. Byrne, K. Park, and N. a. Peppas, "Molecular imprinting within hydrogels," *Adv. Drug Deliv. Rev.*, vol. 54, no. 1, pp. 149–161, 2002.
- [231] J. Liu, Q. Deng, D. Tao, K. Yang, L. Zhang, Z. Liang, and Y. Zhang, "Preparation of protein imprinted materials by hierarchical imprinting techniques and application in selective depletion of albumin from human serum.," *Sci. Rep.*, vol. 4, p. 5487, 2014.
- [232] K. Zhao, T. Chen, B. Lin, W. Cui, B. Kan, N. Yang, X. Zhou, X. Zhang, and J. Wei, "Adsorption and recognition of protein molecular imprinted calcium alginate/polyacrylamide hydrogel film with good regeneration performance and high toughness," *React. Funct. Polym.*, vol. 87, pp. 7–14, 2015.
- [233] M. Zayats, A. J. Brenner, and P. C. Searson, "Protein imprinting in polyacrylamide-based gels," *Biomaterials*, vol. 35, no. 30, pp. 8659–8668, 2014.

- [234] G. Pan, Q. Guo, C. Cao, H. Yang, and B. Li, "Thermo-responsive molecularly imprinted nanogels for specific recognition and controlled release of proteins," *Soft Matter*, vol. 9, no. 14, pp. 3840–3850, 2013.
- [235] L. Qin, X. W. He, X. Yuan, W. Y. Li, and Y. K. Zhang, "Molecularly imprinted beads with double thermosensitive gates for selective recognition of proteins," *Anal. Bioanal. Chem.*, vol. 399, no. 10, pp. 3375–3385, 2011.
- [236] J. Xu, S. Ambrosini, E. Tamahkar, C. Rossi, K. Haupt, and B. Tse Sum Bui, "Toward a Universal Method for Preparing Molecularly Imprinted Polymer Nanoparticles with Antibody-like Affinity for Proteins," *Biomacromolecules*, vol. 17, no. 1, pp. 345–353, 2016.
- [237] A. Poma, A. Guerreiro, M. J. Whitcombe, E. V Piletska, A. P. F. Turner, and S. a Piletsky, "Solid-Phase Synthesis of Molecularly Imprinted Polymer Nanoparticles with a Reusable Template – ‘Plastic Antibodies,’" *Adv. Funct. Mater.*, pp. 2821–2827, 2013.
- [238] L. Feng, B. Kan, K. Zhao, J. Wei, D. Zhu, and L. Zhang, "Preparation and characterization of protein molecularly imprinted polysiloxane using mesoporous calcium silicate as matrix by sol–gel technology," *J. Sol-Gel Sci. Technol.*, vol. 71, no. 3, pp. 428–436, 2014.
- [239] M. Kempe, M. Glad, and K. Mosbach, "An approach towards surface imprinting using the enzyme ribonuclease A.," *J. Mol. Recognit.*, vol. 8, no. 1–2, pp. 35–9, 1995.
- [240] H. Shi, W. B. Tsai, M. D. Garrison, S. Ferrari, and B. D. Ratner, "Template-imprinted nanostructured surfaces for protein recognition.," *Nature*, vol. 398, no. 6728, pp. 593–597, 1999.
- [241] P. C. Chou, J. Rick, and T. C. Chou, "C-reactive protein thin-film molecularly imprinted polymers formed using a micro-contact approach," *Anal. Chim. Acta*, vol. 542, no. 1 SPEC. ISS., pp. 20–25, 2005.
- [242] K. El Kirat, M. Bartkowski, and K. Haupt, "Probing the recognition specificity of a protein molecularly imprinted polymer using force spectroscopy," *Biosens. Bioelectron.*, vol. 24, no. 8, pp. 2618–2624, 2009.
- [243] E. Yilmaz, K. Haupt, and K. Mosbach, "The use of immobilized templates - a new approach in molecular imprinting.," *Angew. Chemie, Int. Ed.*, vol. 39, no. 12, pp. 2115–2118, 2000.
- [244] R. Üzek, L. Uzun, and A. Denizli, "Surface imprinting approach for preparing specific adsorbent for IgG separation," vol. 25, no. 9, pp. 881–894, 2014.
- [245] Q. Li, K. Yang, J. Liu, L. Zhang, Z. Liang, and Y. Zhang, "Transferrin recognition based on a protein imprinted material prepared by hierarchical imprinting technique," *Microchim. Acta*, vol. 180, no. 15–16, pp. 1379–1386, 2013.
- [246] M. M. Titirici and B. Sellergren, "Peptide recognition via hierarchical imprinting," *Anal. Bioanal. Chem.*, vol. 378, pp. 1913–1921, 2004.
- [247] A. Nematollahzadeh, W. Sun, C. S. a Aureliano, D. Lütkemeyer, J. Stute, M. J. Abdekhodaie, A. Shojaei, and B. Sellergren, "High-capacity hierarchically imprinted polymer beads for protein recognition and capture," *Angew. Chemie - Int. Ed.*, vol. 50, pp. 495–498, 2011.
- [248] Y. Lv, T. Tan, and F. Svec, "Molecular imprinting of proteins in polymers attached to the surface of nanomaterials for selective recognition of biomacromolecules," *Biotechnol. Adv.*, vol. 31, no. 8, pp. 1172–1186, 2013.
- [249] A. Rachkov and N. Minoura, "Recognition of oxytocin and oxytocin-related peptides in aqueous media using a molecularly imprinted polymer synthesized by the epitope approach," *J. Chromatogr. A*, vol. 889, no. 1–2, pp. 111–118, 2000.
- [250] H. Nishino, C. S. Huang, and K. J. Shea, "Selective protein capture by epitope imprinting," *Angew. Chemie - Int. Ed.*, vol. 45, no. 15, pp. 2393–2396, 2006.
- [251] D.-Y. Li, Y.-P. Qin, H.-Y. Li, X.-W. He, W.-Y. Li, and Y.-K. Zhang, "A ‘turn-on’ fluorescent receptor for detecting tyrosine phosphopeptide using the surface imprinting procedure and the epitope approach," *Biosens. Bioelectron.*, vol. 66, pp. 224–230, 2015.



- [252] L. Tan, Z. Yu, X. Zhou, D. Xing, X. Luo, R. Peng, and Y. Tang, "Antibody-free ultra-high performance liquid chromatography/tandem mass spectrometry measurement of angiotensin I and II using magnetic epitope-imprinted polymers," *J. Chromatogr. A*, vol. 1411, pp. 69–76, 2015.
- [253] A. M. Bossi, P. S. Sharma, L. Montana, G. Zoccatelli, O. Laub, and R. Levi, "Fingerprint-imprinted polymer: Rational selection of peptide epitope templates for the determination of proteins by molecularly imprinted polymers," *Anal. Chem.*, vol. 84, no. 9, pp. 4036–4041, 2012.
- [254] L. Cenci, A. Anesi, M. Busato, G. Guella, and A. M. Bossi, "Molecularly imprinted polymers coupled to matrix assisted laser desorption ionization mass spectrometry for femtomoles detection of cardiac troponin I peptides," *J. Mol. Recognit.*, vol. 29, no. 1, pp. 41–50, 2016.
- [255] Z. Iskierko, P. S. Sharma, K. Bartold, A. Pietrzyk-Le, K. Noworyta, and W. Kutner, "Molecularly imprinted polymers for separating and sensing of macromolecular compounds and microorganisms," *Biotechnol. Adv.*, 2015.
- [256] C. Alexander and E. N. Vulfson, "Spatially functionalized polymer surfaces produced via cell-mediated lithography," *Adv. Mater.*, vol. 9, no. 9, pp. 751–755, 1997.
- [257] a. Aherne, C. Alexander, M. J. Payne, N. Perez, and E. N. Vulfson, "Bacteria-mediated lithography of polymer surfaces," *J. Am. Chem. Soc.*, vol. 118, no. 36, pp. 8771–8772, 1996.
- [258] S. Tokonami, Y. Nakadoi, M. Takahashi, M. Ikemizu, T. Kadoma, K. Saimatsu, L. Q. Dung, H. Shiigi, and T. Nagaoka, "Label-free and selective bacteria detection using a film with transferred bacterial configuration," *Anal. Chem.*, vol. 85, pp. 4925–4929, 2013.
- [259] F. L. Dickert and O. Hayden, "Bioimprinting of polymers and sol-gel phases. Selective detection of yeasts with imprinted polymers," *Anal. Chem.*, vol. 74, no. 6, pp. 1302–1306, 2002.
- [260] E. Yilmaz, D. Majidi, E. Ozgur, and A. Denizli, "Whole cell imprinting based Escherichia coli sensors: A study for SPR and QCM," *Sensors Actuators B Chem.*, vol. 209, pp. 714–721, 2015.
- [261] Z. Altintas, M. Gittens, J. Pocock, and I. E. Tothill, "Biosensors for waterborne viruses: Detection and removal," *Biochimie*, vol. 115, pp. 144–154, 2015.
- [262] Z. Altintas, J. Pocock, K.-A. Thompson, and I. E. Tothill, "Comparative investigations for adenovirus recognition and quantification: Plastic or natural antibodies?," *Biosens. Bioelectron.*, vol. 74, pp. 996–1004, 2015.
- [263] C.-H. Lu, Y. Zhang, S.-F. Tang, Z.-B. Fang, H.-H. Yang, X. Chen, and G.-N. Chen, "Sensing HIV related protein using epitope imprinted hydrophilic polymer coated quartz crystal microbalance," *Biosens. Bioelectron.*, vol. 31, no. 1, pp. 439–444, 2012.

## *Chapter II*

*Preparation and characterization of hydrogels synthesized by biochemically-initiated free radical polymerization*

*Results and discussion*

## II.1. Introduction

A hydrophilic gel, referred to as hydrogel, is a network of cross-linked polymer chains that can be extensively swollen in presence of water [1]. Since the early 1960s, hydrogels have been a topic of extensive research in biomaterials science. They are well-known to be biocompatible and closely mimic natural living tissue due to their high water content, porosity, and consistency [2]. Network morphology and equilibrium swollen state of hydrogels are responsible for several important properties such as mechanical strength, internal and external transport. For this, hydrogels, including microgels and nanogels, have emerged as the most versatile and viable platform for sustained protein release, targeted drug delivery and tissue engineering [2-6].

In the past decades, many approaches have been developed and applied to obtain hydrogels. These methods are classified into two categories: chemical or physical cross-linking [2, 7, 8, 9]. Chemical hydrogels are covalently cross-linked, and thus, exhibit enhanced mechanical strength and better stability than physically cross-linked hydrogels. Despite this advantage, the use of additives to form chemical bonds, e.g. organic solvents, initiators, and cross-linkers, increases the cytotoxicity of the polymeric matrix, resulting in reduced biocompatibility. Physical cross-linking of hydrogels is achieved when the networks are held together by ionic and/or hydrophobic interactions or by crystallization [9]. This type of cross-linking provides reversibility of the hydrogels and a great tool for controlled drug delivery due to the absence of chemical reactions which are potentially harmful for cells [10]. However, their mechanical stability *in vivo* may be negatively affected by ion concentration or pH changes, as in any normal inflammatory response, leading to gel collapse or denaturing [11].

In the past few years, mild crosslinking methods have been investigated. Synthesis of hydrogels has been performed by click chemistry due to its high reactivity, specificity and yield [12]. Enzymatically cross-linked hydrogels have also been developed. This mainly attracted attention due to the mildness of this type of reactions, which occurs at neutral pH, in aqueous media at moderate temperature. Moreover, unwanted chemical reactions or toxicity can be avoided within a hydrogel and good mechanical stability is maintained [11, 13]. Horseradish peroxidase is the most important enzyme that has been used to cross-link linear polymers [11, 13, 14]. For



instance, dextran-tyramine conjugates were synthesized by thermo-initiated radical polymerization. Then, hydrogels were prepared by HRP-coupling reaction of phenol moieties in the dextran-tyramine conjugates, in presence of hydrogen peroxide [13]. To date, only one example of HRP-mediated polymerization for hydrogel synthesis has emerged [15]. A ternary enzymatic system (HRP/Acac/H<sub>2</sub>O<sub>2</sub>) was used to initiate the co-polymerization of *N,N*-dimethylacrylamide and acryloylated human serum albumin to entrap the HRP within the hydrogel. High catalytic activity of the immobilized enzyme was attained in different solvents compared to covalent immobilization achieved in literature.

Based on this approach, the scope of this chapter is to study the enzymatic synthesis of hydrogels. We proposed to investigate their synthesis by free-radical polymerization with enzyme-mediated initiation using an oxidoreductase as catalyst. The aim of this work was to combine the advantages of both chemical and physical hydrogels, by keeping a good mechanical strength and the biocompatibility. Here, the enzymatic system catalyzes the free-radical polymerization (FRP) of acrylic and vinyl monomers instead of the traditionally chemical initiating systems. HRP is among the enzymes that predominate in the field of enzyme-initiated radical polymerization. It is used, as well as other oxidoreductases such as laccases, to catalyze the polymerization of different vinyl and aromatic compounds [16]. Since the catalytic mechanism of laccases uses molecular oxygen (which inhibits radical polymerization), we preferred to use HRP for the catalysis of hydrogels synthesis.

**Figure II-1** shows the principle of the catalytic cycle of HRP for the formation of radical species, which is presented in detail in **Chapter I, Figure I-15**. This cycle includes the initial oxidation of the enzyme active site by hydrogen peroxide to form compound I and water. Then, the compound I can interact with a reducing species, such as acetylacetone, in an oxido-reduction step leading to radical formation and compound II. Finally, a second radical is formed by another oxido-reduction step, in which compound II is transformed to the enzyme in its initial state, thus achieving the catalytic cycle.

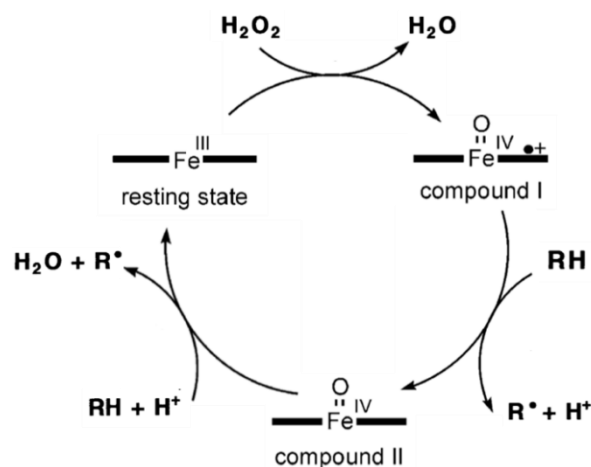


**Figure II-1: Representation of the accepted HRP catalytic cycle, showing compounds I and II as enzyme intermediates, and the formation of radical species.**

The radical species, which are generated within the HRP biocatalytic cycle, have the potential to initiate the polymerization for subsequent hydrogel synthesis (**Figure II-2**).

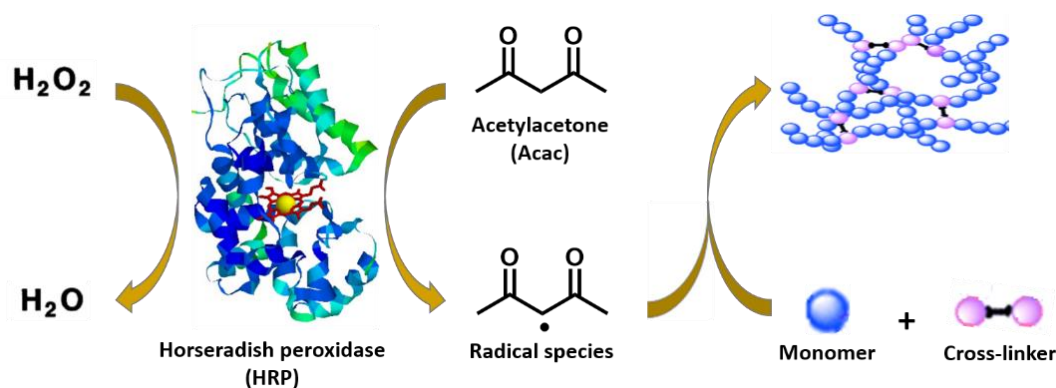


**Figure II-2: Representation of the enzyme-mediated free-radical polymerization for hydrogel preparation.**

Although emphasis is on the use of HRP, in this chapter, the generation of radicals by different enzymes is discussed together with the underlying mechanism. The influence of different experimental parameters on the hydrogels characteristics of resulting hydrogels is also investigated. Finally, this initiating system is compared to the traditional chemical approach.

## II.2. Materials and Methods

### II.2.1. Materials

- Functional and cross-linking monomers

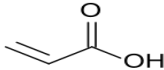
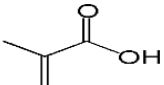
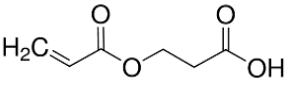
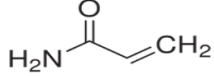
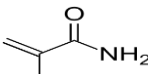
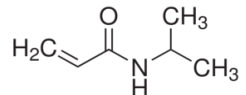
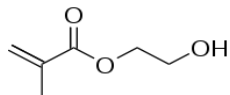
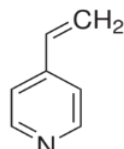
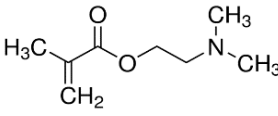
The functional monomers methacrylic acid (MAA), acrylic acid (AA), carboxyethyl acrylate (CEA), acrylamide (Aam), methylacrylamide (MeAAM), *N*-isopropylacrylamide (NiPAM), (hydroxyethyl)methacrylate (HEMA), 4-vinylpyridine (4-VP), 2-(diethylamino)ethylmethacrylate (DEAEM), and cross-linking monomers, e.g. *N,N'*-methylenebisacrylamide (MeBAAM), *N,N'*-ethylenebis(acrylamide) (EbAAM), and 1,4-bis(acryloyl)piperazine (PDA) were purchased from Sigma-Aldrich. 4-VP was vacuum-distilled before use. **Tables II-1** and **II-2** show the chemical structures and molecular weights of the functional and cross-linking monomers used in this study.

- Biochemical system components and chemical initiators

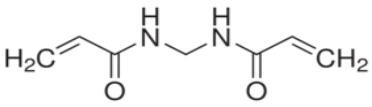
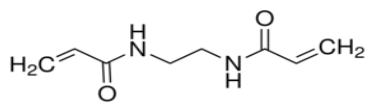
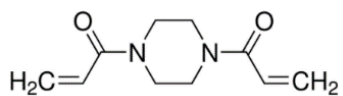
For biochemical initiation, myoglobin from skeletal muscle (Myo), cytochrome *c* from horse heart (Cyt *c*), hemoglobin from bovine blood (Hb), peroxidase from horseradish roots (HRP), hemin and protoporphyrin, the substrates hydrogen peroxide (35 wt. % solution in water), acetylacetone  $\geq 99\%$  (Acac) and 2,2'-azino-bis(3-ethylbenzothiazoline-6-sulfonic acid) diammonium salt (ABTS) were purchased from Sigma-Aldrich.

For photochemical initiation, Vazo<sup>®</sup>56 (2,2'-Azobis(2-amidinopropane) dihydrochloride), potassium persulfate (KPS) and tetramethylethylenediamine (TEMED) were purchased from Chemours or Sigma-Aldrich.

Table II-1: Chemical structure and molecular weight of functional monomers used in this study

Functional monomer	Chemical Structure	Molecular Weight (g/mol)
Acrylic acid		72.06
Methacrylic Acid		86.06
Carboxyethyl acrylate		144.13
Acrylamide		71.08
Methacrylamide		85.11
N-isopropylacrylamide		113.6
(Hydroxyethyl)methacrylate		130.14
4-Vinylpyridine		105.14
2-(diethylamino)ethylmethacrylate		185.27

**Table II-2: Chemical structure and molecular weight of cross-linking monomers used in this study**

Cross-linking monomer	Chemical structure	Molecular Weight (g/mol)
<b><i>N,N'</i>-Methylenebisacrylamide</b>		154.17
<b><i>N,N'</i>-Ethylenebis(acrylamide)</b>		168.19
<b>1,4-Bis(acryloyl)piperazine</b>		194.23

- Solvents

Methanol was from Sigma-Aldrich and used without further purification. Water was purified with a RiOs Progard<sup>®</sup> 2 Silver, and a milli-Q Q-Gard<sup>®</sup> 1 systems from Millipore ('ultrapure water', 18.2 MΩ/cm). The buffer solutions were prepared from the commercial salts dissolved in ultrapure water, and the pH was adjusted, using a pH-meter, by a concentrated sodium hydroxide solution, or diluted solution of hydrochloric acid.

## II.2.2. Synthesis of linear polymers

### Synthesis of linear polyacrylamides

The synthesis of linear polyacrylamide was based on a modified protocol reported earlier [17-21]. The polymerization procedure was as follows: 1.23 mmol (100 mg) of commercial acrylamide were dissolved in 900 μl of water introduced into a glass vial and 17 mmol (1.75 μl) of Acac were added. The solution was stirred, and then 0.1 ml of 0.023 mM biocatalyst solution in water were added to the mixture. The solution was purged in nitrogen during 5 minutes on ice and 106 μl of 0.1 M hydrogen peroxide in water was added with a microsyringe. After polymerization for 4 hours at room temperature, the reaction mixture was added dropwise to 15

ml of methanol to precipitate the polyacrylamide. The polymer was recovered by centrifugation, then washed in methanol for 3 times and dried under vacuum. Only polymerization of acrylamide by the catalysis of iron, protoporphyrin, and hemin was studied in 0.1 M phosphate buffer pH 7.0. The other polymerizations were carried out in ultrapure water.

For the polyacrylamide synthesis by FRP with photochemical initiation, the same monomer concentration was employed. The chemical initiator Vazo<sup>®</sup>56 was used instead of the Acac/H<sub>2</sub>O<sub>2</sub>/biocatalyst system, and kept at 1 mol-% of the monomer double bonds. The sample was irradiated under UV light for 5 minutes, and the samples treated as described above. The weight of chemical initiator was calculated by using the upcoming equation 1:

$$\% \text{ Initiator} = \frac{\text{Number of moles of initiator}}{\text{Number of moles of the double bonds within monomers}} \times 100 \quad (\text{Eq.1})$$

### Synthesis of linear polyacrylates

The procedure for the polymerization of acrylic and vinyl monomers was the same as for the acrylamide polymerization. 1.23 mmol of the functional monomer were dissolved in a total volume of 1 ml of solvent. The polymerization of acidic monomers was performed in distilled water and in phosphate buffer pH 7.0 with different molarities, whereas the polymerization of different neutral and alkaline monomers was done in distilled water.

For the precipitation, the polymers based on neutral and acidic monomers (poly(acrylic acid) and poly(methacrylic acid)) were precipitated in methanol, and subsequently washed with the same solvent for 2 times, while for alkaline monomers, the polymers were washed in water.

### II.2.3. Synthesis of Hydrogels

Hydrogels were prepared by free-radical polymerization, in which functional monomer is polymerized in the presence of water-soluble bifunctional cross-linker. For each hydrogel, 0.58 mmol of cross-linking monomer were mixed with 0.145 mmol of the functional monomer in ultrapure water or buffer. The required volume of solvent was calculated depending on total monomer concentration, according to the following equation 2:

$$[\text{Monomers}](\%) = \frac{\text{Total monomers weight}}{\text{Total Weight (monomers+solvent)}} \times 100 \quad (\text{Eq.2})$$

The standard protocol for biochemical initiation was: 0.1 ml of 0.023 mM solution of biocatalyst were added to the monomers mixture with 0.035 mmol (3.6  $\mu$ l) Acac solution. The solution was kept on ice and degassed for 10 minutes. 216  $\mu$ l of a 103 mM solution of hydrogen peroxide in water were then introduced. In order to study the influence of the different parameters, the amounts of each component in this protocol were varied.

For chemical initiations, 2% of initiator was used instead of the Acac/H<sub>2</sub>O<sub>2</sub>/biocatalyst system. The initiator quantity was calculated according to the equation **Eq. 1**. It corresponds to 3 mg of Vazo<sup>®</sup>56 and 7 mg of KPS. For the redox couple, the ratio of KPS/TEMED is fixed to 7.5:1, so 0.0035 mmol of TEMED are used.

#### II.2.4. Polymer characterization

**Polymerization Yield:** The polymerization yield corresponds to the weight ratio of dry polymer recovered after the polymerization reaction and washing steps to the monomers quantity introduced initially. The relative percentage is calculated according to the following equation 3:

$$\text{Polymerization Yield } (\%) = \frac{\text{Polymer weight}}{\text{Total monomers amount}} \times 100 \quad (\text{Eq.3})$$

**Gel Permeation Chromatography (GPC):** For all water-soluble linear polymers synthesized by both enzymatic and chemical initiations, GPC was performed to determine the molecular weight. The experiments were performed by asymmetrical flow field-flow fractionation coupled to detection by multi-angle laser light scattering (AF4-MALLS) on a Wyatt Helios 8 angles.

**Particle size measurements** by dynamic light scattering for the determination the hydrodynamic size were performed with a Zetasizer Nano (Malvern Instruments Ltd., Worcestershire, UK) at 25°C. The laser used is a 4 mW He-Ne,  $\lambda=632$  nm, 173°, backscatter. The samples were

prepared by different dilutions in water (0.1 mg/l) followed by 30 minutes sonication prior to the measurement.

**Particles morphology:** the morphology of the particles was studied by Scanning Electron Microscopy (SEM). SEM imaging was performed on a Quanta feg 250 environmental microscope at the Physico-Chemical Analysis Platform from UTC. The samples were prepared in ethanol at 50 ppm. A drop of this solution was deposited on a cleaned glass surface and dried in air. A thin gold layer (0.5 nm) was then vacuum-deposited on the sample prior to analysis.

### II.2.5. Study of the polymerization kinetics

The polymerization kinetics by different oxidoreductases were investigated by measuring the particles sizes and the polymerization yields at different times during the polymerization. The kinetics of HRP, myoglobin, and cytochrome *c* were investigated for the polymerization of different functional monomers and PDA as cross-linker.

Different hydrogels were synthesized, for every biocatalyst, *via* the typical procedure described in II.2.3. The polymerization was stopped by introducing oxygen in the reaction mixture. The particles sizes are measured directly by DLS and the hydrogels were recovered by washing steps with water in order to measure the polymerization yield.

### II.2.6. Evaluation of HRP entrapment within hydrogel matrix

In order to study the entrapment of HRP within the hydrogel matrix, two hydrogels were synthesized by the typical protocol described above (cf II.2.3), using HRP final concentrations of 0.08 mg/ml or 0.4 mg/ml in 0.1 mM phosphate buffer pH 7.0 were prepared. For this, 0.1 ml of 10 mg/ml and 50 mg/ml HRP solutions were used for the enzymatic synthesis of **Hydrogel 1** and **Hydrogel 2**, respectively.



The polymerization was carried out at room temperature for three days. The hydrogels were then washed with phosphate buffer 3 times and polymers were recovered by centrifugation. In order to determine the polymerization yields, 1 ml of each hydrogel was dialyzed in water and lyophilized. The polymerization yields were 63 % and 79 % for Hydrogels **1** and **2**, respectively.

**Protein quantification:** the amount of horseradish peroxidase entrapped in the hydrogels was determined by the Bradford spectroscopic assay [22]. The standard curve was plotted measuring the absorbance at 595 nm of a solution consisting of HRP serial standards from 0.02 g.L<sup>-1</sup> to 0.1 g.L<sup>-1</sup> and 0.9 ml of the Bradford reagent solution, as shown in **Figure II-3**. The protein concentrations in the reaction media before and after polymerization were determined by the Bradford protein assay using this standard curve. The amount of immobilized peroxidase was the difference between the initial enzyme concentration in the media and ones measured in the washing liquids after polymerization.

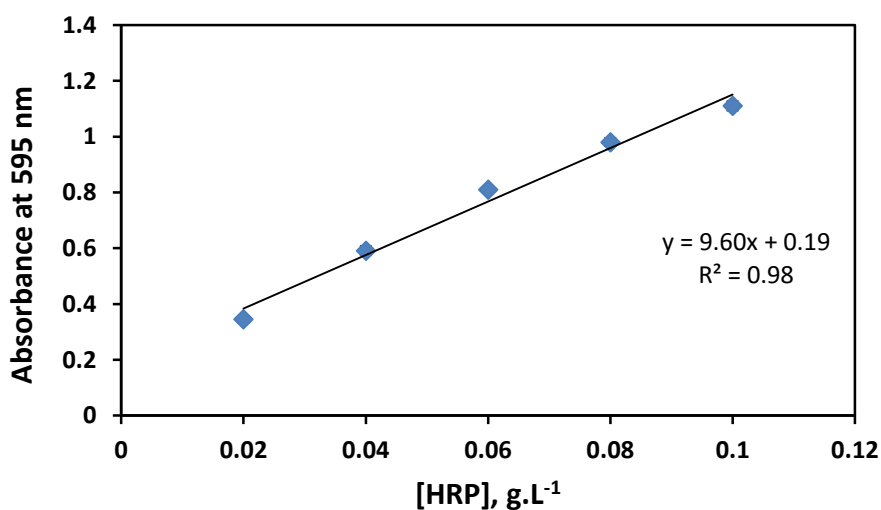


**Figure II-3: Standard curve for protein quantification by Bradford**

**Activity:** Enzyme activity assays were done measuring the oxidation of ABTS by UV-Visible spectrophotometry on a Cary-60 spectrophotometer. One unit of enzyme activity is defined as the amount of oxidized ABTS (in  $\mu\text{mol}$ ) formed per minute. For free enzyme, HRP solution (0.5

mg/L; 100  $\mu$ l) is added to 2,2'-azino-bis(3-ethylbenzothiazoline-6-sulfonate) (ABTS) solution (1.1 mM; 1.35 ml) in 50 mM phosphate buffer pH 7.0. The reaction was initiated by adding 50  $\mu$ l of 30 mM H<sub>2</sub>O<sub>2</sub>. Kinetics were measured for 2 minutes by following the absorption at 405 nm. A blank reaction without enzyme was subtracted to correct for the oxidation of ABTS by hydrogen peroxide.

The same protocol was used to study the activity of the entrapped enzyme with some modification. The specific activity of hydrogels **1** and **2** was determined by adding 0.5 ml of 30 mM H<sub>2</sub>O<sub>2</sub> solution to an ABTS solution in 50 mM phosphate buffer pH 7.0 (1.04 mM; 14.5 ml) containing different concentrations of polymer solution. The oxidation of ABTS was followed by UV/Vis spectrophotometry for 5 minutes at 405 nm.

**SDS-PAGE Electrophoresis:** The presence of HRP within the particles was also checked by SDS-PAGE analysis under reducing conditions. Polyacrylamide separation and stacking gels of 12 % and 5 % respectively were prepared and the solutions were introduced in the wells as following:

- Molecular weight markers (dual color) in lane 1
- 40  $\mu$ l of 0.1 mg/ml HRP solution in lane 2
- 40  $\mu$ l of **Hydrogel 1** homogenous solution (theoretically estimated at 25 mg/ml) *prior to any treatment*, in lane 3.
- 60  $\mu$ l of a concentrated specimen of *washed* **Hydrogel 1** (by means of ultrafiltration on Centriprep, the estimated concentration of polymer is 15 mg/ml) in lane 4.
- 20  $\mu$ l of **Hydrogel 2** homogenous solution (theoretically estimated at 35 mg/ml), prior to washing, in lane 6.
- 20  $\mu$ l of a concentrated specimen of **Hydrogel 2** at 7 mg/ml, in lane 7.

An electric field of 100 V/cm is applied across the gel for 1h 30 for protein migration. After migration, the gel was stained with Coomassie Brilliant blue.

### II.2.7. Cytotoxicity test of nanoparticles

The relative cytotoxicity of nanoparticles against HaCat cells was evaluated *in vitro* by a standard MTT test.

Cells are seeded, at 37°C, in 96-well plates at about 10000-20000 cells per well (except for the first column, which stays empty and is used as blank). 200 µl of Dulbecco's modified Eagle (DMEM) medium supplemented with 10% (v/v) fetal bovin serum (FBS) and 1% streptomycin and penicillin is added to each well, and the cells are cultured in 5% CO<sub>2</sub> atmosphere. After 48 h of incubation, the cell medium is changed to DMEM with 1% of streptomycin and penicillin and just 1% of FBS and the cells are grown again for 24 h in the presence of nanoparticles, prepared in the same medium at 1% v/v form stock solution, which is added to the cells at different concentrations (0-200 mg/L). After incubation with NPs, the cells are washed three times with PBS and a solution of 90% of medium (DMEM low glucose, 10% FRBS, 1% Pen/Strep; 1% L-glutamine) and 10% MTT reagent (3-(4,5-dimethylthiazol-2-yl)-2,5-diphenyltetrazolium bromide, 5mg/ml in PBS) is added, followed by a 3-4 h incubation. The medium is then discarded and 200 µl of DMSO is added to each well. The DMSO dissolves the blue MTT crystals that are produced through living cells. The plates are shaken for 10 minutes and then 25 µl of Sorencens Glycine Buffer is added. The plates are analyzed with a plate reader, at 570/620 nm, where 570 nm is the absorbance wavelength of the MTT, and 620 nm is the reference to make sure that there is no dirt or cell fragments influencing the measurement. Cell viability is then calculated by the following formula (Equation 4):

$$Cell\ viability = \frac{Absorbance\ (test\ cell) - Absorbance\ (blank)}{Absorbance\ (controlled\ cell) - Absorbance\ (blank)} \times 100$$

(Eq.4)

Absorbance of the control corresponds to the wells without nanoparticles and the absorbance of blank represents the wells without cells.

## II.3. Results and discussion

### II.3.1. Linear polymers synthesis by biochemical initiation

#### II.3.1.1. Synthesis of linear polyacrylamides

The synthesis of linear polyacrylamides by HRP-initiated polymerization was already reported in the literature and, as expected, the concentration of the components in the enzymatic system affected the polymer characteristics in term of yields and molecular weight [19]. In this part, we therefore first verify the synthesis of linear polyacrylamides by biochemically-initiated free radical polymerization using different oxidoreductases. We highlight the effect of the biocatalyst, the mediator, and the oxidant on the polymer synthesis. The performance of the enzymatic ternary system is then compared to the photo-chemically synthesized linear polyacrylamides. **Table II-3** summarizes the tested experimental conditions combined with the polymers yields.

**Table II-3: Linear polymerization assays of acrylamide by free radical polymerization initiated by different catalyts**

Entry	Biocatalyst	Acac	H <sub>2</sub> O <sub>2</sub>	Yield (%)
1	-	+	+	0
2	HRP	-	+	0
3	HRP	+	-	0
4	Protoporphyrin	+	+	0
5	Fe <sup>2+</sup>	+	+	5
6	Hemin	+	+	99
7	HRP	+	+	92
8	Cyt <i>c</i>	+	+	82
9	Myo	+	+	86
10	Hb	+	+	0

a. Effect of the ternary enzymatic system

Polyacrylamides were synthesized in distilled water with high yield (92 %) by adding in the HRP (1 mg/ml), hydrogen peroxide (0.01 mmol) and acetylacetone (17 mmol) to initiate the free radical polymerization of acrylamide. In the absence of one these components (entries 1, 2, and 3 in **Table II-3**), no polymerization occurred. These results highlight the importance of each component of the initiating system in the mechanism of the free radical formation and confirmed the classical horseradish peroxidase cycle, which is represented in **Figure II-1** and **Figure I-15**.

These results differ from those described by Derango *et al.* [23], where the polymerization was achieved in the absence of the reducing molecule. The formation of linear polyacrylamide in this condition was explained by the formation of a ferric  $\pi$ -dication radical resulting from the interaction of HRP with excess of hydrogen peroxide. It seemed that this ferric  $\pi$ -dication radical could contribute to the polymerization. The results described by our experimental work and involving the functionalized reducing molecule, strongly confirm the results shown in the study of Lalot *et al.* (2001) [19]. The importance of the mediator is emphasized as well as that of the enzyme in the formation of the polymer. Thus, in our case the possibility of the self-polymerization of acrylamide can be then rejected, as well as the autoxidation of Acac by HRP for the formation of linear polyacrylamides.

Furthermore, HRP is a metalloprotein containing a heme as its active site. The polymerization of acrylamide was also carried out with either the protoporphyrin organic component, the iron atom, the heme or the total enzyme (**Table II-3**, entries 4, 5, 6, and 7).

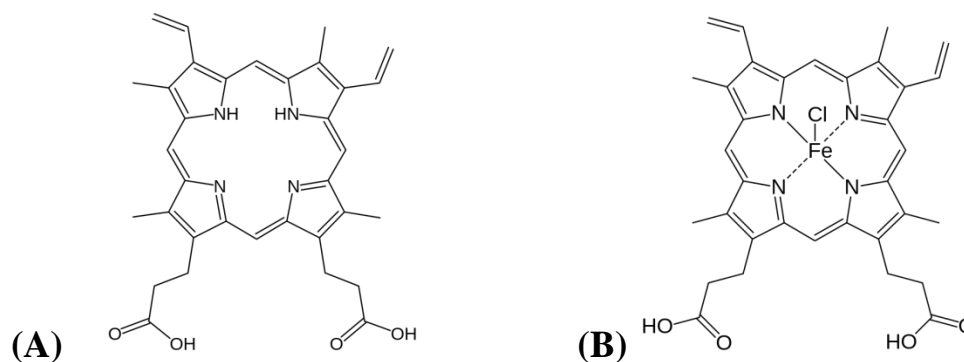


**Figure II-4: Chemical structures of (A) Protoporphyrin IV and (B) Hemin.**

**Figure II-4A** shows the chemical structure of protoporphyrin, which is widely used as carrier molecule for divalent cations, and together with iron ( $\text{Fe}^{2+}$ ), they form the body of the heme-group of many heme-containing enzymes and proteins. As can be seen from the results in **Table II-3**, the presence of only protoporphyrin does not lead to any polymer, which means that Acac cannot be oxidized in this way.

The Fenton reaction [24] was also examined (Entry 5) for the polymerization of acrylamide. Indeed, iron and hydrogen peroxide are capable of oxidizing a wide range of substrates. However, in this work, the iron ( $\text{Fe}^{2+}$ ) and hydrogen peroxide were not very efficient to oxidize Acac since only 5% yield in polyacrylamide was obtained. Whereas with hemin (**Figure II-4B**), which is the prosthetic group of different metalloproteins such as hemoglobin, myoglobin, and horseradish peroxidase, polyacrylamide could be synthesized with a high yield, similar to that with the whole enzyme. We can conclude that in the presence of Acac and hydrogen peroxide, the whole active site of the enzyme is required for an efficient radical formation and acrylamide polymerization.

#### b. Nature of the biocatalyst

As we have shown that the heme group is crucial for the radical generation mechanism, different heme-containing proteins including horseradish peroxidase, myoglobin, cytochrome *c*, and hemoglobin were tested for polyacrylamide synthesis. In general, heme proteins perform diverse important biological functions, such as oxygen transport (hemoglobin and myoglobin), electron transfer (cytochrome *c*), and catalysis (horseradish peroxidase) [25-27]. Moreover, they can all show peroxidase activity by metabolizing hydrogen peroxide in order to protect cells from endogenous oxidative damage after hypoxia.

Different oxidoreductases were investigated in the initiation of acrylamide polymerization in water (Entries 5, 8, 9, and 10 in **Table II-3**). The same molar quantity of each biocatalyst was introduced in the presence of hydrogen peroxide and acetylacetone. In addition, polymerization was also carried out by photochemical initiation with Vazo 56 (used at 1 mol-% of the polymerizable double bonds, similar to the concentration of Acac in enzymatic initiations). All the tested enzymes led to polyacrylamides with different kinetics and yields, except for

hemoglobin (Hb, entry 10 in **Table II-3**). The highest polymerization yield was obtained in the case of HRP (**Table II-3**).

The absence of polymerization with hemoglobin can be explained based on molecular basis of the peroxidase activity within hemoglobin. Hemoglobin is an oxygen transport protein within the cytosol of red blood cells in the bloodstream of vertebrates, it binds and offloads both oxygen and carbon dioxide at each tissue, serving the oxygen needed for cellular metabolism and removing the resulting waste product, carbon dioxide. Moreover, Hb has a great potential to be an oxidative stressor. The oxidation of Hb by autoxidation (oxyhemoglobin) can produce superoxide ions [28-31]. These reactive oxygen species are potential inhibitors of free-radical polymerization.

Linear polyacrylamides obtained by the catalysis of different enzymes, as well as by photochemical initiation, were characterized by gel permeation chromatography (**Table II-4**).

**Table II-4: Yields and average molecular weights of linear polyacrylamides synthesized by enzyme-mediated initiation of free-radical polymerization, through different biocatalysts.**

Entry	Biocatalyst	Yield (%)	Mw ( $10^5$ g/mol)	Mn ( $10^5$ g/mol)	Polydispersity*
1	HRP	92	7.379	5.213	1.416
2	Myoglobin	86	4.068	2.733	1.489
3	Cytochrome C	82	4.931	3.521	1.401
4	Photo-initiation	98	6.963	4.677	1.489

*\*All the measurements were achieved in ultrapure water.*

*\*Mw is the weight average molecular weight and Mn is the number average molecular weight.*

*\*The polydispersity index corresponds to the ratio of Mw/Mn.*

The results with all catalytic systems were similar, but higher yield and molecular weights were obtained with HRP as biocatalyst and with photochemical initiation, compared to the other proteins. The polymers prepared with the different enzymes show similar polydispersity. however, the weight average and number average molecular weights (Mw and Mn) show higher value in case of HRP compared to Myo and Cyt c. HRP-catalysis led to the highest polymer molecular weight, superior to that of photo-initiation.

Because of the higher yield and molecular weight, HRP was kept for subsequent experiments of polymer synthesis.

### II.3.1.2. Polymerization of other acrylic and vinyl monomers

We also studied the polymerization of a number of other monomers currently used in the field of molecular imprinting, by the HRP system and by conventional photochemical initiation. The results are shown in **Table II-5**.

**Table II-5: Yields of linear polymers based on neutral and basic monomers by free-radical polymerization initiated by enzyme-mediation.**

Polymer	Functional Monomer	Yield (%)
<b>PolyMethylAAM</b>	MethylAAM	98
<b>PolyHEMA</b>	HEMA	70
<b>PolyNIPAm</b>	NIPAm	92
<b>Poly4-VP</b>	4-Vinylpyridine	85
<b>PolyDEAEM</b>	2-(diethylamino)ethyl methacrylate	82

All neutral and basic monomers led to polymers with high polymerization yields. Enzyme-initiated polymerization of acidic monomers such as acrylic acid (AA), methacrylic acid (MAA) and carboxyethyl acrylate (CEA) is also investigated with the same experimental conditions. However, no polymer was obtained, in water or in 0.1 M sodium phosphate buffer pH 7.0, with the acidic monomers AA, MAA and CEA. This may be due to the interactions between the acidic monomer and the enzyme active site at this rather high concentration of acidic groups [32].

### II.3.2. Hydrogel synthesis by biocatalyst-mediated initiation

After the successful synthesis of linear polymers, we now wanted to attempt the enzyme-mediated synthesis of highly chemically cross-linked copolymers. This is in the context of our main goal, the synthesis of molecularly imprinted polymers (MIPs). First, bis-acryloylpiperazine (PDA)-crosslinked 4-vinylpyridine-based hydrogels were synthesized, and the morphology of the particles and possible enzyme entrapment within the hydrogel matrix were investigated. We chose poly(4-VP/PDA) as a model polymer since it will later be used to prepare MIPs (**Chapter**



IV). Again, the effect of different oxidoreductases was studied in terms of particle size and the polymerization yield.

### II.3.2.1. Characterization of hydrogels synthesis by HRP-mediated free radical polymerization

Since it is the first time the enzymatic initiation of co-polymerized hydrogels is reported, it is crucial to study the polymer formation. For the hydrogels synthesis in our study, poly(4-VP/PDA) with cross-linking ratios of 80% were prepared, since high cross-linking ratios are generally preferred in MIPs, in order to generate materials with high 3D structural integrity and mechanical stability. Hydrogels were prepared at 1% total monomers concentration, by both enzyme-mediated and photochemical initiations of free-radical polymerization. After polymerization, the particles were washed in water and characterized by scanning electron microscopy and protein assay.

**Figure II-5** shows the results of the particles characterization by SEM. The images show a clear difference between the two initiation methods. For enzyme-mediated polymerization, small-sized polydisperse nanoparticles with a diameter around 50 nm were obtained with irregular shapes (**Figure II-5A**), while larger particles were formed by photochemical synthesis with an average size of 200 nm (**Figure II-5B**).

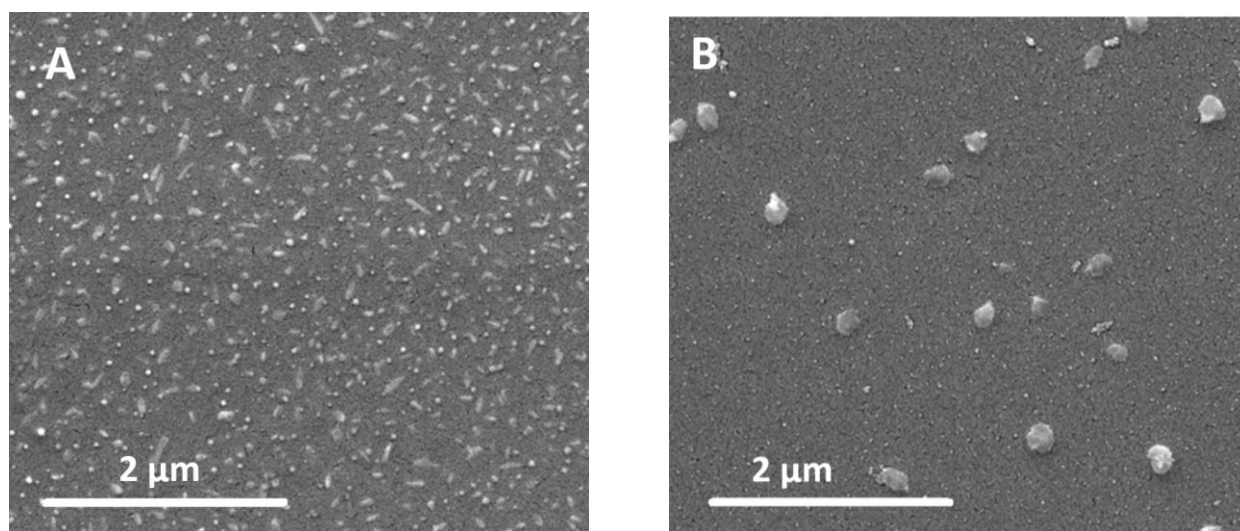


**Figure II-5: SEM images for poly(4-VP/PDA) nanoparticles synthesized by free-radical polymerization initiated by: (A) HRP catalysis; (B) UV with Vazo<sup>®</sup> 56.**

Since horseradish peroxidase was present in the solution during polymerization, it could be entrapped within the polymeric matrix. We verified this with two hydrogels synthesized by HRP-mediated free-radical polymerization using two different enzyme concentrations: 0.08 and 0.4 mg/ml for **Hydrogel 1** and **Hydrogel 2**, respectively.

After several washing steps of the hydrogels in sodium phosphate buffer, the residual peroxidase activity was determined in the hydrogels by activity measurements (ABTS test). **Figure II-6** shows the activities of the horseradish peroxidase remaining in **Hydrogels 1 and 2** for different polymer concentrations. For **Hydrogel 2**, an HRP activity of 0.2  $\mu\text{mol}/\text{min}$  was obtained. No activity has been detected in **Hydrogel 1** even when higher polymer amounts were employed.

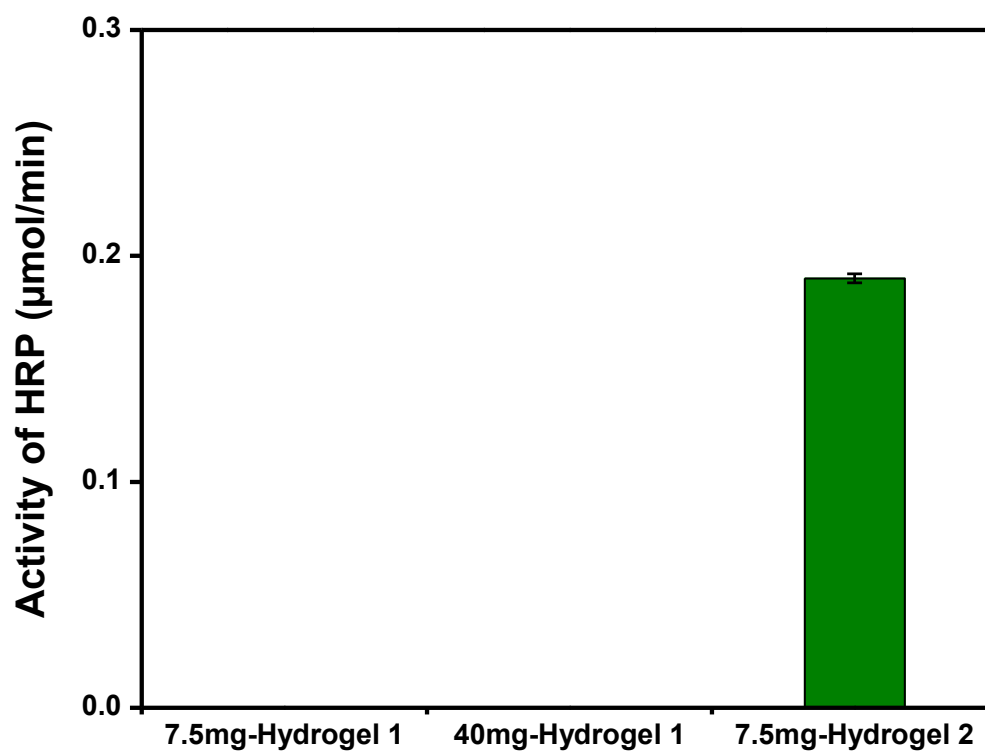


**Figure II-6:** Activity of the possibly entrapped HRP within Hydrogels 1 and 2.

The quantity of protein entrapped within **Hydrogel 1** and **2** is assessed by the Bradford method. The difference between the initial enzyme concentration in the polymerization mixture and that of washing liquids was determined for the both polymers. No protein has been detected in **Hydrogel 1** with the Bradford method, which is congruent with the absence of activity and shows that this absence is not due to enzyme inactivation. The quantity of entrapped enzyme has been estimated at 11.7  $\mu\text{g}/\text{mg}$  of polymer for **Hydrogel 2** corresponding to the entrapment of 27% of the initial enzyme amount. The entrapped enzyme in **Hydrogel 2** corresponds, thus, to 1.3 % its residual activity after the polymerization and washing steps.

In order to confirm the absence of entrapped protein within the matrix of **Hydrogel 1**, we performed SDS-PAGE electrophoresis under reducing conditions. **Figure II-7** represents the gel.

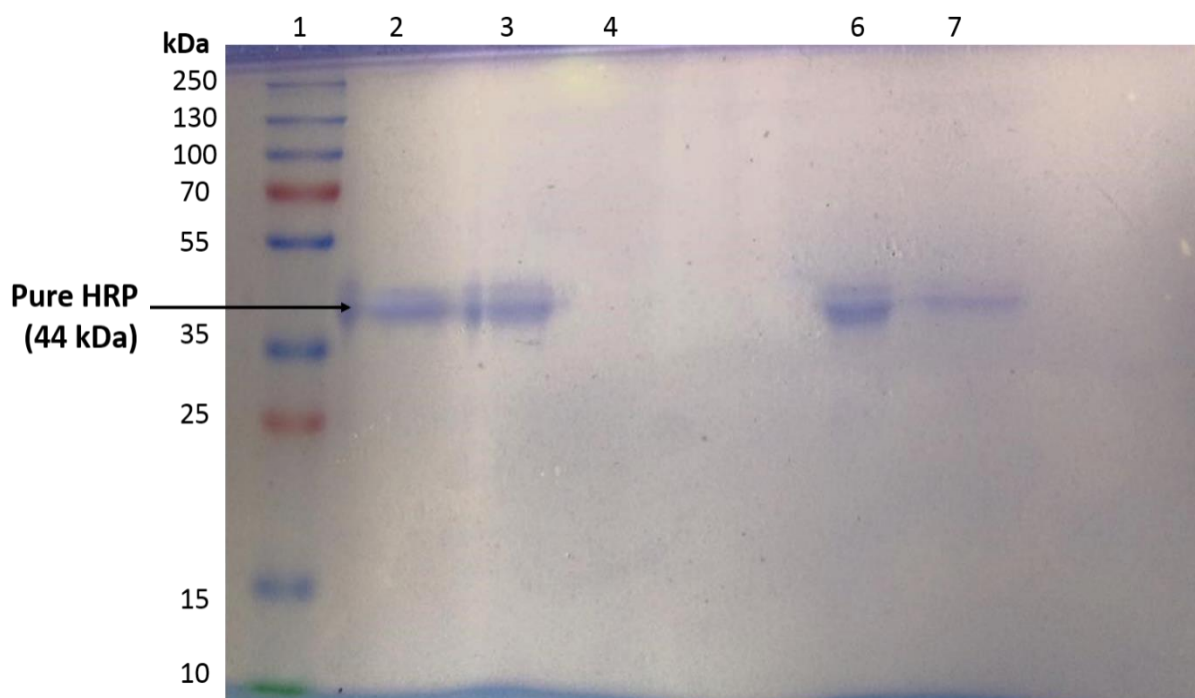


**Figure II-7: Sodium Dodecyl Sulfate Gel Electrophoresis (SDS-PAGE) under reducing conditions of nanoparticles. Lane 1: molecular weight markers (10000-250000 Da), Lane 2: commercial pure HRP solution, Lane 3: Hydrogel 1 prior to washing, Lane 4: Hydrogel 1 after washing, Lane 6: Hydrogel 2 prior to washing, Lane 7: Hydrogel 2 after washing**

Lane 2 represents the pure commercial enzyme with a molecular weight around 44 kDa. Lane 3 represents the presence of HRP in **Hydrogel 1** prior to washing. The absence of any band in Lane 4 indicates that there is no enzyme within the **Hydrogel 1** after washing. In other terms, as the sensibility of Coomassie Brilliant Blue staining is 5 ng [33], we can conclude that probably less than 5 ng of protein/mg of polymer is present in the polymeric matrix. However, the presence of a small band corresponding to the presence of protein in **Hydrogel 2** (lane 7) indicates that HRP is still present in the polymer even after 3 cycles of washing, which is coherent with the previous results of protein and peroxidase activity quantification.

Therefore, we may conclude that HRP can be entrapped when used with high concentrations for the initiation of hydrogels-free radical polymerization. HRP concentration should be fixed at 0.08 mg/ml or less in order to avoid the entrapment of the enzyme within the polymeric network, and the contamination of the final material by the biocatalyst.

### II.3.2.2. Efficiency of different heme-containing proteins for FRP

We have already shown that acrylamide can be polymerized by initiation with different biocatalysts. These different enzyme-mediated initiations have also been applied to hydrogel synthesis. For this, hydrogels based on PDA as cross-linker and different acidic, neutral, and basic functional monomers, such as MAA, Aam, and 4-VP were prepared.

Hydrogels are synthesized at 1% total monomers concentration using the ternary system acetylacetone/hydrogen peroxide/biocatalyst for initiation. **Table II-6** and **Figure II-8** show the resulting yields and particles sizes, respectively, after 3 days.

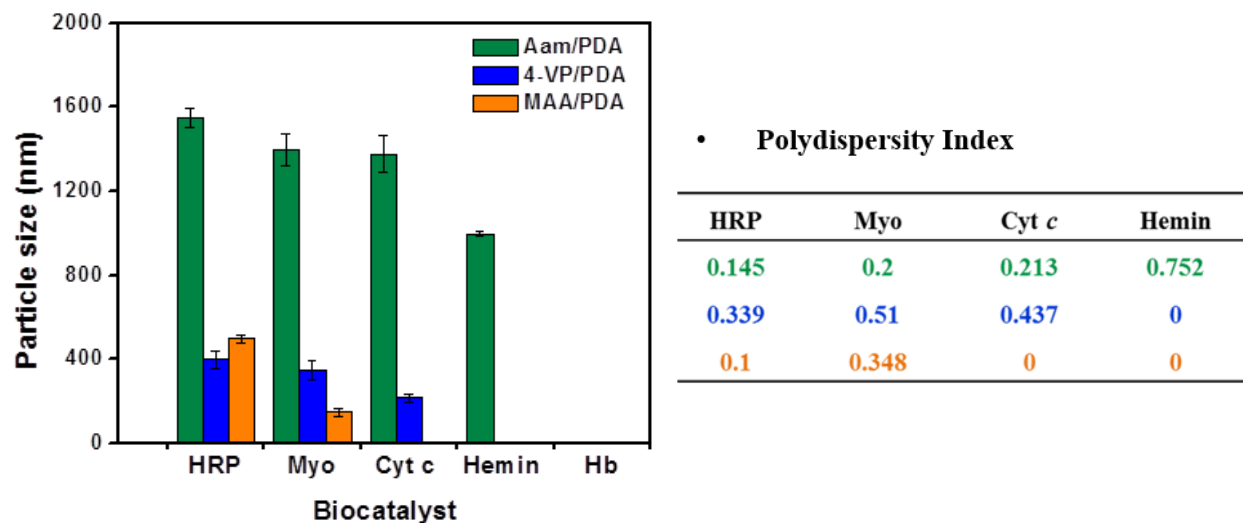


**Figure II-8:** Hydrodynamic diameters and PDI (as obtained by DLS) of the particles obtained by free radical polymerization of different functional monomers and PDA as cross-linker, initiated by different biocatalysts, using  $[\text{Monomers}]_0 = 57.2 \text{ mmol/l}$ ,  $[\text{Biocatalyst}]_0 = 0.023 \text{ mM}$ ,  $[\text{Acac}]_0 = 2.8 \text{ mM}$ , and  $[\text{H}_2\text{O}_2]_0 = 1.76 \text{ mM}$ , in  $0.1 \text{ M}$  phosphate buffer pH 7.0.

**Table II-6:** Polymerization yields obtained with different functional monomers and PDA as cross-linker, initiated by different biocatalysts, using  $[\text{Monomers}]_0 = 57.2 \text{ mmol/l}$ ,  $[\text{Biocatalyst}]_0 = 0.023 \text{ mM}$ ,  $[\text{Acac}]_0 = 2.8 \text{ mM}$ , and  $[\text{H}_2\text{O}_2]_0 = 1.76 \text{ mM}$ , in  $0.1 \text{ M}$  phosphate buffer pH 7.0.

Yield (%)	HRP	Myo	Cyt c	Hemin
<b>AAm/PDA</b>	96	97	68	12
<b>4-VP/PDA</b>	85	48	68	0
<b>MAA/PDA</b>	93	93	0	0

As we can observe, hydrogels based on the three different monomers (Aam, 4-VP, MAA) can only be obtained by the catalysis of HRP and myoglobin. The Cyt *c*-mediated initiation can lead to poly(4-VP/PDA) and poly(MAA/PDA), whereas hemin can only catalyze the synthesis of cross-linked polyacrylamide. As for the linear polymers, hemoglobin catalysis didn't result in any polymer in the case of hydrogels.

The absence of any polymerization mediated by hemoglobin is already justified in **II.3.1.1.b**. Moreover, knowing that all the tested oxidoreductases have their optimum pH between 6-7 [34-

37], the absence of any MAA/PDA polymerization by Cyt *c*-mediation cannot be due to reduced enzyme activity in the medium, since the pH in the medium is coherent with the optimum pH for the enzyme activity.

On the other hand, the fact that hemin couldn't catalyze the polymerization of 4-VP and MAA is related to the hypothesis that Fe<sup>2+</sup> of the hemin can be complexed by 4-VP [38, 39], and MAA [32]. Indeed, iron in both hemin (Fe<sup>3+</sup>) and heme (Fe<sup>2+</sup>) can be occupied and reduced by the pyridine nitrogen atom of 4-vinylpyridine [38, 39]. In literature, the formation of strong bonds between functional groups of methacrylic acid (COO<sup>-</sup>) and iron has been demonstrated [32].

The complexation of iron ions in the heme prosthetic group is probably the main reason behind the absence of any polymerization in the case of MAA/PDA by Cyt-*c* catalysis. Thus, the most probable hypothesis here is that myoglobin and horseradish peroxidase seem to have their active site more protected than that of cytochrome *c*.

In term of polymerization yields, very high polymerization yields are obtained with HRP- and Myo- initiations for poly(Aam/PDA). However, the yields decreased slightly for Cyt *c*, and greatly decreased with hemin. For basic monomer, the best yield is obtained with HRP and the smallest amount of polymer has been recovered with Myo. For acidic monomers, myoglobine- and horseradish peroxidase catalyzed initiations had led to similar yields.

In term of particles sizes, the nature of the biocatalyst has an effect on the particles size, shown in **Figure II-8**. For acrylamide-based hydrogels, somewhat smaller particles (1400 nm) were obtained with the catalysis of Cyt *c* and larger ones (1648 nm) with HRP-mediation. Hemin yielded the smallest particles in this group (1000 nm). Smaller particles were obtained with charged monomers. Particles of 200-400 nm were obtained for 4-VP-based polymers. Poly(MAA/PDA) particles had a diameter of ~500 nm (HRP catalyzed) and 128 nm (Myo).

The morphology of nanoparticles synthesized by enzyme-initiated FRP, was examined by scanning electron microscopy (SEM) for poly(4-VP/PDA) as shown in **Figure II-9**. All biocatalysts yielded spherical nanoparticles with apparently smooth surface. The particles synthesized by HRP-catalysis are twice bigger (~60 nm) than the others (~30 nm), confirming the DLS results (**Figure II-8**).



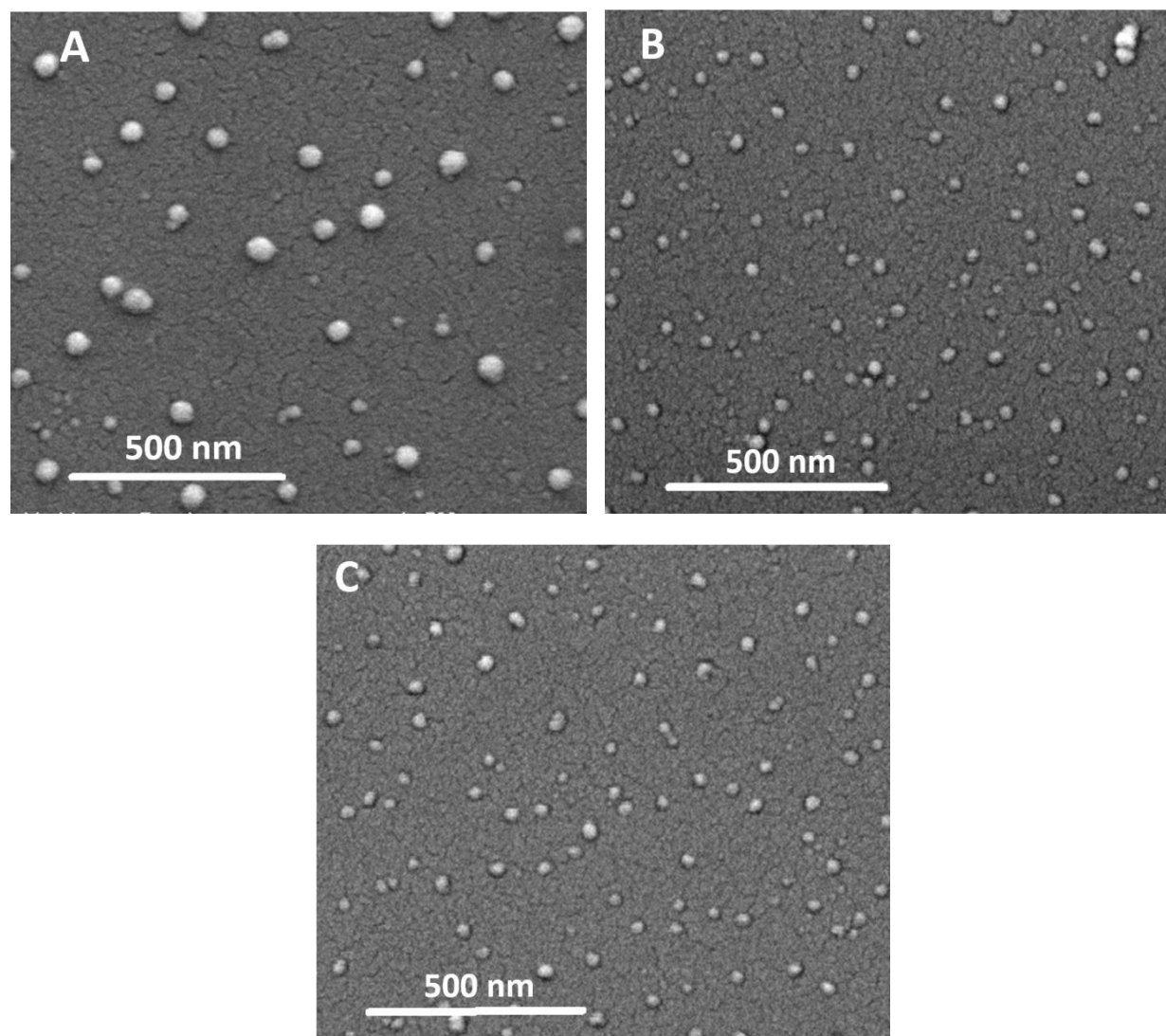


**Figure II-9: SEM images of poly(4-VP/PDA) particles synthesized by free radical polymerization initiated by (A) HRP, (B) cytochrome *c*, (C) myoglobin, using  $[\text{Monomers}]_0 = 57.2$  mM,  $[\text{Biocatalyst}]_0 = 0.023$  mM,  $[\text{Acac}]_0 = 2.8$  mM, and  $[\text{H}_2\text{O}_2]_0 = 1.76$  mM, in 0.1 M phosphate buffer pH 7.0.**

The variation in particles size and polymerization yield for the different biocatalyst with a given polymer can be attributed to the enzyme activity resulting in the production of free radicals with different kinetics. We have therefore studied the polymerization kinetics for each enzyme and also determined the time required for full polymerization. First, the co-polymerization of acrylamide and PDA was carried out by free radical polymerization in buffer using  $\text{H}_2\text{O}_2$  (1.76 mM), Acac (2.8 mM) and enzyme (0.023 mM) to initiate the reaction. We chose polyacrylamides as model polymers and HRP, Cyt *c* and Myo as biocatalysts in this study. The reaction was

interrupted at different time intervals to measure the polymerization yields and particles sizes.

**Figure II-10** summarizes the results.

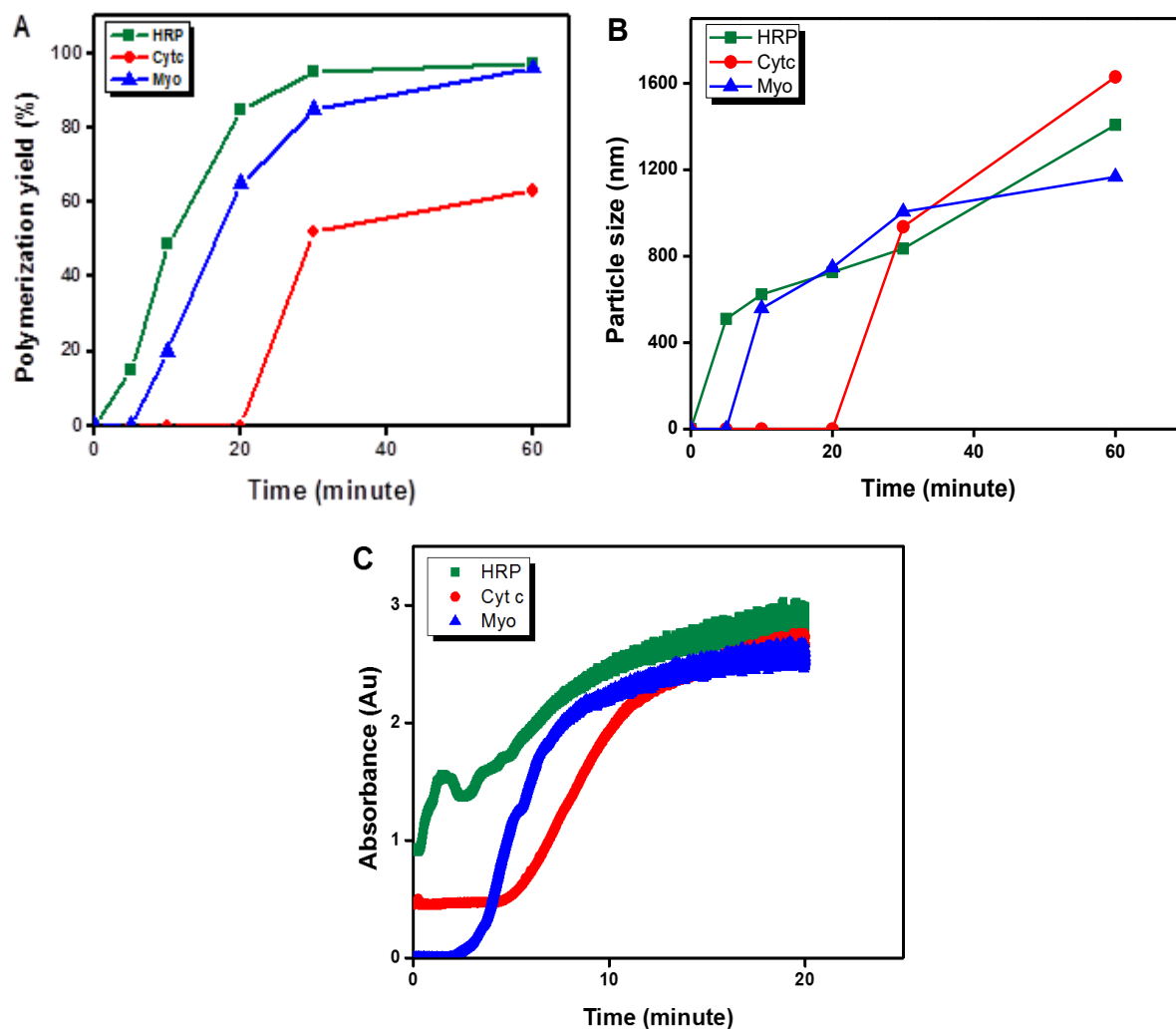


**Figure II-10: Kinetics for acrylamide-based hydrogels synthesis by free-radical polymerization via different biocatalysts, in term of: (A) Polymerization yield (%), (B) Particles size (nm) measured by DLS and (C) spectrophotometric monitoring.**

We can notice, from the DLS results, that the polymerization started at different times, the first being HRP-mediated polymerization, followed by myoglobin and cytochrome *c*. the difference in the polymerization's starting time is emphasized by the spectrophotometric monitoring of the polymerization achieved using Cary 60 U.V-Visible spectrophotometer. The yields increased exponentially to attain a maximum at 30 minutes for HRP-mediated polymerization and for 60 minutes for Myo and Cyt *c* catalysis. HRP and Myo led to 100% yield; however, 60% are only reached for Cyt *c* within 1h. The particles size increased also with the polymerization yield to



reach rapidly microgel range. However, we can observed a continuous increase in the particles size even when the maximum yield is attained that could be explained by microgel swelling.

In order to see if the incubation of 3 days is enough to get high polymerization yields for all types of hydrogels synthesized by HRP-initiated FRP, polymerization kinetics were studied during the 16 hours following the synthesis. **Figure II-11A** and **Figure II-11B** show the polymerization yields and particles size, respectively.

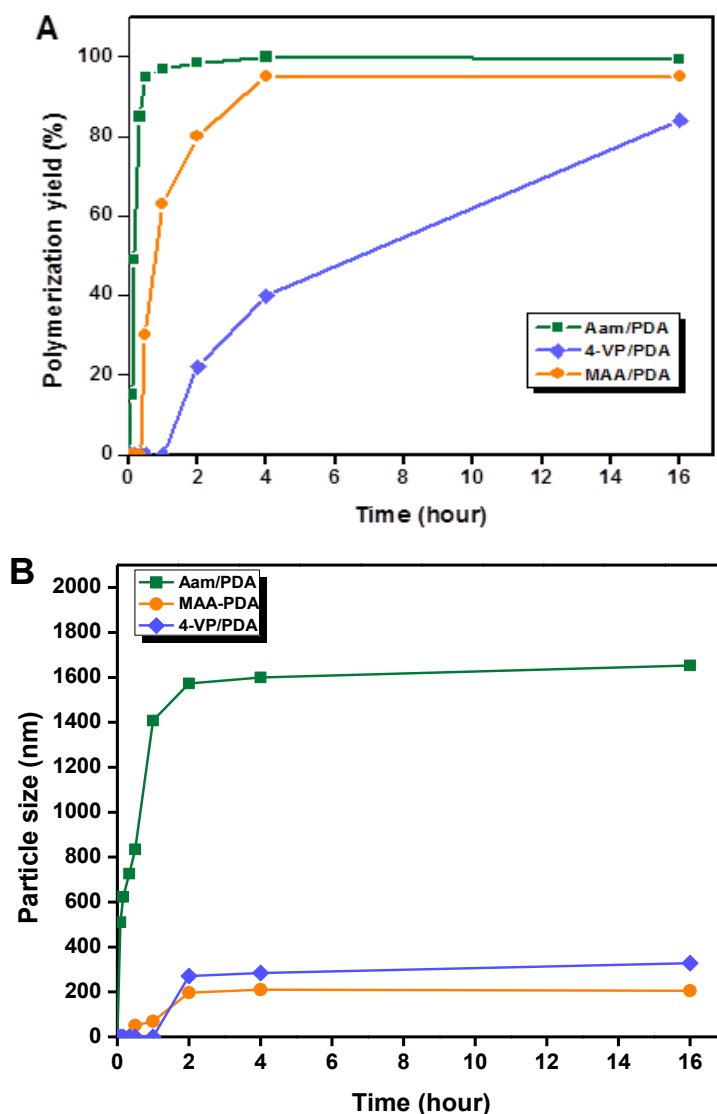


**Figure II-11: Kinetics for HRP-initiated polymerization of different functional monomers in presence of PDA as cross-linker, in term of: (A) Polymerization yield (%) and (B) Particles size (nm), using  $[\text{Monomers}]_0 = 57.2 \text{ mM}$ ,  $[\text{Biocatalyst}]_0 = 0.023 \text{ mM}$ ,  $[\text{Acac}]_0 = 2.8 \text{ mM}$ , and  $[\text{H}_2\text{O}_2]_0 = 1.76 \text{ mM}$ , in 0.1 M phosphate buffer pH 7.0.**

It can be observed that the polymerization of the different monomers is achieved *via* different kinetics. For Aam-based polymers, the polymerization starts early, a few minutes after the enzyme addition and is faster since it is finished after 2 hours. For acid-based polymer, the polymerization is a slower, and the maximum for particles sizes and yields is attained within four hours. However, the hydrogel based on 4-vinylpyridine is synthesized through overnight, for a duration of 16 hours, attaining a yield lower than 100 %.

To resume, independently from the type of functional monomer, the polymerization can be completed in 16 hours. Particles sizes and yields are quite similar to those obtained after 3 days of incubation for all of hydrogels. Incubation for overnight seems to be enough for the hydrogel synthesis by HRP-mediated initiation.

As a short conclusion for this part, horseradish peroxidase is the best biocatalyst among all the ones that have been tested for the polymerization of acrylic monomers. It will be used, in the next chapters, to study its immobilization and its application for MIP particles synthesis, as well as the synthesis of molecularly imprinted polymers.

### II.3.2.3. Versatility of enzyme-mediated polymerization for hydrogel synthesis

Polymerization of different vinyl and acrylic functional monomers was studied in the presence of the HRP and its reaction substrates, in order to extend the enzyme induced polymerization to the synthesis of different hydrogels compositions. Scores of functional monomers, which are commonly used for molecular imprinting by the non-covalent approach, were studied. Moreover, a number of water-soluble cross-linkers were also evaluated, since cross-linkers are well-known to control the morphology of the polymer matrix [40]. **Table II-7** and **Figure II-12** show the polymerization yields and particles sizes obtained for the different hydrogels.

**Table II-7: Yield of the particles based on various functional and cross-linking monomers by HRP-mediated free-radical polymerization using  $[\text{monomers}]_0 = 57.2 \text{ mmol/l}$ ,  $[\text{H}_2\text{O}_2]_0 = 1.76 \text{ mM}$ ,  $[\text{Acac}]_0 = 2.78 \text{ mM}$ , and  $[\text{HRP}]_0 = 0.023 \text{ mM}$  (0.08 g/l), in 0.1 M phosphate buffer pH 7.0.**

	AA	MAA	Aam	NIPAm	MeAAm	HEMA	4-VP
PDA	76%	69%	95%	61%	68%	72%	85%
MeBAAm	93%	91%	98%	84%	92%	99%	90%
EbAAm	68%	93%	75%	80%	91%	85%	66%

The yields are relatively high, without any significant difference among the different types of the acidic, neutral, and basic monomers. For the difference according to the type of cross-linker, all polymerization yields are high, but we noticed that the highest values are obtained with MeBAAm.

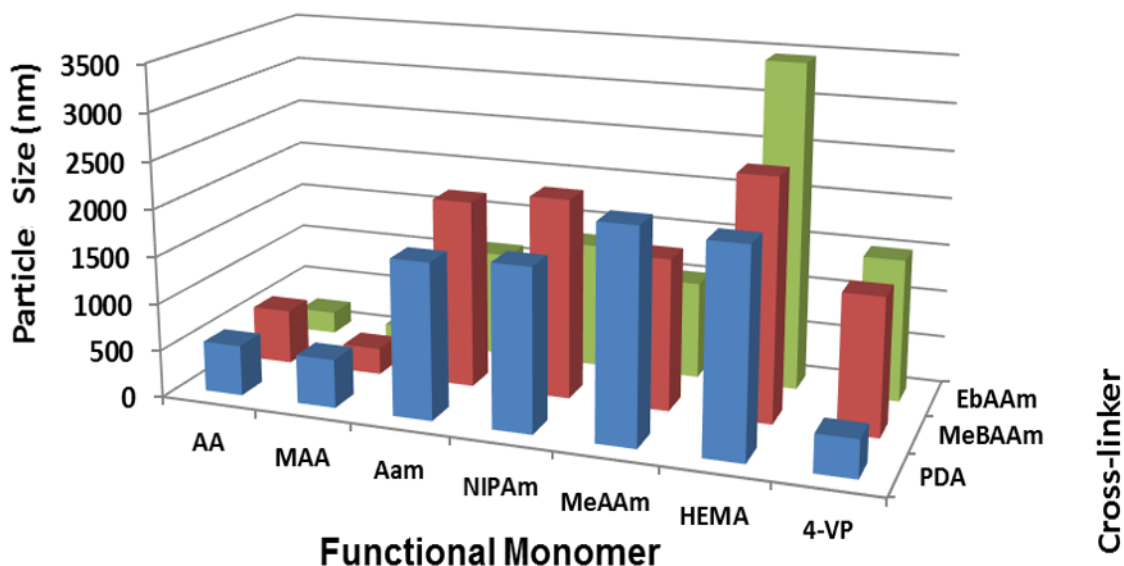


**Figure II-12: Sizes of the particles obtained by HRP-initiated free radical polymerization of different functional and cross-linking monomers, using  $[\text{Monomers}]_0 = 57.2 \text{ mM}$ ,  $[\text{HRP}]_0 = 0.023 \text{ mM}$  (0.08 g/l),  $[\text{Acac}]_0 = 2.8 \text{ mM}$ , and  $[\text{H}_2\text{O}_2]_0 = 1.76 \text{ mM}$ , in 0.1 M phosphate buffer pH 7.0.**

According to particles sizes, hydrogels are usually classified into different groups: macrogels, microgels (from submicron to  $100 \mu\text{m}$ ) [41] and nanogels (smaller than 200 nm) [42]. From what was shown in the above figure, nanogels were obtained with acidic monomers and EbAAm. Microgels with small particles were obtained for the same acidic monomers with MeBAAm and

PDA, whereas neutral monomers resulted in microgel formation with bigger particles sizes whatever the cross-linker is.

Moreover, the effect of the total monomers concentration was studied for several polymers that differ by the acidic, neutral or alkaline nature of their functional monomers. The yields are presented in **Table II-8**, and the particles sizes for the different hydrogels are shown in **Figure II-13**, according to the polymer and the total monomers concentrations. The results show an increase in particles size with monomer concentration, whereas the polymerization yields are not much affected except for the 4-VP/PDA system.

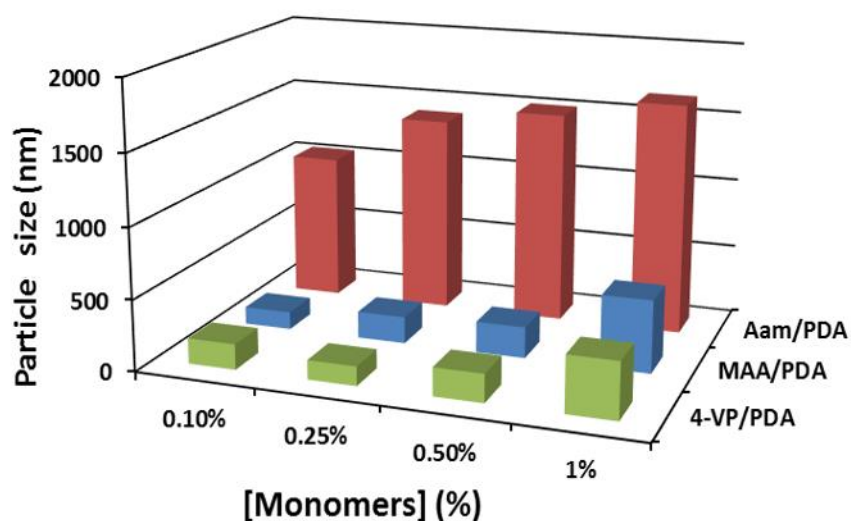


**Figure II-13:** Sizes of the particles obtained by HRP-initiated free radical polymerization of different functional and cross-linking monomers, using different monomer concentrations.

**Table II-8:** Hydrogels yields based on various functional monomers in different monomers concentrations by HRP-mediated free-radical polymerization.

Monomères	0.10%	0.25%	0.5%	1%
MAA/PDA	72%	76%	77%	69%
Aam/PDA	77%	81%	76%	95%
4-VP/PDA	54%	44%	47%	85%

#### II.3.2.4. Optimization of the enzymatic initiation system

It has been shown earlier by others that changing the nature or the concentration of each component in the enzymatic ternary system can have consequences for the molecular weight or the yield of linear polymer [19]. We therefore wanted to investigate the influence of each component on the hydrogel particles size and the polymerization yield.

##### *A. Influence of hydrogen peroxide initial concentration on hydrogels synthesis*

In the HRP biocatalytic cycle, hydrogen peroxide ( $H_2O_2$ ) is involved not only in the catalytic oxidation of Acac, but also in oxidation of Acac and the irreversible inactivation of the HRP. A side-reaction between HRP-II and excess of hydrogen peroxide leads to the formation of the compound III (**Figure I-16** in **Chapter I**), well-known as the irreversibly inactive form of the enzyme [19, 21]. Based on this fact, the study of the effect of hydrogen peroxide initial concentration was required to avoid the undesirable inactivation of HRP and to control also the particles size and yield. Several polymerizations of 4-VP/PDA at a total monomer concentration of 1 % were carried out at room 25°C using hydrogen peroxide initial concentrations from 0.7  $\mu$ M to 6.8 mM. The particles sizes and yields were determined after 3 days of reaction and are shown in **Figure II-14**.

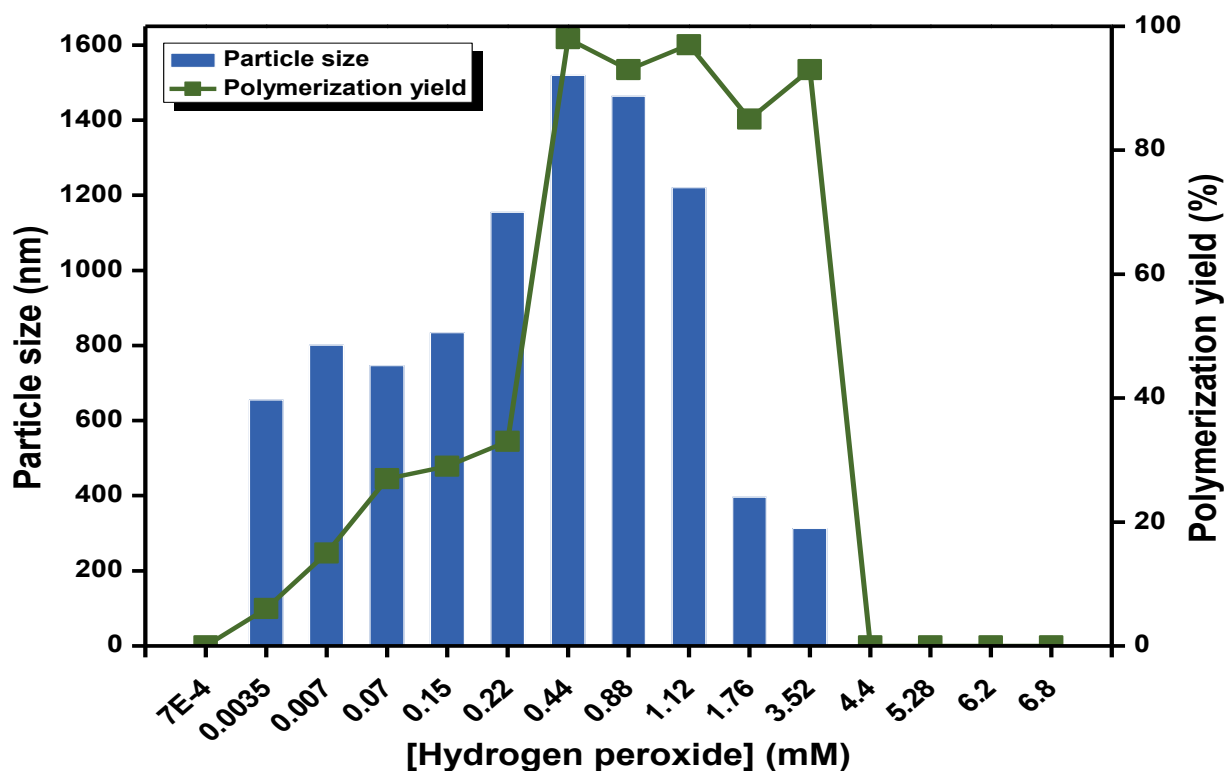


**Figure II-14: Sizes and yields of poly(4-VP/PDA) particles obtained by free radical polymerization initiated with different hydrogen peroxide concentrations, using  $[\text{monomers}]_0 = 57.2 \text{ mM}$ ,  $[\text{HRP}]_0 = 0.023 \text{ mM}$  (0.08 g/l), and  $[\text{Acac}]_0 = 2.78 \text{ mM}$ .**

The polymerization occurs in a range of hydrogen peroxide concentrations 3.5  $\mu\text{M}$  and 3.5 mM for an HRP concentration of 0.08 g/l. With a hydrogen peroxide concentration below 3.5  $\mu\text{M}$  or above 3.5 mM, no polymer was obtained. The absence of any polymerization below a minimum concentration of hydrogen peroxide can be explained by radical inactivation by side reactions being faster than polymerization, or the total consumption of the hydrogen peroxide by side reactions. Indeed, side reactions of oxidation of Acac produce a cyclic compound, the cycloperoxide, and not the free radical required for the polymerization [19]. It can be detected by the yellowish color that appears in the polymerization mixture [43]. In contrast, the upper limit is explained by the enzyme inactivation due to the excess of the  $\text{H}_2\text{O}_2$  as described before.

Within these two limit concentrations, the particles sizes are 600-800 nm and increased with the  $\text{H}_2\text{O}_2$  concentration until a concentration of 0.88 mM. The highest particle size ( $> 1400 \text{ nm}$ ) corresponds to 0.44 and 0.88 mM as hydrogen peroxide concentrations. Beyond, the particle size decreases and smaller nanoparticles are obtained for higher concentration of  $\text{H}_2\text{O}_2$ .

The polymerization yield increases to attain a plateau around 85-95 % between 0.44 and 0.88 mM, whereafter it decreases. Moreover, we observed that the polymerization kinetics was quick for concentrations between 3.5  $\mu$ M and 0.88 mM. Beyond, it decreases with the increase in hydrogen peroxide concentrations. The slow initiation rate, due to the partially inactivation of HRP, can explain the decrease in particle size.

Therefore, for the next experiments, we set its ideal concentration with respect to the theoretical stoichiometry for [Acac]/[H<sub>2</sub>O<sub>2</sub>] that is 2:1 [20, 44]. In practice, we fixed the ratio of Acac/ H<sub>2</sub>O<sub>2</sub> closer to 1.5:1 (1.76 mM), since hydrogen peroxide is liable to dismute.

### *B. Influence of Acetylacetone initial concentration*

One of the main characteristics of HRP is its broad substrate specificity. It can act on several reducing substrates, such as phenol, hydroquinone, catechol, resorcinol, pyrogallol, aniline, *p*-aminobenzoate and others. [16, 45].

The choice of the reducing species in our experiment is crucial. The reducing molecule should meet two essential conditions: to be able to be oxidized by HRP, as substrate, and to behave as a potential initiator of the monomers polymerization. Lalot *et al.* have demonstrated that the enolic form of the  $\beta$ -diketones was found to be the key compounds in the biocatalytic cycle of HRP for the initiation mechanism of acrylamide linear polymerization. Moreover, among the  $\beta$ -diketone structures, 2,4-pentanedione or acetylacetone (Acac), led to the highest polymerization yield and molecular weight of linear polyacrylamide [20, 44].

The influence of acetylacetone initial concentration (0.93 mM to 11.12 mM) was investigated for the co-polymerization of 4-VP and PDA at 1 % as monomers concentration. The particles size and polymerization yield are represented in **Figure II-15**.

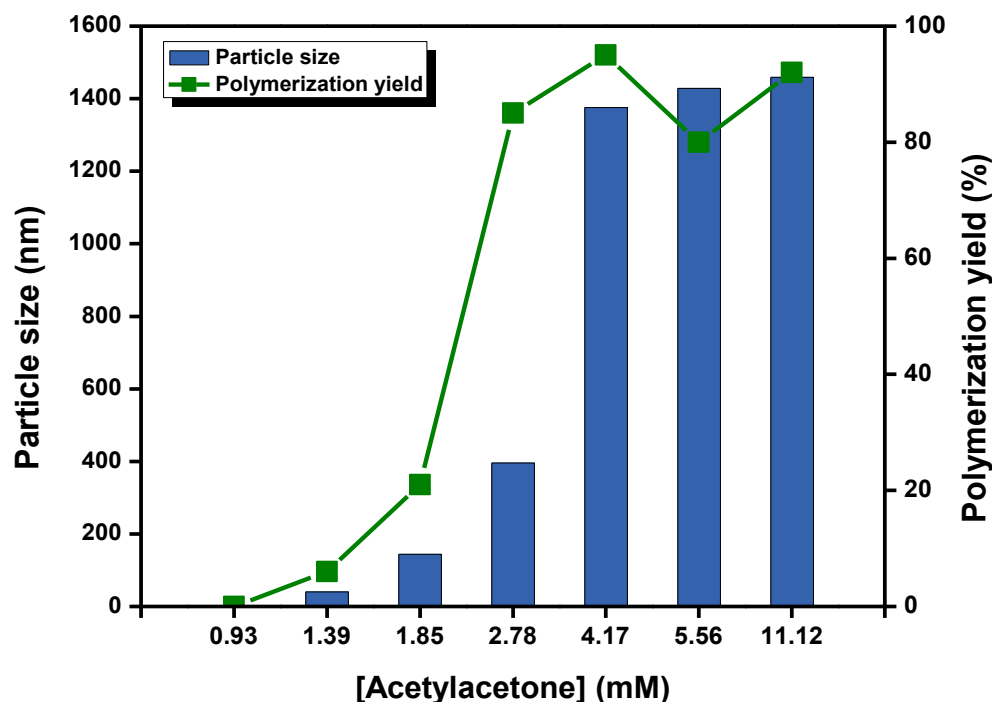


**Figure II-15: 4-VP/PDA particle sizes and yields obtained by free radical polymerization initiated by HRP and different acetylacetone concentrations, using  $[\text{monomers}]_0 = 57.2 \text{ mM}$ ,  $[\text{HRP}]_0 = 0.023 \text{ mM}$  (0.08 g/l), and  $[\text{H}_2\text{O}_2]_0 = 1.76 \text{ mM}$ .**

There is a lower limit Acac concentration ( $[\text{Acac}] < 1.4 \text{ mM}$ ), since no polymer can be recovered probably due to a too low radical generation rate to initiate the polymer propagation. For 1.4 mM, very small particles (30 nm) were obtained with a very low yield (5%). Above this concentration, an exponential increase in size and yield was observed. Particle size attains a maximum around 1400 nm for an Acac concentration of 4.2 mM. Beyond this concentration, there is no significant increase in the size. Moreover, 80 - 95 % yield is reached for an Acac concentration higher than 2.8 mM.

These results strongly differ from those described by Derango *et al.* [23], who showed a polymerization in the absence of the reducing molecule, but is in accordance with those described by Lalot *et al.* who showed an increase in the yields of linear polyacrylamides when Acac concentration is increased [17-21].



### C. Influence of enzyme initial concentration

As enzyme concentration affects the kinetics of radical generation, we have also studied the effect of this parameter by varying the initial HRP concentration from 0.01 to 0.4 g/l (0.029 to 0.113 mM). The ratios of [Acac]/[Monomers] and [Acac]/[H<sub>2</sub>O<sub>2</sub>] have been fixed at 0.05 and 1.5:1 respectively. The particles sizes and polymerization yields of poly(4-VP/PDA) synthesis are presented in **Figure II-16**.

The results of the polymers yields and sizes clearly indicate a strong influence of the enzyme initial concentration on the polymerization efficiency. By increasing the HRP concentrations, both particles size and polymerization yield are enhanced.

For [HRP]<sub>0</sub> < 0.04g/l (0.0115 mM), no polymer was obtained resulting probably from a competition between “inactivation” and “initiation” processes in the biocatalytic cycle of horseradish peroxidase. This means that the initiation rate is too low to give rise to the polymerization and the enzyme could also be irreversibly inactivated due to the excess of hydrogen peroxide [18]. When [HRP] is higher than 0.08g/L (0.023 mM), no significant variation of the yield can be detected. No evident variation of the particles size can be observed for [HRP]<sub>0</sub> above 0.24g/l (0.069 mM). We also noticed a faster polymerization kinetics with an increase in HRP concentration.

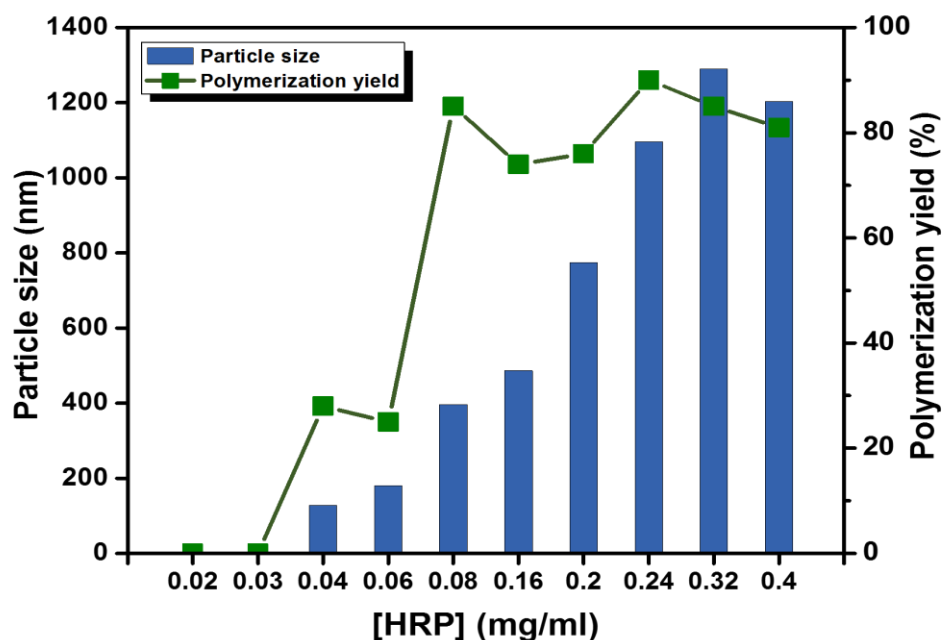


**Figure II-16:** 4-VP/PDA particle sizes and yields obtained by free radical polymerization initiated by different HRP concentrations, using  $[\text{monomers}]_0 = 57.2 \text{ mM}$ ,  $[\text{Acac}]_0 = 2.8 \text{ mM}$ , and  $[\text{H}_2\text{O}_2]_0 = 1.76 \text{ mM}$ .

As a conclusion, for all further experiments, the enzyme initial concentration is fixed at 0.08 g/L (0.023 mM) for which we can obtain small-sized particles (393 nm) with a high polymerization yield (85%).

#### *D. Influence of $[\text{HRP}]/[\text{H}_2\text{O}_2]$ ratio*

As hydrogen peroxide is both a substrate and an inhibitor of HRP, it was important to examine the influence of both variations of HRP and  $\text{H}_2\text{O}_2$  by using the molar ratio ( $\alpha$ ) of initial molar hydrogen peroxide concentration to that of HRP. **Table II-9** summarizes the polymerization yields and particles sizes obtained for different molar ratios  $\alpha$  of hydrogen peroxide and enzyme initial concentrations.

**Table II-9: yield of the 4-VP/PDA particles with different HRP and hydrogen peroxide initial concentrations ([Monomers]<sub>0</sub> = 57.2 mM, and [Acac]<sub>0</sub> = 2.78 mM).**

Entry	[H <sub>2</sub> O <sub>2</sub> ] <sub>0</sub> (mM)	[HRP] <sub>0</sub> (g/L)	$\alpha^a$	Yield (%)
1	0.0007	0.08	0.39	0
2	0.0035	0.08	1.93	6
3	0.007	0.08	3.85	15
4	0.073	0.08	40	27
5	0.22	0.08	121	33
6	0.44	0.08	242	93
7	1.12	0.08	616	97
8	1.76	0.08	986	85
9	4.4	0.08	2420	0
10	6.8	0.08	3740	0
11	1.76	0.03	2581	0
12	1.76	0.04	1936	28
13	1.76	0.06	1291	25
14	1.76	0.16	484	74
15	1.76	0.2	387	76
16	1.76	0.24	323	90
17	1.76	0.32	242	85
18	1.76	0.4	194	81

<sup>a</sup> = [H<sub>2</sub>O<sub>2</sub>]<sub>0</sub>/[HRP]<sub>0</sub>; the ratio is calculated with molar concentrations of HRP and H<sub>2</sub>O<sub>2</sub>.

When  $\alpha$  is below 2, no polymerization is observed due to a very low concentration in hydrogen peroxide. When  $\alpha$  is  $\geq 2420$ , no polymerization was observed, whatever the effective change in either [H<sub>2</sub>O<sub>2</sub>] or [HRP], due to the competition between “inactivation” and “initiation” processes. Best yields are obtained when  $\alpha$  is between 250 and 600. Our observations strongly confirm those of Lalot *et al.* who found that  $\alpha$  is a very important parameter for optimization of the HRP catalytic activity. This study included the formation of linear polyacrylamides with 100% as yield with  $\alpha$  between 250 and 370 [21].

As a result, general guidelines are provided in order to apply these enzymatically catalyzed redox system for the synthesis of hydrogels with control of particles sizes and polymerization yields.

To conclude for this part, we can see that each component of the enzymatic system has a great impact on the yield and size of the particles. An interaction among these different parameters is also detected. HRP and Acac concentrations should be wisely chosen for the control of the particles sizes. However, these concentrations should not be too high when small-sized particles are required. High concentrations of hydrogen peroxide should be avoided in order to prevent the enzyme inactivation.

#### *E. Effect of the solvent*

In hydrogel chemistry, the solvent plays a crucial role since it is responsible for creating the pores within the gel matrix. The nature of a porogenic solvent can be used to control the morphology of the hydrogel and the total pore volume. Indeed, the use of thermodynamically good solvent will lead to well-developed hydrogel structure, whereas a thermodynamically poor solvent will cause the precipitation of particles with poorly developed structure [46]. On the other hand, the solvent and the pH are crucial parameters for the enzyme activity. The effect of solvent has been studied on the particle size and the polymerization yield.

The polymerization is studied in water and in 0.1 M phosphate buffer pH 7.0. We chose for this study acrylamide (Aam) as a neutral functional monomer, which does not lead to significant change in pH when dissolved in water. The polymerization was achieved by using three different cross-linkers in these solvents. **Table II-10** shows the results of polymerization yields for the different hydrogels.

**Table II-10: Polymerization yields obtained by free radical polymerization, in water or in 0.1 M PB pH 7.0, using  $[\text{Monomers}]_0 = 57.2 \text{ mM}$ ,  $[\text{HRP}]_0 = 0.023 \text{ mM}$  (0.08 g/l),  $[\text{Acac}]_0 = 2.8 \text{ mM}$ , and  $[\text{H}_2\text{O}_2]_0 = 1.76 \text{ mM}$**

Yield (%)	PDA	EbAm	MEbAm
Water	84	72	90
Phosphate buffer	95	75	98

The synthesis of hydrogels succeeded for all the cross-linkers in both media. High polymerization yields between 85% and 98% are obtained. In fact, HRP can be qualified as robust biocatalyst since polymers can be formed in other than buffered media where no control on the medium pH is achieved. However better yields have been obtained in buffer media for all the polymers.

Buffered media is required for maintaining optimal enzyme activity. It is also well-known that HRP is active from pH 4 to 9 with the optimum pH between 6 and 7. [34, 47]. The influence of the polymerization medium pH was also investigated for the synthesis of poly(4-VP/PDA) hydrogels. Polymerization of 4-VP and PDA was performed, during three days, in several buffers covering a range of pH from 4 to 9. The particles sizes and polymerization yields are presented in **Figure II-17**.

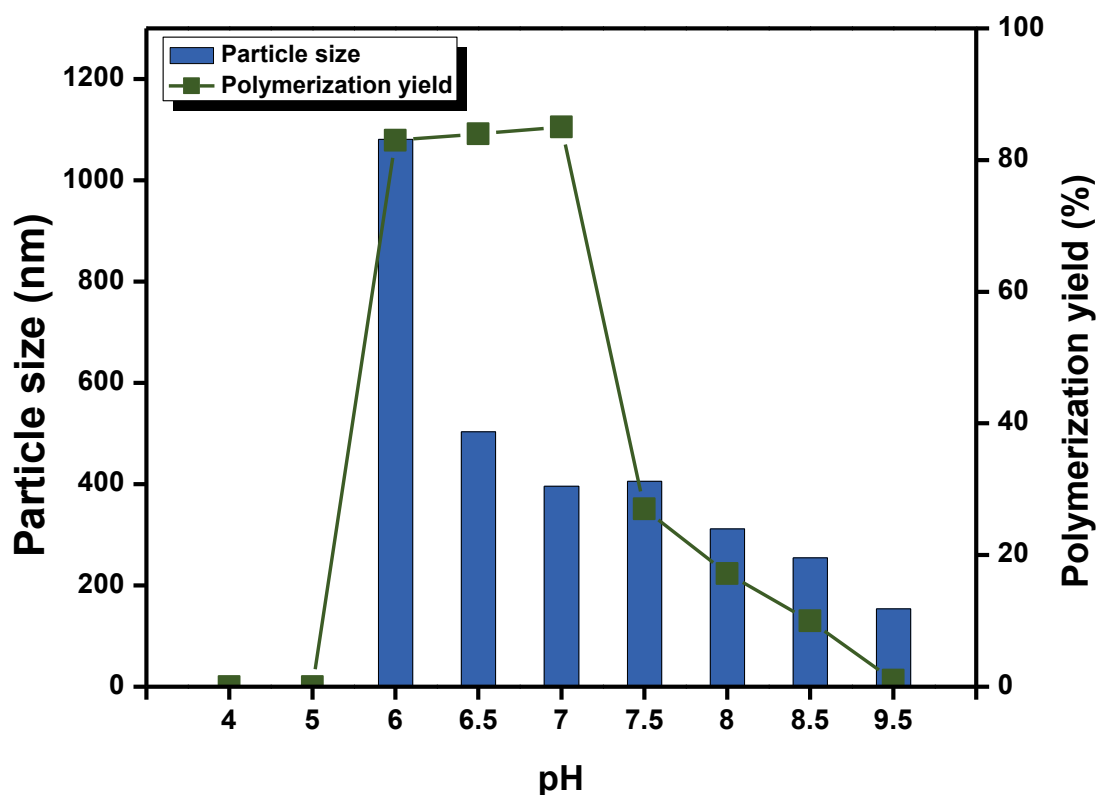


**Figure II-17: 4-VP/PDA particle sizes and yields obtained by free radical polymerization initiated in different buffers using  $[\text{monomers}]_0 = 57.2 \text{ mM}$ ,  $[\text{HRP}]_0 = 0.023 \text{ mM}$  (0.08 g/l),  $[\text{Acac}]_0 = 2.8 \text{ mM}$ , and  $[\text{H}_2\text{O}_2]_0 = 1.76 \text{ mM}$**

For pH 4 and 5 no gel was obtained. The polymerization yield show an optimum at pH 6-7, within which we can observe a decrease in the particles sizes. Beyond pH 7.0, the polymerization yield decrease significantly to attain ~2% with a pH value of 9.5. These results confirm that the optimum pH is between 6 and 7. Interestingly, pH optimum range for this hydrogel synthesis is larger than the range studied for linear polyacrylamides (pH 5.4-8) by Lalot *et al.* [21].

An optimal pH value of 7 is fixed for the following experiments, due to the optimal polymerization yield combined with a small particle size obtained.

#### II.3.2.5. Comparison between HRP-mediated and chemical initiations of free radical polymerization

Free-radical polymerization is normally triggered by the decomposition of chemical initiator in different ways, such as light, heat, or electrochemical or redox reactions [46]. As the initiation method has an effect on the polymer characteristics [48], it was interesting in this chapter to compare the traditional initiation methods of free-radical polymerization to the enzymatic one.

The biochemical redox using HRP system is compared to other chemical initiations traditionally used for the co-polymerization of different functional monomers (Aam, 4-VP, MAA) and PDA. For this, different polymers are synthesized at 1% as total monomers concentration. Vazo® 56 and potassium persulfate are used as initiators for the photochemical and redox initiations, respectively, at 1 mol %. The particles sizes and polymerization yields are shown in **Figure II-18** and **Table II-11**, respectively.

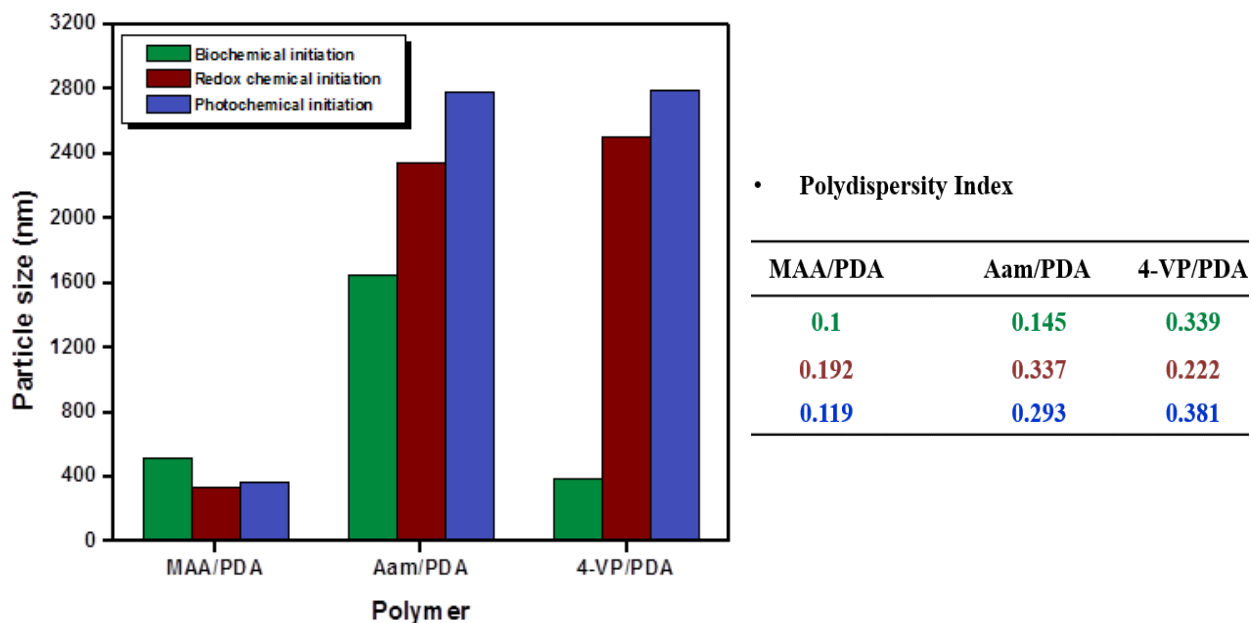


**Figure II-18: Particle sizes with their corresponding PDI obtained by different initiations methods for the free radical polymerization of acidic, neutral, and basic monomers cross-linked by PDA.**

No significant difference is observed in particles size of MAA-based polymers, prepared by different initiation systems. However, smaller particles, for Aam- and 4-VP- based polymers are obtained by using the HRP-mediated initiation, as compared to both of chemical initiations.

**Table II-11: Polymerization yields for polymer based on acidic, neutral, and basic functional monomers, synthesized by free-radical polymerization initiated by enzyme catalysis, redox chemical and photochemical initiation**

Yield (%)	MAA/PDA	Aam/PDA	4-VP/PDA
<b>Biochemical initiation</b>	69	95	85
<b>Redox chemical initiation</b>	87	87	91
<b>Photochemical initiation</b>	96	99	94

The HRP-mediated initiation performance in terms of polymerization yield is similar to those obtained by other chemical initiations except for HRP-synthesized poly(MAA/PDA).

The photochemical initiation is triggered by the decomposition of an azo initiator, leading to the formation of carbon-centered radicals. These compounds are usually known to be less reactive than the oxygen-centered radicals generated by the decomposition of peroxides in the electrochemical initiation. The lower reactivity results in the decrease of the branch grafting and the preliminary chain termination as well as the increase of the polymer chain growth [48]. This can explain the bigger particle sizes and partially the polymerization yields obtained for all polymers in the photochemical initiations than the KPS/TEMED initiation.

Peroxides can be generated not only in KPS/TEMED initiation, but also in the catalytic cycle of HRP. Therefore, the difference in particles sizes is not necessarily due to the nature of the generated radicals neither to their concentration. It is mainly due to the effect of the other components of the enzymatic redox system. The HRP cycle includes a ternary system composed of HRP, Acac, and H<sub>2</sub>O<sub>2</sub>. The change in a concentration of one component can modify either particles size or polymerization yield, or even both. The concentrations of the enzymatic reactants used here are those optimized in this chapter, and are the origin of this difference in particles sizes compared to KPS/TEMED, especially for poly(4-VP/PDA).

In conclusion, this study shows that HRP-mediated initiation is a good alternative to other chemical initiations of free-radical polymerizations for hydrogels preparation.

#### II.3.2.6. Cytotoxicity of the enzymatically synthesized nanoparticles

The cytotoxicity test of poly(4-VP/PDA) nanoparticles against HaCat cells was evaluated *in vitro* by a standard MTT assay. Two batches of nanoparticles synthesized by photochemical (Vazo<sup>®</sup>56) or enzyme-mediated initiations are evaluated. The **Figure II-19** shows the results of HaCat cell viability for the two polymers.



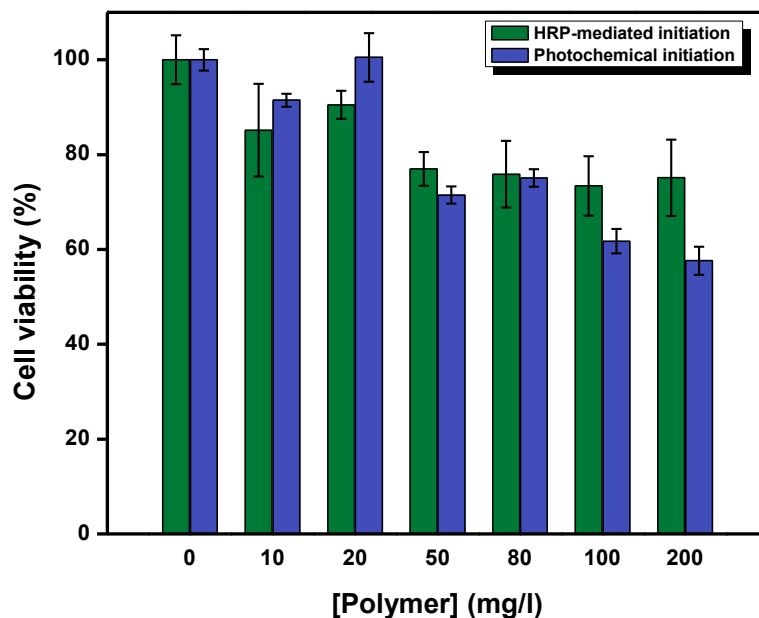


**Figure II-19: HaCat Cells viability for different polymer concentrations of (4-VP/PDA) nanoparticles polymerized by HRP-mediated initiation (green bars), and photochemical initiation with Vazo<sup>®</sup>56 (blue bars). The errors bars are means of 5 replicates.**

The polymers, synthesized by both initiations, showed a quantity-dependent cytotoxicity. It seems that the polymeric matrix is toxic for cells, whatever the initiation method. This may be due to the pyridine moieties in the material. However, a difference in cell viability for high polymer concentrations (100 and 200 mg/l) can be observed between the two polymers. The photochemically synthesized particles led to up to 40% of cell death, while the enzymatically prepared polymer was less toxic. These preliminary results show the advantage for enzyme-initiated polymerization as a good alternative for nanoparticles synthesis in biomedical applications. This new method can be applied for the preparation of biocompatible nanogels with less cytotoxicity and residual initiator compared to traditional initiation ways using toxic chemical compounds.

## II.4. Conclusion

The work in this chapter promoted the biochemically initiated polymerization, using different enzymes, as an efficient approach for hydrogels synthesis.

High polymerization yields can be obtained by the catalysis of different oxidoreductases such as cytochrome *c*, myoglobin, horseradish peroxidase, as well as their active group, heme, for the synthesis of linear polymers based on acrylamide and different other acrylic and vinyl monomers.

For hydrogel synthesis, polymers with different composition and particles sizes are easily prepared by enzyme-mediated polymerization. A wide variety of monomers, which are commercially available and used in polymer chemistry, can be polymerized *via* this approach. The variation of one of the enzymatic system components, such as biocatalyst nature or its concentration, substrates concentrations affect the particles yields and sizes, allowing the synthesis from small-sized nanoparticles to microgels. Horseradish peroxidase was verified to be the best biocatalyst among other oxidoreductases. This enzyme can be applied for the synthesis of a wide range of hydrogels with high polymerization yield and fast kinetics comparable to those of other chemical initiations.

This research work provides a greener alternative for hydrogel synthesis. In this approach, eco-friendly and less toxic polymerization conditions have been proposed especially for the initiators and the polymerization solvent, while maintain same polymerization performances. The enzymatic initiation is readily shown as a very good alternative to other chemical initiations for free radical polymerization, since it implicates a robust and low-cost enzyme, as well as the ability to control the initiator amount in the final product.

---

## References

- [1] E. M. Ahmed, "Hydrogel: Preparation, characterization, and applications: A review," *J. Adv. Res.*, vol. 6, no. 2, pp. 105–121, 2015.
- [2] A. S. Hoffman, "Hydrogels for biomedical applications," *Adv. Drug Deliv. Rev.*, vol. 64, no. SUPPL., pp. 18–23, 2012.
- [3] A. V. Kabanov and S. V. Vinogradov, "Nanogels as pharmaceutical carriers: Finite networks of infinite capabilities," *Angew. Chemie - Int. Ed.*, vol. 48, no. 30, pp. 5418–5429, 2009.
- [4] G. Soni and K. S. Yadav, "Nanogels as potential nanomedicine carrier for treatment of cancer: A mini review of the state of the art," *Saudi Pharm. J.*, 2014.
- [5] S. a. Ferreira, F. M. Gama, and M. Vilanova, "Polymeric nanogels as vaccine delivery systems," *Nanomedicine Nanotechnology, Biol. Med.*, vol. 9, no. 2, pp. 159–173, 2013.
- [6] S. Sant, S. L. Tao, O. Z. Fisher, Q. Xu, N. a. Peppas, and A. Khademhosseini, "Microfabrication technologies for oral drug delivery," *Adv. Drug Deliv. Rev.*, vol. 64, no. 6, pp. 496–507, 2012.
- [7] N. a. Peppas, P. Bures, W. Leobandung, and H. Ichikawa, "Hydrogels in pharmaceutical formulations," *Eur. J. Pharm. Biopharm.*, vol. 50, no. 1, pp. 27–46, 2000.
- [8] L. Klouda and A. G. Mikos, "Thermoresponsive hydrogels in biomedical applications," *Eur. J. Pharm. Biopharm.*, vol. 68, no. 1, pp. 34–45, 2008.
- [9] G. Erdodi and J. P. Kennedy, "Amphiphilic conetworks: Definition, synthesis, applications," *Prog. Polym. Sci.*, vol. 31, no. 1, pp. 1–18, 2006.
- [10] Y. Qiu and K. Park, "Environment-sensitive hydrogels for drug delivery," *Adv. Drug Deliv. Rev.*, vol. 64, no. SUPPL., pp. 49–60, 2012.
- [11] L. S. Moreira Teixeira, J. Feijen, C. a. van Blitterswijk, P. J. Dijkstra, and M. Karperien, "Enzyme-catalyzed crosslinkable hydrogels: Emerging strategies for tissue engineering," *Biomaterials*, vol. 33, no. 5, pp. 1281–1290, 2012.
- [12] Y. Jiang, J. Chen, C. Deng, E. J. Suuronen, and Z. Zhong, "Click hydrogels, microgels and nanogels: Emerging platforms for drug delivery and tissue engineering," *Biomaterials*, vol. 35, no. 18, pp. 4969–4985, 2014.
- [13] R. Jin, C. Hiemstra, Z. Zhong, and J. Feijen, "Enzyme-mediated fast in situ formation of hydrogels from dextran-tyramine conjugates," *Biomaterials*, vol. 28, no. 18, pp. 2791–2800, 2007.
- [14] J. a. Yang, J. Yeom, B. W. Hwang, A. S. Hoffman, and S. K. Hahn, "In situ-forming injectable hydrogels for regenerative medicine," *Prog. Polym. Sci.*, vol. 39, no. 12, pp. 1973–1986, 2014.
- [15] T. Su, D. Zhang, Z. Tang, Q. Wu, and Q. Wang, "HRP-mediated polymerization forms tough nanocomposite hydrogels with high biocatalytic performance.," *Chem. Commun.*, vol. 49, no. 73, pp. 8033–5, 2013.

- 
- [16] F. Hollmann and I. W. C. E. Arends, "Enzyme initiated radical polymerizations," *Polymers (Basel)*, vol. 4, no. 1, pp. 759–793, 2012.
- [17] T. Lalot, M. Brigodiot, and E. Maréchal, "A kinetic approach to acrylamide radical polymerization by horse radish peroxidase-mediated initiation," *Polym. Int.*, vol. 48, no. 4, pp. 288–292, 1999.
- [18] D. Teixeira, T. Lalot, M. Brigodiot, and E. Maréchal, "β-Diketones as Key Compounds in Free-Radical Polymerization by Enzyme-Mediated Initiation," *Macromolecules*, vol. 32, no. 1, pp. 70–72, 1998.
- [19] A. Durand, T. Lalot, M. Brigodiot, and E. Maréchal, "Enzyme-mediated radical initiation of acrylamide polymerization: Main characteristics of molecular weight control," *Polymer (Guildf)*, vol. 42, no. 13, pp. 5515–5521, 2001.
- [20] O. Emery, T. Lalot, M. Brigodiot, and E. Maréchal, "Free-radical polymerization of acrylamide by horseradish peroxidase-mediated initiation," *J. Polym. Sci. Part A Polym. Chem.*, vol. 35, no. 15, pp. 3331–3333, 1997.
- [21] A. Durand, T. Lalot, M. Brigodiot, and E. Maréchal, "Enzyme-mediated initiation of acrylamide polymerization: reaction mechanism," *Polymer (Guildf)*, vol. 41, no. 23, pp. 8183–8192, 2000.
- [22] M. M. Bradford, "A rapid and sensitive method for the quantitation of microgram quantities of protein utilizing the principle of protein-dye binding," *Anal. Biochem.*, vol. 72, pp. 248–254, 1976.
- [23] R. A. Derango, L. Chiang, R. Dowbenko, and J. G. Lasch, "Enzyme-mediated polymerization of acrylic monomers," *Science (80- )*, vol. 6, no. 6, pp. 523–526, 1992.
- [24] C. C. Winterbourn, "Toxicity of iron and hydrogen peroxide: The Fenton reaction," *Toxicol. Lett.*, vol. 82–83, pp. 969–974, 1995.
- [25] M. A. Gilles-Gonzalez and G. Gonzalez, "Heme-based sensors: Defining characteristics, recent developments, and regulatory hypotheses," *J. Inorg. Biochem.*, vol. 99, no. 1, pp. 1–22, 2005.
- [26] H. Y. Song, J. Z. Liu, L. P. Weng, and L. N. Ji, "Activity, stability, and unfolding of reconstituted horseradish peroxidase with modified heme," *J. Mol. Catal. B Enzym.*, vol. 57, no. 1–4, pp. 48–54, 2009.
- [27] J. Zeng, Y. Zhao, W. Li, X. Tan, G.-B. Wen, and Y.-W. Lin, "Hydrogen-bonding network in heme active site regulates the hydrolysis activity of myoglobin," *J. Mol. Catal. B Enzym.*, vol. 111, pp. 9–15, 2015.
- [28] H. P. Misra and I. Fridovich, "ARTICLE: The Generation of Superoxide Radical during the Autoxidation of Hemoglobin The Generation the Awtoxidation of Superoxide Radical of Hemoglobin \* during," pp. 6960–6962, 1972.
- [29] C. E. Cooper, R. Silaghi-Dumitrescu, M. Rukengwa, A. I. Alayash, and P. W. Buehler, "Peroxidase activity of hemoglobin towards ascorbate and urate: A synergistic protective strategy

- against toxicity of Hemoglobin-Based Oxygen Carriers (HBOC),” *Biochim. Biophys. Acta - Proteins Proteomics*, vol. 1784, no. 10, pp. 1415–1420, 2008.
- [30] Y. Wang, X. Barbeau, A. Bilimoria, P. Lagüe, M. Couture, and J. K.-H. Tang, “Peroxidase Activity and Involvement in the Oxidative Stress Response of *Roseobacter denitrificans* Truncated Hemoglobin,” *PLoS One*, vol. 10, no. 2, p. e0117768, 2015.
- [31] C. E. Cooper, D. J. Schaer, P. W. Buehler, M. T. Wilson, B. J. Reeder, G. Silkstone, D. a. Svistunenko, L. Bulow, and A. I. Alayash, “Haptoglobin Binding Stabilizes Hemoglobin Ferryl Iron and the Globin Radical on Tyrosine  $\beta$ 145,” *Antioxid. Redox Signal.*, vol. 18, no. 17, p. 120806113112009, 2012.
- [32] L. Khenkin, T. Baluyan, a Novakova, I. Rebrin, and E. Makhaeva, “Iron complexes embedding influence on PMAA hydrogel,” *IOP Conf. Ser. Mater. Sci. Eng.*, vol. 38, p. 012029, 2012.
- [33] V. J. Gauci, M. P. Padula, and J. R. Coorsen, “Coomassie blue staining for high sensitivity gel-based proteomics,” *J. Proteomics*, vol. 90, pp. 96–106, 2013.
- [34] S. a. Mohamed, A. a. Darwish, and R. M. El-Shishtawy, “Immobilization of horseradish peroxidase on activated wool,” *Process Biochem.*, vol. 48, no. 4, pp. 649–655, 2013.
- [35] S. Liu and H. Ju, “Electrocatalysis via Direct Electrochemistry of Myoglobin Immobilized on Colloidal Gold Nanoparticles,” *Electroanalysis*, vol. 15, no. 18, pp. 1488–1493, 2003.
- [36] H. Essa, E. Magner, J. Cooney, and B. K. Hodnett, “Influence of pH and ionic strength on the adsorption, leaching and activity of myoglobin immobilized onto ordered mesoporous silicates,” *J. Mol. Catal. B Enzym.*, vol. 49, no. 1–4, pp. 61–68, 2007.
- [37] X. Gao, Y. Xin, and R. E. Blankenship, “Enzymatic activity of the alternative complex III as a menaquinol:auracyanin oxidoreductase in the electron transfer chain of *Chloroflexus aurantiacus*,” *FEBS Lett.*, vol. 583, no. 19, pp. 3275–3279, 2009.
- [38] E. Tsuchida, K. Honda, and H. Sata, “Hydrophobic Environmental Effects on Oxygenation of Polymeric Hemochrome in Aqueous Solution,” vol. 2261, pp. 2251–2261, 1975.
- [39] E. Tsuchida and E. Hasegawa, “Reduction of Ferriprotoporphyrin IX to the Ferroderivative by Copoly( 4-Vinylpyridine-N-(pVinylbenzyl) -3-Car bamoyl- 1,4-Dihydropyridine) in Dimethyl Sulfoxide,” *Biopolymers*, vol. 16, pp. 845–855, 1977.
- [40] B. H. karsten, V. L. Ana, B. Marc, and Tse Sum Bui, “Molecularly Imprinted Polymers,” *Top Curr Chem*, vol. 325, pp. 1–28, 2012.
- [41] H. Kawaguchi, “Thermoresponsive microhydrogels: Preparation, properties and applications,” *Polym. Int.*, vol. 63, no. 6, pp. 925–932, 2014.
- [42] M. M. Yallapu, M. Jaggi, and S. Chauhan, “Design and engineering of nanogels for cancer treatment,” *Drug Discov. Today*, vol. 16, no. 9–10, pp. 457–463, 2011.
- [43] W. D. Hewson and H. B. Dunford, “Stoichiometry of the reaction between horseradish peroxidase and p-cresol,” *J. Biol. Chem.*, vol. 251, no. 19, pp. 6043–6052, 1976.

- 
- [44] A. P. Rodrigues, L. M. da Fonseca, O. M. de Faria Oliveira, I. L. Brunetti, and V. F. Ximenes, "Oxidation of acetylacetone catalyzed by horseradish peroxidase in the absence of hydrogen peroxide," *Biochim. Biophys. Acta - Gen. Subj.*, vol. 1760, no. 12, pp. 1755–1761, 2006.
- [45] A. M. Azevedo, V. C. Martins, D. M. F. Prazeres, V. Vojinović, J. M. S. Cabral, and L. P. Fonseca, "Horseradish peroxidase: A valuable tool in biotechnology," *Biotechnol. Annu. Rev.*, vol. 9, no. 03, pp. 199–247, 2003.
- [46] P. a G. Cormack and A. Z. Elorza, "Molecularly imprinted polymers: synthesis and characterisation.," *J. Chromatogr. B. Analyt. Technol. Biomed. Life Sci.*, vol. 804, no. 1, pp. 173–182, 2004.
- [47] Q. Chang and H. Tang, "Immobilization of Horseradish Peroxidase on NH<sub>2</sub>-Modified Magnetic Fe<sub>3</sub>O<sub>4</sub>/SiO<sub>2</sub> Particles and Its Application in Removal of 2,4-Dichlorophenol," *Molecules*, vol. 19, no. 10, pp. 15768–15782, 2014.
- [48] A. Rachkov, M. Hu, E. Bulgarevich, T. Matsumoto, and N. Minoura, "Molecularly imprinted polymers prepared in aqueous solution selective for [Sar<sup>1</sup>,Ala<sup>8</sup>]angiotensin II," *Anal. Chim. Acta*, vol. 504, no. 1, pp. 191–197, 2004.

## *Chapter III*

*Immobilization of horseradish peroxidase for the initiation of the free-radical polymerization*

*Results and discussion*

### III.1. Introduction

Enzyme immobilization is a procedure to enhance the physical and chemical stability of biocatalysts. It is important in many different biotechnology fields, such as food industries [1-3], biochips and biosensors development [4, 5], and also for enzymatic polymerizations [6]. It has many advantages such as the efficient recovery of costly enzyme and their easier separation from the reaction medium for reuse. Another main benefit of the immobilization is avoiding the contamination of the final product by the protein.

In the 'green' synthesis of polymers, enzymes have attracted a specific attention for their ability to catalyze reaction under mild conditions with good regio- and enantioselectivity. Apart from using free enzymes in the medium, their immobilization was also investigated, as an important route to improve their performance in non-natural environments such as organic solvents and at high reaction temperatures. Different immobilization methods were applied such as adsorption, covalent attachment or even incorporation in organic or inorganic materials *via* a polymerization or a sol-gel process [6]. Immobilization has been thus achieved for a wide range of enzymes such as lipases [7, 8], amylases [9], laccases [10, 11] and peroxidases [12-14]. What makes horseradish peroxidase (HRP) interesting for enzymatic solid-phase polymerization is its natural function as radical initiator for lignin degradation and defense against pathogens [15, 16]. Immobilization of HRP on a wide range of supports *via* different methods has been applied in the treatment of industrial wastewater streams for the efficient removal of phenol and chlorophenol from water by enzymatic polymerization. Among all the immobilization methods, covalent attachment to water-insoluble solid carriers, such as magnetic or glass beads, is one of the simplest and most used methods. It helps recovering and reusing the immobilized HRP for many cycles with optimal enzyme behavior in aqueous and hydro-organic mixtures.

In this chapter, the enzymatic polymerization mediated by immobilized HRP is investigated. The main purpose was to provide a novel system for free-radical polymerization to prepare hydrogels free from any radical source residues, and to be able to reuse the enzyme more than once. For



this, covalent attachment of the enzyme to a solid carrier was chosen to facilitate the separation of the enzyme from the final polymeric product after synthesis. Another reason behind using covalent immobilization is to ensure efficient substrate diffusion resulting in good enzymatic kinetics compared to enzyme encapsulation or entrapment in which mass transfer is limited. The selected support in this study was glass beads to avoid the potential co-polymerization of functional monomers with other susceptible polymeric supports. Glass beads are also well-known for their reactivity with different coupling agents facilitating the protein immobilization.

**Figure III-1** illustrates, in details, the steps of the HRP immobilization on glass beads as solid carrier. Our basic protocol for HRP immobilization consists in an activation of the glass beads by silanization followed by grafting a spacer to the support to link the protein.

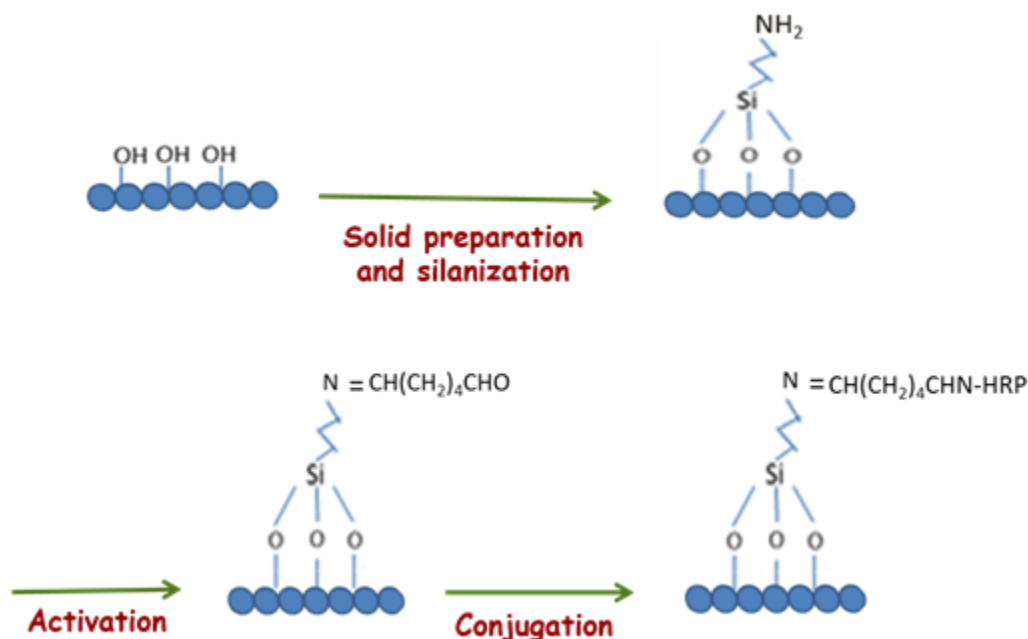


**Figure III-1: Schematic representation of the detailed protocol for HRP immobilization.**

Glass beads of 0.1 mm pore diameter are used for immobilization. The first step is for their activation, where hydroxyl groups ( $-\text{OH}$ ) are formed on the surface of the beads by surface hydrolysis of the silica. Silane-modification of the carrier is then performed. An anchoring layer of silane groups bearing active amine functions is fixed on the beads using (3-

aminopropyl)triethoxysilane (APTES). A bifunctional amine-reactive coupling agent (spacer) is attached to the aminosilane, allowing in turn the grafting of the enzyme. This is based on the formation of covalent bonds (Schiff base) between the spacer and the enzyme's surface  $-NH_2$  residues. In this chapter, the immobilization of horseradish peroxidase is studied and the protocol is optimized to obtain a stable and efficient biocatalyst for enzymatic polymerization. Indeed, enzyme-carrier interactions involve a wide range of dynamic processes depending on both the physicochemical parameters of the immobilization system and on the intrinsic properties of the biocatalyst [17]. For this, we proceeded by optimizing in details every step in the immobilization protocol, in order to ensure best experimental conditions to obtain an optimal enzyme activity. An overall discussion for every step in the dynamic immobilization process is provided with its impact on the enzyme catalytic activity.

The second part of this chapter is dedicated to the synthesis of poly(4-VP/PDA) hydrogel by immobilized enzyme-mediated polymerization. The ternary enzymatic system including hydrogen peroxide, acetylacetone and immobilized HRP were optimized for the polymerization initiation by an experimental design to determine the effect of each initiator system component on the enzymatic polymerization performance.

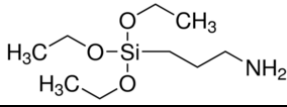
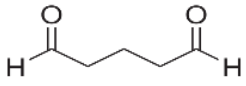
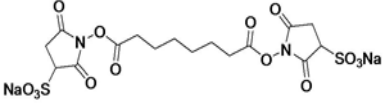
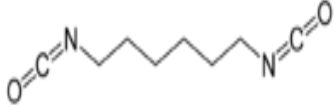
This new system is considered a green approach for hydrogel preparation. Less toxic conditions induce the formation of hydrogels that are clean from any enzymatic radical source.

## III.2. Materials and Methods

### III.2.1. Materials

Immobilization solid supports such as glass beads with a diameter of 0.1 and 0.5 mm are purchased from BioSpec. For glass activation and the coupling step, (3-aminopropyl) triethoxysilane (APTES), glutaraldehyde 50% and hexamethyl diisocyanate (HMDI) were from Sigma-Aldrich. Bis(sulfosuccinimidyl) suberate (BS<sub>3</sub>) was from Fisher Scientific. **Table III-1** shows the chemical composition of these chemicals.

**Table III-1: The chemical structure of the chemicals used in this study for activation and coupling steps.**

Chemical compound	Chemical Structure
(3-aminopropyl)triethoxysilane	
Glutaraldehyde	
Bis(sulfosuccinimidyl) suberate	
Hexamethyl diisocyanate	

Horseradish peroxidase (HRP) and its substrates, including hydrogen peroxide (H<sub>2</sub>O<sub>2</sub>), acetylacetone (Acac) and 2,2'-azino-bis(3-ethylbenzothiazoline-6-sulfonic acid) diammonium salt (ABTS) were all from Sigma.

For hydrogels synthesis, 4-vinylpyridine (4-VP) and 1.4-bis(acryloyl)piperazine (PDA) are purchased from Sigma. 4-VP is distilled under vacuum prior to use.

Organic solvents were of Chromasolv<sup>®</sup> quality or anhydrous and are used in this study without further purification. Ultrapure water (18.2 M $\Omega$ /cm) is obtained by a RiOs Progard<sup>®</sup> 2 Silver, and a milli-Q Q-Gard<sup>®</sup> 1 systems from Millipore. Buffers are prepared from commercial salts and medium pH is adjusted by using NaOH or HCl solutions.

### III.2.2. HRP immobilization

#### Preparation of the carrier

Beads (of 0.1 or 0.5 mm) were activated by incubation in either acidic or basic solutions. For acidic conditions, glass beads were washed in 5 % HNO<sub>3</sub> at 85°C for 1 hour, then rinsed with distilled water and dried in an oven at 100°C.

For basic conditions, glass beads are incubated in a solution of 4 M NaOH at 100°C for 10 minutes to 3 hours. Then, they were washed with water, acetone and then dried in an oven at 100 °C.

#### Silanization step

Different protocols were evaluated for the silanization step of glass beads with APTES. Solutions of  $\gamma$ -APTES (2 or 10%, v/v) were prepared either in water or in toluene and added to the glass beads. For aqueous solutions, pH was adjusted to between pH 3 and 4 with 6 M HCl. The mixtures were incubated either for 2 hours at 75 ° C or for overnight at room temperature.

After incubation, glass beads were washed with water and dried in an oven at 100°C. For glass beads incubated with APTES in toluene, washing steps with toluene and acetone were performed prior to the washing in water.

**Activation of the solid support**

The silanized beads were reacted with different coupling agents: 2.5% (v/v) glutaraldehyde in 50 mM phosphate buffer pH 7.0 for 0.5 to 6 hours, 4 mM bis(sulfosuccinimidyl) suberate in water for 30 minutes, or 37% (v/v) hexamethylene diisocyanate in toluene for 6 hours. All incubations were performed at 25°C under gentle agitation. Upon activation, the glass beads were intensively washed in the same solvent used for the incubation.

**HRP immobilization**

1 gram of activated glass beads was incubated overnight at 25°C with 2 ml of a standard 2 mg/ml HRP solution prepared in 50 mM phosphate buffer pH 7.0 for glutaraldehyde and BS3-activated beads. For HMDI-activated beads, the conjugation was done in 50 mM borate buffer pH 9.2. Then, the unreacted coupling groups were blocked by incubation in 50 µl ethanolamine for 30 min prior to washing. All glass beads were washed and stored at 4°C in buffer.

**III.2.3. Characterization of the immobilized enzyme****Quantification of amino groups**

After the silanization step, the glass beads were washed to eliminate the unreacted functional groups. The amount of amino groups available on the silanized beads surface was estimated by the Orange Test. It is based on a colorimetric assay using an anionic dye, Orange II. 100 mg of glass beads were introduced in 1 ml of 40 mM Orange II acidic solution (Milli-Q water adjusted to pH 3 with 1 M HCl) and stirred for 30 minutes at 40°C. The sample was then intensively rinsed with the same acidic solution to remove unbound dye. Once air-dried the colored glass beads were immersed in 1 mL of basic solution (Milli-Q water adjusted to pH 12 with 1 M NaOH) to release the adsorbed dye. The pH in the basic solution, which contains the desorbed dye analyte, was adjusted to 3 by adding 1 M HCl. 100 µl of this solution were added to 0.9 ml of water acidic solution in a disposable cuvette. The absorbance of the solution was measured at

485 nm by UV/Vis spectroscopy on a Cary-60 spectrometer. As a control, the same protocol was applied to original not activated beads.

The total amount of amino groups is calculated according to a standard curve (**Figure III-2**).

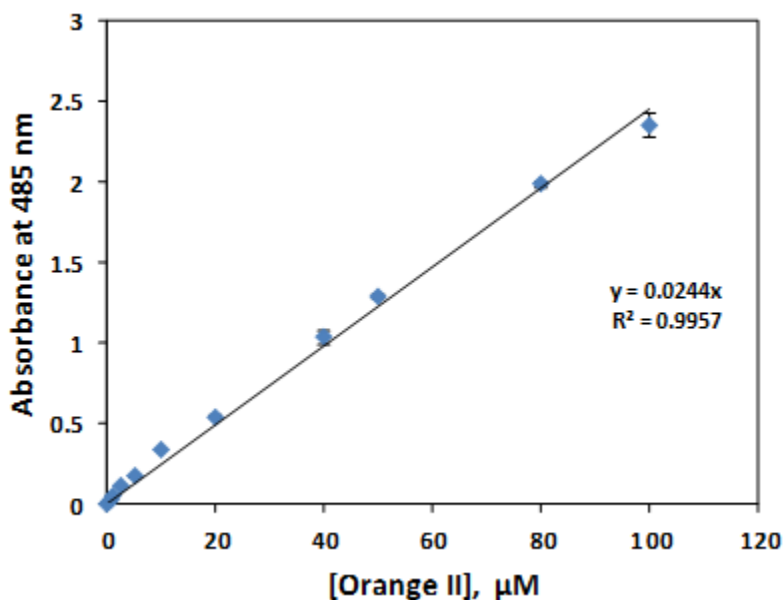


**Figure III-2: Calibration curve for Orange Test.**

### Protein quantification

Horseshradish peroxidase immobilized on the glass beads was quantified by the Bradford protein assay. It is based on the absorbance shift at 595 nm of Coomassie Brilliant Blue upon adsorption to a protein. The amount of protein in the immobilization medium before and after immobilization was determined using the standard curve initially plotted (cf. **Chapter II**, II.2.6). The amount of coupled peroxidase was the difference among the initial enzyme concentration and ones measured in the final enzyme solution and the washing liquids.

### Activity measurements of the free and immobilized HRP

In order to measure the activity of free horseradish peroxidase, we used the same ABTS Test described in **Chapter II** (II.2.5). For the immobilized enzyme, the specific activity of HRP-charged glass beads (200 mg) was measured in a total volume of 6 ml, including 0.2 ml of 30

mM ABTS and 0.2 ml of 30 mM hydrogen peroxide solution. After the introduction of H<sub>2</sub>O<sub>2</sub> solution, the absorbance at 405 nm was monitored on a UV/Vis spectrophotometer for 10 minutes. The specific activity was calculated using the following equation:

$$a_i = \frac{\Delta Abs}{\Delta t \times \varepsilon} \times \frac{1}{V} \times \frac{1}{m(GB)}$$

(Eq.1)

Where  $a_i$  is the specific activity in mol/min/g of GB,  $\varepsilon$  is the extinction coefficient at 405 nm being 36000 mol/l/min as determined experimentally,  $V$  is the solution total volume (L) and  $m$  is the total amount of beads, which is here 200 mg.

### **Storage stability**

Storage stability experiments were conducted in order to determine the stability of free and immobilized HRP upon storage in 50 mM phosphate buffer pH 7.0 at 4°C for 72 days. Free and immobilized HRP residual activities were measured every 7 days using the activity measurements protocol described above.

### **Scanning electron microscopy (SEM)**

SEM analysis of glass beads at the different steps in the immobilization protocol done at the Physico-Chemical Analysis Platform at UTC by using a Quanta feg 250 environmental microscope.

### III.2.4. Synthesis of hydrogels using immobilized HRP and their characterization

#### III.2.4.1. Experimental design

##### Protocol of hydrogels preparation

Doehlert's experimental design, a second-order uniform shell design, was used for the optimization of HRP-mediated synthesis of hydrogels. We wanted to determine the optimal experimental conditions that allow us to obtain small-sized hydrogels combined with high polymerization yields.

The system is a uniform shell design for the modeling of a measured response by the second-order function of distinct variables and their interactions, as illustrated by the following equation 2:

$$Y = \beta_0 + \sum_{i=1}^f \beta_i X_i + \sum_{i=1}^f \beta_{ii} X_i^2 + \sum_{i=1}^{f-1} \sum_{j=i+1}^f \beta_{ij} X_i X_j$$

(Eq.2)

Where  $f$  is the number of parameters,  $Y$  is the measured response,  $X_i$  and  $X_j$  are the distinct variables,  $\beta_0$  is the intercept,  $\beta_i$  and  $\beta_j$  are the linear coefficients, and  $\beta_{ij}$  are interaction coefficients.

Doehlert experimental design is well adapted for modeling the phenomena that are based on the complex interactions of different factors in hydrogels preparation by immobilized HRP-catalyzed synthesis. Four parameters, which may influence the process, are studied:

- Quantity of HRP-charged beads (2 g to 20 g)
- Total monomers concentration (0 to 10%)
- Amount of acetylacetone (0.017 mmol to 0.136 mmol)



- Amount of hydrogen peroxide (5.5  $\mu\text{mol}$  to 44  $\mu\text{mol}$ )

The process is evaluated by characterizing a final result that is called response (Y). For our study, 2 types of responses are registered. Each hydrogel is characterized in terms of particles size (nm) ( $Y_1$ ) and the polymerization yield (%) ( $Y_2$ ).

The Doehlert matrix gives the number of experiments and the corresponding experimental conditions to apply the studied process for every experiment. The values obtained for every experimental parameter, also called factor, are given in a normalized space. In order to study the influence of the four factors already mentioned, the Doehlert matrix is represented in **Table II-2**.

Each row of the table corresponds to one experiment for the formation of one hydrogel. In addition, the columns in the table are representing the studied factors in their two forms: coded values of the normalized form of the factor as well as its real experimental value.

The conversion of the coded values in real space is necessary to know the experimental factors that should be applied for hydrogel synthesis. It is achieved using the following equation 1:

$$x_i = \frac{n_i - n_i^0}{\Delta n_i} \quad (\text{Eq.3})$$

Where  $x_i$  is the coded value of the normalized form ( $X_i$ ) of the factor  $N_i$ ,  $n_i$  is the real value of the factor  $N_i$ ;  $n_i^0$  is the real value of the factor  $N_i$  at the center of the experimental domain and  $\Delta n_i$  the step of variation of the real variable  $N_i$ .

An ANOVA test was performed to check the adequacy of the fitted model. The run in the center of each factor is repeated one more time in order to estimate the reproducibility of the results.

Experimentally, hydrogels were prepared by the dilution method of free radical polymerization. Radical generation is achieved by the oxidation of acetylacetone catalyzed by the immobilized HRP. 4-vinylpyridine and 1,4-bis(acryloyl)piperazine are used as model functional and cross-linking monomers, respectively. 0.58 mmol of PDA and 0.145 mmol of 4-VP were dissolved in an adequate volume of 0.1 M sodium phosphate buffer pH 7.0, depending on the total monomer concentration. This mixture was placed in a 20 ml glass tube fitted with an airtight septum. The required volume of Acac was added to the solution with the HRP-charged glass beads. The mixture, kept in ice, was purged with nitrogen for 10 minutes. Finally, a predetermined volume

of 103 mM solution of hydrogen peroxide according to the experimental design was added after degassing to start the polymerization. After 4 days of polymerization at 25°C on a rotor, the polymers were recovered by pipetting, and the glass beads were washed by 10 ml of the same buffer for 5 times. The hydrogels are washed by dialysis in water for 2 days at room temperature and lyophilized.

**Table II-2: Four-parameter Doelhart matrix showing the number of experiments and the factors.**

N° of runs	Factor 1	Beads (g)	Factor 2	[Monomers] (%)	Factor 3	n(Acac) (mmol)	Factor 4	n(H <sub>2</sub> O <sub>2</sub> ) (mmol)
1	0	11	0	5	0	0.0767	0	0.025
2	1	20	0	5	0	0.0767	0	0.025
3	0.5	15.5	0.866	9.33	0	0.0767	0	0.025
4	-0.5	6.5	0.866	9.33	0	0.0767	0	0.025
5	-1	2	0	5	0	0.0767	0	0.025
6	-0.5	6.5	-0.866	0.67	0	0.0767	0	0.025
7	0.5	15.5	-0.866	0.67	0	0.0767	0	0.025
8	0.5	15.5	0.289	6.445	0.816	0.125	0	0.025
9	-0.5	6.5	0.289	6.445	0.816	0.125	0	0.025
10	0	11	-0.577	2.115	0.816	0.125	0	0.025
11	0.5	15.5	-0.289	3.555	-0.816	0.0283	0	0.025
12	-0.5	6.5	-0.289	3.555	-0.816	0.0283	0	0.025
13	0	11	0.577	7.885	-0.816	0.0283	0	0.025
14	0.5	15.5	0.289	6.445	0.204	0.0887	0.791	0.04
15	-0.5	6.5	0.289	6.445	0.204	0.0887	0.791	0.04
16	0	11	-0.577	2.115	0.204	0.0887	0.791	0.04
17	0	11	0	5	-0.612	0.0404	0.791	0.04
18	0.5	15.5	-0.289	3.555	-0.204	0.0646	-0.791	0.01
19	-0.5	6.5	-0.289	3.555	-0.204	0.0646	-0.791	0.01
20	0	11	0.577	7.885	-0.204	0.0646	-0.791	0.01
21	0	11	0	5	0.612	0.113	-0.791	0.01

### **Polymerization Yield**

The polymerization yield was determined after the polymer washing step and lyophilization. The yield corresponds to the weight ratio of dry polymer recovered after the polymerization reaction to the monomer amount that was initially introduced.

### **Particle size measurements**

The hydrodynamic diameter of the particles was determined by dynamic light scattering (DLS) measurements on a Malvern Instruments ZetaSizer Nano ZS in water. Directly after synthesis, 50  $\mu\text{l}$  of each hydrogel is mixed with water in a total volume of 1 ml, and the particles are sonicated in an ultrasonic bath for at least 30 minutes in order to break the aggregates of particles.

### **Particles morphology**

The characterization of the nanoparticles in term of size and surface morphology was done in the physico-chemical Analysis Unit at UTC, by Scanning electron microscopy on a Quanta feg 250 environmental microscope.

#### **III.2.4.2. Entrapment of HRP in the hydrogel matrix**

SDS-PAGE electrophoresis was performed under reducing agents in order to control the absence of HRP within the polymeric matrices after synthesis. Polyacrylamide gels of 12% and 5% concentrations for running and stacking gels, respectively, were prepared. The following solutions were put in the well:

- Molecular weight markers (Dual color) in Lane 1
- 20  $\mu\text{l}$  of 0.1 mg/ml HRP solution in Lane 2
- 40  $\mu\text{l}$  of 0.25  $\mu\text{g}/\text{ml}$  HRP solution in Lane 3
- 40  $\mu\text{l}$  of 100 mg/ml of hydrogel solution in Lane 4
- 50  $\mu\text{l}$  of 200 mg/ml of hydrogel solution in Lane 6

The electric field of 100 mV/cm applied across the gel caused the negatively charged proteins to migrate within the gel towards the anode (+). After electrophoresis, the gel was stained by

---

Coomassie Brilliant Blue for 30 minutes at room temperature. The bands are revealed by a discoloration step.

#### III.2.4.3. Comparison of free and immobilized enzyme for hydrogels synthesis

Hydrogel synthesis was performed by both free and immobilized enzymes. The same polymerization procedure was used. 2.32 mmol of PDA were dissolved with 0.58 mmol of 4-VP in 5 ml of ultra-pure water (10% as total monomer concentration). 0.035 mmol of Acac were added. For the immobilized enzyme, 10 g of HRP-charged beads of  $3 \times 10^{-7}$  mol/min/g of GB as specific activity were used. To compare, free enzyme with the same activity was used for synthesis, estimated to 0.14 mg of HRP having a specific activity  $1.6 \times 10^{-5}$  mol/min/mg. Both polymerization mixtures were degassed in ice for 10 minutes and 0.022 mmol of hydrogen peroxide were finally added. The glass tubes were left on a rotor for 4 days at room temperature. The hydrogels were dialyzed against water for 2 days and lyophilized. The polymerization yields and particles sizes were determined as previously described.

### **III.3. Results and discussion**

#### **III.3.1. HRP immobilization**

The methodology presented in this chapter emerges as a potential solution for the preparation of hydrogels free from any radical source. This part includes the development of an immobilized HRP system and its application in the enzymatically initiated free radical polymerization of hydrogels. For this purpose, HRP was immobilized on a solid carrier, here the glass beads, by covalent bonding. Every step in the immobilized protocol is optimized in terms of immobilized HRP amount and residual activity. The optimal protocol is characterized and applied for hydrogel preparation.

##### **III.3.1.1. Optimization of HRP immobilization**

In this study, the solid carrier for HRP immobilization was glass beads, according to an enzyme immobilization protocol already developed in our group [18]. The protocol includes different steps. The preparation of the carrier consists in the activation and the silanization of the beads. A bifunctional coupling agent is then bound to the  $-NH_2$  functional groups on the surface of the beads, and used for covalent enzyme immobilization. The final material will be applied to enzymatic polymer particles synthesis. Since, polymerization yield has been shown to depend on the enzyme kinetics, it was crucial to optimize the immobilization of the enzyme.

##### **A. Activation of the glass beads**

Glass beads were selected as HRP solid carrier mainly for their physical stability and the ease of activation. Various approaches for the activation and silanization were carried out. The main purpose for the optimization of this step is the increase in the amount of amino groups grafted on

the surface of the beads, since the increase in  $-\text{NH}_2$  should theoretically should lead to an increase in the enzyme amount that will be immobilized.

First, we have evaluated different sizes of glass beads (0.1 or 0.5 mm as diameter) for protein immobilization. For this, glass beads were activated by incubation in 4 M NaOH solution at  $100^\circ\text{C}$  for 5 minutes. Then, they were washed with water and acetone and dried in the oven at  $100^\circ\text{C}$ . The activated GBs were then incubated in APTES/toluene 2% v/v. solution for overnight at room temperature. The quantity of amino groups per g of glass beads were determined by spectroscopic methods using Orange test. As expected, glass beads with a diameter of 0.5 mm had two times less amino groups ( $0.126 \mu\text{mol/g}$  of GB  $\pm 0.1$ ) than the ones of 0.1 mm ( $0.21 \mu\text{mol/g}$  of GB  $\pm 0.01$ ), which is due to the higher specific surface area of the latter [19]. 0.1 mm beads were thus used in all further experiments.

- Beads activation

The first step is the activation of glass beads to reveal reactive silanoyl groups on the surface. This activation can be performed by two approaches either in acidic [20] or basic [21] solutions. The activation in basic conditions consisted in boiling the glass beads in 4 M NaOH solution, whereas the acidic one aimed to incubated the glass beads in 5%  $\text{HNO}_3$  at  $75^\circ\text{C}$ . The efficiency of this step was assessed by determining the amount of  $\text{NH}_2$  groups grafted after the silanization step on the beads surface. For each activation method, two different protocols of silanization have been evaluated by incubating the activated beads either in APTES/toluene solution (2% v/v) or in an aqueous acidic solution of APTES (10%), both at room temperature for overnight. **Figure III-3** shows the results obtained for the two activations methods and silanization protocols.

For both silanization protocols, the activation of glass beads in basic media led clearly to a higher amino group density on the support surface. Higher amounts of  $\text{NH}_2$  groups grafted on glass beads was obtained in basic conditions than in acidic ones. Therefore, glass beads activation by basic solution is thus preferred suggesting a higher efficiency of the silane grafting.

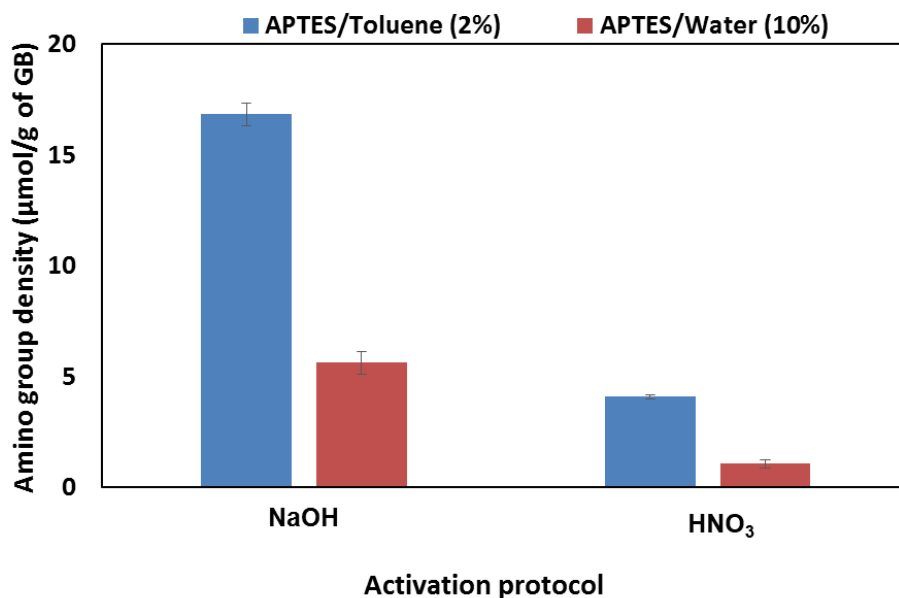


**Figure III-3:** Amounts of amino groups on the surface of activated glass beads according to different activation and silanization protocols.

The effect of activation time boiling 4 M NaOH solution was also examined for a period ranging from 5 minutes to 3 hours. Different batches of glass beads were activated and then silanized by APTES/toluene 2% prior to HRP coupling. The amino group density on the solid support and the quantity of immobilized protein were determined for different activation times (**Figure III-4**).

We noticed that the activation time strongly affects the amino group density on the support and thus, the quantity of immobilized HRP. A linear increase in the amino group density on glass beads can be observed as a function of the activation time until 120 minutes, as shown in **Figure III-4A**. The maximal  $\text{NH}_2$  amount of 32  $\mu\text{mol/g}$  of GBs was obtained at 2 hours of incubation in boiling 4 M NaOH. Afterwards, the amino group density rapidly decreased due to the deterioration of the beads. **Figure III-4B** shows that increasing the  $-\text{NH}_2$  groups on the beads surface will lead to a proportional increase in the immobilized enzyme load with an  $R^2$  of 0.998.

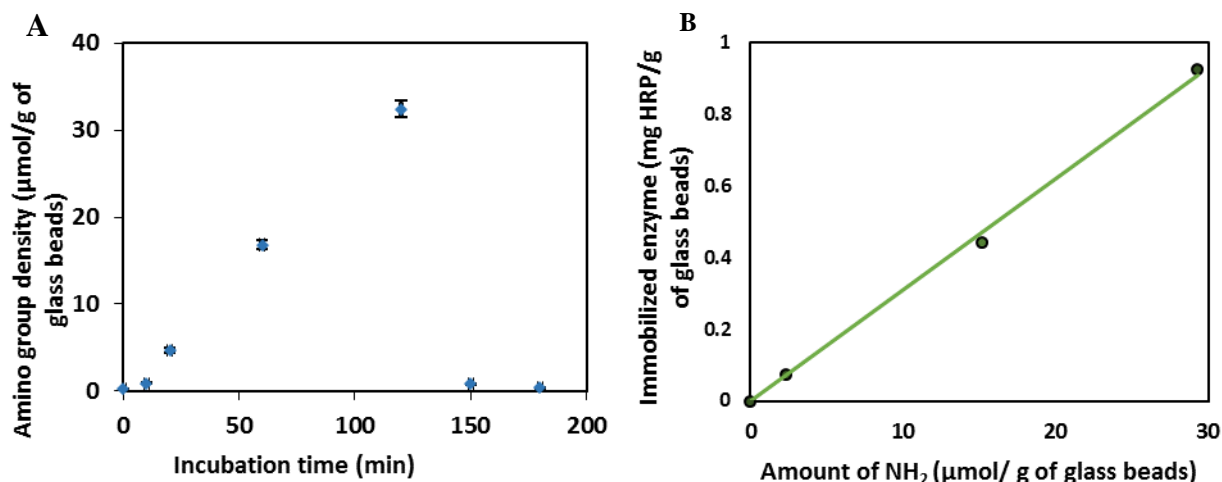


**Figure III-4 Optimization of the activation step by boiling in 4 M NaOH. (A) Effect of the incubation time on the amino group density. (B) Effect of the increase in amino groups number on the amount of the immobilized HRP. The immobilization reactions were conducted using 2% APTES/toluene for silanization, 2.5 wt% glutaraldehyde for 1 hour, and 2 mg/ml HRP solution for overnight at 25°C.**

In consequence, activation of glass beads in 4 M NaOH for 2 hours will be used for all the upcoming experiments for enzyme immobilization.

- Optimization of the silanization step

After activation, the following step is a silanization process in order to introduce amino groups onto the carrier surface. It is well-known that (3-aminopropyl)triethoxysilane (APTES) is the most used silane coupling agent for enzyme immobilization in the literature [20, 22, 23].

Different experimental conditions were evaluated for the silanization of glass beads by incubating the beads in aqueous and organic solutions of APTES at different concentrations. The influence of the solvent, APTES concentration and incubation time on the amino group density is represented in **Figure III-5**.



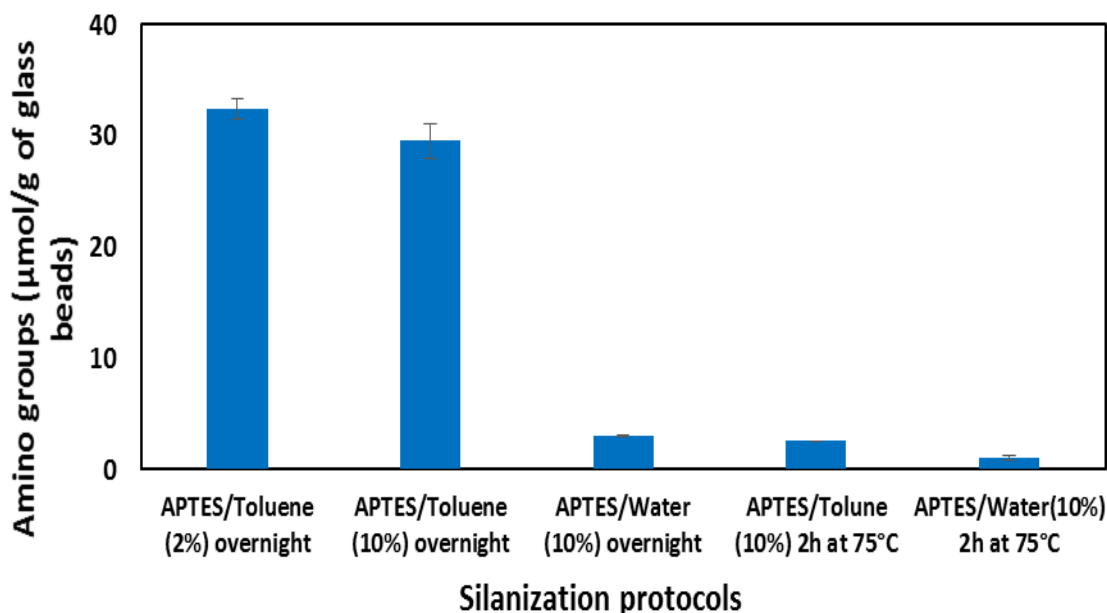


**Figure III-5: Effect of the different silanization protocols on the amino group density on the surface of the glass beads. Activation was by boiling in 4 M NaOH for 2 hours.**

It seems that incubation temperature and time have a great effect on the amount of amino groups grafted onto the beads. Incubating the glass beads at room temperature for overnight always gives better results than the incubation at 75°C for 2 hours whatever the solvent nature and concentration are. Concerning the nature of the solvent, higher amino group quantities are grafted on the support when silanization occurs in toluene rather than in acidic water whatever the incubation time is. Keeping fixed the incubation protocol, the increase in the silane coupling agent concentration (from 2% to 10% v/v) has no significant effect on the amino groups density. Therefore, the optimal recipe for silanization of glass beads with APTES is the incubation in APTES/toluene (2% v/v) for overnight at room temperature leading to a  $\text{NH}_2$  groups density of 32  $\mu\text{mol/g}$  of GBs on the carrier surface.

### **B. Influence of the coupling agent on the enzyme immobilization**

The coupling agent or linker is a symmetric molecule that reacts on one side with the primary amine on the beads surface, and, on the other side, forms a covalent bond with the enzyme by reacting with the primary amine of an accessible lysine residue. In this work, the coupling agent

grafting step has been studied to optimize the protein immobilization by studying the effect of the incubation time and nature of the linkers.

### *1. Optimization of the coupling step using glutaraldehyde*

Glutaraldehyde is by far the most applied linker in the enzyme immobilization on solid carriers [8, 13, 18, 21, 22, 24]. Prior to any experiment, it was crucial to fix the glutaraldehyde concentration. It was shown in literature that changing the linker concentration can greatly affect the amount and the residual activity of the immobilized enzyme. Optimal glutaraldehyde concentration was shown to be 2.5-wt% [12, 14, 20, 24]. A linker concentration below the optimal one is not able to adequately immobilize the protein for the intended application, resulting in a relatively low amount of immobilized enzyme [23]. However, high concentrations can lead to extensive crosslinking among enzymes and aldehyde groups on the surface of the solid carrier, which may result in lower enzyme activity [12, 23].

- *Effect of the glutaraldehyde incubation time on the HRP immobilization*

As well as the concentration parameter, the incubation time of glass beads in glutaraldehyde solution is a major parameter affecting the HRP immobilization in terms of residual enzyme activity and immobilization yield.

After the incubation of activated glass beads for 0.5, 1, and 6 hours with glutaraldehyde solution of 2.5-wt% at room temperature, HRP was immobilized on the activated solid support., at room temperature and under gentle agitation. The specific activities of the immobilized enzyme, as well as the immobilized enzyme amount at different times are represented in **Figure III-6**.

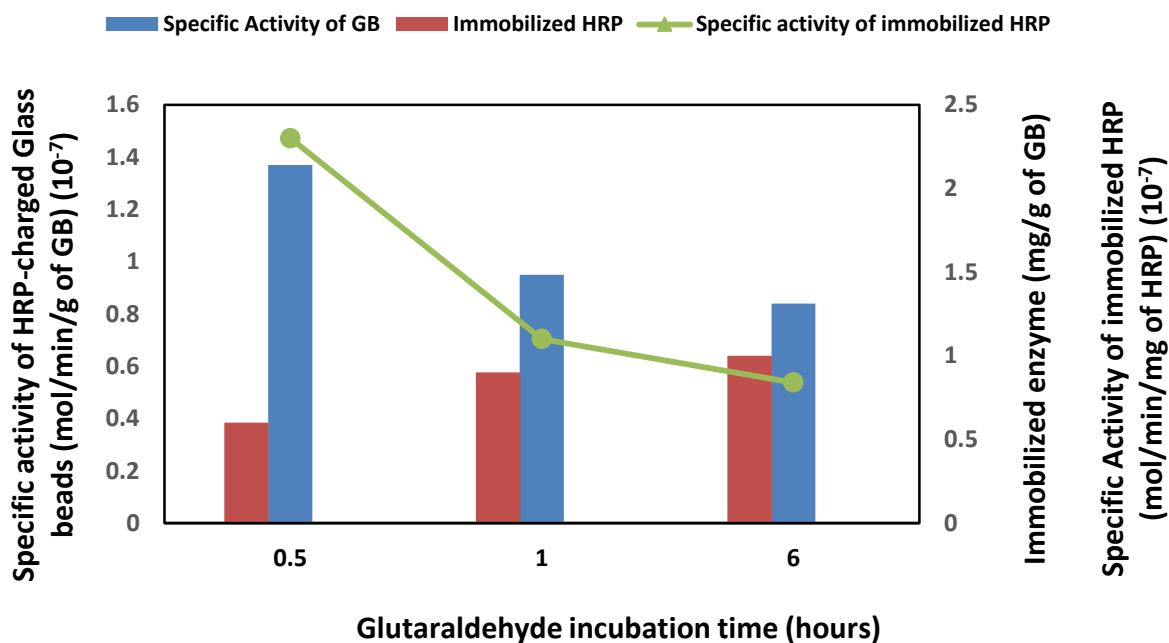


**Figure III-6: Influence of the glutaraldehyde incubation time on HRP immobilization.** The reactions were achieved by boiling the beads for 2 hours in 4 M NaOH and incubation in 2% APTES/toluene overnight. The HRP coupling Step is achieved at 25°C, with an enzyme concentration of 2 mg/ml.

As the figure shows, the amount of immobilized HRP is enhanced with the increase of the glutaraldehyde incubation time. An increase in time from 0.5 hour to 6 hours allowed an increase in immobilized enzyme amount from 0.6 mg to 1 mg per g of solid carrier. In contrast, the specific activity of HRP-charged glass beads is inversely proportional to the increase of glutaraldehyde incubation time and the immobilized enzyme load. Optimal activity is obtained at 0.5 hour. The low amount of immobilized enzyme at short incubation time is due to the fact that glutaraldehyde had no enough time to adequately react with the solid carrier. However, with too long glutaraldehyde incubation time, the enzyme can change its conformation [12]. Longer activation can even lead to a too high amount of glutaraldehyde coupled, which results in the enzyme denaturation by excessive cross-linking. An optimal activation time of 1 hour was fixed for subsequent experiments. However, the reduced specific activity of the HRP-charged beads, and so the enzyme residual activity, is a drawback.

- Influence of the micro-environment of the enzyme

It is known that water plays an important role in enzyme structure and function. When the enzyme is immobilized, the hydrophilicity of the support may therefore largely affect the catalytic residual activity of the enzyme, that is, if the support is too hydrophobic the enzyme may be denatured during attachment. Thus, hydration of the support may help maintaining enzyme activity [7, 25-27]. Therefore, a washing step with water was added after the silanization to create an aqueous micro-environment in all immobilization steps, providing efficient amount of water that can be absorbed by the glass beads. Glass beads were first activated in basic conditions and then silanized in APTES/toluene (2% v/v.). In order to remove the unreacted silane groups, beads are washed with toluene and acetone, then a third washing step with distilled water was added in order to create the aqueous micro-environment prior to the glutaraldehyde activation and the enzyme conjugation. The specific activities of the immobilized HRP as well as the immobilization performance are shown in **Figure III-7**. The addition of a washing in water step led to a slight decrease in the amount of the immobilized enzyme. However, the specific activity of the HRP-charged beads greatly improved from  $1 \cdot 10^{-7}$  to  $3 \cdot 10^{-7}$  mol/min/g of glass beads. The residual activity thus increased from 1% to 2.1%. These results show that our hypothesis that the aqueous micro-environment during coupling influences well the enzyme specific activity is valid.

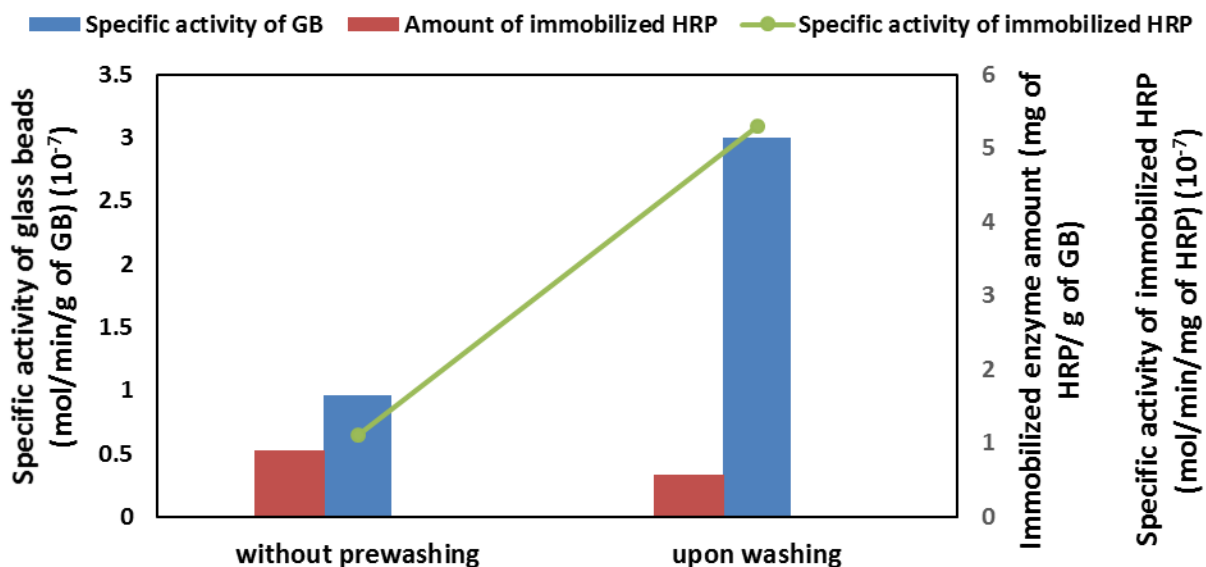


**Figure III-7: Influence of the pretreatment with water prior to glutaraldehyde incubation on HRP immobilization.** The reactions were achieved by boiling the beads for 2 hours in NaOH 4M, and incubation in 2% APTES/toluene overnight, and by activating in 2.5-wt% glutaraldehyde for 1 hour. The HRP coupling step is achieved at 25°C, with an enzyme concentration of 2 mg/ml.

## 2. Influence of the spacer on HRP immobilization

Glutaraldehyde, a linear dialdehyde of 5 carbon atoms, is commonly used as an anchoring agent for protein immobilization [28]. However, the immobilization efficiency can be strongly affected by the spacer length and its reactivity towards the protein. Several other coupling agents have also been used in literature. In this part, we have examined the efficiency of different coupling agents for HRP immobilization to improve the enzyme residual activity and the quantity of immobilized protein.

For this purpose, two more coupling agents, bis(sulfosuccinimidyl) suberate (BS<sub>3</sub>) and hexamethylene diisocyanate (HMDI), in addition to glutaraldehyde, were studied. BS<sub>3</sub> is able, like glutaraldehyde, to covalently react with –NH<sub>2</sub> group of the enzyme under mild conditions in aqueous media [29], whereas the isocyanate group of HMDI can react with the amino and hydroxyl groups of the protein. Protocols for the two new spacers were adapted from the PhD

thesis of Ana-Valvanuz Linares from in our group [30]. **Figure III-8** shows the performance of the HRP immobilization using these three coupling agents on the specific activity and immobilized enzyme amount.

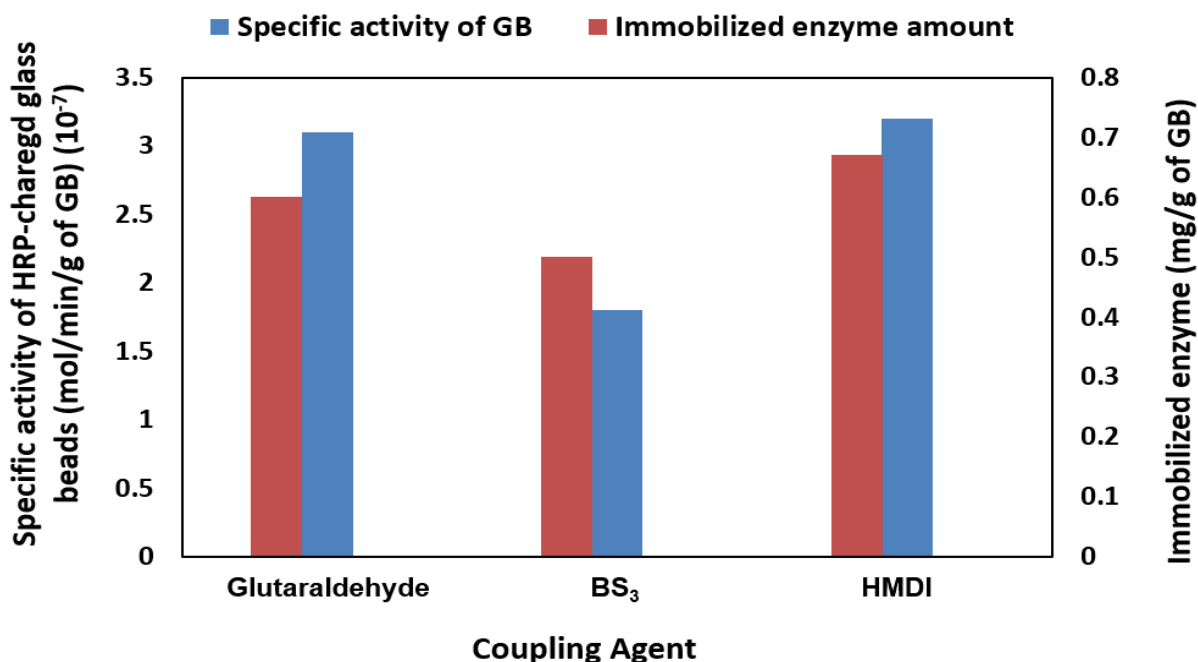


**Figure III-8: Influence of the coupling agent on HRP immobilization.** The reactions were carried out by boiling the beads for 2 hours in 4 M NaOH and incubating in 2% APTES/toluene overnight. The HRP coupling step is achieved at 25°C, with an enzyme concentration of 2mg/ml.

No significant difference was detected between the specific activities of the beads activated with glutaraldehyde and HMDI nor the immobilized HRP amount. Protein loading and specific activities achieved with BS<sub>3</sub> were lower than with the other methods.

Glutaraldehyde and HMDI activation both yield good results for HRP immobilization. However, glutaraldehyde-modified beads allow better polymerization yields upon synthesis of MIP particles than HMDI-modified ones. For this reason, glutaraldehyde immobilization will be used for the all subsequent studies.

### C. Optimization of enzyme coupling step

HRP is normally immobilized *via* covalent bonds with glutaraldehyde. This covalent immobilization of enzyme is achieved by the interaction of aldehyde groups with the terminal –NH<sub>2</sub> groups within the enzyme, forming a Schiff base. However, reaction is also possible with thiol groups (-SH) [28]. Different parameters such as incubation time, temperature, and enzyme concentration can affect the coupling step.

- Effect of the immobilization process : incubation time and temperature

It was described in the literature that increasing the conjugation time up to 12 hours results in increasing immobilization yield. No significant variations are detected with even longer incubation [23, 24, 28]. In order to define standard optimal conditions for HRP immobilization, the incubation temperature in the enzyme coupling step is investigated for two values, 4°C and 25°C commonly applied in the literature [20, 24, 31]. The immobilization yield and the enzyme specific activity of HRP immobilization depending on the incubation temperature are detailed in **Figure III-9**.

The same immobilization yield (~10%) was obtained for the both incubation temperatures keeping identical the experimental conditions in all the immobilization step, whereas a difference in the enzyme residual activity was observed (1.5 % and 2.1 % for 4°C and 25°C, respectively). Thus, room temperature incubation is chosen for the final protocol.

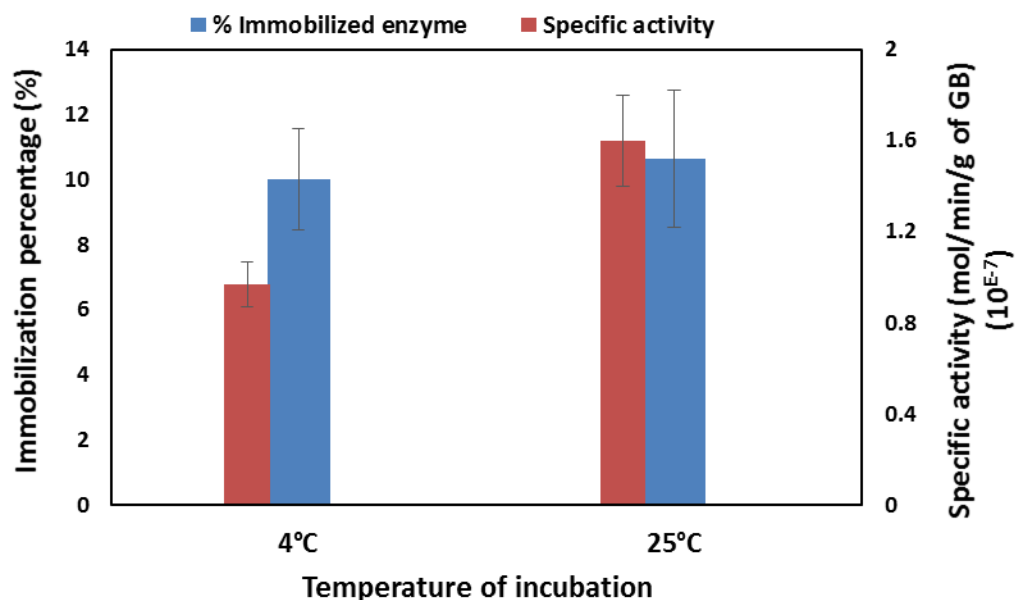


**Figure III-9: Influence of the incubation temperature on HRP immobilization.** The reaction is carried out by boiling the beads for 2 hours in 4 M NaOH, then by incubating successively in 2% APTES/toluene overnight, 2.5-wt% glutaraldehyde for 1 hour, and 2 mg/ml HRP solution.

- *Effect of the enzyme*

Two different isoenzymes, HRP II and HRP IV, were evaluated for use as immobilized catalyst. The quantity of immobilized protein was 1.6 and 1 mg per g of solid carrier for HRP IV and II, respectively. However, the residual activities were the same for both of isoenzymes. Since HRP IV is much more expensive and no significant different are observed for the immobilized enzyme characteristics, HRP II was used for the enzymatic polymerization.

The effect of HRP concentration on the immobilization was studied. The experiments were carried out at the optimum conditions of the immobilization process mentioned above. Different HRP concentrations ranging from 0.5 to 10 mg/ml were examined and the results are illustrated in **Figure III-10**.



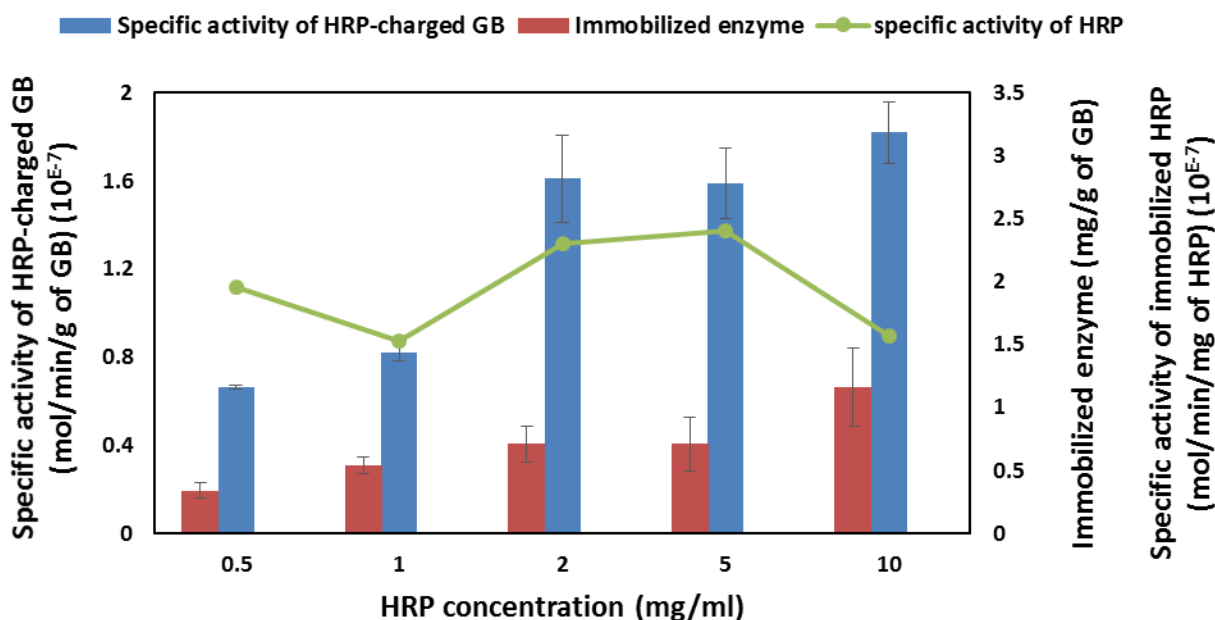


**Figure III-10: Influence of the enzyme concentration on HRP immobilization.** The reaction is carried out by boiling the beads for 2 hours in 4 M NaOH, then by incubating successively in 2% APTES/toluene overnight, in 2.5 wt-% glutaraldehyde for 1 hour. The HRP coupling step is done at 25°C.

The enzyme load increased with the increase of HRP concentration from 0.34 mg HRP/g of GB with 0.5 mg/ml of HRP solution to 1.16 mg/g GB with 10 mg/ml, as expected. For the specific activity of the HRP-charged glass beads, it increases between 0.5 and 2 mg/ml of HRP solutions. Beyond, there is no significant change with the increase of the enzyme concentration inducing a decrease in the specific activity of the immobilized HRP from 2.4 to 1.57 mol/min/ mg of HRP for 5 and 10 mg/ml of HRP solution, respectively.

Only about 0.1% of the amino groups were, thus, occupied by the immobilized enzyme. So, it should be possible to improve the immobilization yield on the solid carrier. However, further increase in enzyme concentrations may cause more important decrease in the specific activities of the immobilized HRP, with no significant changes in the specific activities of the glass beads. Indeed, the immobilization of a too large amount of protein could result in a steric hindrance limiting the accessibility and the diffusion of substrate molecules [24, 31].

Maximal residual activity of the immobilized enzyme, even at optimal conditions, will not exceed 3% of the free HRP. This is explained by the covalent bond created within the immobilization of HRP *via* the coupling with glutaraldehyde, which is well-known to trigger the extensive protein denaturation and to limit the protein flexibility and its orientation [24].

As a conclusion, an enzyme concentration of 2 mg/ml seems to be the optimal protein concentration enabling a compromise to be reached between high specific activity and immobilization yield while minimizing cost and protein losses.

### III.3.1.2. Characterization of HRP immobilization

Based on our findings in the previous section, the optimum immobilization conditions were defined and applied to one batch of glass beads in order to characterize each step of the immobilization process by SEM. The stability of the enzyme was investigated under different experimental conditions. Immobilization of HRP was done as follows:

- Activation step: 0.1 mm glass beads are activated by incubating in 4 M NaOH for 2 hours at 100°C under gentle agitation. Then they are washed with water and acetone, and dried in an oven at 100°C.
- Silanization step: NH<sub>2</sub>-modification of the beads is performed by their incubation in APTES/toluene (2% v/v.) for overnight at room temperature. They are washed with toluene, acetone and distilled water, then dried at 100°C.
- Grafting of the coupling agent: by using glutaraldehyde in a 2.5 wt-% solution prepared in 50 mM sodium phosphate buffer, pH 7.0. The incubation is for 1 hour and the beads are washed with distilled water.
- HRP immobilization: the enzyme is coupled by incubating in a 2 mg/ml protein solution in 50 mM phosphate buffer pH 7.0 for overnight at 25°C. The beads are washed with the same buffer and stored in the same buffer at 4°C.

With this protocol, the amino groups density on the surface of the beads is  $32 \mu\text{mol/g}$  of GBs and 1 mg of HRP is immobilized on 1 g of glass beads. In terms of activities, the specific activities of HRP and beads are  $5.3 \cdot 10^{-7}$  mol/min per 1 mg of immobilized enzyme and  $3 \cdot 10^{-7}$  mol/min per 1 g of glass beads. The residual activity of the immobilized HRP is thus estimated to 2.1% of the native enzyme's specific activity and the immobilization yield to 25 % of the enzyme total amount. These characteristics are satisfactory compared to those achieved by others on HRP immobilization on magnetic beads where the immobilization was 18 % [32], or to those obtained when HRP was immobilized on aminopropyl glass beads (amino group density of  $130 \mu\text{mol/g}$ ) and the immobilization yield 37% was however the residual activity did not exceed 3% [24].

The glass beads were characterized by scanning electron microscopy. SEM images were obtained for every step in the immobilization protocol as represented in **Figure III-11**.

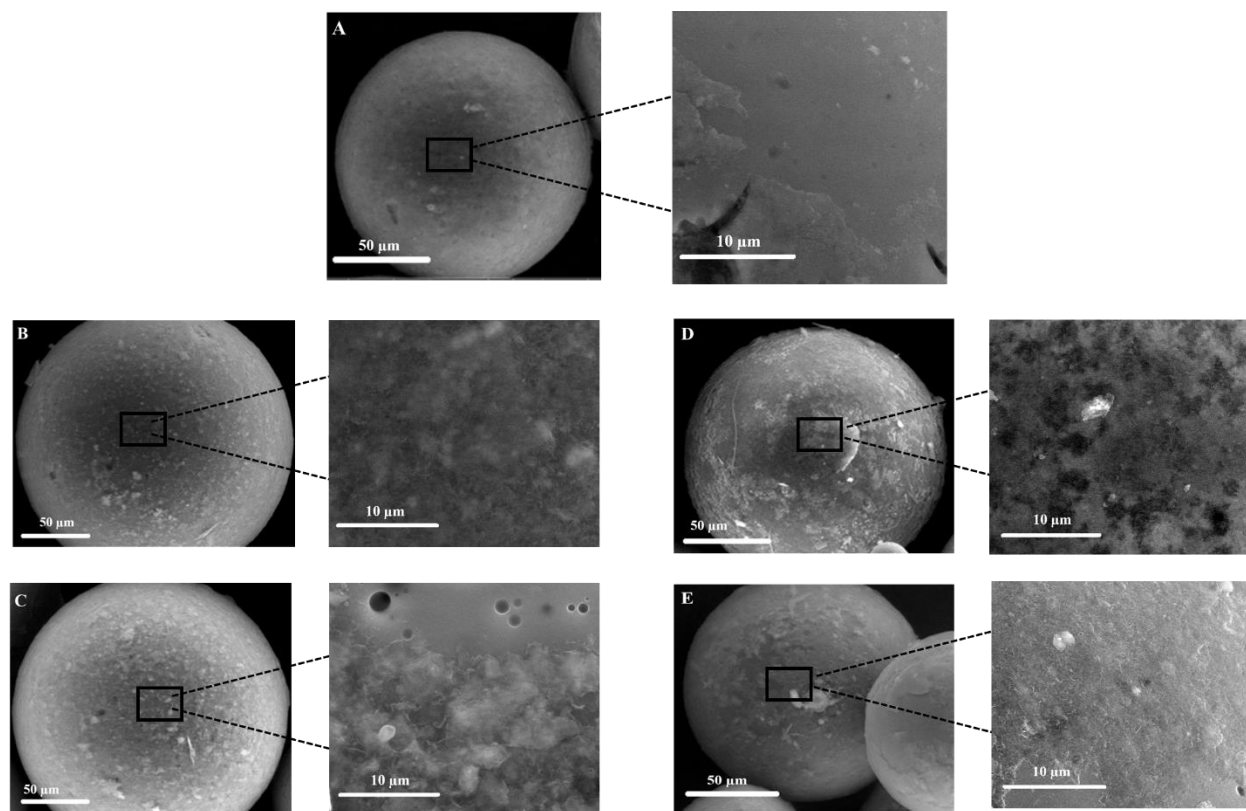


**Figure III-11: SEM images of glass beads (GB) at the different stages of the HRP immobilization protocol: (A): Native GB; (B): GB after activation by 4 M NaOH (C): GB after silanization in APTES/toluene; (D): GB after activation via glutaraldehyde; (E): GB after coupling of HRP.**

The SEM images show beads of spherical shape with relatively smooth surface prior to any modification (**Figure III-11A**). After activation by NaOH and silanization by APTES, rougher surfaces are observed in **Figure III-11 B** and **C** and a clear homogenous layer covered the beads. After the reaction with glutaraldehyde (**Figure III-11D**), the glass beads show contrasted areas evenly distributed all over the beads. Finally, almost no further modifications are induced by protein immobilization except that some contrast is flattened out (**Figure III-11E**).

Since it was expected that HRP should covalently bind onto the glass beads, the release of HRP in the media due to its physical adsorption on the support was studied in buffer after 24-hour storage at 4°C. The enzyme activity was measured in the storage buffer, but no activity has been detected suggesting that HRP is not present in the sample. HRP is thus probably not released upon immobilization, which confirms the covalent bond between the enzyme and the solid carrier.

### III.3.1.3. Enzyme activities in hydro-organic mixtures

Hydrogels synthesis is interesting not only in water, but also in hydro-organic mixtures, especially for molecularly imprinted hydrogels. In order to extend the use of immobilized enzyme system to a wide range of hydrogel synthesis, we evaluated the enzyme activity in aqueous and hydro-organic mixtures of the immobilized biocatalyst. The results are compared to those of the free enzyme.

The enzyme activity of free and immobilized enzymes was studied in different hydro-organic mixture composed of organic solvent such as methanol (MeOH), acetonitrile (ACN) and dimethyl sulfoxide (DMSO) in a 50 mM sodium phosphate buffer pH 7.0 at different ratio (0, 5, 10, 20, 50, 80, 100 % v/v). All experiments throughout this study were repeated at least three times, being subject to less than 10% error for each data point. The enzymes activity profiles shown in **Figure III-12** are quite similar.

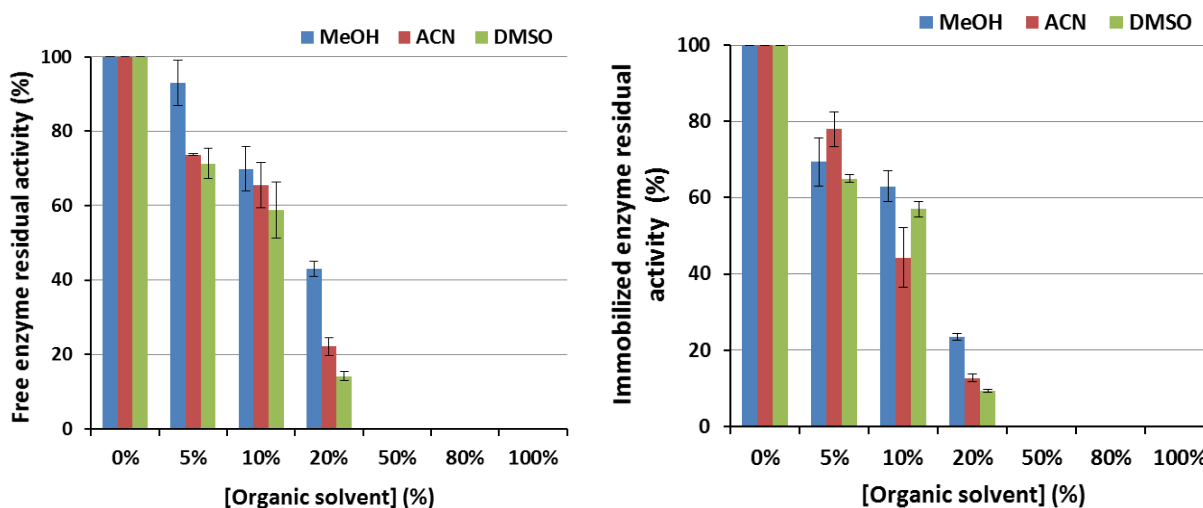


**Figure III-12: Residual enzyme activity of free and immobilized HRP in hydro-organic solvents according to the percentage of organic solvents in 50 mM sodium phosphate buffer (pH 7.0). The remaining activities (%) refers to the percentages of the initial reaction rates obtained for the free and immobilized HRP measured directly upon dissolving the free HRP in buffer, and directly upon immobilization and washing of the glass beads.**

Both free and immobilized enzymes showed a decrease in activity proportional to the increase of the solvent percentage. Regarding the activity data, the enzyme maintains at least 50% of its activity in 10% of all organic solvents. The immobilized enzyme remains as active as the free HRP, but immobilization did not improve the HRP stability in organic solvent. The activities dropped noticeably to lower levels when the concentration of the solvents attain 20%. At higher concentrations of organic solvents, both free and immobilized HRP are completely inactivated. So, the HRP-mediated free radical polymerization can be achieved in water-compatible media up to 10% of organic solvents.

#### III.3.1.4. Storage stability

An enzyme in solution is not stable and its activity will gradually decrease. The effect of immobilization was studied on the storage stability of the enzyme. Free and immobilized HRP were stored in 50 mM sodium phosphate buffer pH 7.0 at 4°C for 70 days. The remaining

activities of the enzymes, represented in **Figure III-13**, were measured using  $H_2O_2$  and ABTS as substrates, by U.V.-visible spectrophotometry.

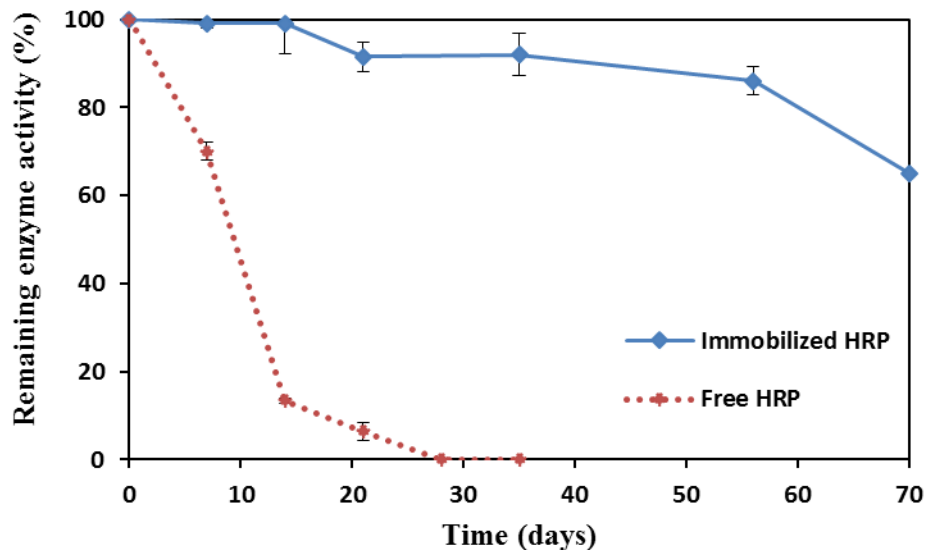


**Figure III-13: Storage stabilities of free and immobilized HRP in 50 mM phosphate buffer pH 7.0. The remaining activity (%) refers to the percentages of the initial reaction rates obtained for the free and immobilized HRP measured directly after dissolving the free HRP in buffer, and directly after immobilization and washing of the glass beads.**

The activity of the free HRP decreases much faster than the immobilized HRP. Free HRP has lost about 85% during the first 14 days and all its activity within 28 days, whereas the immobilized HRP maintained its full activity for the first 14 days and 85% of its initial activity within the following 42 days. Thus, the immobilized HRP exhibits a higher storage stability than that of the free HRP. This confirms similar data already reported in the literature [20, 28].

### III.3.2. HRP-mediated synthesis of hydrogels

Biotechnology provides many opportunities for the synthesis of functional polymeric materials and many enzymatic polymerizations have been reported [33, 34]. Biocatalysts are immobilized by different processes onto hybrid materials or solid carriers in order to improve the enzyme

recovery from the reaction solutions [6]. Immobilization of horseradish peroxidase is a prominent example of biocatalysts immobilization for enzymatic polymerization of phenol considering that phenol is at the same time the enzyme substrate and the monomer [28, 35]. However, immobilized HRP was not used, until now, for the enzyme-mediated initiation of free radical polymerization of hydrogels. In this chapter, we demonstrate for the first time, that immobilized HRP can be a powerful mean for the preparation of chemically cross-linked hydrogels traditionally prepared by toxic photo-initiations of free radical polymerization.

### III.3.2.1. Influence of the experimental conditions on the hydrogels synthesis

The generally accepted mechanism for the preparation of hydrogels by immobilized HRP-mediated free radical polymerization involves three components in the enzymatic system: immobilized HRP as biocatalyst, acetylacetone and hydrogen peroxide as electron donor and acceptor, respectively. Horseradish peroxidase is immobilized on the beads throughout the optimized protocol described in the previous section. The catalytic properties of HRP have been maintained and thus, the enzyme should oxidize acetylacetone in presence of  $H_2O_2$  leading to the formation of water and generation of free radical species. The free radicals produced within this mechanism will initiate the co-polymerization of the functional and the cross-linking monomers.

As hydrogel composition, we selected 4-vinylpyridine and 1.4-bis(acryloyl)piperazine as functional monomer and water-soluble cross-linker, respectively. The reasons behind our choice are that the same monomers were used in **Chapter II** in similar studies with soluble HRP. Moreover, these chemicals will be used for the imprinting of small molecules in **Chapter VI**. Molar quantities of functional and cross-linking monomers are fixed during the whole experiment at a 1:4 ratio (functional monomer: cross-linker) as for MIPs synthesis. Nevertheless, all the syntheses are carried out in 0.1 M sodium phosphate buffer pH 7.0 at room temperature.

It was reported in literature, that changing the concentration of each component of the enzymatic system can have evident consequences on the resulting polymer characteristics [36]. In the previous chapter, we showed that these parameters, as well as the total monomers concentrations greatly affected the particles sizes and the polymerization yields in enzyme-mediated synthesis of hydrogels. As for free enzyme, the interaction among the experimental factors might be

observed in the case of immobilized enzyme mediated synthesis. For this, we wanted to elaborate the underlying interactions within these factors during preparation of hydrogels by this new approach.

In order to lower the number of necessary experiments, we proposed to use a multivariate design. This method is also advantageous to determine the interactions among parameters owing to simultaneous variation of all studied factors. In this context, the second-order plan proposed by Doehlert fits this study particularly well. Within this design, the factors are equally distributed inside centered spheres. Herein, we illustrate the potential of second-order Doehlert's experimental design for the systematic optimization of four important parameters in hydrogels synthesis:

- The amount of HRP-charged beads (2 g to 20 g)
- The total monomers concentration (0 to 10%)
- The molar quantities of acetylacetone (0.017 mmol to 0.136 mmol)
- The molar quantity of hydrogen peroxide (5.5  $\mu$ mol to 44  $\mu$ mol)

As for **Chapter II**, the hydrogels are characterized in terms of 2 responses: the particles size (nm) and the polymerization yield (%). **Table III-3** shows all real values of the different experimental factors studied, as well as the values of the responses in all the runs. 21 experiments (Runs **1- 21**) of hydrogels synthesis were required to draw the experimental design. Run 22 is performed under the same experimental conditions as the first run, in which all the factors values are in the center, in order to study the reproducibility of the results.

An analysis of variance (ANOVA) of the response model is performed in order to estimate the explicative power of the model. The correlation coefficients indicate a good adjustment to the proposed models. R values obtained are higher than 0.88. Consequently, the performing models can be considered satisfactory and significant for such types of second-order design for four factors. The evolution of the two responses according to the relative variation of the four factors is registered and presented in **Table III-4** and **Table III-5** for particles sizes and polymerization yields, respectively.



**Table III-3: Four-parameter Doelhart matrix showing the number of experiments, the real values of the factors and the responses values obtained for 22 runs of hydrogels synthesis by immobilized HRP-mediated initiation of free-radical polymerization.**

N° of runs	Beads (g)	[Monomers] (%)	n(Acac) (mmol)	n(H <sub>2</sub> O <sub>2</sub> ) (mmol)	Response 1:		Response 2:
					Particle size (nm)	PDI	Polymerization Yield (%)
1	11	5	0.0767	0.025	131	0.415	9
2	20	5	0.0767	0.025	105	0.504	12.5
3	15.5	9.33	0.0767	0.025	240.7	0.258	17
4	6.5	9.33	0.0767	0.025	226.2	0.563	10
5	2	5	0.0767	0.025	65	0.272	4
6	6.5	0.67	0.0767	0.025	91.28	0.652	2.5
7	15.5	0.67	0.0767	0.025	108.6	0.789	5
8	15.5	6.445	0.125	0.025	1471	0.276	44
9	6.5	6.445	0.125	0.025	1427	0.452	26
10	11	2.115	0.125	0.025	864.3	0.784	10
11	15.5	3.555	0.0283	0.025	78	0.385	3
12	6.5	3.555	0.0283	0.025	59	0.521	3.5
13	11	7.885	0.0283	0.025	116	0.253	5
14	15.5	6.445	0.0887	0.04	989	0.159	12
15	6.5	6.445	0.0887	0.04	814	0.264	10
16	11	2.115	0.0887	0.04	501.7	0.461	10
17	11	5	0.0404	0.04	324	0.209	4.5
18	15.5	3.555	0.0646	0.01	163.6	0.451	5.5
19	6.5	3.555	0.0646	0.01	134.5	0.783	4
20	11	7.885	0.0646	0.01	235.5	0.263	5
21	11	5	0.113	0.01	531.2	0.381	6
22	11	5	0.0767	0.025	179.2	0.299	8.5

**Polymerization yield**

The analysis of the factors probabilities shows that only X2 and X3 have an impact on the polymerization yield of the synthesized hydrogel, as shown in **Table III-4**. The increase in the yield is, thus, mostly achieved by the increase of initial concentration of acetylacetone and then by the increase of the total monomer concentration to a lesser extent.

**Table III-4: Sorted parameter estimates of the polymerization yield (%), where X1= amount of glass beads, X2= [Monomers], X3= amount of acetylacetone, X4= amount of H<sub>2</sub>O<sub>2</sub>**

Term	Estimate	Std Error	t Ratio	t Ratio	Prob> t
X3	12.088803	2.470163	4.89		0.0018
X2	6.6108545	2.468733	2.68		0.0316
X2*X3	16.627609	7.130134	2.33		0.0525
X1	4.75	2.468661	1.92		0.0957
X3*X3	9.8802303	5.291523	1.87		0.1041
X1*X3	10.415605	7.13157	1.46		0.1875
X3*X4	9.0982905	7.406456	1.23		0.2590
X4	2.5263556	2.467317	1.02		0.3399
X4*X4	-4.469005	5.083736	-0.88		0.4085
X2*X4	-3.558363	7.401694	-0.48		0.6454
X1*X4	-3.319405	7.402426	-0.45		0.6674
X1*X2	2.5981524	6.374242	0.41		0.6957
X1*X1	-0.5	5.520093	-0.09		0.9304
X2*X2	-1.42e-14	5.520417	-0.00		1.0000

The normalized model, without the non-significant values is represented by the equation 4 below:

$$\text{Polymerization Yield (\%)} = 8.75 + 12.1 \times n(\text{Acac}) + 6.6 \times [\text{Monomers}]$$

(Eq.4)

The evolution of the polymerization yield as a function of the relative Acac amount and the total monomers concentration is visualized by the response surface in the following **Figure III-14**.

Analysis of the response surfaces shows that the polymerization yield increases significantly with the total monomers concentration as well as Acac amount.

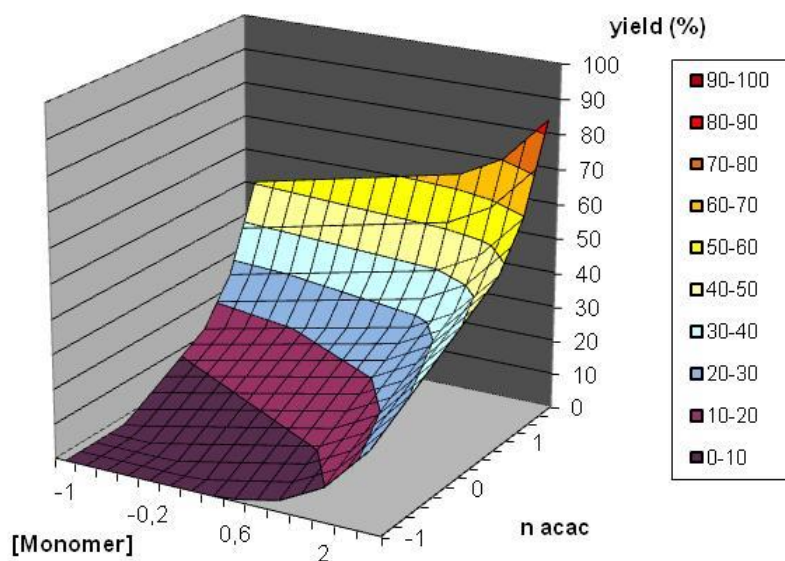


**Figure III-14: 3D representation of response surfaces for the polymerization yield according to total monomers (%) concentrations and the Acac amount (mmol).**

Experimentally, the radicals formed by HRP catalysis increase with the acetylacetone amount resulting in an increase of the number of grafted polymer chains. The effect of total monomer concentration on the polymerization yield has also been observed for the hydrogel synthesis via free HRP catalysis. Moreover, the interaction between these two factors, representing the molar ratio of  $[Acac]/[Monomers]$  shows a probability very near to the significance threshold.

For the hydrogen peroxide amount, hydrogels was always formed even with a high  $H_2O_2$  concentration compared to the amount of the immobilized enzyme. Immobilized HRP was not inactivated by the excess of hydrogen peroxide within the range of tested concentration.

### Particles size

The same study was done for the factors influencing on the particles size. **Table III-5** shows the sorted parameter estimates with their probabilities for every factor or their combinations.

**Table III-5: Sorted parameter estimates of the particles size (nm), where X1= amount of glass beads, X2= [Monomers], X3=amount of acetylacetone, X4=amount of H<sub>2</sub>O<sub>2</sub>**

Term	Estimate	Std Error	t Ratio	t Ratio	Prob> t
X3	671.08439	59.56908	11.27		<.0001
X3*X3	779.77074	127.6074	6.11		0.0005
X4	247.08426	59.50044	4.15		0.0043
X2	175.40185	59.53459	2.95		0.0215
X4*X4	340.57413	122.5965	2.78		0.0274
X3*X4	480.58884	178.6099	2.69		0.0311
X2*X3	418.60431	171.9463	2.43		0.0451
X2*X4	160.48317	178.4951	0.90		0.3985
X1	37.892	59.53284	0.64		0.5447
X1*X1	-70.1	133.1195	-0.53		0.6147
X1*X4	88.720489	178.5128	0.50		0.6344
X2*X2	38.828945	133.1273	0.29		0.7790
X1*X3	15.895273	171.981	0.09		0.9290
X1*X2	-1.628176	153.7176	-0.01		0.9918

We can observe that the acetylacetone amount is the most important factor that affects the particles sizes. The hydrogen peroxide amount as well as the total monomer concentration have also an impact of the size. Interactions among this factor affect as well the particles size. We can summarize the model in the following equation 5:

$$\begin{aligned}
 \text{Particle size} = & 155 + 671 \times n(\text{Acac}) + 779.8 \times n(\text{Acac})^2 + 247.1 \times n(\text{H}_2\text{O}_2) + 175.4 \\
 & \times [\text{Monomer}] + 340.6 \times n(\text{H}_2\text{O}_2)^2 + 480.6 \times n(\text{Acac}) \times n(\text{H}_2\text{O}_2) + 418.6 \\
 & \times [\text{Monomers}] \times n(\text{Acac})
 \end{aligned}$$

(Eq.5)

Particle size evolution is illustrated in **Figure III-15** by the response surfaces as a function of different parameters.

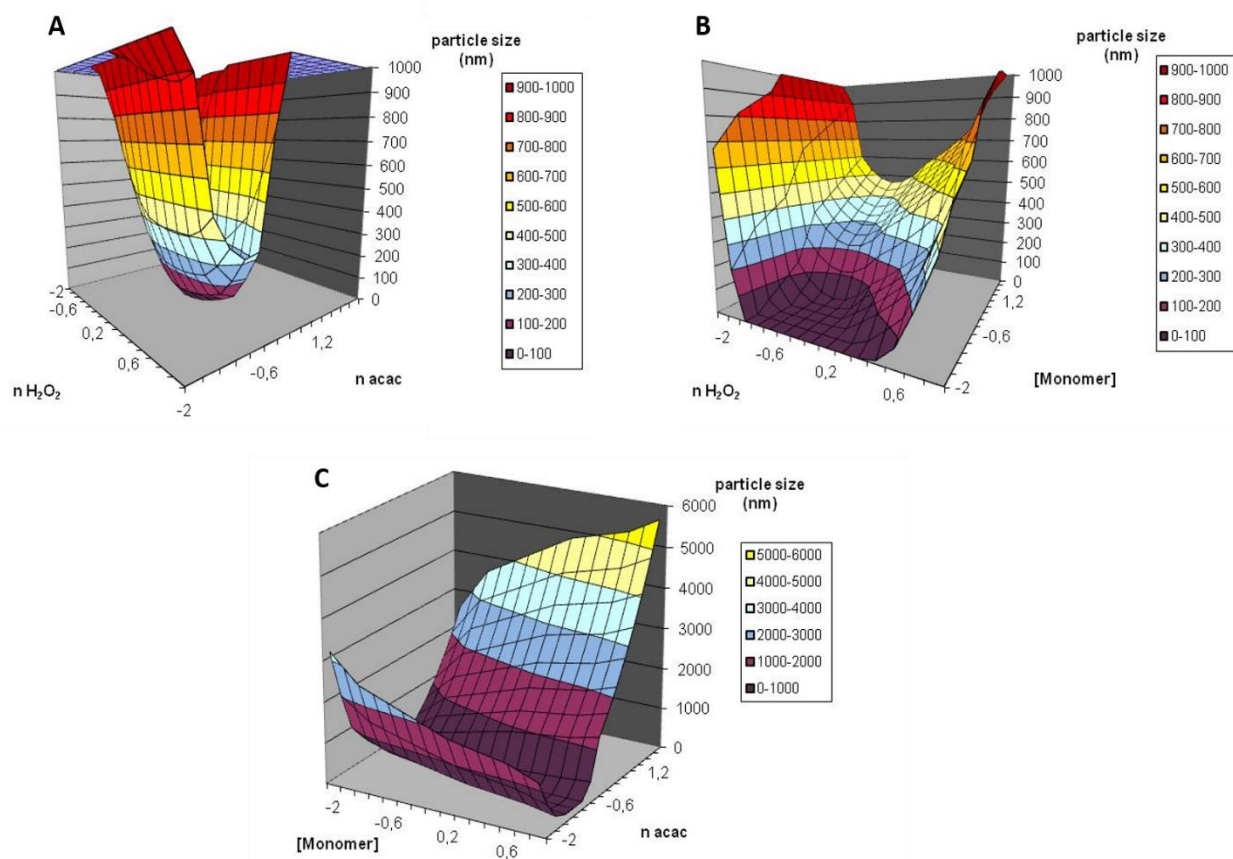


**Figure III-15: 3D representation of response surfaces for the particles size according to different parameters: (A)  $\text{H}_2\text{O}_2$  and Acac; (B)  $\text{H}_2\text{O}_2$  and  $[\text{Monomers}]$ ; (C)  $[\text{Monomers}]$  and Acac.**

As shown previously, particles size increases significantly with the Acac amount and the total monomer concentration. Thus, a lower Acac concentration can be compensated by an increase in total monomers concentrations. Concerning the relative hydrogen peroxide amount, a tendency is also observed. The highest sizes are obtained around the center. Smaller particles are obtained at the extrema of this parameter.

As conclusion, the influence on the particles size involves at least four experimental factors as well as their interactions. These four factors are related and their interaction greatly affects also the initiation rate and so the polymerization kinetics. Indeed, any change, either an increase or a decrease, in the radical generation rate will induce a change in the particle size, which is not necessarily combined with a change in the polymerization yield.

### III.3.2.2. Models validation

After the analysis of the factors impact and the establishment of the two models, they have to be validated by confronting experimental datas to the predictive responses of a selected set value of the factors. Each response function can be used in order to predict the combination of the four factors values leading to the hydrogels synthesis with a predetermined yield and particles size. As this hydrogel means to be applied for molecular imprinting, we search to obtain values of the factors resulting in small-sized hydrogel combined with high polymerization yield. **Figure III-16** shows the prediction profile that study the combination of the four factors in order to obtain optimal values for size and yield response.

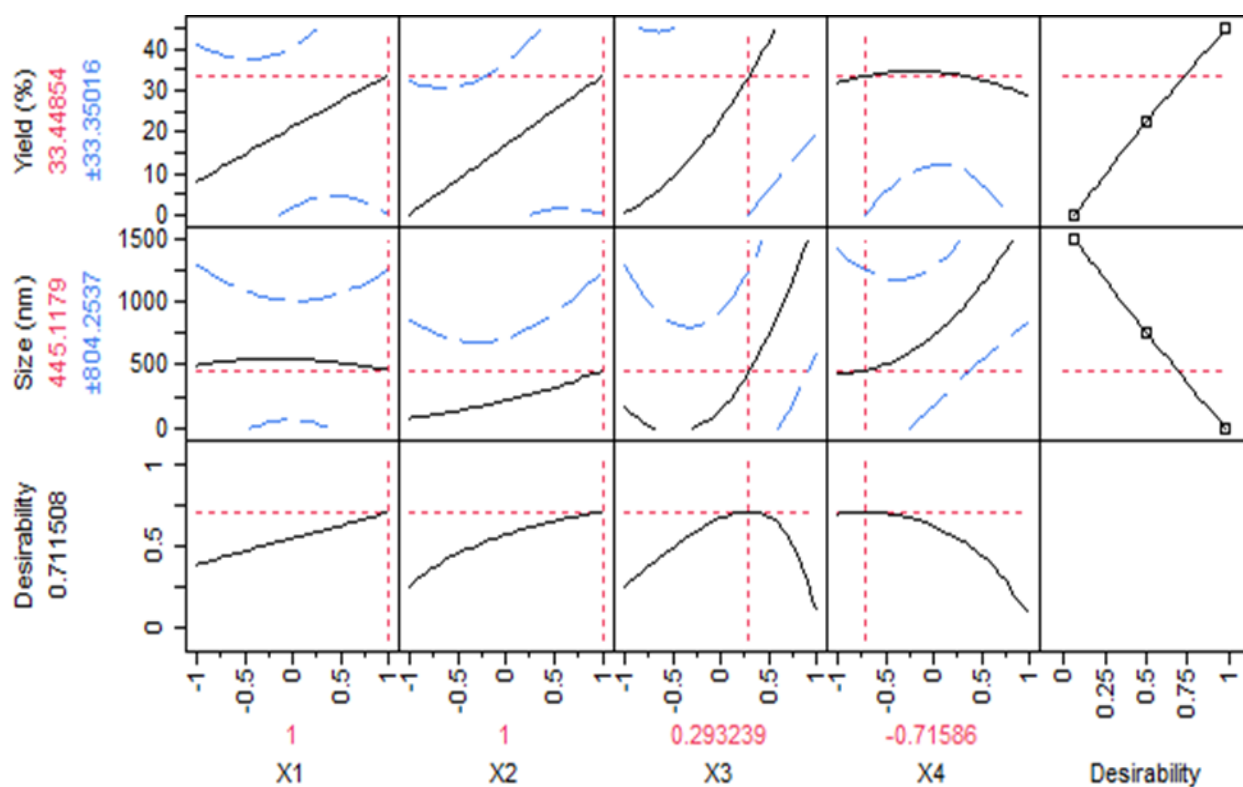


**Figure III-16: Prediction profile of the optimum experimental conditions in order to obtain small-sized hydrogel with high polymerization yield.**

The desirability conditions are determined for every coded value of the four factors. Since particles sizes and polymerization yields are influenced in the same manner and their evolutions are in the same way, it was difficult to obtain the smallest particle size for the highest polymerization yield. Nevertheless, the optimal value for the different parameters has been determined and presented in **Table III-6**. This optimal combination should produce hydrogel with a 445 nm as particles size and 33% as polymerization yield according to the prediction of the two models.

**Table III-6: Coded and real values of the factors in the optimal protocol in the Doelhart experimental design**

Factor1	Beads (g)	Factor 2	[Monomers] (%)	Factor 3	n(Acac) (mmol)	Factor 4	n(H <sub>2</sub> O <sub>2</sub> ) (mmol)
1	20	1	10	0.293239	0.095	-0.71586	0.011

An experiment was carried out for the synthesis of hydrogel in the optimal conditions indicated in the **Table III-6** by immobilized HRP-catalyzed polymerization. The experimental results, presented in **Table III-7**, for size and yield were compared to those that were predicted from the model.

**Table III-7: Comparison of the predicted values in the Doelhart's experimental design and the real experimental ones for the particles sizes (nm) and the polymerization yield (%) in HRP-mediated synthesis of hydrogels**

	Particles size	Polymerization yield
<b>Predicted values</b>	445 nm	33%
<b>Experimental values</b>	410 nm	23%

The particles size obtained experimentally by immobilized HRP-mediated polymerization is close to what was predicted. **Figure III-17** shows the results obtained by DLS measurements.

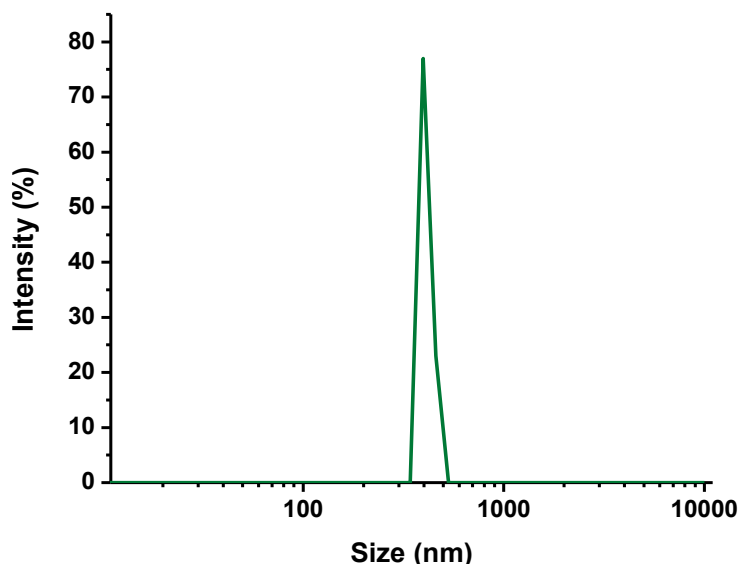


**Figure III-17: Particles size of the poly(4-VP/PDA) hydrogel synthesized by the optimal synthesis protocol predicted by the desirability function.**

However, for the polymerization yield, the real value was somewhat lower than the predicted value, although it is still considered relatively high. The difference might be due to the difference in the immobilized HRP behavior among the different batches of beads, to the small total volume of the solution (1.2 ml) compared to the large amount of beads (20 g) and to the probably incomplete recovery of polymer.

### **III.3.2.3. Emphasis of the enzyme absence within the hydrogel matrix**

We tended, for the first time, in this work to develop any new approach for the preparation of hydrogels clean from any radical source. Once the hydrogels are synthesized in a wide range of experimental conditions, it was crucial to verify that the resulting cross-linked polymers did not entrap any enzyme within the polymer matrix.

For this study, SDS-PAGE electrophoresis was performed under reducing conditions. The gel is represented in **Figure III-18**.



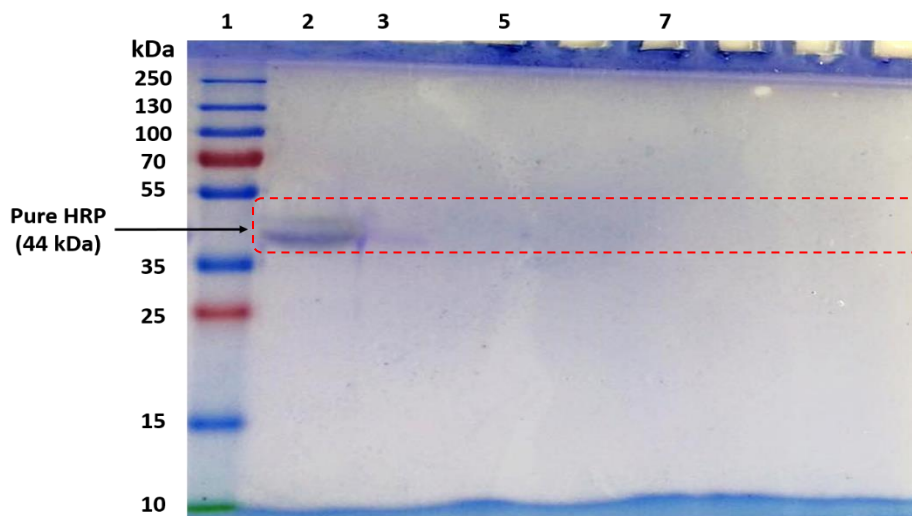


**Figure III-18: Sodium dodecyl sulfate gel electrophoresis (SDS-PAGE) under reducing conditions of hydrogels. Lane 1: molecular weight markers (10000-250000 Da), Lane 2: commercial pure HRP (2  $\mu$ g), Lane 3: commercial pure HRP (10 ng), Lane 5: Hydrogel solution (5 mg), Lane 7: Hydrogel solution (10 mg)**

The electrophoretogram shows two bands within the gel, in addition to the bands of the molecular weight markers. These two bands (lane 2 and lane 3) represent to the pure commercial enzyme with two different concentrations. The first band is dark and appears well since the enzyme amount is relatively high (2  $\mu$ g), whereas the band in lane 3 is much lighter due to the low HRP amount (10 ng), but still clearly visible. The absence of any band in Lanes 5 and 7 verifies the absence of any enzyme in the polymer solution. As the sensibility of Coomassie Brilliant Blue staining is 5 ng, the absence of any band in lane 5 and 7 indicates that there is less than 0.5 ng of HRP per mg of particles.

In term of sensibility, these results are significant and allow verifying that the hydrogels are free from HRP.

#### **III.3.2.4. Comparison between the free and immobilized HRP-mediated syntheses of hydrogels**

In an experimental condition different from what was done above, hydrogels were synthesized in water with high acetylacetone and hydrogen peroxide amounts, by both free and immobilized

HRP-initiated free radical polymerization. Same polymer formulation is used for both hydrogels, as well as the amount of oxidant and reducing species in the ternary enzymatic system. HRP catalytic activity was also kept constant. The only difference was the enzyme state, either free or immobilized. The **Table III-8** summarizes the experimental conditions as well as particles sizes and yields of the hydrogels obtained by the two protein states.

**Table III-8: Experimental conditions and polymer characteristics for the hydrogels synthesized by free and immobilized HRP-initiated polymerization via an enzymatic catalytic activity of  $3 \cdot 10^{-6}$  mol/min in the polymerization medium.**

Enzyme state	[Monomers] (mM)	[Monomers] (%)	n(Acac) (mmol)	n(H <sub>2</sub> O <sub>2</sub> ) (mmol)	Particle size (nm)	Yield (mg)
Immobilized HRP	2.9	10	0.035	0.022	60	7
Free HRP	2.9	10	0.035	0.022	45	5

Interestingly, for the same experimental conditions, HRP-initiated radical polymerization led to similar particles size and yield whether the enzyme is immobilized or not. For the particle sizes, the polydispersity index was 0.532 and 0.36 for the particles prepared with immobilized and free HRP, respectively. Thus, immobilization of HRP has no major drawback with respect to polymer synthesis. It has, however, advantages such as easy separation of the biocatalyst from the final product and its reuse in other syntheses.

In a general comparison between free and immobilized enzyme's behaviors, results that were obtained in **Chapters II** and **III** show that variation in experimental parameters can lead to similar effect on particles sizes and yields. For instance, the increase in the total monomer concentration leads in both cases to an increase in particles sizes and yields. Similar interpretation can be observed with the variation of acetylacetone amount, which plays a major role in hydrogels synthesis. However, an increase in the free HRP concentration induces also to the increase in both responses, which is not necessarily the same with immobilized HRP. The effect of H<sub>2</sub>O<sub>2</sub> concentration seems also not completely similar for the free and the immobilized HRP.

### **III.4. Conclusion**

In this chapter, we developed a standardized protocol for covalent immobilization of HRP on solid carrier and we succeeded in applying this enzymatic system for the development of a versatile approach in hydrogels synthesis by green chemistry.

Glass beads are used as carrier for the enzyme immobilization. The HRP immobilization protocol has been optimized in terms of specific activity of HRP-charged beads, immobilized enzyme residual activity and HRP immobilization load to produce efficient biocatalyst for enzymatic polymerization.

The immobilization procedure comprises 4 steps: (1) the glass beads activation in NaOH 4M solution for 2 hours, (2) the silanization in APTES/toluene (2% v/v) providing an amino groups density of 32  $\mu\text{mol/g}$  on the beads surface, (3) the linker coupling using glutaraldehyde, (4) the protein grafting by incubating in 2 mg/ml HRP solution. With this procedure, up to 1mg of HRP could be immobilized on 1g of solid support with 2 % as residual activity, in accordance with the literature. Interestingly, no protein release has been observed in the storage media and higher storage stability has been obtained with immobilized HRP than the free one.

The application of the immobilized HRP for the nanoparticles synthesis was investigated. The immobilized HRP was used to catalyze the oxidation of acetylacetone (Acac) in the presence of hydrogen peroxide. The radical species are potential initiators of the free radical polymerization for hydrogel synthesis. A Doehlert's experimental design was used to study the effect of different parameters and their interactions on the particles sizes and the polymerization yields of the hydrogels. Our study was focused on the amount of HRP-charged beads, the total monomer concentrations and the total amounts of acetylacetone and/or hydrogen peroxide, which can affect the hydrogel characteristics. It appeared as a powerful tool not only to study the interaction of these experimental conditions, but also to determine the best formulation for the hydrogel synthesis in order to obtain particles with a targeted size combined with high yield of polymerization. Indeed, a good correlation between the model and the experiment has been

observed and hydrogels prepared by the corresponding enzymatic system are free from any source of radicals. This fact can largely increase the application of hydrogels in domains where biocompatibility is important.

Finally, we believe that the developed HRP-catalyzed system is a versatile approach for biochemical synthesis of hydrogels, and it can be extended for the preparation of other hydrogels, based on a wide range of functional and cross-linking monomers. Moreover, it can be applied to prepare molecularly imprinted nanoparticles. This perspective will be developed in **Chapter IV**.

## References

- [1] A. K. Chandel, R. Rudravaram, L. V. Rao, P. Ravindra, and M. L. Narasu, "Industrial enzymes in bioindustrial sector development: An Indian perspective," *J. Commer. Biotechnol.*, vol. 13, no. 4, pp. 283–291, 2007.
- [2] J.-M. Choi, S.-S. Han, and H.-S. Kim, "Industrial applications of enzyme biocatalysis: Current status and future aspects," *Biotechnol. Adv.*, 2015.
- [3] N. An, C. H. Zhou, X. Y. Zhuang, D. S. Tong, and W. H. Yu, "Immobilization of enzymes on clay minerals for biocatalysts and biosensors," *Appl. Clay Sci.*, vol. 114, pp. 283–296, 2015.
- [4] Y. Huang, W. Wang, Z. Li, X. Qin, L. Bu, Z. Tang, Y. Fu, M. Ma, Q. Xie, S. Yao, and J. Hu, "Horseradish peroxidase-catalyzed synthesis of poly(thiophene-3-boronic acid) biocomposites for mono-/bi-enzyme immobilization and amperometric biosensing," *Biosens. Bioelectron.*, vol. 44, no. 1, pp. 41–47, 2013.
- [5] C. C. Akoh, S.-W. Chang, G.-C. Lee, and J.-F. Shaw, "Biocatalysis for the Production of Industrial Products and Functional Foods from Rice and Other Agricultural Produce," *J. Agric. Food Chem.*, vol. 56, no. 22, pp. 10445–10451, 2008.
- [6] N. Miletić, A. Nastasović, and K. Loos, "Immobilization of biocatalysts for enzymatic polymerizations: Possibilities, advantages, applications," *Bioresour. Technol.*, vol. 115, pp. 126–135, 2012.
- [7] M. Arroyo, J. M. Sánchez-Montero, and J. V. Sinisterra, "Thermal stabilization of immobilized lipase B from *Candida antarctica* on different supports: Effect of water activity on enzymatic activity in organic media," *Enzyme Microb. Technol.*, vol. 24, no. 1–2, pp. 3–12, 1999.
- [8] N. Chauhan, J. Narang, and C. S. Pundir, "Covalent Immobilization of lipase, glycerol kinase, glycerol-3-phosphate oxidase & horseradish peroxidase onto plasticized polyvinyl chloride (PVC) strip & its application in serum triglyceride determination," *Indian J Med Res*, vol. 139, pp. 603–609, 2014.
- [9] M. V. Kahraman, G. Bayramoğlu, N. Kayaman-Apohan, and A. Güngör, "α-Amylase immobilization on functionalized glass beads by covalent attachment," *Food Chem.*, vol. 104, no. 4, pp. 1385–1392, 2007.
- [10] A. Kunamneni, F. J. Plou, A. Ballesteros, and M. Alcalde, "Laccases and their applications: a patent review," *Recent Pat. Biotechnol.*, vol. 2, no. 1, pp. 10–24, 2008.
- [11] F. Hollmann, Y. Gumulya, C. Tölle, A. Liese, and O. Thum, "Evaluation of the laccase from *Myceliophthora thermophila* as industrial biocatalyst for polymerization reactions," *Macromolecules*, vol. 41, no. 22, pp. 8520–8524, 2008.
- [12] W. Liu, W. C. Wang, H. S. Li, and X. Zhou, "Immobilization of horseradish peroxidase on silane-modified ceramics and their properties: potential for oily wastewater treatment," *Water Sci. Technol.*, vol. 63.8, pp. 1621–1628, 2011.
- [13] S. Dalal and M. N. Gupta, "Treatment of phenolic wastewater by horseradish peroxidase immobilized by bioaffinity layering," *Chemosphere*, vol. 67, no. 4, pp. 741–747, 2007.
- [14] T. Marchis, G. Cerrato, G. Magnacca, V. Crocellà, and E. Laurenti, "Immobilization of soybean peroxidase on aminopropyl glass beads: Structural and kinetic studies," *Biochem. Eng. J.*, vol. 67, pp. 28–34, 2012.
- [15] M. Hamid and Khalil-ur-Rehman, "Potential applications of peroxidases," *Food Chem.*, vol. 115, no. 4, pp. 1177–1186, 2009.
- [16] N. C. Veitch, "Horseradish peroxidase: A modern view of a classic enzyme," *Phytochemistry*, vol. 65, no. 3, pp. 249–259, 2004.

- [17] N. Aissaoui, L. Bergaoui, S. Boujday, J.-F. Lambert, C. Méthivier, and J. Landoulsi, "Enzyme immobilization on silane-modified surface through short linkers: fate of interfacial phases and impact on catalytic activity.," *Langmuir*, vol. 30, no. 14, pp. 4066–77, 2014.
- [18] S. Ambrosini, S. Beyazit, K. Haupt, and B. Tse Sum Bui, "Solid-phase synthesis of molecularly imprinted nanoparticles for protein recognition.," *Chem. Commun. (Camb)*, vol. 49, no. 60, pp. 6746–8, 2013.
- [19] M. Tascan and K. Gaffney, "Effect of Glass-Beads on Sound Insulation Properties of Nonwoven Fabrics," *J. Eng. Fiber. Fabr.*, vol. 7, no. 1, pp. 101–105, 2012.
- [20] J. L. Gómez, a. Bódalo, E. Gómez, J. Bastida, a. M. Hidalgo, and M. Gómez, "Immobilization of peroxidases on glass beads: An improved alternative for phenol removal," *Enzyme Microb. Technol.*, vol. 39, no. 5, pp. 1016–1022, 2006.
- [21] A. Poma, A. Guerreiro, M. J. Whitcombe, E. V Piletska, A. P. F. Turner, and S. a Piletsky, "Solid-Phase Synthesis of Molecularly Imprinted Polymer Nanoparticles with a Reusable Template –‘ Plastic Antibodies ,’" *Adv. Funct. Mater.*, pp. 2821–2827, 2013.
- [22] S. G. Beads, "Comparison of Some Properties of Immobilized and Soluble Forms of Fungal Peroxidase," *Biotechnol. Bioeng.*, vol. XXIII, pp. 2161–2165, 1981.
- [23] Q. Chang and H. Tang, "Immobilization of Horseradish Peroxidase on NH<sub>2</sub>-Modified Magnetic Fe<sub>3</sub>O<sub>4</sub>/SiO<sub>2</sub> Particles and Its Application in Removal of 2,4-Dichlorophenol," *Molecules*, vol. 19, no. 10, pp. 15768–15782, 2014.
- [24] Y. C. Lai and S. C. Lin, "Application of immobilized horseradish peroxidase for the removal of p-chlorophenol from aqueous solution," *Process Biochem.*, vol. 40, no. 3–4, pp. 1167–1174, 2005.
- [25] M. Persson, D. Costes, E. Wehtje, and P. Adlercreutz, "Effects of solvent, water activity and temperature on lipase and hydroxynitrile lyase enantioselectivity," *Enzyme Microb. Technol.*, vol. 30, no. 7, pp. 916–923, 2002.
- [26] L. Ma, M. Persson, and P. Adlercreutz, "Water activity dependence of lipase catalysis in organic media explains successful transesterification reactions," *Enzyme Microb. Technol.*, vol. 31, no. 7, pp. 1024–1029, 2002.
- [27] E. Wehtje, D. Costes, and P. Adlercreutz, "Enantioselectivity of lipases: Effects of water activity," *J. Mol. Catal. - B Enzym.*, vol. 3, no. 5, pp. 221–230, 1997.
- [28] G. Bayramoğlu and M. Y. Arica, "Enzymatic removal of phenol and p-chlorophenol in enzyme reactor: Horseradish peroxidase immobilized on magnetic beads," *J. Hazard. Mater.*, vol. 156, no. 1–3, pp. 148–155, 2008.
- [29] L. H. Chen, Y. S. Choi, J. W. Park, J. Kwon, R. S. Wang, T. Lee, S. H. Ryu, and J. W. Park, "Effect of linker for immobilization of glutathione on BSA-assembled controlled pore glass beads," *Bull. Korean Chem. Soc.*, vol. 25, no. 9, pp. 1366–1370, 2004.
- [30] Ana-Valvanuz Linares, "Hierarchically structured molecularly imprinted nanomaterials as recognition elements in biochips," 2010.
- [31] S. a. Mohamed, A. a. Darwish, and R. M. El-Shishtawy, "Immobilization of horseradish peroxidase on activated wool," *Process Biochem.*, vol. 48, no. 4, pp. 649–655, 2013.
- [32] K. Tatsumi and S. Wada, "Removal of Chlorophenols from Wastewater," *Biotechnology*, vol. 51, pp. 126–130, 1996.
- [33] S. Kobayashi and A. Makino, "Enzymatic polymer synthesis: an opportunity for green polymer chemistry," *Chem. Rev.*, vol. 109, no. 11, pp. 5288–5353, 2009.
- [34] F. Hollmann and I. W. C. E. Arends, "Enzyme initiated radical polymerizations," *Polymers (Basel)*, vol. 4, no. 1, pp. 759–793, 2012.
- [35] H. J. Kim, "Removal of phenol using horseradish peroxidase immobilized in the nano-scale porous structural material," vol. 1, pp. 105–108, 2011.
- [36] A. Durand, T. Lalot, M. Brigodiot, and E. Maréchal, "Enzyme-mediated radical initiation of acrylamide polymerization: Main characteristics of molecular weight control," *Polymer (Guildf)*, vol. 42, no. 13, pp. 5515–5521, 2001.

## *Chapter IV*

*Enzyme-mediated synthesis of molecularly imprinted hydrogels*

*Results and discussion*

## IV.1. Introduction

Molecularly imprinted polymers (MIPs), also referred to as plastic antibodies, are synthetic polymers that are capable of binding specifically a target molecule [1]. The binding sites are complementary to the target by their size, shape, and chemical functionalities [2, 3]. This is achieved by a moulding process at the molecular level during polymerization. A complex is formed between a template (the target or a derivative thereof) and appropriate functional monomers, which is then co-polymerized with a cross-linker. After the subsequent removal of the template, nano-sized cavities are revealed in the polymer [4, 5]. Due to their chemical and thermal stabilities, MIPs have been widely applied in several areas [6, 7], such as chromatography and solid-phase extraction [9-11], immunoassays [8, 9], optical and chemical sensing [5, 10, 11], as well as catalysis [12, 13]. Recently, the interaction of MIPs with biological systems is getting attention, and the application of MIPs in drug delivery and medical treatment is being studied [14-17].

To generate these polymeric materials, free-radical polymerization is the most commonly used method for its simplicity and universality. It is normally triggered by the decomposition of a chemical initiator that is controlled by different ways, such as light, heat, or electrochemical means, depending on the chemical nature of the initiator [18]. Recently, controlled/living radical polymerization such as atom transfer radical polymerization (ATRP) [19] or reversible addition-fragmentation Chain transfer (RAFT) [20] has been also applied to MIP synthesis allowing an improvement of their molecular recognition properties, and resulting in an higher homogenous polymeric network and binding sites distribution [1]. However, the use of these free-radical polymerization reagents leads to toxic final compounds. This sometimes limits the use of these materials, in particular in biomedical, pharmaceutical and environmental applications [6, 21, 22].

In order to overcome this drawback and develop more biocompatible MIP, we propose an enzyme-mediated synthesis of molecularly imprinted nanoparticles. An enzyme, horseradish peroxidase (HRP) is used to catalyze the generation of free radicals using a substrate ( $H_2O_2$ ) and a mediator (acetylacetone, Acac) of low toxicity. Synthesis of polymers by enzymatic



polymerization have been already described in literature [23]. Indeed, HRP predominates for the catalysis of radical polymerization [24].

We used the principle of enzymatic initiation for a novel strategy to prepare MIPs in aqueous media. A ternary enzymatic system is used and includes, other than HRP, hydrogen peroxide and acetylacetone as oxidant and reducing species, respectively. The classical cycle of HRP depends on the oxidation of the enzyme active site in presence of  $H_2O_2$ , and involves the formation of the so-called compounds HRP I and HRP II. It results in the production of acetylacetone radicals that are liable to interact with a wide variety of monomers to start the propagation of the polymer.

In this work, molecularly imprinted polymers are synthesized exclusively in aqueous media for different templates by free radical polymerization using enzyme-mediated initiation. Small molecules with low molecular weight such as 2,4-dichlorophenoxyacetic acid (2,4-D), which is known as toxic herbicide, were imprinted *via* the ternary initiating system. MIPs for pharmaceuticals like salicylic acid (SA) are also prepared. Then, the application of this system is extended to the synthesis of MIP nanogels for proteins such as trypsin.

Despite the great potential of the enzymatic catalysis in polymer chemistry, major drawbacks limit the application of enzymes for industrial production, such as the difficult recovery of the enzymes from the reaction solution and their easy denaturation. A workaround is the immobilization of the enzymes on a solid carrier in order to improve their physical and thermal stability, as well as their recovery and their reusability [25-27]. Horseradish peroxidase immobilization had been investigated in literature earlier, for enzymatic removal of phenols from waters as well as in biosensing [28-33].

In this chapter, we also develop for the first time the free-radical polymerization of molecularly imprinted nanoparticles initiated by the catalysis of an immobilized enzyme. **Figure IV-1** illustrated the basic principle of the HRP immobilization and its application in MIP synthesis. Horseradish peroxidase (HRP) is widely used among other oxidoreductases and other enzyme categories for free radical polymerization [24, 34-38]. It was immobilized on 0.1 mm glass beads (GB) to catalyze the polymerizations of MIPs according to the methods developed in **Chapter**

III. The HRP-immobilized glass beads were applied for the synthesis of a MIP for 2,4-D in aqueous media.

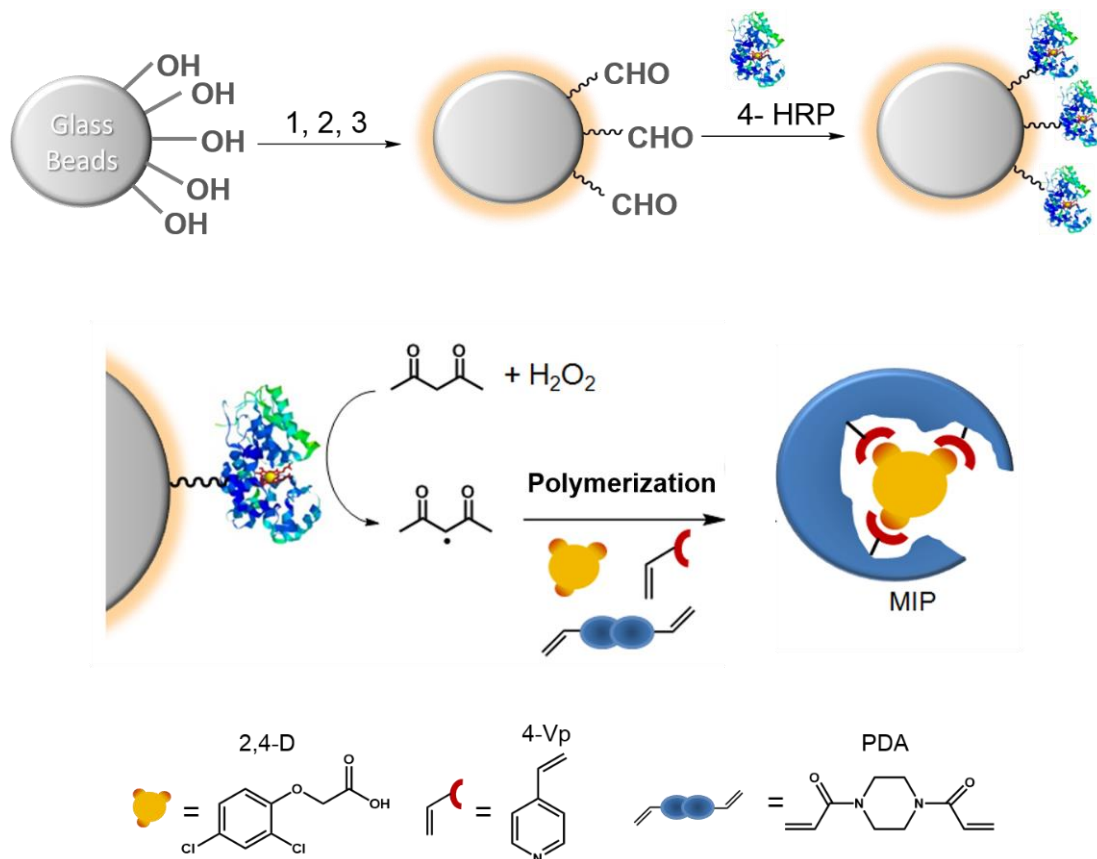


**Figure IV-1: Schematic representation of HRP immobilization and the synthesis of molecularly imprinted nanoparticles by immobilized HRP-initiated free-radical polymerization. (1): preparation of the solid carrier by activation in 4 M NaOH solution at 100°C for 2 hours, (2): silanization step with (3-Aminopropyl)triethoxysilane solution prepared in toluene at 2% (v/v), (3): glass beads activation *via* glutaraldehyde 2.5% (v/v, in 50 mM sodium phosphptate buffer pH 7.0), (4): coupling of HRP on activated glass beads by 2 mg/ml HRP solution (prepared in the same buffer).**

## IV.2. Materials and Methods

### IV.2.1. Materials

All functional monomers (4-VP, NiPAm) and cross-linkers (PDA, EbAAm) used for the imprinting were purchased from Sigma-Aldrich. The chemical structures of all the compounds are illustrated in **Chapter II**. They are all used without any further purification, except for 4-VP, which was vacuum-distilled and stored at -80°C prior to use.

All templates and chemicals, such as 2,4-dichlorophenoxyacetic acid (2,4-D), salicylic acid (SA), phenoxyacetic acid (Ph-AcOH), chlorophenoxyacetic acid (CPOAc) and trypsin from porcine pancreas were from Sigma-Aldrich.

For the imprinting of trypsin, an anchoring monomer, *N*-acryloyol-*p*-aminobenzamidine.HCl (AB) was synthesized according to a protocol developed in our group [22]. 34 g (0.41 mol) of sodium acetate were dissolved in 200 mL of Milli Q water. 2.0 g (9.6 mmole) of 4-aminobenzamidine dihydrochloride was added. The solution was cooled to < 5 °C in an ice bath. 4 mL (49 mmole) of acryloyl chloride was added dropwise in 10 minutes. The reaction was left to proceed for 1 hour. The pH was then adjusted to 4.0 with hydrochloric acid and precipitation was observed. After filtration, the precipitate was redissolved in hot water. Hydrochloric acid was again added this time to pH 1.0, until precipitation was observed. The precipitate was collected by filtration and dried at 50 °C. <sup>1</sup>H NMR (400 MHz, DMSO-d<sub>6</sub>): δ (ppm) = 10.56 (s, 1H), 8.99 (s, 3H), 7.86 (s, 2H), 7.81 (s, 2H), 6.31 (d, 1H), 6.46 (d, 1H), 5.85 (s, 1H).

As initiating systems, chemical initiators such as Vazo<sup>®</sup> 56 and potassium persulfate (KPS) were used. *N,N,N',N'*-tetramethylethylenediamine (TEMED) is used as accelerator for electrochemical initiation. The ternary system including horseradish peroxidase (HRP), acetylacetone (Acac), and hydrogen peroxide (H<sub>2</sub>O<sub>2</sub>) was used for the polymerization and all its reactants were from Sigma-Aldrich. HRP immobilization on 0.1 mm glass beads of was done as described in **Chapter III**.

For 2,4-D MIP binding experiments, radiolabeled 2,4-dichlorophenoxyacetic acid [carboxyl- $^{14}\text{C}$ ]-2,4-D (specific activity 50mCi/mmol, 100 mCi) was obtained from Biotrend Chemicals (Köln, Germany). The radiolabeled compound was dissolved in methanol (200  $\mu\text{l}$ ) so as to constitute a stock solution.

Binding properties of MIPs for trypsin are assessed by activity tests. The enzyme substrate, *N* $\alpha$ -*p*-tosyl-L-arginine-methyl ester hydrochloride (TAME) was from Sigma.

All organic solvents were of analytical grade and purchased from VWR International or Sigma-Aldrich. Buffers were prepared using ultrapure water (18.2 M $\Omega$ /cm $^2$ ), purified using a Milli-Q system (Millipore, Molsheim, France).

## IV.2.2. Synthesis of MIP Hydrogels

### IV.2.2.1. Molecular imprinting of 2,4-dichlorophenoxyacetic acid

Molecularly imprinted micro- and nanoparticles against 2,4-D were synthesized using high dilution polymerization by different biochemical and photochemical initiations.

#### A. *Polymerization using soluble biocatalyst*

##### Free HRP-mediated initiation

In a typical procedure, 2.32 mmol of PDA (cross-linker), 0.58 mmol of 4-VP (functional monomer), 0.145 mmol of 2,4-D (template) were dissolved in 25 ml of ultrapure water (2% as a total monomers concentration). 0.035 mmol of acetylacetone (Acac) corresponding to 0.7 mol-% of the polymerizable double bonds, were added to the mixture with 2 mg of HRP. The 50 ml glass vial sealed with a silicon rubber septum was put in ice and purged with a gentle flow of nitrogen for 10 minutes. Finally, 216  $\mu\text{l}$  of a 0.1 M solution of hydrogen peroxide were added to the mixture. Control Polymers (NIP) were prepared using the same recipe, but without adding the template. Polymerization was carried out at 25°C for 3 days under gentle agitation.

### Photochemical initiation

For UV polymerization, Vazo® 56 is used as photochemical initiator at 1 mol-% of the monomers polymerizable double bonds. The MIPs and NIPs are put under UV irradiation by using a Spectroline UV<sub>312nm</sub> lamp transilluminator for 6 hours. The whole system was covered with a box lined with aluminum foil.

The particles, in both syntheses, were then dialyzed in water for 2 days, lyophilized and then re-washed by incubation in methanol/acetic acid (8:2) (3 times), methanol/acetic acid (9:1) (3 times), methanol (2 times) and acetonitrile (1 time) for 1 hour each time, followed by centrifugation for 30 minutes at 21000 rpm. Then, the particles were dried in vacuum.

### ***B. Immobilized HRP-mediated initiation***

Glass beads of 0.1 mm are activated by incubation in a solution of 4 M NaOH at 100°C for 2 hours. Then, they are washed with water and acetone and dried in an oven at 100°C. For silanization, a solution of  $\gamma$ -APTES (2 %, v/v) is prepared in toluene and added to the activated glass beads. The mixture is incubated overnight at room temperature and the glass beads are washed in toluene, acetone and water, and dried in an oven at 100°C. The silanized beads are reacted with 2.5% (v/v) glutaraldehyde (Sigma) solution in 50 mM phosphate buffer pH 7.0 for 1 hour at 25°C under gentle agitation. After that, the glass beads are intensively washed in the same buffer. 1 gram of activated glass beads are incubated, overnight at 25°C with 2 ml of a standard 2 mg/ml HRP solution prepared in 50 mM phosphate buffer pH 7.0. The glass beads are finally washed and stored at 4°C in the same buffer.

Molecularly imprinted nanoparticles are prepared similarly to those prepared by soluble-HRP catalysis (see above Protocol A). The same polymerization mixtures are used in terms of monomers, solvent, molar quantities of acetylacetone and H<sub>2</sub>O<sub>2</sub>, as well as the ratios of template/monomer/cross-linker. However, the total monomer concentration is 5 % and 10 % instead of 2 %. 10g of glass beads with immobilized HRP and MIP precursors solution are used for each batch. Polymerization is carried out in 20 ml glass tubes on a rotor at 25°C for 4 days.

The polymers are then recovered by pipetting. The glass beads are washed 5 times with 10 ml of distilled water and can then be reused for a new synthesis.

The polymers are dialyzed and washed in the same manner as the ones synthesized with soluble HRP. The washings in organic mixtures are performed in 2 ml polypropylene Eppendorf tubes in a volume of 1.5 ml for each. The 1-hour-washing is followed by a centrifugation at 17500 rpm for 40 minutes for solvent removal.

#### IV.2.2.2. Molecular imprinting of salicylic acid

For the imprinting of salicylic acid (SA), the polymers are prepared by free radical polymerization under high dilution conditions in a glass vial fitted with a septum. 0.29 mmol of 4-vinylpyridine (4-VP) are mixed with 1.45 mmol of 1.4-bis(acryloyl)piperazine (PDA) in 31 ml as a total volume distilled water. 0.0725 mmol of SA, already dissolved in 100  $\mu$ l of ethanol are added to the mixture. Total monomers concentration is 1%. Non-imprinted polymers (NIP) are synthesized, as control, in the same manner of MIPs but without adding the template

For enzyme-mediated initiation, 2 mg of HRP are added together with 0.035 mmol of Acac. The mixture is put in ice and purged with nitrogen for 10 minutes. Finally, 108  $\mu$ l of 103 mM hydrogen peroxide solution are introduced into the mixture. Polymerization is carried out for 3 days at room temperature under gentle agitation.

For photochemical initiation, 7 mg of Vazo® 56 is added to the mixture prior to degassing. Mixtures are polymerized under UV light for 6 hours.

After polymerization, hydrogels are transferred to 50 ml centrifuge tubes and washed in 15 ml of 0.5 M HCl solution containing 14.25 ml of methanol (3 times) and methanol (3 times) for at least one hour at room temperature. The polymers are then dried under vacuum for overnight.

### IV.2.2.3. Trypsin imprinting

PolyNiPAm-based nanogels for trypsin recognition were prepared by free-radical polymerization under high dilution conditions, with a total monomers concentration of 0.5 %. The polymerization was carried out in 50 ml glass vials with screw caps and septum. The mixture was prepared by mixing 2.17 mmol of NiPAm with 0.114 mmol of EbAm (95:5 molar ratio) in 25 mM sodium phosphate buffer pH 7.0. 0.12  $\mu$ mol of trypsin (2.8 mg) was incubated with a stoichiometric amount of the anchoring monomer (AB) in 3 ml of the same buffer during 30 min at 6°C to form the trypsin-AB complex. This complex is then added to the polymerization mixture to yield a total volume of 53 ml (protocol adapted from [39]). For enzymatic initiation, the ternary system is applied as follows: 5.25  $\mu$ l of Acac are added with 3 mg of HRP. After purging with nitrogen for 10 minutes, 32  $\mu$ l of 10 mM hydrogen peroxide solution are finally introduced to the solution by a syringe. The polymerization is allowed to proceed for 3 days at room temperature under a gentle agitation. A control polymer is synthesized by the same procedure, but without adding the target protein.

For the template removal, electro-migration is performed on the MIP particles as described in [40]. After polymerization, the thermoresponsive gels, in their swollen state, are incubated for 15 minutes at 40°C to precipitate. Particles are then recovered by centrifugation at 21000 rpm during 30 minutes at 40°C. The polymers are re-suspended in 15 ml of HEPES buffer (200 mM, pH 7.2). A cylindrical Millipore centrifugal concentrator with a cellulose ultra-filtration membrane (150 kDa MW cut-off), is used on the cathode compartment, and is filled with 15 ml of the particles solution. The membrane is immersed into the anode compartment, which is filled with 100 ml of the same buffer. The whole cell is put in ice. Platinum electrodes are introduced in each compartment and are connected to an electrophoresis power supply. A voltage of 75 V is applied during 3 days to elute trypsin. Due to its positive charge, this protein migrates in the electric field from the cathode to the anode compartment, whereas the MIP particles are retained by the membrane. Finally, the particles are dialyzed against water in order to remove buffer salts. For the sake of comparison, the same washing procedure is applied to NIPs.

### IV.2.3. Polymers characterization

#### IV.2.3.1. Particle size measurements

A Zetasizer Nano (Malvern Instruments Ltd., Worcestershire, UK) system is used for dynamic light scattering measurements. The hydrodynamic diameter of the nanoparticles is determined at 25°C by a laser of 4 mW (He-Ne),  $\lambda=632$  nm, 173°, backscatter. 0.1 mg/l dilutions are prepared in 1.5 ml polypropylene Eppendorf tubes in the solvent of synthesis and the mixture is sonicated for at least 30 minutes until no aggregation can be observed.

#### IV.2.3.2. Polymer morphology

The characterization of the particles morphology is performed by Scanning Electron Microscopy (SEM) on a Quanta feg 250, or Scanning Transmission Electron Microscopy (STEM) on a JEM 2100 F at the Physico-Chemical Analysis Platform at UTC.

#### IV.2.3.3. Binding properties of MIPs

In order to assess the binding properties of the MIPs, different methods were used according to the template that was imprinted. Radioligand binding assays for 2,4-D were performed as well as spectrophotometric methods including fluorescence for SA and enzymatic activity measurements for trypsin.

For binding experiments, the percentage of the template bound to the polymer is determined for each polymer concentration by the following equation:

$$\text{Amount of bound template (\%)} = \frac{\text{total } n(\text{template}) - \text{free } n(\text{template})}{\text{total } n(\text{template})} \times 100$$

Where n is the amount of template in mol.

The imprinting factor is also calculated to evaluate the MIP specificity *i.e.* the imprinting effect. It is calculated from the ratio of the template bound to MIP over the one bound to the control:



$$IF = \frac{\% \text{ bound MIP}}{\% \text{ bound NIP}}$$

- 2,4-dichlorophenoxyacetic acid MIP binding assay

For radioligand binding assays, the polymers particles are suspended in 20 mM sodium phosphate buffer pH 7; 0.1% triton X-100, and appropriate volumes are added into the test tubes, followed by the radioligand [<sup>14</sup>C]-2,4-D (0.04 nmol), varying amounts of a solution of a competing ligand if appropriate, and solvent to complete to a total volume of 1 ml. The samples are incubated on a rotor at room temperature for 2 hours. After centrifugation, a 500 µl aliquot of the supernatant is added to 4 ml of scintillation liquid (Ultima Gold, Perkin-Elmer) in scintillation vials. The concentration of the free template is measured by liquid scintillation counter (Beckman LS-6000 IC).

Binding isotherms were recorded as follows: for soluble-HRP mediated synthesis, 0.5 to 7 mg/ml concentrations of MIP and NIP solutions were analyzed, whereas concentrations from 0.1 to 1 mg/ml of polymers were studied for immobilized HRP-catalyzed polymerization. The values of the maximum amount bound at equilibrium ( $Q_{\max}$ ), as well as the polymer concentration yielding half maximum binding ( $K_{50}$ ) were determined by non-linear regression analysis with GraphPad software.

Langmuir binding isotherms were used in order to assess the dissociation constant ( $K_d$ ) as well as the maximum binding capacity ( $B_{\max}$ ). The MIP amount is fixed at the necessary amount for half-maximum binding of [<sup>14</sup>C]-2,4-D. Polymers are incubated with 40 pmol of radioligand and increasing concentrations of the normal (not radio-labeled) 2,4-D, called cold 2,4-D.  $K_d$  is defined as the concentration of the 2,4-D that causes the complexation of half of the polymer binding sites at equilibrium.  $B_{\max}$  is the maximum number of accessible binding sites for 2,4-D within the MIP.

For competitive binding assays, the same amount of polymers as used for Langmuir isotherms is used. The polymer is incubated with 40 pmol of [<sup>14</sup>C]-2,4-D and with increasing concentrations of cold 2,4-D and of two other competitors: phenoxyacetic acid (Ph-AcOH) and chlorophenoxyacetic acid (CPOAc). The competitor concentrations replacing 50% of the

radioligand ( $IC_{50}$ ) were determined from the competition curves by nonlinear regression, and cross-reactivities were calculated by dividing  $IC_{50}$  values for 2,4-D by that obtained for each compound as shown below:

$$\text{cross - reactivity (\%)} = \frac{IC_{50 (2,4-D)}}{IC_{50 (competitor)}} \times 100$$

- Salicylic acid MIP binding assays

Equilibrium binding experiments are carried out using the fluorescence of SA for detection. Fluorescence measurements were carried out on a Cary-Eclipse spectrofluorimeter. The excitation/Emission wavelengths are set to 306/410 nm. All binding tests are done in the dark.

A 4 mM stock solution of SA was first prepared in anhydrous acetonitrile and stored at 4°C. For every binding test, a diluted aliquot of 0.1 mM is freshly prepared in acetonitrile from the stock solution. The polymer stock solutions of 10 mg/ml are prepared either in acetonitrile or acetate buffer 20 mM pH 6.0. Polymer concentrations from 0.1 to 3 mg/ml are prepared in 1.5 ml polypropylene microcentrifuge tubes and 100  $\mu$ l of SA solution is added. The final volume is adjusted to 1 ml with the same solvent. The tubes are incubated overnight at room temperature on the rotor and then centrifuged at 17500 rpm for 30 minutes. The amount of the free SA in the supernatant was quantified by fluorescence measurements. The amount of SA bound to the polymers, can be calculated by subtracting the amount of free analyte from the initial amount of SA added to the mixture (10 nmol).

- Trypsin MIP binding assays

Enzymatic activity measurements were used to quantify trypsin. They were performed by spectrophotometry on a CARY60 UV-Vis spectrophotometer (Agilent Technologies). A 60  $\mu$ M stock solution of trypsin was prepared in 1 mM HCl, 10 mM  $CaCl_2$ . Activity assays are carried out at 25°C with TAME as substrate [39, 40]. The reaction mixture of 1 ml contains 50  $\mu$ l of 10 mM TAME (final concentration: 500  $\mu$ M) in 50 mM Tris-HCl pH 8.0, 10 mM  $CaCl_2$ . The enzymatic reaction is triggered by adding different volumes of trypsin solutions using standard 1

cm path length quartz cuvettes. TAME hydrolysis was monitored by the absorbance change at 247 nm against a reference cuvette. A calibration curve was plotted with various trypsin concentrations ranging from 25 to 120 nM as shown in **Figure IV-2**.

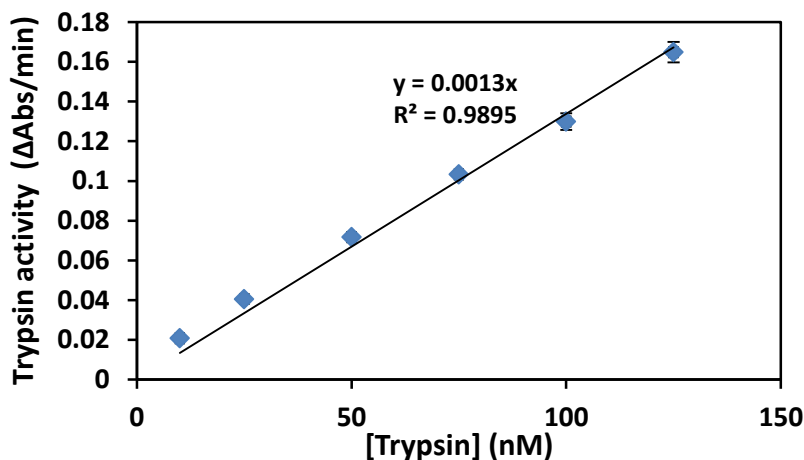


**Figure IV-2: Calibration curve of trypsin between 20 and 120 nM in 50 mM Tris-HCl pH 8.0.**

For equilibrium binding assays, the binding capacity of the trypsin-imprinted nanogels was determined from saturation studies. In 4 ml glass vials, increasing amounts of particles were suspended in 5 mM Tris.HCl buffer pH 8.0, 10 mM CaCl<sub>2</sub>. 100 μl of a trypsin solution (600 nM as a final concentration) was added and the volume adjusted to 1 ml. the samples were incubated at 6°C overnight under gentle agitation. Control incubations of trypsin without polymer were performed in parallel. The vials are incubated at 40°C for 10 minutes prior to centrifugation in order to precipitate the particles. The polymers are then moved to 1.5 ml polypropylene microcentrifuge tubes and separated from the solution by centrifugation at 10000 rpm during 15 min. the remaining trypsin in the supernatant is quantified by activity measurements as described above with TAME as substrate.

### IV.3. Results and discussion

#### IV.3.1. Free HRP-mediated synthesis of MIPs

Molecularly imprinted polymers (MIPs) for different templates, such as small molecules like herbicides (2,4-dichlorophenoxyacetic acid) and pharmaceuticals (salicylic acid), as well as biomacromolecules like trypsin were synthesized. Free radical polymerization of the MIPs was initiated by enzyme-mediated catalysis using the horseradish peroxidase free (not immobilized) in the polymerization solution. The particles were characterized in terms of size and morphology, and their molecular recognition properties of the MIPs were evaluated. The results with enzymatic initiation were compared to other traditional chemical initiation methods.

##### IV.3.1.1. Synthesis of MIP for 2,4-dichlorophenoxyacetic acid

2,4-Dichlorophenoxyacetic acid (2,4-D) an herbicide of the phenoxy acid family. It was used to protect crops, in particular rice. Today it is still authorized for use in private gardens and parks to protect lawns from weeds. The toxicology and human health effects of 2,4-D had been studied extensively and repeatedly since 1946. These studies indicated that 2,4-D has a low-to-moderate toxicity, and chronic toxicity responses (carcinogenicity and teratogenicity) in high doses (25 mg/kg/day) [41]. Due to its toxicity, many attempts have been made to develop detection systems for 2,4-D, for example based on molecular imprinting technology [10, 42, 43].

For the molecular imprinting of the 2,4-D, the MIP formulation was adapted from Haupt *et al.* [43]. The 4-vinylpyridine (4-VP) was used as functional monomer since it forms ionic and hydrophobic/ $\pi$ -stacking interactions with the carboxyl group and the aromatic ring of the template, respectively. Instead of using methanol/water (4:1) as solvent as in the original publication, the polymerization was performed in purely aqueous media. For solubility, we substituted the cross-linker (EGDMA) with a highly water-soluble cross-linker, 1,4-bis(acryloyl)piperazine (PDA). The ratio T: FM: CL was fixed at (1:4:16) in order to maintain

the chemical and physical stability of the MIP. The polymers were prepared in high dilution polymerization and the MIP behaviors were compared to those of photochemically prepared polymers.

#### *IV.3.1.1.1. Effect of the acetylacetone and hydrogen peroxide concentrations on the MIP synthesis*

In **Chapter II**, we noticed that the Acac and hydrogen peroxide concentration greatly affected the enzyme-mediated synthesis of hydrogels, both in terms of particles sizes and polymerization yields. Thus, we studied the influence of these parameters on MIP synthesis, especially on the imprinting effect.

The effect of Acac concentration on the MIP synthesis was examined by preparing different MIPs and their corresponding controls using HRP-initiated free radical polymerization with different acetylacetone concentrations ranging from 0.8 mM to 2.8 mM. After synthesis, all the polymeric materials are characterized in terms of particles size and polymerization yields. **Table IV-1** shows the results of this characterization.

**Table VI-1: Particles sizes and polymerization yields of the MIP/NIP polymers according to different acetylacetone initial concentrations**

	Particles size (nm)		Yield (%)	
	MIP	NIP	MIP	NIP
<b>0.9 mM</b>	289	129	10	4
<b>1.4 mM</b>	180	54	27	20
<b>2.1 mM</b>	296	23	80	24
<b>2.8 mM</b>	287	29	96	29

No significant variation could be detected for the MIP particles sizes, whereas NIP size has slightly decreased with the increase of Acac concentrations. Nevertheless, polymerization yields of both MIPs and NIPs are increased by increasing the Acac initial concentration. It is also noticeable that the MIP yield is always higher than that of the NIP. The lower polymerization yields obtained for the NIP could be explained by the fact that the functional monomer interacts

with the enzyme's active site and inhibits the reaction. In the case of the MIP, the monomer is complexed with the template and therefore less available, thus this negative effect is avoided. Binding properties of the MIPs and NIPs were determined by radioligand binding assays in 20 mM phosphate buffer pH 7.0 using [ $^{14}\text{C}$ ]-2,4-D. The binding isotherms for MIP prepared with different amount of Acac are shown in **Figure IV-3**.  $Q_{\text{max}}$ , the maximum amount of radiolabeled template bound at the equilibrium, and  $K_{50}$ , the amount of polymer needed to attain half maximum binding were obtained from the resulting isotherms (**Table IV-2**).

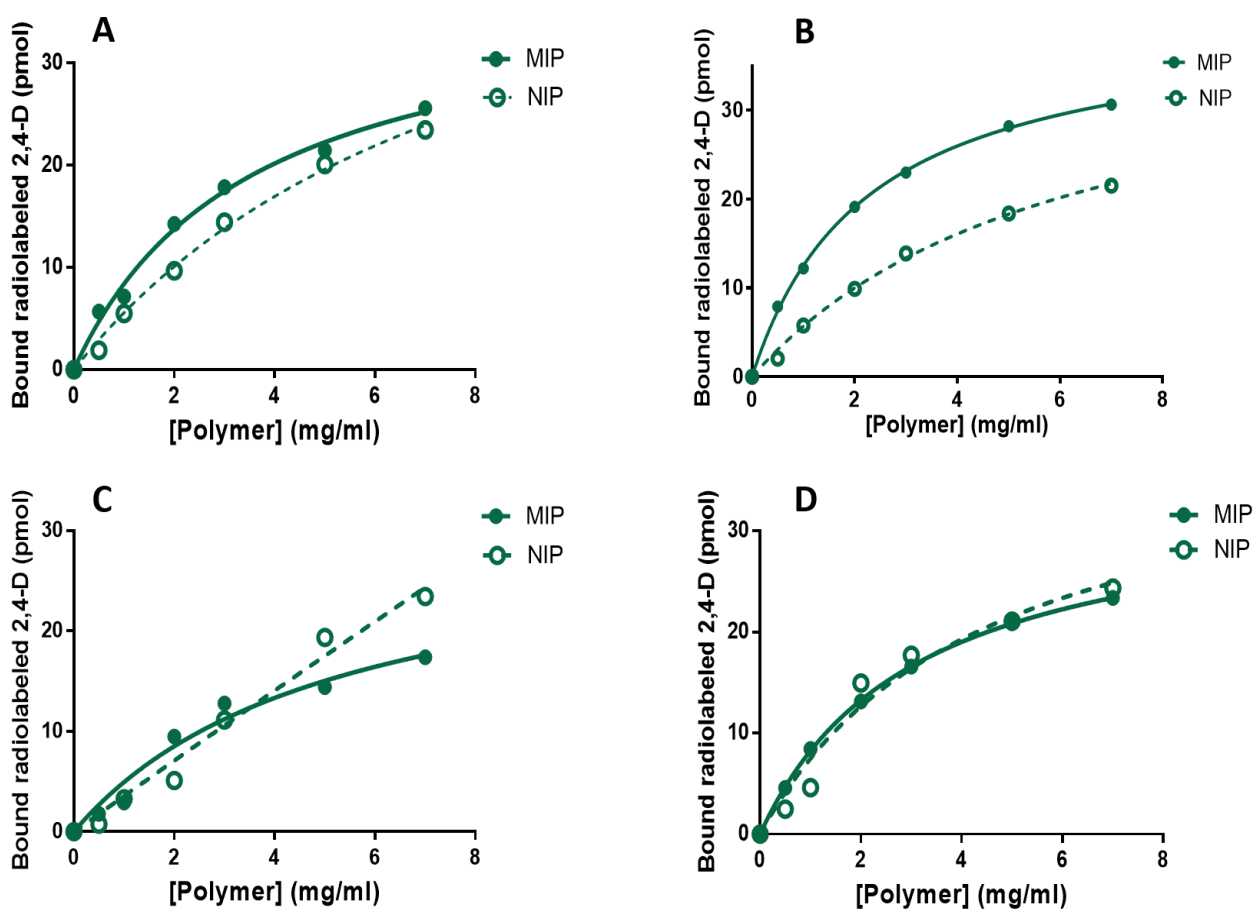


**Figure IV-3:** Effect of the acetylacetone (Acac) initial concentrations on the 2,4-D binding on MIPs and NIP synthesized *via* HRP-catalysis : (A) 0.9 mM; (B) 1.4 mM; (C) 2.1 mM; (D) 2.8 mM. The synthesis was achieved by using  $[\text{HRP}]_0 = 0.08 \text{ g/l}$ , and  $[\text{H}_2\text{O}_2]_0 = 0.88 \text{ mM}$ . The binding tests are carried out by radioactive assays, in 20 mM pH 7.0 sodium phosphate buffer + 0.1% triton X-100 using [ $^{14}\text{C}$ ]-2,4-D (0.04 nmol, 2 nCi).

**Table IV-2:  $Q_{\max}$  and  $K_{50}$  of MIPs synthesized via HRP-catalysis by different acetylacetone (Acac) initial concentrations.**

[Acac] (mM)	$Q_{\max}$ (pmol)	$K_{50}$ (mg/ml)	$IF_{\max}$ (0.5 mg/ml)
0.9	38	3.5	2.8
1.4	40	2.2	3.8
2.1	33	5.2	2.3
2.8	34	3	1.5

MIP nanoparticles prepared with a [Acac] = 1.4 mM showed best binding performance and the highest imprinting factor (IF) value (3.8). No difference in MIP and NIP binding properties was observed for polymers prepared with an Acac initial concentration above 1.4 mM.

To conclude, like all initiators, the Acac initial concentration influences polymer binding properties. This may probably result in the loss of imprinting.

On the other hand, the modification of the acetylacetone initial concentration can change different ratios, such as [Acac]/[Monomer] and [Acac]/[H<sub>2</sub>O<sub>2</sub>], which are particularly important in enzymatic polymerization as shown in **Chapter II**. For this, MIPs and NIPs with different hydrogen peroxide initial concentrations were prepared. 1.76 mM of H<sub>2</sub>O<sub>2</sub> was used for MIP synthesis with 2.8 mM of Acac. This polymer is compared to the previous ones prepared with [Acac] of 1.4 and 2.8 mM. No significant variation was observed in particle sizes. However, the polymerization yield decreased, due to the increase in hydrogen peroxide that might cause the partial inactivation of HRP. **Table IV-3** shows the IF value and the yield for each MIP.

**Table IV-3: Yields and imprinting factors for the MIPs and NIPs synthesized according to different molar ratios of [Acac]/[Monomer] and [Acac]/[H<sub>2</sub>O<sub>2</sub>]**

N°	[Monomer] (mM)	[H <sub>2</sub> O <sub>2</sub> ] (mM)	[Acac] (mM)	[Acac]/[H <sub>2</sub> O <sub>2</sub> ]	[Acac]/[Monomer]	Yield (%)		IF*
						MIP	NIP	
1	116	0.88	1.4	1.59	0.012	27	20	3.8
2	116	0.88	2.8	3.2	0.024	96	29	1.8
3	116	1.76	2.8	1.59	0.024	48	14	1.8

\*: maximal imprinting factor obtained for 0.5 mg/ml of polymer concentration.

As summarized in the **Table IV-3**, an increase in Acac concentrations, which led to a change in both ratios, had resulted in a decrease of the imprinting factor. However, for a fixed Acac concentration, an increase in hydrogen peroxide didn't improve the binding. Therefore,  $[\text{Acac}]/[\text{Monomer}]$  has a direct effect on the MIP binding properties and thus must be fixed to 0.012.

#### IV.3.1.1.2. Effect of the initial HRP concentration

The influence of HRP concentration on the molecular recognition of MIP was also investigated. Several concentrations of horseradish peroxidase were used for the synthesis of MIP from 0.04 g/L to 0.4 g/L, using  $[\text{Acac}]_0 = 1.4$  mM, and  $[\text{H}_2\text{O}_2]_0 = 0.88$  mM. The other experimental conditions were kept constant. **Table IV-4** shows the particle sizes and the polymerization yields of the MIPs.

**Table IV-4: Particles sizes and polymerization yields of the MIP/NIP polymers according to different HRP initial concentrations**

	Particles size (nm)		Yield (%)	
	MIP	NIP	MIP	NIP
<b>0.04 g/L</b>	280	100	16	5
<b>0.08 g/L</b>	180	54	27	20
<b>0.16 g/L</b>	386	25	80	25
<b>0.4 g/L</b>	537	28	89	36

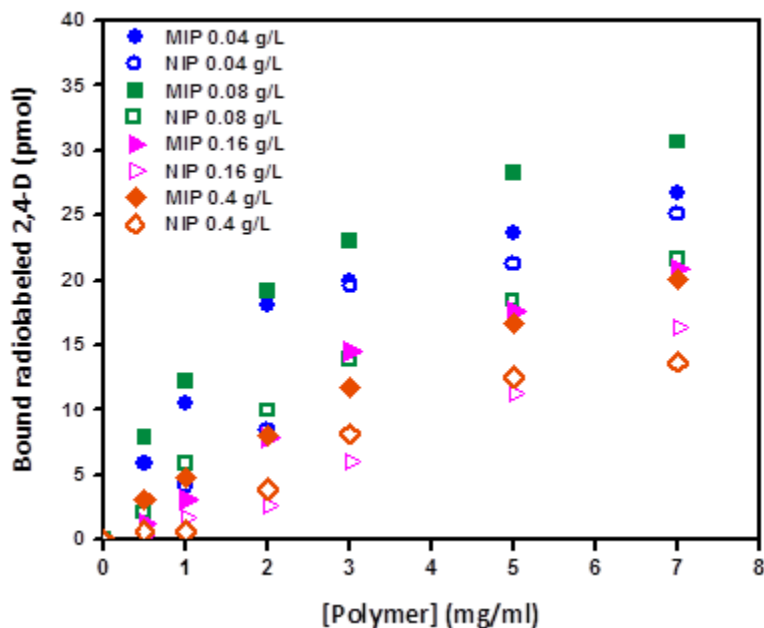
By increasing the enzyme concentration, MIP size increases. We can also notice that the yields of both MIPs and NIPs have been greatly influenced by of the HRP initial concentration. Higher yields were obtained for high HRP concentrations.

MIP binding properties are studied by radioactivity assays in order to assess the molecular recognition of the MIPs. The binding isotherms of MIPs and NIPs prepared with different HRP concentration are presented in **Figure VI-4** and the corresponding  $Q_{\text{max}}$  and  $K_{50}$  are summarized in **Table VI-5**.



**Table IV-5:  $Q_{\max}$ ,  $K_{50}$  and imprinting factors of the different MIPs synthesized via HRP-catalysis by different HRP initial concentrations**

	$Q_{\max}$ (pmol)	$K_{50}$ (mg/ml)	$IF_{\max}$ (0.5 mg/ml)
0.04 g/L	34.7	1.5	2.4
0.08 g/L	40	2.2	4
0.16 g/L	34	8	3.2
0.4 g/L	34	10	3.2

**Figure IV-4: Effect of the HRP concentrations (from 0.04 g/l to 0.4 g/l) on the binding isotherms of MIPs and NIP synthesized *via* HRP-catalysis in 20 mM pH 7.0 sodium phosphate buffer + 0.1% triton X-100 using [ $^{14}$ C]-2,4-D (0.04 nmol, 2nCi), [Acac] $_0$ = 1.4 mM, and [H $_2$ O $_2$ ] $_0$ = 0.88 mM.**

Highest 2,4-D binding and imprinting factors are obtained for 0.08g/l HRP concentration. Below this concentration, the MIP shows lower 2,4-D binding and specificity. The inefficient amount of enzyme has resulted in lowering the polymerization kinetics, which in turn seems to have affected the MIP binding properties, similar to what was observed with the Acac concentration. When the HRP concentration is higher, lower binding performance has been also obtained.

As conclusion, the HRP concentration affects the MIP binding properties, but also the polymerization yield in a reverse manner. Therefore, a compromise has to be made between a good imprinting effect and the recovery of a high quantity of polymer. As specificity is crucial for MIP applications, we selected a HRP concentration of 0.08 g/l as the optimal one for this work.

### IV.3.1.1.3. Effect of the imprinting solvent

The previous 2,4-D MIP synthesis in our study was done in ultrapure water. As the HRP optimal activity is at pH 7.0, we studied the synthesis of MIP in sodium phosphate buffer at this pH in order to determine its effect on the MIP binding properties. The MIP and NIP were prepared using  $[\text{Acac}] = 1.4 \text{ mM}$  and  $[\text{HRP}] = 0.08 \text{ g/l}$ .

The particles size of MIP and NIP synthesized in phosphate buffer, being 855 nm and 52 nm, respectively, were higher than the ones prepared in distilled water. Higher yields are also obtained for MIP (76%) and NIP (30%) compared to the same polymers synthesized in water probably due to a higher enzymatic activity of HRP in buffered media.

2,4-D bindings are performed by radioactivity tests and the curves are plotted in the upcoming **Figure IV-5**. Little difference between the binding of MIP and NIP prepared in buffer can be observed with a negligible imprinting effect suggesting a lower specificity compared to the MIP synthesized in water, whereas  $Q_{\text{max}}$  and  $K_{50}$ , being 39 pmol, and 3.6 mg/ml respectively, are close to the values of the polymer prepared in water.

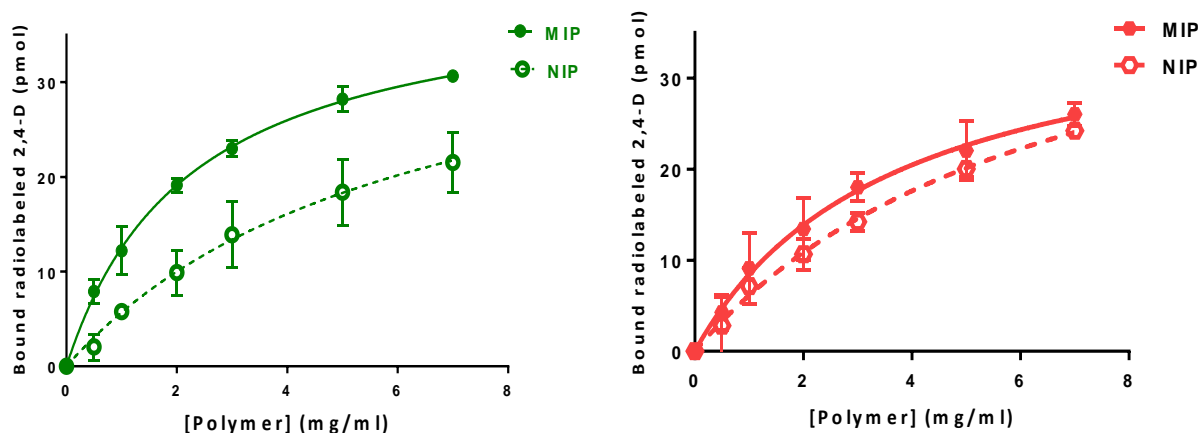


**Figure IV-5:** Effect of polymerization media on the 2,4-D binding by MIPs and NIP synthesized via HRP-initiated free radical polymerization in water (left) or in 20 mM phosphate buffer pH 7.0 (right). The radioligand binding assays were performed in 20 mM sodium phosphate buffer pH 7.0 + 0.1% triton X-100 with  $^{14}\text{C}$ -2,4-D (0.04 nmol, 2nCi).

At pH 7.0, the 4-VP is neutral since its pKa is 5.62 and the 2,4-D, which is a weak acid (pKa=2.6), is negatively charged [44]. So, the interactions between the template and the functional monomer are probably weaker in phosphate buffer than in water where ion pairs can be formed between template and monomer, resulting in a lower affinity.

In conclusion, MIPs are prepared in distilled water for the upcoming syntheses.

#### *IV.3.1.1.4. Comparison of the HRP-mediated and UV-initiated MIP synthesis*

MIPs for the molecular recognition of 2,4-D were synthesized by HRP-mediated and U.V-initiated free radical polymerization. Total monomers concentration is fixed at 2% and the synthesis is performed in ultra-pure water. For enzymatic synthesis, MIPs were prepared by using 0.08 mg/ml of HRP solution, 1.4 mM of Acac and 0.88 mM of H<sub>2</sub>O<sub>2</sub>. The photochemically-initiated synthesis was however achieved by using the initiator Vazo 56<sup>®</sup> at 1 mol %.

##### *A. Particles size characterization*

Dynamic light scattering measurements show particles of 200 nm and ~60 nm for MIPs and NIPs, respectively, for HRP-catalyzed polymerization. The sizes of the photochemically-prepared MIPs were ~1000 nm and ~700 nm for both MIP and NIP. The morphology of the micro/nanoparticles was characterized by scanning electron microscopy (SEM) analysis and the images for both polymers are shown in **Figure IV-6** and **Figure IV-7**.

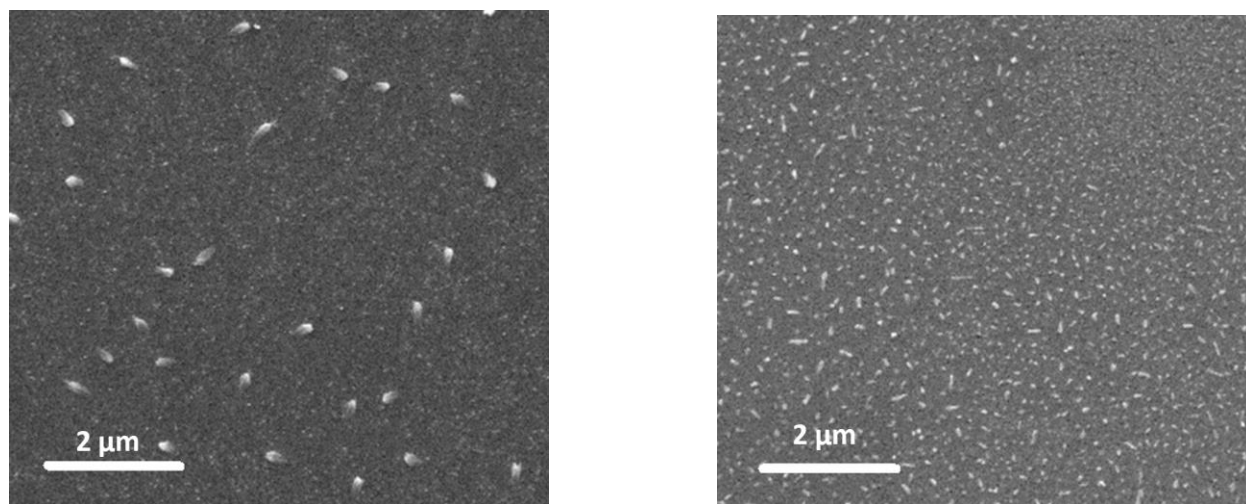


**Figure IV-6: SEM images of the MIPs (left) and NIPs (right) synthesized by HRP-mediated initiation of free radical polymerization.**

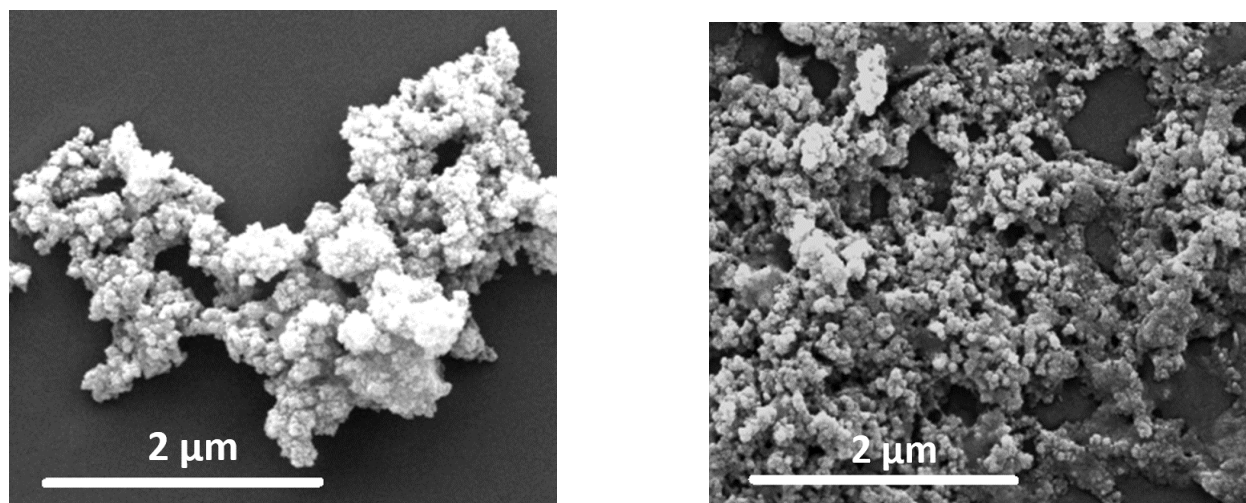


**Figure IV-7: SEM images of the MIPs (left) and NIPs (right) synthesized by U.V-initiated free radical polymerization.**

A significant effect of the initiation method on the polymer morphology can be observed. Monodisperse small-sized nanoparticles with irregular shape are obtained by HRP-mediated initiation of FRP. The average sizes of  $\sim 200$  nm and  $\sim 60$  nm of MIPs and NIPs, respectively, confirm the results obtained by DLS. UV-initiated polymerization led to large aggregates of spherical nanoparticles. The large size obtained by DLS was due to aggregation. The morphology initiation depending on the initiation method was previously also observed in the synthesis of non-imprinted hydrogels in **Chapter II**.

### B. Evaluation of the imprinting effect

The enzymatically initiated MIPs binding properties were compared to those of the traditionally prepared MIPs. The binding isotherms are shown in **Figure IV-8**.

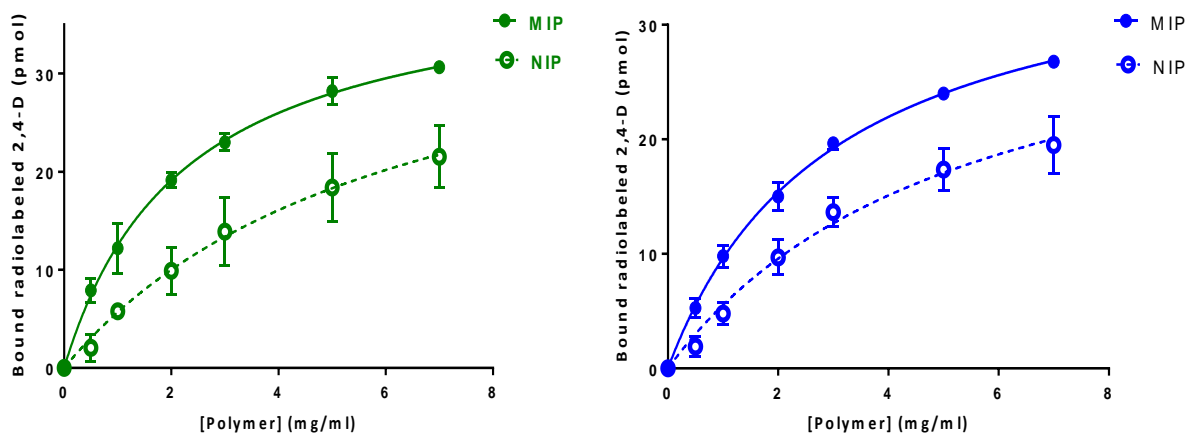


**Figure IV-8:** Comparison of the binding isotherms of the MIPs and NIPs synthesized by free radical polymerization initiated by enzyme-catalysis (left) or UV (right), using 4-VP and PDA as functional and cross-linking monomers at 2%. The tests are performed by radioactivity binding assays in 20 mM sodium phosphate buffer pH 7.0 + 0.1% triton X-100 using [ $^{14}$ C]-2,4-D (0.04 nmol, 2nCi).

Similar binding properties were observed for the two initiation methods in terms of binding capacity and specificity, even if a slightly higher imprinting factor has been obtained for the enzymatic initiation. Interestingly, for a polymer concentration of 0.5 mg/ml, the IF is 4 for enzymatically initiated MIP and only 2.7 for the UV-initiated MIP. The  $Q_{\max}$  is 40 pmol and 38 pmol for the HRP MIP and the UV MIP, respectively.  $K_{50}$  is 2.2 mg/ml for the enzymatic MIP, and 2.9 mg/ml for U.V-polymerized MIP.

In order to generalize the optimized enzymatic system for MIPs preparation, a MIP for 2,4-D was synthesized by using EbAAm as cross-linker instead of PDA with a total monomer concentration of 1%. The other conditions were the same. A conventional photochemical MIP was used as reference. **Figure IV-9** shows the binding isotherms obtained for the two initiation methods.

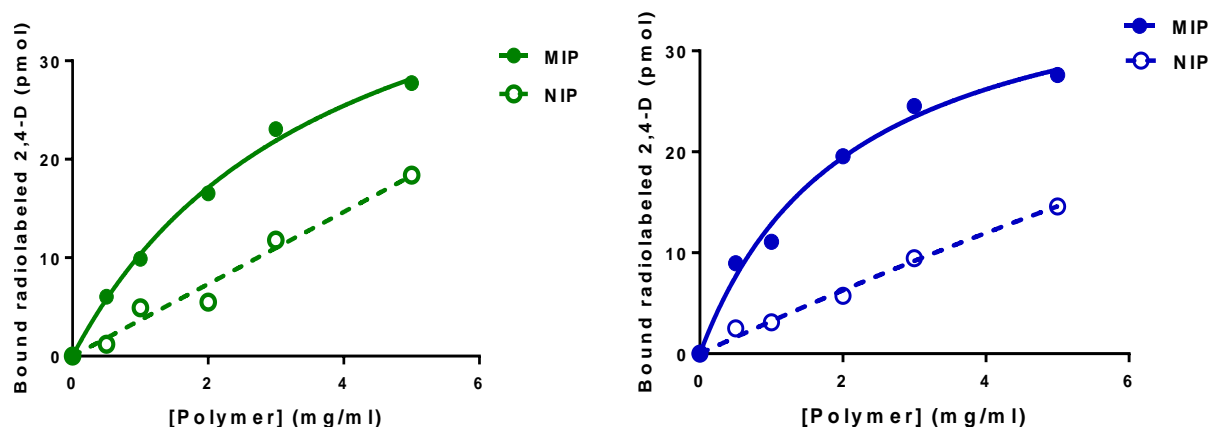


**Figure IV-9: Comparison of the binding for MIPs and NIPs synthesized by free radical polymerization initiated by enzyme-catalysis (left) or UV (right), using 4-VP and EbAAM as functional and cross-linking monomers at 1% total concentration. The binding tests were performed by radioligand binding assays in 20 mM sodium phosphate buffer pH 7.0 + 0.1% triton X-100 with [<sup>14</sup>C]-2,4-D (0.04 nmol, 2nCi).**

Even by changing the cross-linker, similar binding results are obtained for MIPs synthesized by the two initiation methods.  $K_{50}$  for enzymatic MIPs is 3.7 mg/ml with 50 pmol as  $Q_{max}$ , whereas for the UV-polymerized MIP, these values are 2.2 mg/ml and 40 pmol, respectively. As previously with PDA-based MIP, a higher imprinting factor is obtained for HRP-mediated MIP than UV-polymerized MIP both being 5 and 3.5 (for 0.5 mg/ml as polymer concentration), respectively.

In conclusion, these results show that enzyme-mediated initiation is an interesting alternative for the preparation of water-compatible MIPs. It can lead to not only similar, but also better molecular recognition properties than photochemical initiation.

### *C. Langmuir binding isotherms*

In order to determine the true dissociation constants for template binding to the MIP, binding isotherms for enzyme initiated and UV-polymerized MIPs were recorded by varying the ligand concentration at a constant low polymer concentration. They were fitted with the Langmuir

model (mono-site). Dissociation constant ( $K_d$ , the ligand concentration that causes complexation of half of the polymer binding sites at equilibrium) and maximum capacity ( $B_{max}$ , maximum number of accessible binding sites) are determined according to the following equation:

$$B = \frac{B_{max} \times F}{K_d + F}$$

$F$  and  $B$  represent the concentrations at the equilibrium of 2,4-D in the liquid and adsorbed phases, respectively. **Figure IV-10** shows the corresponding results.

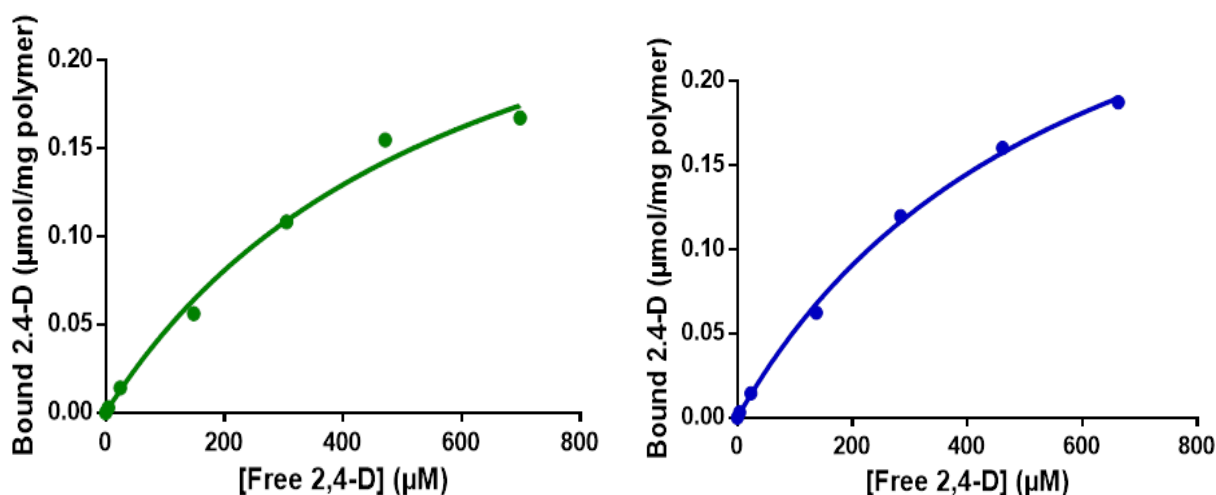


**Figure IV-10:** Langmuir isotherms of the MIPs synthesized by free radical polymerization initiated by enzyme-catalysis (left) or U.V (right), using 4-VP and PDA as functional and cross-linking monomers at 2%. The binding tests are performed by radioactive binding assays in 20 mM pH 7.0 sodium phosphate buffer + 0.1% triton X-100 using [ $^{14}$ C]-2,4-D (0.04 nmol, 2nCi) and increasing concentrations of cold (not labeled) 2,4-D.

**Table IV-6:** Maximum capacities and dissociation constants of the MIPs synthesized *via* different initiation methods.

Initiation	$B_{max}$ (μmol/mg)	$K_d$ (μM)
HRP-mediated catalysis	$0.33 \pm 0.04$	$607 \pm 90$
Photochemical	$0.36 \pm 0.02$	$596 \pm 69$



As shown in **Figure IV-10** and **Table IV-6**, no significant difference is observed in the affinities of MIPs prepared by the 2 initiations methods. A slight difference in maximum capacity with higher value for HRP-mediated polymerization is observed.

#### *D. MIPs selectivity*

The selectivity of the MIPs was evaluated by competitive binding assays. The competition curves between the radioligand and a number of non-labeled molecules, including the template molecule, are recorded. The selectivity of the plastic antibody can then be assessed by comparing the competition power (IC<sub>50</sub>, the lower the stronger) of the different related molecules with that of the template. The tests are done using a constant amount of MIPs and radio-labeled 2,4-D and increasing concentrations of competitors. The competition curves of the three competitors (2,4-D, PhAcOH, and CPOAc) for MIPs synthesized by the two initiation methods are illustrated in **Figure IV-11**. B/B<sub>0</sub> is the ratio of the radio-labeled 2,4-D bound in the presence of competing ligand (B) to the amount bound in the absence of competing ligand (B<sub>0</sub>). The corresponding values of IC<sub>50</sub> and cross-reactivities are in **Table IV-7**.

**Table IV-7: Parameters of cross-reactivity for MIP of enzymatic and photochemical initiations.**

	HRP-mediated catalysis		Photochemical initiation	
	IC <sub>50</sub> (mM)	Cross-reactivity (%)	IC <sub>50</sub> (mM)	Cross-reactivity (%)
<b>2,4-Dichlorophenoxyacetic acid (2,4-D)</b>	0.18	100	0.22	100
<b>Phenoxyacetic acid (PhAcOH)</b>	1.17	15.5	1.6	13
<b>4-Chlorophenoxyacetic acid (CPOAc)</b>	0.63	29	0.36	59



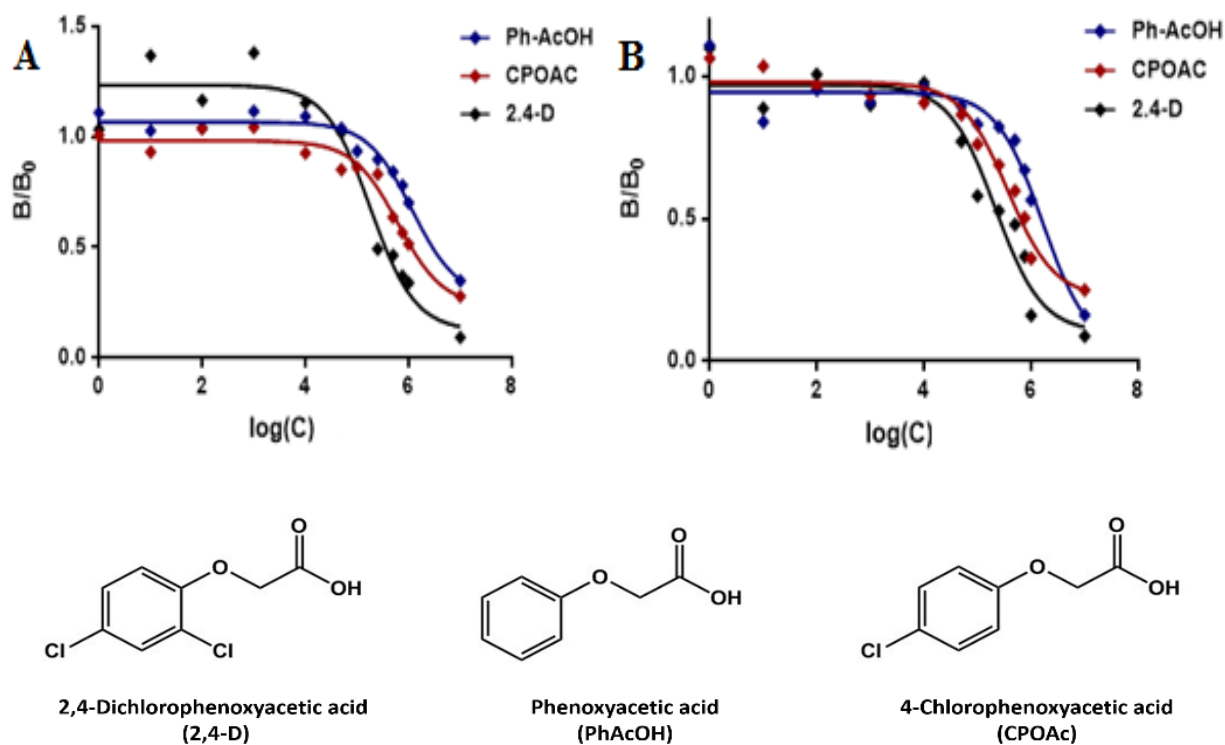


**Figure IV-11: Displacement of [<sup>14</sup>C]-2,4-dichlorophenoxyacetic (0.04nmol, 2nCi) , binding to (A) enzyme-mediated synthesized MIPs and to (B) photochemically synthesized MIPs (right), by increasing concentrations of competing ligands, in 20mM sodium phosphate buffer pH 7.0 +0.1% triton X-100. Chemical structures of the corresponding competitors are drawn below.**

As it can be observed from the curves and the values, there is a difference between the 2 MIPs. Similar cross-reactivities are obtained for PhAcOH, they are 15.5 % and 13 % for the enzymatic and photochemical MIPs, respectively. However, MIPs that are synthesized by HRP-catalysis have 29% cross-reactivity against CPOAc, whereas photochemically-synthesized MIPs have 59%.

#### IV.3.1.2. Synthesis of a MIP for salicylic acid

Salicylic acid is a phenolic acid that is used as an anti-inflammatory drug. In addition, SA is well-known for its use as a key ingredient in topical anti-acne products and a safe choice for the control of localized psoriasis and other skin diseases [45, 46]. A MIP for this molecule would therefore be interesting for pharmaceutical or cosmetic applications, in order to control and

maximize the efficacy of this drug during the treatment and to develop a drug delivery system. There are several MIPs in the literature specific for SA, not only for drug delivery [46], but also chemical sensing [47] and its separation or recovery [48, 49].

In this study, we used salicylic acid as a second model system to synthesize a MIP by enzyme-mediated initiation. We prepared water-soluble molecularly imprinted nanoparticles for SA HRP-initiated free radical polymerization using 4-VP and PDA as functional and cross-linking monomers, respectively, at 1 % total monomer concentration. Photochemical synthesis of the same MIPs was also performed in order to compare the data to the conventional ways of MIP preparation.

Enzymatic polymerization yields were low, and higher for the mIP than for the NIP (~22% for MIP and ~3% for NIP). Much higher yields are obtained with UV-polymerization, the yields for MIP and NIP being roughly the same with this initiation system (~64% and ~60% for MIP and NIP, respectively). DLS results show small sizes for HRP-catalyzed particles. MIP and NIP were of 200 nm and 50 nm, respectively. Larger particles were obtained with UV-polymerization. Microgels are formed with ~900 nm and ~450 nm particles sizes for MIP and NIP, respectively.

The binding properties of the MIPs from UV and enzymatic polymerizations were determined using fluorescence methods in 20 mM acetate buffer pH 6.0. They are shown in **Figure IV-12**.

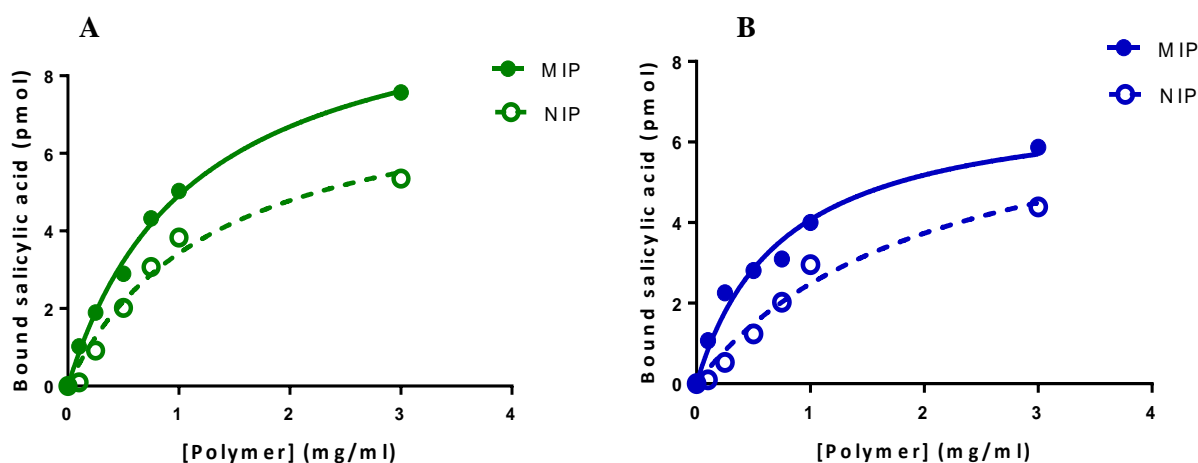


**Figure IV-12: Equilibrium binding isotherms in 20 mM acetate phosphate buffer, pH 6.0 with 10 nmol SA, on MIP (full symbols) and NIP (open symbols) nanoparticles that have been prepared through: (A) HRP-catalysis, (B) UV-initiation.**

Similar SA binding was obtained for MIPs synthesized by the two initiation methods, with  $K_{50}$  of 1.1 mg/ml and 0.8 mg/ml and  $Q_{\max}$  values of 10.5 pmol and 7 pmol for the enzymatic and UV MIPs, respectively. Both MIPs show good imprinting factors for low polymer concentrations, being 10 and 2 for 0.1 and 0.25 mg/ml, respectively. However, IF decreased to 1.5 and less with increasing polymer concentrations.

#### IV.3.1.3. Molecular imprinting of a protein: trypsin

In this study, we applied the enzymatic ternary system for the preparation of thermo-responsive imprinted nanogels for trypsin as an example for a larger (protein) template. An adapted protocol from a previous study in our group was applied [39]. The main component (95 %) in the polymer formulation is *N*-isopropylacrylamide (NiPAm) for its ability to undergo a volume-phase transition at its critical solution temperature (LCST) of 32°C. MIP nanogels were synthesized by HRP-mediated initiation at 25°C, which means in the swollen state, using 5 % EbAm as cross-linker in 25 mM phosphate buffer pH 7.0. Conventional KPS/TEMED-initiated synthesis of MIPs was performed as reference. For the two initiation methods, molecularly imprinted gels were prepared in the presence and the absence of the anchoring monomer aminobenzamidinium (AB), which is used in a stoichiometric amount with respect to trypsin. This monomer, presented in **Figure IV-13**, is based on a well-known inhibitor of trypsin. It was previously used as an affinity ligand and strong anchoring monomer for MIP synthesis [40].

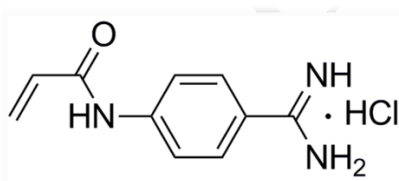


**Figure IV-13:** Chemical structure of the anchoring *N*-acryloyl-*p*-aminobenzamidinium.HCl monomer (AB).

Polymer characteristics in terms of particles sizes and polymerization yields are summarized in **Table IV-8**. From these values, both initiations had led to very small-sized nanogels without any

significant difference. High polymerization yields are obtained *via* HRP-initiated polymerization, but slightly higher for the KPS/TEMED initiation.

**Table IV-8: Particles sizes and polymerization yields of the MIP/NIP polymers according to the initiation way of free-radical polymerization.**

Initiation system	Anchoring monomer	Particles size (nm)		Yield (%)	
		MIP	NIP	MIP	NIP
Ternary enzymatic system	With AB	28	21	67	79
	Without AB	28	22	78	82
KPS/TEMED couple	With AB	18	16	73	83
	Without AB	25	21	84	91

The MIPs binding properties were determined by enzymatic activity assays to determine the quantity of absorbed protein. **Figure IV-14** shows the binding results for the polymers prepared by HRP-catalyzed polymerization with and without the anchoring monomer AB.

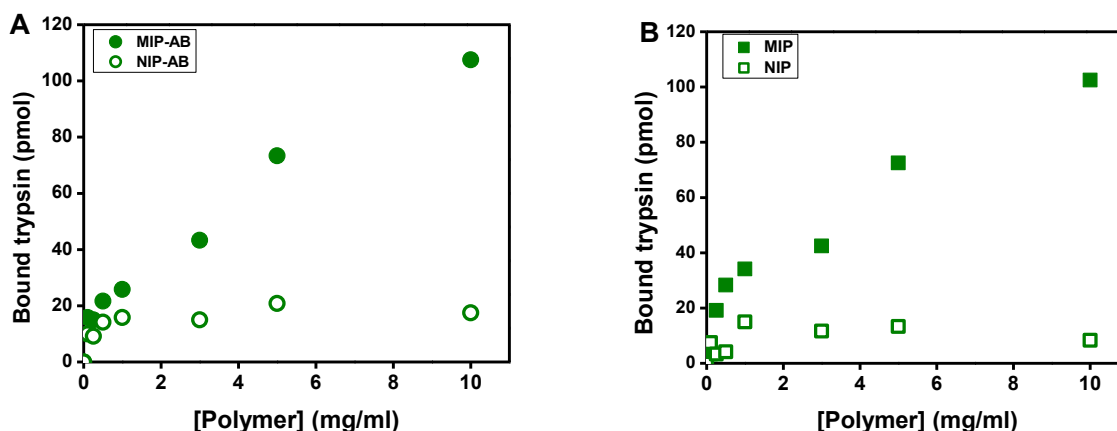


**Figure IV-14: Equilibrium binding isotherms of MIP and NIP nanoparticles for trypsin (0.6 nmol) in 5 mM Tris-HCl buffer pH 8.0 + 10 mM CaCl<sub>2</sub>, in: (A) the presence of the anchoring monomer AB, and (B) the absence of AB in the polymer formulation. Polymerization was initiated by HRP.**

Similar results were obtained with the two MIPs. The IF are high, which is due to a low binding to the NIPs.

In conclusion, soluble HRP-initiated free radical polymerization was successfully applied for MIP synthesis for acidic and basic templates of small size, and for a protein. Green chemistry approach was used as versatile tool for the preparation of imprinted hydrogels based on different co-monomers for the recognition of different templates.

### **IV.3.2. Synthesis of MIP nanoparticles by immobilized HRP**

Free enzymes may be entrapped in the polymeric matrices upon synthesis and contaminate the final product, Moreover, they cannot be reused although their price is typically higher than that of conventional initiators, which will increase production cost. We therefore wanted to investigate whether immobilized HRP can be used to initiate the polymerization of MIP NPs in a solid-phase reactor. In that way, the enzyme can be easily separated from the polymerization mixture, washed to eliminate excess of chemicals, and may be reused. HRP was immobilized on a solid carrier using the protocol developed in **Chapter III**. Different experimental conditions were studied in order to optimize the synthesis. The specificity and the selectivity of the particles are then examined and the reusability of the same batch of beads is investigated for subsequent MIP synthesis.

#### **IV.3.2.1. Optimization of MIP synthesis**

MIPs for 2,4-D were synthesized by free radical polymerization using immobilized HRP to initiate the reaction. Experimental conditions such as total monomers concentration, and molar amounts of Acac and hydrogen peroxide were varied in order to determine the best combination of ternary system components resulting in high polymerization yield with controlled particles sizes and high molecular recognition properties.

Since we had already shown that the molar ratio  $[Acac]/[monomers]$  greatly affected the imprinting properties of the polymers, we studied its influence on the immobilized HRP-

catalyzed synthesis of MIP. First, the same protocol as used for MIP synthesis with soluble HRP was reproduced with immobilized HRP. In a standard protocol, cross-linking and functional monomers (PDA and 4-VP, respectively) as well as template are used with a molar ratio of 16:4:1 in a total monomer concentration of 5 % in water. Molar ratios of 0.05 for [Acac]/[Monomers] and 1.5 for [Acac]/ [H<sub>2</sub>O<sub>2</sub>] are employed. Free HRP was substituted by 10 g of HRP-charged glass beads. After polymerization, the results of particles size and polymerization yield for different [Acac]/[Monomers] are indicated in **Table IV-9** (entry 1).

Second, the total monomer concentration was fixed, but the Acac concentration was increased from 3.5 mM to 14.8 mM (thus the ratio [Acac]/[monomers] increased from 0.012 to 0.05, entry 2). Smaller particles were obtained for MIP and NIP prepared with increased [Acac]/[Monomers] ratio. Moreover, the yield was greatly improved.

**Table IV-9: Influence of total monomers concentrations and the acetylacetone concentration on the characteristics of MIP-NPs synthesized by immobilized-HRP catalyzed free radical polymerization.**

N°	Beads <sup>(1)</sup> (g)	[Mono] <sup>(2)</sup> (%)	[Acac]/[Mono]	IF <sup>(3)</sup>	Bound [ <sup>14</sup> C]- 2,4-D (pmol) <sup>(4)</sup>		Particle size <sup>(5)</sup> (nm)		Yield (mg)	
					MIP	NIP	MIP	NIP	MIP	NIP
<b>1</b>	10	5	0.012	5.5	2.5	0.45	342	109	9	4
<b>2</b>	10	5	0.05	1	2.4	2.32	140	63	31	130
<b>3</b>	10	10	0.012	4.4	3.25	0.75	280	60	10	7

<sup>(1)</sup> For 1 g of HRP-charged glass beads, the amount of immobilized enzyme is 1 mg of HRP and the residual HRP activity is  $3 \cdot 10^{-7}$  mol/min/mg of HRP.

<sup>(2)</sup> Total monomer concentration.

<sup>(3)</sup> Imprinting factor corresponds to the ratio binding to MIP/binding to NIP.

<sup>(4)</sup> at 0.5 mg/ml polymer concentration

<sup>(5)</sup> Particle size measured by dynamic light scattering (DLS).

The binding properties of these polymers for 2,4-D were evaluated by radioligand binding assays for two polymer concentrations (0.5 and 1 mg/ml). The results are presented in **Figure IV-15A**. With an [Acac]/[monomers] ratio of 0.012, good imprinting factors were obtained, 4.8 and 2.5 for 0.5 and 1 mg/ml, respectively. No imprinting effect was observed when this ratio was increased.

Since the yields in MIP particles obtained with a [Acac]/[monomers] ratio of 0.012 were very low, new trials were performed to increase the yield. In **Chapter III**, we showed that experimental parameters affecting the polymerization yield in this solid-phase synthesis are the molar amount of acetylacetone and the total monomer concentration. Since the increase of Acac has a negative effect on imprinting, our only option is increasing the total monomer concentration. For this, the total monomer concentration was increased from 5% to 10%, keeping the parameters fixed. The results are shown in **Table IV-9** (Entry 3). The particles size of the MIP decreased slightly, but the yield increased only insignificantly. It appears therefore that 10% total monomers concentration and a molar ratio of [Acac]/[Monomers] of 0.012 are the best choice for MIP-NP synthesis with initiation by immobilized HRP. These conditions were subsequently used.

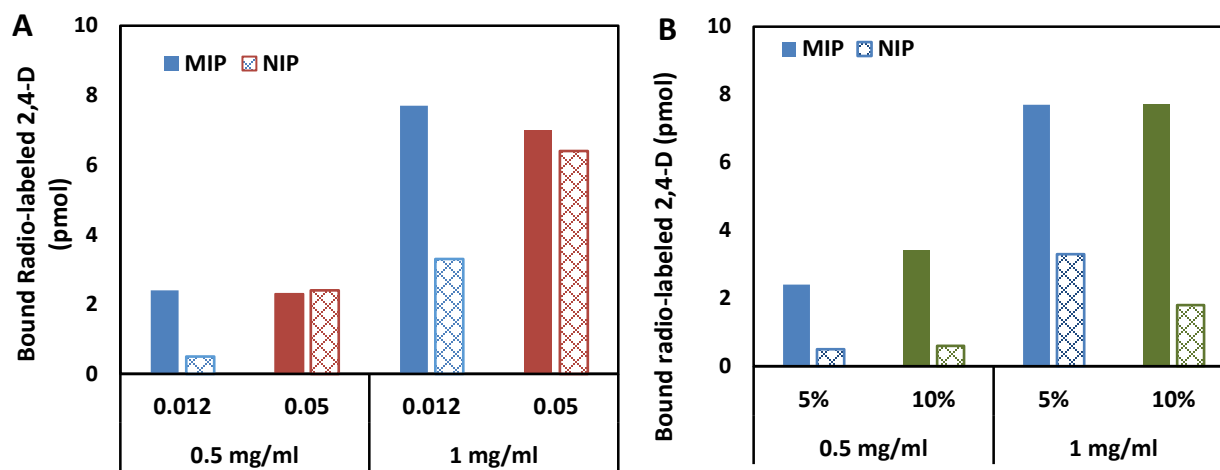


**Figure IV-15: 2,4-D radioactive binding assays in 20 mM pH 7.0 sodium phosphate buffer + 0.1% triton X-100 with [<sup>14</sup>C]-2,4-D (0.04 nmol, 2nCi) for MIPs/NIPs prepared by immobilized HRP catalysis in: (A) different molar ratios of [Acac]/[Monomers], (B): different total monomers concentrations.**

### IV.3.2.2. Molecular recognition properties

MIPs nanoparticles were prepared in the optimized experimental conditions (10% total monomer concentration and 0.012 as [Acac]/[Monomers] ratio). In order to evaluate the binding properties of the MIP, 2,4-D binding isotherms for the MIP and the control polymer were performed in 20 mM phosphate buffer pH 7.0 by radioligand binding assays [43]. The results are shown in the following **Figure IV-16**. A good imprinting effect is obtained, good specificity of the MIP with binding to the NIP being surprisingly low even for the higher polymer concentrations.

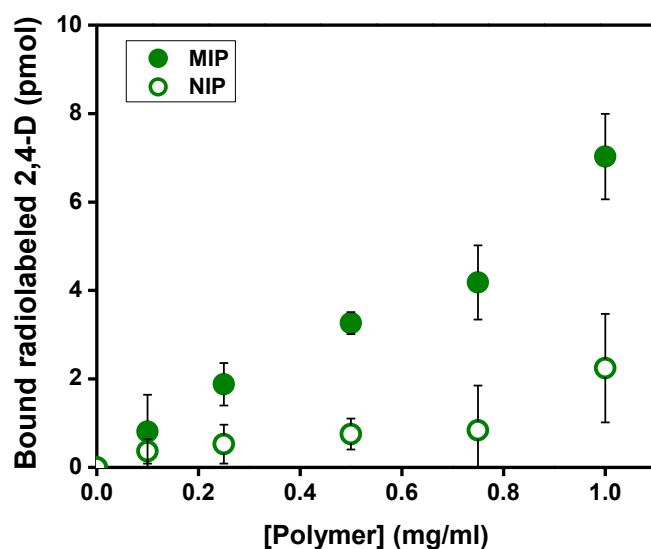


**Figure IV-16:** Equilibrium binding isotherms using [ $^{14}\text{C}$ ]-2,4-D (0.04 nmol, 2 nCi), in 20 mM sodium phosphate buffer pH 7.0 + 0.1% triton X-100 for MIP (filled symbols) and NIP (open symbols) nanoparticles prepared with immobilized HRP catalysis. Data points are means from three independent experiments with three different polymer batches issued from different HRP immobilizations.

The selectivity of the MIP nanoparticles was evaluated by competitive binding assays as outlined under **IV.3.1.1.4.D**. The competition curves are shown in **Figure IV-17**.  $\text{IC}_{50}$  values were 260  $\mu\text{M}$ , 590  $\mu\text{M}$ , and 1618  $\mu\text{M}$ , for 2,4-D, CPOAc and PhAcOH, respectively. Based on this, the MIP shows 16% and 44% as cross-reactivity for PhAcOH and CPOAc, respectively. These



results are similar to those obtained with the MIP synthesized by free HRP mediated polymerization even though a higher cross-reactivity to CPOAc was obtained.

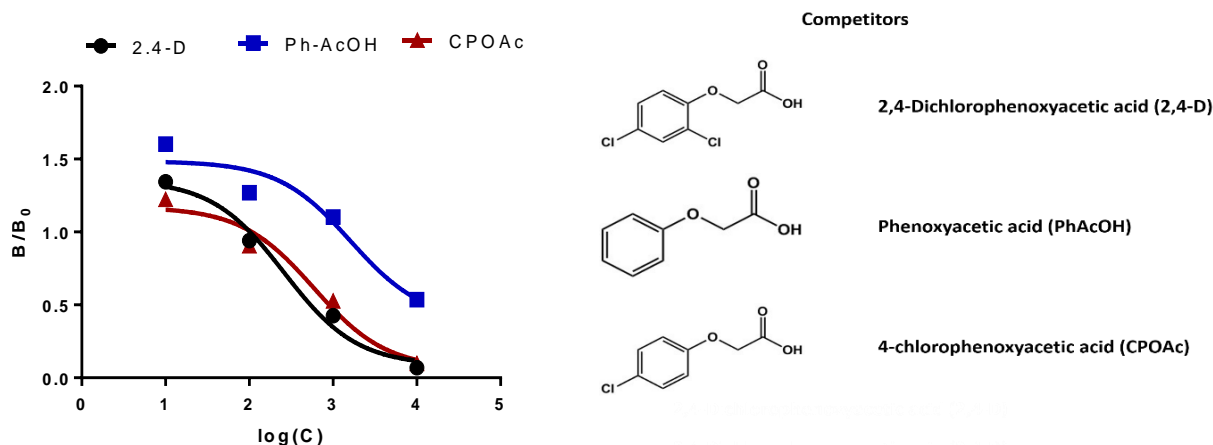


**Figure IV-17:** Displacement of [ $^{14}\text{C}$ ]-2,4-D (0.04 nmol, 2nCi) binding to 1.5 mg of MIP, by increasing concentrations of competing ligands, in 20 mM pH 7.0 sodium phosphate buffer + 0.1% triton X-100.  $B/B_0$  is the ratio of the amounts of radioactive 2,4-D bound in the presence and absence of displacing ligand.

#### IV.3.2.3. Reusability of the immobilized HRP

After the synthesis of the first MIP and NIP with catalysis by the immobilized enzyme, the HRP-charged glass beads were washed and re-suspended in new polymerization mixture. In that way, MIP synthesis was repeated several times with the same batch of immobilized HRP. As a result, it was possible to reuse the immobilized enzyme for four cycles.

The results in terms of particle size, yield and 2,4-D binding are shown in **Figure IV-18** and in **Table IV-10**. The particle sizes did not vary significantly during the cycles, while the yield decreased slightly. In each batch, a clear imprinting effect is obtained, while the binding of [ $^{14}\text{C}$ ]-2,4-D increases until batch 3 whereafter it decreases slightly. This might be due to improved polymerization kinetics with respect to the imprinting, as a result of a slight inactivation of the

immobilized enzyme. Thus, the immobilized enzyme can be reused at least 4 times for the synthesis of fully functional MIP-NPs in a reproducible manner.

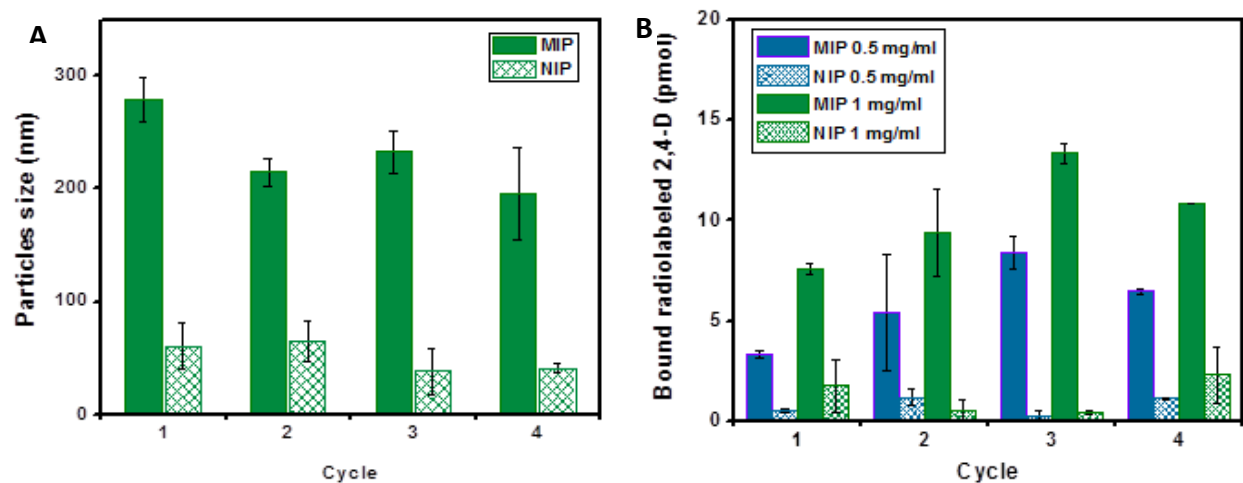
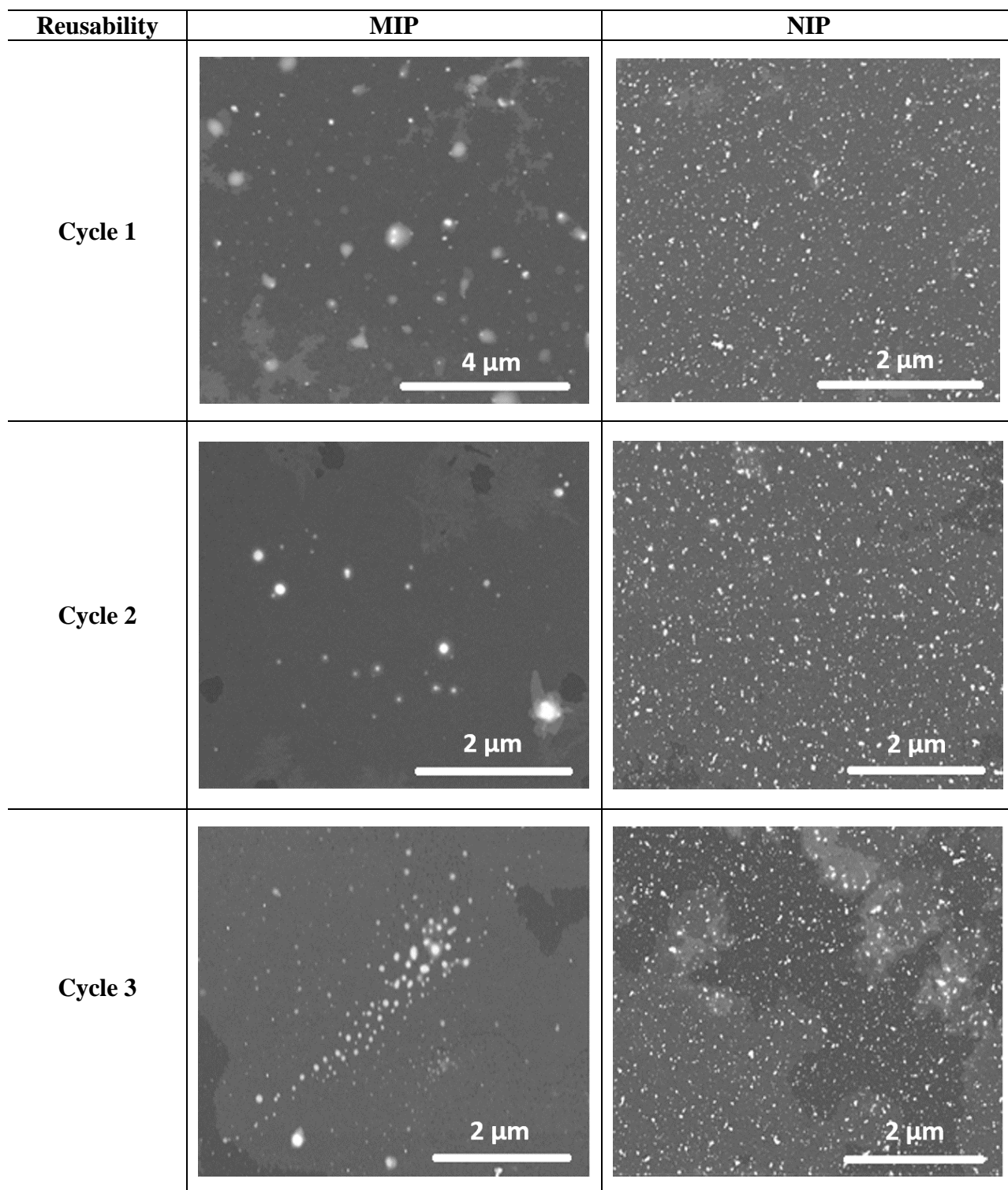


**Figure IV-18: (A):** DLS measurement of particle sizes for MIP and NIP obtained in every cycle of free radical polymerization catalyzed by the same immobilized HRP. **(B):** Binding assays using [<sup>14</sup>C]-2,4-D (0.04 nmol, 2 nCi) for MIP and NIP nanoparticles (1 mg/ml) synthesized in every cycle by immobilized HRP-mediated FRP in 20 mM pH 7.0 sodium phosphate buffer + 0.1% triton X-100.0 Data are mean values from three different batches of polymers synthesized within 3 separate HRP immobilizations.

**Table IV-10: Polymerization yields (mg) for the MIPs and NIPs in every cycle.**

	Cycle 1	Cycle 2	Cycle 3	Cycle 4
MIP	9	7.5	6	5
NIP	4	6	5	4

Finally, scanning transition electron microscopy (STEM) were used to analyze MIP and NIP in every cycle. The images are represented in **Figure IV-19** indicating the formation of polydisperse MIPs and NIPs. For the first batch, ~350 nm MIP and ~40 nm NIP are observed similar to what was measured in DLS. It is also observed that the MIP size decreased after the first cycle and became stable around ~100-150 nm, whereas the NIP had the same size in every cycle.



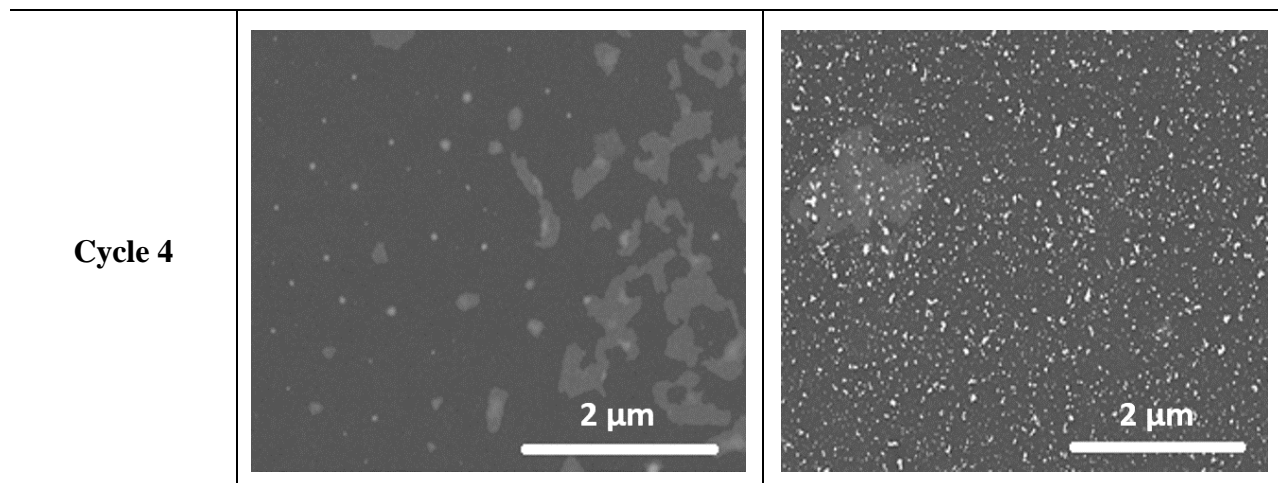


**Figure IV- 19:** Particles sizes, measured by STEM, upon washing and drying, of the MIP (left) and NIP (right) nanoparticles synthesized by free radical polymerization catalyzed by the reusable HRP immobilized on glass beads in every cycle.

#### IV.4. Conclusion

Synthesis of molecularly imprinted hydrogels was achieved by HRP-mediated initiation of free radical polymerization. Different templates were been successfully imprinted. Molecules with low molecular weight (2,4-D, salicylic acid) were studied as well as proteins (trypsin).

'Green' synthesis of MIPs was performed by free radical polymerization using, for the first time, enzyme-mediated initiation with soluble and immobilized HRP. We found that experimental conditions such as the molar ratios of the ingredients have an impact on the MIP characteristics. In order to obtain optimal imprinting effect, ratio of [Acac]/[Monomers] and HRP concentration should be 0.012 and 0.08 mg/ml, respectively. With these optimal conditions, the 'green' MIPs have the same binding properties as those synthesized by traditional photoinitiation of FRP.

Initiation with immobilized HRP allowed to reuse the initiator for at least 4 cycles, which should be a great advantage in terms of production cost.

## References

- [1] B. H. Karsten, V. L. Ana, B. Marc, and Tse Sum Bui, "Molecularly Imprinted Polymers," *Top Curr Chem*, vol. 325, pp. 1–28, 2012.
- [2] B. Ekberg and K. Mosbach, "Molecular imprinting: A technique for producing specific separation materials," *Trends Biotechnol.*, vol. 7, no. 4, pp. 92–96, 1989.
- [3] G. Wulff, "Forty years of molecular imprinting in synthetic polymers: Origin, features and perspectives," *Microchim. Acta*, vol. 180, no. 15–16, pp. 1359–1370, 2013.
- [4] H. Yan, K. H. Row, and G. Yang, "Water-compatible molecularly imprinted polymers for selective extraction of ciprofloxacin from human urine," *Talanta*, vol. 75, no. 1, pp. 227–232, 2008.
- [5] G. Wulff, "Enzyme-like catalysis by molecularly imprinted polymers," *Chem. Rev.*, vol. 102, no. 1, pp. 1–27, 2002.
- [6] R. Schirhagl, "Bioapplications for Molecularly Imprinted Polymers," *Anal. Chem.*, vol. 86, pp. 250–261, 2014.
- [7] M. J. Whitcombe, N. Kirsch, and I. a. Nicholls, "Molecular imprinting science and technology: A survey of the literature for the years 2004-2011," *J. Mol. Recognit.*, vol. 27, no. 6, pp. 297–401, 2014.
- [8] R. J. Ansell, "Molecularly imprinted polymers in pseudoimmunoassay," *J. Chromatogr. B Anal. Technol. Biomed. Life Sci.*, vol. 804, no. 1, pp. 151–165, 2004.
- [9] Z. X. Xu, H. J. Gao, L. M. Zhang, X. Q. Chen, and X. G. Qiao, "The Biomimetic Immunoassay Based on Molecularly Imprinted Polymer: A Comprehensive Review of Recent Progress and Future Prospects," *J. Food Sci.*, vol. 76, no. 2, 2011.
- [10] X. A. Ton, B. Tse Sum Bui, M. Resmini, P. Bonomi, I. Dika, O. Soppera, and K. Haupt, "A versatile fiber-optic fluorescence sensor based on molecularly imprinted microstructures polymerized in situ," *Angew. Chemie - Int. Ed.*, vol. 52, no. 32, pp. 8317–8321, 2013.
- [11] N. Atar, T. Eren, and M. L. Yola, "A molecular imprinted SPR biosensor for sensitive determination of citrinin in red yeast rice," *Food Chem.*, vol. 184, pp. 7–11, 2015.
- [12] A. Katz and M. Davis, "Molecular imprinting of bulk, microporous silica," *Nature*, vol. 403, no. 6767, pp. 286–9, 2000.
- [13] P. Bonomi, A. Servant, and M. Resmini, "Modulation of imprinting efficiency in nanogels with catalytic activity in the Kemp elimination," *J. Mol. Recognit.*, vol. 25, no. 6, pp. 352–360, 2012.
- [14] D. L. Rathbone, "Molecularly imprinted polymers in the drug discovery process," *Adv. Drug Deliv. Rev.*, vol. 57, no. 12, pp. 1854–1874, 2005.
- [15] Y. Yu, L. Ye, K. Haupt, and K. Mosbach, "Formation of a class of enzyme inhibitors (drugs), including a chiral compound, by using imprinted polymers or biomolecules as molecular-scale reaction vessels," *Angew. Chemie - Int. Ed.*, vol. 41, no. 23, pp. 4459–4463, 2002.
- [16] D. Cunliffe, A. Kirby, and C. Alexander, "Molecularly imprinted drug delivery systems," *Adv. Drug Deliv. Rev.*, vol. 57, no. 12, pp. 1836–1853, 2005.
- [17] K. Çetin and A. Denizli, "5-Fluorouracil delivery from metal-ion mediated molecularly imprinted cryogel discs," *Colloids Surfaces B Biointerfaces*, vol. 126, pp. 401–406, 2015.
- [18] P. a G. Cormack and A. Z. Elorza, "Molecularly imprinted polymers: synthesis and characterisation," *J. Chromatogr. B. Analyt. Technol. Biomed. Life Sci.*, vol. 804, no. 1, pp. 173–182, 2004.



- [19] Z. Adali-Kaya, B. T. S. Bui, A. Falcimaigne-Cordin, and K. Haupt, "Molecularly Imprinted Polymer Nanomaterials and Nanocomposites: Atom-Transfer Radical Polymerization with Acidic Monomers," *Angew. Chemie-International Ed.*, vol. 54, no. 17, pp. 5192–5195, 2015.
- [20] C. Gonzato, M. Courty, P. Pasetto, and K. Haupt, "Magnetic molecularly imprinted polymer nanocomposites via surface-initiated RAFT polymerization," *Adv. Funct. Mater.*, vol. 21, no. 20, pp. 3947–3953, 2011.
- [21] M. Shirangi, J. Sastre Toraño, B. Sellergren, W. E. Hennink, G. W. Somsen, and C. F. van Nostrum, "Methylenation of Peptides by *N*, *N*, *N*, *N*-Tetramethylethylenediamine (TEMED) under Conditions Used for Free Radical Polymerization: A Mechanistic Study," *Bioconjug. Chem.*, vol. 26, no. 1, pp. 90–100, 2015.
- [22] M. Panagiotopoulou, S. Beyazit, S. Nestora, K. Haupt, and B. T. Sum Bui, "Initiator-free synthesis of molecularly imprinted polymers by polymerization of self-initiated monomers," *Polymer (Guildf.)*, 2015.
- [23] S. Kobayashi and A. Makino, "Enzymatic polymer synthesis: an opportunity for green polymer chemistry," *Chem. Rev.*, vol. 109, no. 11, pp. 5288–5353, 2009.
- [24] F. Hollmann and I. W. C. E. Arends, "Enzyme initiated radical polymerizations," *Polymers (Basel)*, vol. 4, no. 1, pp. 759–793, 2012.
- [25] N. Miletic, A. Nastasovic, and K. Loos, "Immobilization of biocatalysts for enzymatic polymerizations: Possibilities, advantages, applications," *Bioresour. Technol.*, vol. 115, pp. 126–135, 2012.
- [26] N. An, C. H. Zhou, X. Y. Zhuang, D. S. Tong, and W. H. Yu, "Immobilization of enzymes on clay minerals for biocatalysts and biosensors," *Appl. Clay Sci.*, vol. 114, pp. 283–296, 2015.
- [27] J. M. Bolivar, I. Eisl, and B. Nidetzky, "Advanced characterization of immobilized enzymes as heterogeneous biocatalysts," *Catal. Today*, pp. 15–19, 2015.
- [28] Y. C. Lai and S. C. Lin, "Application of immobilized horseradish peroxidase for the removal of p-chlorophenol from aqueous solution," *Process Biochem.*, vol. 40, no. 3–4, pp. 1167–1174, 2005.
- [29] J. L. Gómez, a. Bódalo, E. Gómez, J. Bastida, a. M. Hidalgo, and M. Gómez, "Immobilization of peroxidases on glass beads: An improved alternative for phenol removal," *Enzyme Microb. Technol.*, vol. 39, no. 5, pp. 1016–1022, 2006.
- [30] G. Bayramoğlu and M. Y. Arica, "Enzymatic removal of phenol and p-chlorophenol in enzyme reactor: Horseradish peroxidase immobilized on magnetic beads," *J. Hazard. Mater.*, vol. 156, no. 1–3, pp. 148–155, 2008.
- [31] G. Shtenberg, N. Massad-Ivanir, S. Engin, M. Sharon, L. Fruk, and E. Segal, "DNA-directed immobilization of horseradish peroxidase onto porous SiO<sub>2</sub> optical transducers," *Nanoscale Res. Lett.*, vol. 7, no. 1, p. 443, 2012.
- [32] I. Alemzadeh and S. Nejati, "Phenols removal by immobilized horseradish peroxidase," *J. Hazard. Mater.*, vol. 166, no. 2–3, pp. 1082–1086, 2009.
- [33] T. Zhang, X.-L. Xu, Y.-N. Jin, J. Wu, and Z.-K. Xu, "Immobilization of horseradish peroxidase (HRP) on polyimide nanofibers blending with carbon nanotubes," *J. Mol. Catal. B Enzym.*, vol. 106, pp. 56–62, 2014.
- [34] A. Durand, T. Lalot, M. Brigodiot, and E. Maréchal, "Enzyme-mediated radical initiation of acrylamide polymerization: Main characteristics of molecular weight control," *Polymer (Guildf.)*, vol. 42, no. 13, pp. 5515–5521, 2001.
- [35] O. Emery, T. Lalot, M. Brigodiot, and E. Maréchal, "Free-radical polymerization of acrylamide by horseradish peroxidase-mediated initiation," *J. Polym. Sci. Part A Polym. Chem.*, vol. 35, no. 15, pp. 3331–3333, 1997.

- [36] T. Lalot, M. Brigodiot, and E. Maréchal, "A kinetic approach to acrylamide radical polymerization by horse radish peroxidase-mediated initiation," *Polym. Int.*, vol. 48, no. 4, pp. 288–292, 1999.
- [37] R. L. Shogren, J. L. Willett, and A. Biswas, "HRP-mediated synthesis of starch-polyacrylamide graft copolymers," *Carbohydr. Polym.*, vol. 75, no. 1, pp. 189–191, 2009.
- [38] B. Kalra and R. a Gross, "Horseradish peroxidase mediated free radical polymerization of methyl methacrylate.," *Amani*, vol. 1, no. 3, pp. 501–5, 2000.
- [39] S. Ambrosini, S. Beyazit, K. Haupt, and B. Tse Sum Bui, "Solid-phase synthesis of molecularly imprinted nanoparticles for protein recognition.," *Chem. Commun. (Camb.)*, vol. 49, no. 60, pp. 6746–8, 2013.
- [40] A. Cutivet, C. Schembri, J. Kovensky, and K. Haupt, "Molecularly imprinted microgels as enzyme inhibitors," *J. Am. Chem. Soc.*, vol. 131, no. 41, pp. 14699–14702, 2009.
- [41] J. S. Bus and L. E. Hammond, "Regulatory progress, toxicology, and public concerns with 2,4-D: Where do we stand after two decades?," *Crop Prot.*, vol. 26, no. 3, pp. 266–269, 2007.
- [42] K. Haupt, A. G. Mayes, and K. Mosbach, "Herbicide assay using an imprinted polymer-based system analogous to competitive fluoroimmunoassays," *Anal. Chem.*, vol. 70, no. 18, pp. 3936–3939, 1998.
- [43] K. Haupt, A. Dzgoev, and K. Mosbach, "Assay system for the herbicide 2,4-dichlorophenoxyacetic acid using a molecularly imprinted polymer as an artificial recognition element," *Anal. Chem.*, vol. 70, no. 3, pp. 628–631, 1998.
- [44] A. Boivin, S. Amellal, M. Schiavon, and M. T. Van Genuchten, "2,4-Dichlorophenoxyacetic acid (2,4-D) sorption and degradation dynamics in three agricultural soils," *Environ. Pollut.*, vol. 138, no. 1, pp. 92–99, 2005.
- [45] P. R. a O. K, K. Khaliq, S. S. Kharat, P. Sagare, and P. Sk, "PREPARATION AND EVALUATION O / W CREAM FOR SKIN PSORIASIS," *Int. J. Pharma Bio Sci.*, vol. 1, no. 3, 2010.
- [46] B. Li, J. Xu, A. J. Hall, K. Haupt, and B. Tse Sum Bui, "Water-compatible silica sol-gel molecularly imprinted polymer as a potential delivery system for the controlled release of salicylic acid.," *J. Mol. Recognit.*, vol. 27, no. 9, pp. 559–565, 2014.
- [47] J. Kang, H. Zhang, Z. Wang, G. Wu, and X. Lu, "A Novel Amperometric Sensor for Salicylic Acid Based on Molecularly Imprinted Polymer-Modified Electrodes," *Polym. Plast. Technol. Eng.*, vol. 48, no. 6, pp. 639–645, 2009.
- [48] Q. P. You, M. J. Peng, Y. P. Zhang, J. F. Guo, and S. Y. Shi, "Preparation of magnetic dummy molecularly imprinted polymers for selective extraction and analysis of salicylic acid in *Actinidia chinensis*," *Anal. Bioanal. Chem.*, vol. 406, no. 3, pp. 831–839, 2014.
- [49] M. Meng, Y. Feng, M. Zhang, Y. Liu, Y. Ji, J. Wang, Y. Wu, and Y. Yan, "Highly efficient adsorption of salicylic acid from aqueous solution by wollastonite-based imprinted adsorbent: A fixed-bed column study," *Chem. Eng. J.*, vol. 225, pp. 331–339, 2013.



## *General conclusions and perspectives*

For many decades, polymers have played a prominent role in technology, as extraordinary versatile and diversified structural and multifunctional macromolecular materials. Over the recent years, interest in biocompatible materials has been increasing proportionally with the more and more demanding applications of such materials in the environmental, biomedical and other fields. The use of enzymes as catalysts for organic synthesis has become an increasingly attractive alternative to conventional chemical catalysts. Enzymes offer several advantages including high selectivity, ability to operate under mild conditions, as well as the catalyst recyclability and most importantly the biocompatibility. Thus, many examples of biocatalytic routes to greener polymers have been widely discussed in literature, by using both free and immobilized biocatalysts. The most important examples are polycondensation, oxidative polymerization, and ring-opening polymerization.

Among the many different functional polymers emerging in the biomedical and environmental applications, molecularly imprinted polymers (MIP) have recently attracted special attention for their specificity and selectivity, and for their plethora of different applications. However, as for other synthetic materials, concerns about MIP toxicity for human and environment safety are of great importance. Therefore, biocompatibility of these imprinted materials should be investigated in order to enlarge the use of MIPs in these fields.

In this multidisciplinary PhD thesis, the main goal was to establish a green biocatalytic route for molecularly imprinted hydrogels synthesis by enzyme-initiated free radical polymerization. First, hydrogels have been synthesized by enzyme-initiated free radical polymerization using free HRP as potential biocatalyst. Many different hydrogels have been prepared and characterized. Different experimental conditions were investigated to understand the effect of the initiating

---

system on hydrogels characteristics. Immobilization of the biocatalyst on solid carrier was then studied and optimized for particles synthesis. Finally, MIPs for the recognition of small molecules and protein were synthesized for environmental, cosmetic or pharmaceutical applications. The green approach was used for the MIP synthesis by both free and immobilized enzymes.

Biocatalyst-mediated free radical polymerization was successfully applied to synthesize linear and highly cross-linked polymers. Different oxidoreductases were used to prepare linear polyacrylamides with emphasis on the yield and the polymer molecular weight. Moreover, hydrogels were also synthesized by this approach. The enzymatic initiation method was shown to be a low-cost, robust and fast alternative for preparing hydrogels. Horseradish peroxidase was verified to be the best among all the tested biocatalysts including myoglobin, cytochrome *c*, hemoglobin, and hemin for the preparation of hydrogels based on a wide range of functional and cross-linking monomers. The role of each component in the ternary system was investigated, to optimize the yield and to control the size of the particles. The hydrogen peroxide concentration showed a special effect by inactivating the enzyme in an irreversible manner at higher extents. However, the increase in acetylacetone or HRP concentration can lead to a variation in particle sizes, from small-sized nanoparticles to microgels, with an increase in the polymerization yield. Finally, HRP-initiated polymerization was compared to the traditional photochemical initiation in terms of particles sizes and yields, as well as the cytotoxicity of the polymers. Better control of the particles size combined with high yields are provided by the enzymatic initiating system being also less cytotoxic at high polymers concentrations.

Horseradish peroxidase has then been covalently immobilized on glass beads, in order to develop a solid-phase synthesis approach of polymer nanoparticles with an immobilized radical source. Different experimental conditions were studied and the results characterized by means of specific activity of HRP-charged beads, immobilized enzyme amount and residual activity. After the optimization of the conditions, the effect of each immobilization step was emphasized by scanning electronic microscopy and the immobilized enzyme *via* the final standard protocol was characterized in term of storage stability and hydro-organic solvents. It was shown that HRP

---

immobilization enhances its stability at the time for at least 56 days compared to the free counterpart.

Immobilized HRP was applied for hydrogels synthesis, and was shown to be a powerful means for the preparation of chemically cross-linked polymers. A model polymer, poly(4-VP/PDA) was used. The synthesis protocol was optimized *via* a second-order experimental design proposed by Doehlert.

Molecularly imprinted hydrogels were successfully synthesized by enzyme-mediated free radical polymerization. Different MIPs were prepared for the molecular recognition of small molecules such as the herbicide 2,4-dichlorophenoxyacetic acid (2,4-D) and the pharmaceutical salicylic acid by means of the ternary system including the HRP free in the media. The effects of the oxidant and reducing species concentrations on the MIP behaviors were studied. Protein imprinting was also successfully investigated. The binding properties of the MIPs prepared by enzymatic initiation were compared to the ones of the traditionally synthesized MIPs.

Moreover, HRP was immobilized on glass beads through different protocols, for MIP synthesis. A glutaraldehyde-based protocol was found to be the best, leading to optimal residual enzyme activity. Synthesis of MIPs for 2,4-D based on immobilized HRP-ternary system was performed. The resulting polymers showed very good specificity and selectivity. The reusability of the same batch of HRP-charged beads was also investigated for subsequent syntheses of MIPs. Different batches of polymers were successfully obtained in 4 cycles. Interestingly, the different MIPs retained their excellent binding properties. The system was thus readily shown to be a very good alternative for traditional MIP synthesis in order to enlarge the use of these functional materials in biocompatible applications.

**As a perspective of this work**, it would be interesting to test this new initiation system for the synthesis of more complex materials, such as nanocomposites. Thereby, it may be possible to combine it with a controlled/living polymerization method, such as atom-transfer radical polymerization (ATRP) or Reversible addition-fragmentation chain transfer (RAFT). Better

---

control of the polymer characteristics as the molecular weights can thus expected. Also, other enzymes could be tested for green synthesis, alone or combined with horseradish peroxidase. For example, glucose oxidase, and enzyme using free oxygen for its reaction, in addition to horseradish peroxidase may permit polymer synthesis in open air by eliminating dissolved oxygen. This would represent an exciting progress toward overcoming the oxygen-free restriction of free radical polymerization. The resulting H<sub>2</sub>O<sub>2</sub> will be a potential substrate in the biocatalytic cycle of HRP leading to the formation of one water molecule with two radical molecules. The cytotoxicity of the polymers can be also repeated with new polymers based on non-toxic monomers (other than 4-vinyl pyridine) in order to establish well the difference in cytotoxicity among the enzyme-based initiations and the chemical ones emphasizing the novel green approach.

It would also be interesting to use our new approach for other types of polymer, for example to study hydrogel synthesis by using phenol, or one of its derivatives, as functional monomers or cross-linkers, thus diversifying the polymeric matrices for molecular imprinting technology or to design multi-functional materials. The final product can, in addition, be characterized in terms of anti-oxidant activity in order to establish green polymers with interesting properties.

The initiation method with the immobilized enzyme could be tested to prepare hydrogels with lower or higher cross-linking degree, in order to provide gels with different mechanical stabilities in order to broaden the use of the materials for a wide range of biocompatible applications and in particular for molecular imprinting. If the enzyme is partly entrapped within the matrix, a higher degree of cross-linking may enhance this effect. The resulting MIPs with an HRP residual catalytic activity can be thus used in order to develop plastic antibody-based bioassays with an integrated detection scheme. It would also be interesting to extent this protocol to MIP nanogels for protein recognition.

---

## Annexes 1 - Achievements

### Publications

*Free-radical polymerization initiated by immobilized horseradish peroxidase for molecularly imprinted nanoparticles synthesis*, **M. Daoud Attieh**, A. Elkak, A. Falcimaigne-Cordin, K. Haupt, submitted.

*Synthesis of molecularly imprinted hydrogels via HRP-initiated free-radical polymerization*, **M. Daoud Attieh**, A. Elkak, A. Falcimaigne-Cordin, K. Haupt, in preparation.

*Application of different heme-based oxidoreductases for hydrogels synthesis via free radical polymerization*, **M. Daoud Attieh**, A. Elkak, A. Falcimaigne-Cordin, K. Haupt, in preparation

### Oral communications

**M. Daoud Attieh**, A. Elkak, A. Falcimaigne-Cordin, K. Haupt, *Development of a new polymerization approach for artificial receptors synthesis in aqueous media*, Nanodrug summer school, Coimbra, Portugal, 29 June - 4 July 2014.

**M. Daoud Attieh**, A. Elkak, A. Falcimaigne-Cordin, K. Haupt, *Optimization of a new polymerization approach for the synthesis of water-compatible imprinted nanoparticles*, LAAS 21, Beirut, Liban, 23 Avril 2015.

**M. Daoud Attieh**, A. Elkak, A. Falcimaigne-Cordin, K. Haupt, *Optimization of a new polymerization approach for the synthesis of water-compatible imprinted nanoparticles*, EMRS, Lille, France, 11 Mai 2015.

### Poster presentations

**M. Daoud Attieh**, A. Elkak, A. Falcimaigne-Cordin, K. Haupt, *Optimization of a new polymerization approach for the synthesis of water-compatible imprinted nanoparticles*, Symposium of Biomacromolecules and their applications, Tripoli, Lebanon, 26 February 2015.

**M. Daoud Attieh**, A. Elkak, A. Falcimaigne-Cordin, K. Haupt, *Development of a new polymerization approach for the synthesis of water-compatible imprinted nanoparticles*, 3<sup>rd</sup> International Symposium on Green Chemistry, La Rochelle, France, 3-7 May 2015.

## Annexes 2 - Posters



## OPTIMIZATION OF A NEW POLYMERIZATION APPROACH FOR THE SYNTHESIS OF WATER-COMPATIBLE IMPRINTED NANOPARTICLES

M. Daoud Attieh<sup>1,2\*</sup>, A. Elkak<sup>3</sup>, A. Falcimaigne-Cordin<sup>4</sup>, K. Haupt<sup>4</sup>.

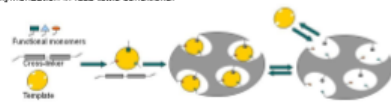
<sup>1</sup> Compiègne University of Technology, FRE-CNRS 3580 Institute for Enzyme and Cell Engineering, Compiègne 60203, France.

<sup>2</sup> Laboratoire de Valorisation des Ressources Naturelles et Produits de Santé (VRNPS), Université Libanaise, Cité Universitaire Rafic Hariri, Hadath, Liban

\* Mira DAOUD ATTIEH (mira.daoud-attieh@utc.fr)

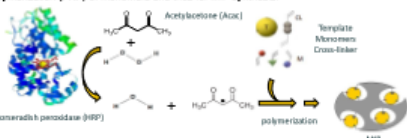
### INTRODUCTION

Molecularly Imprinted polymers (MIPs), also referred to as plastic antibodies, are tailor-made synthetic receptors that are able to specifically recognize and bind target molecules. They can thus be widely used in various applications where selective binding is required, such as immunoassays, affinity separation, and biosensors.<sup>[1]</sup> Recently, it has been suggested that MIPs could be applied in biomedical fields, such as drug delivery systems for their release properties.<sup>[2]</sup> These specific materials are synthesized traditionally by free radical co-polymerization of functional and cross-linking monomers arranged around a molecular template in apolar media. However, exposure to the free-radical polymerization reagents leads to toxic final compounds, and this fact will greatly limit their use in biomedical, pharmaceutical and environmental applications.<sup>[3]</sup> Herein, we describe, for the first time, a new approach for the synthesis of MIP hydrogels by free-radical polymerization in less toxic conditions.



### PEROXIDASE-MEDIATED POLYMERIZATION OF MIPs

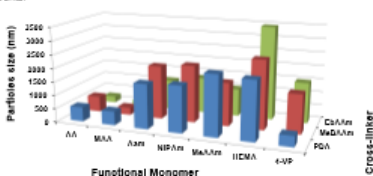
Horseradish peroxidase (HRP) is an enzyme that catalyzes the oxidation of several organic substances (phenols, anilines) by hydrogen peroxide (H<sub>2</sub>O<sub>2</sub>) and a few hydro-peroxides.<sup>[4]</sup> The generally accepted mechanism involves the production of free radicals, that can be thus used for the initiation of the free radical polymerization (FRP) of monomers and thus for MIP synthesis.



### SYNTHESIS OF MIP NANOPARTICLES BY FREE ENZYME-MEDIATION

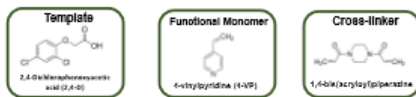
#### Emphasis of the enzymatic system for the hydrogels synthesis

In order to emphasize the enzymatic initiation, several hydrogels were synthesized by using a wide range of acidic, neutral and basic functional monomers that are commonly used for MIP synthesis, and water-soluble cross-linkers. The experiments were carried out in phosphate buffer in order to replace the dipolar aprotic solvents.



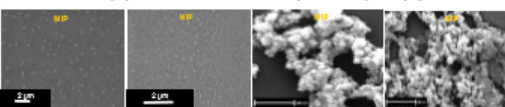
#### MIP Hydrogels formulation

MIP nanogels for 2,4-dichlorophenoxyacetic acid (2,4D) were synthesized with different polymerization processes in aqueous media using 4-VP and PDA as functional and cross-linking monomers, respectively (ratio 1:4:16). The specific binding properties were evaluated radioactivity assays.



4VP/11DA nanoparticles synthesized by HRP<sup>1</sup>-mediated polymerization

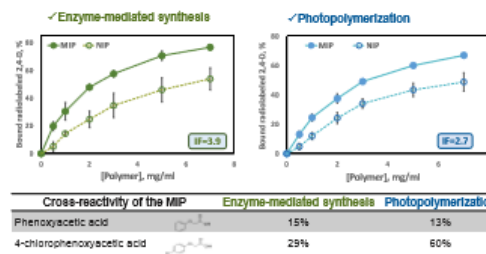
4VP/11DA nanoparticles synthesized by photochemically-mediated polymerization



References

1. Haddad, V. *Anal. Chim. Acta* 2003, 575, 279-300.
2. Sliemers, R.; Schmittmann, C.; Thoenes, H.; Janssen, C.; Obermayer, B.; Dittmar, T. *Journal of Controlled Release* 2004, 104, 175-178.
3. Srinivas, M.; Toranzo, J.; Salgado, J.; Vargiu, V.; Serrano, B.; Hasciuc, C. *Bioorganic Chem.* 2015, 26, 90-100.
4. Gnanou, Y.; Dubois, P. *New J. Chem.* 2007, 31, 2275-2281.
5. Li, Y.; Li, B. *Process Biochemistry* 2005, 41, 1167-1176.

### Molecular recognition of the nanoparticles

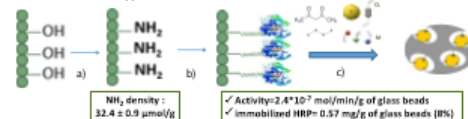


### SYNTHESIS OF MIP NANOPARTICLES VIA IMMOBILIZED PEROXIDASE

Immobilized HRP was developed for nanoparticles synthesis in aqueous media, and applied to the MIP preparation. The resulting polymeric materials will be free of any radical source. The immobilized enzyme can be reused for several polymerization batch.

#### Characterization of HRP immobilization

The HRP immobilization has been studied and optimized. Porous glass beads of 0.1mm have been selected as support for immobilization. First, glass beads are activated by silanization with aminopropyl triethoxysilane, then HRP is attached on the support through covalent grafting with a spacer. The optimal conditions for the beads silanization and HRP immobilization were performed and glutaraldehyde are selected for the attachment of HRP on support.

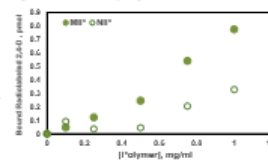


a) Silanization, b) HRP immobilization, c) Polymerization of MIPs

#### MIP Synthesis by immobilized enzyme-mediated polymerization

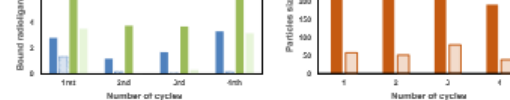
MIP nanogels for 2,4D were synthesized in aqueous media with the same polymer formulation for MIP nanoparticles prepared by free enzyme-mediated polymerization.

The binding test shows that the imprinting is verified, with an imprinting factor of 5.4 for [polymer] = 0.5mg/ml, which is significantly high.



#### MIP nanoparticles synthesis by the reusable immobilized enzyme

Immobilized HRP can be used several time to initiate a free radical polymerization. 4 batches of MIP and NIP have been obtained with the same biocatalyst without any significant change in the particles size and yield, and by changing a high imprinting factor for each couple of polymers.



Immobilized HRP can be used several time to initiate a free radical polymerization. 4 batches of MIP and NIP have been obtained with the same biocatalyst without any significant change in the particles size and yield, and by changing a high imprinting factor for each couple of polymers.

### CONCLUSION - PERSPECTIVES

- Enzyme-mediated initiation of free radical polymerization is a good alternative for the synthesis of hydrogels.
- The Horseradish peroxidase-mediated synthesis of MIPs can lead to the same binding properties of the polymers, as well as the photochemical initiation of FRP.

The authors acknowledge the EU Marie Curie programme (ITK CHEBANA), COSTER Regional de Picardie (ANR09), and ADM SAGE, for funding, as well as the European Union and the Regional Council of Picardy for co-funding of equipment under CPER2007-2013





## OPTIMIZATION OF A NEW POLYMERIZATION APPROACH FOR THE SYNTHESIS OF WATER-COMPATIBLE IMPRINTED NANOPARTICLES.

**M. Daoud Attieh<sup>a,b\*</sup>, A. Elkak<sup>a</sup>, A. Falcimaigne-Cordin<sup>a</sup>, K. Haupt<sup>b</sup>.**

<sup>a</sup> Compiègne University of Technology, FRE-CNRS 3650 Institute for Enzyme and Cell Engineering, Compiègne 60203, France.

<sup>b</sup> Laboratoire de Valorisation des Ressources Naturelles et Produits de Santé (VRNPS), Université Libanaise, Cité Universitaire Rafic Hariri, Hadath, Liban

\* MIRA DADUD ATTIEH (mira.daoud-attieh@utc.fr)

### INTRODUCTION

Molecularly imprinted polymers (MIPs) are synthetic materials with specific binding capacities to a target molecule. Their molecular recognition properties, similar to natural receptors, are obtained by creating a complementary shape in a polymeric matrix using a molecular template. MIPs are applied in several fields, such as immunoassays, affinity separations, biosensors, and recently, in biomedical and cosmetic fields as drug delivery systems. These specific materials are synthesized traditionally by free radical co-polymerization of functional and cross-linking monomers arranged around a molecular template in apolar media. The process of MIPs synthesis are not entirely compatible to water-soluble relevant biological molecules such as drugs and proteins and suitable for their biomedical applications due to the use of toxic solvents and initiators. Herein, we propose a green chemistry approach for the MIPs synthesis by enzyme-initiated polymerization in aqueous media.

### PEROXIDASE-MEDIATED FREE RADICAL POLYMERIZATION

Horseradish peroxidase (HRP) is an enzyme which catalyzes the oxidation of several organic substances (phenols, amines) by hydrogen peroxide (H<sub>2</sub>O<sub>2</sub>) and a few hydro-peroxide. The generally accepted mechanism involves the production of free radicals, that can be used for the initiation of the free radical polymerization (FRP) of acrylamide.

#### ♦ Synthesis of linear polyacrylamide by biochemical initiation

HRP Initiator	HRP	Am	Chemical Initiator	Yield (%)	Molecular weight (kDa)
Chemical Initiator	Opt C	-	-	92.2	7.6
Chemical Initiator	HRP	-	-	88.8	6.9
Chemical Initiator	HRP	Am	-	88.8	8
Photochemical initiation	-	-	-	0	-
Control	-	-	-	0	-
Control	HRP	-	-	0	-
Photochemical initiation	-	-	HRP-30	88.8	8.8

### NANOGELS SYNTHESIS BY ENZYME-INITIATED POLYMERIZATION

#### ♦ Hydrogels formulation

#### ♦ Comparison of photochemical and HRP-mediated initiation

The size and the morphology of Enzyme-mediated free radical polymerization (FRP) synthesized hydrogels, as well as their chemical structures were studied and compared to those obtained with a traditionally photochemical initiator of FRP. The polymerization yield obtained from enzyme-mediated initiation of FRP was lower than the one produced by photochemical initiator.

Time (h)	4-VP/POA	4-VP/MAA	4-VP/POA
Photochemical initiation	30%	20%	20%
Biochemical initiation	55%	35%	55%

References:  
 1. Hsieh, K. *Anal. Chem.* 2003, 75, 231A.  
 2. Dornel, A., Laha, T., Sigaud, M., Hennefort, F. *Polymer* 2003, 44, 5915.

#### ♦ Effect of monomers formulation

The enzyme-mediated initiation can be applied to the hydrogels production with various water-soluble cross-linkers and functional monomers.

The gels size depends on monomer composition and total monomer concentration (Cm). Nanogels have been obtained for 4-VP/POA and MAA/POA as formulation with a Cm = 1%.

#### ♦ Optimization of enzyme initiator system

The values of 4-VP/POA particles (1%) sizes measured by Dynamic Light Scattering, and yield clearly indicate that HRP, H<sub>2</sub>O<sub>2</sub>, and Acac concentrations influence the polymerization:

- The higher [HRP] and [Acac], the bigger the particles and the polymerization yield as well.
- For initial [HRP] < 0.05 mg/ml, no polymerization can occur.
- The lower limit for [Acac] is 1 mM.
- For initial [H<sub>2</sub>O<sub>2</sub>] < 0.5 mM, no polymerization can occur. The upper limit (6 mM) is due to HRP degradation.

### SYNTHESIS OF MOLECULARLY IMPRINTED NANOGELS

MIP hydrogels (2%) for 2,4-dichlorophenoxyacetic acid (2,4-D) were synthesized with different polymerization processes in aqueous media using 4-VP and POA as functional and cross-linking monomers, respectively (ratio 1:4:15). The specific binding properties were evaluated radioactively assays.

#### ♦ Synthesis of molecularly imprinted nanoparticles

##### ♦ Peroxidase-mediated initiation

##### ♦ Photochemical initiation

### CONCLUSION - PERSPECTIVES

- Enzyme-mediated initiation of free radical polymerization is a good alternative for the synthesis of hydrogels.
- The Horseradish peroxidase-mediated synthesis of MIPs can lead to the same binding properties of the polymers, as well as the photochemical initiation of FRP.

The authors acknowledge the EU Marie Curie programme (EV6-GRAM), and ADM MACE for funding, as well as the European Union and the Regional Council of Provence for co-funding of equipment under DRAC2007-2012.